

P

ADA102276

DMC FILE COPY

XEROX

DISTRIBUTION STATEMENT A
Approved for public release;
Distribution Unlimited



81731005

(1) 334

(1)

(9) TECHNICAL REPORT

VOLUME I

(6) TRAINER ENGINEERING REPORT (FINAL)

FOR MILES

CDRL ITEM A002

18 NAVTRAQ EQUIPZ LEVEL DTIC SELECTED JUL 31 1981

(19) 76-2-0010-RTV

(14) XEOS-2350-AD-224-REV

Prepared by:

MILES Technical Staff

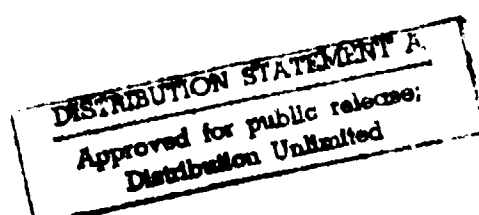
(15) Contract No. N61139-76-C-0060

XEOS Document No. 2350-AD-227
29 May 1980

(11) Rev. /22 April 1981

Xerox Electro-Optical Systems

300 North Halstead Street
Pasadena, California 91107



230650 alt

UNCLASSIFIED

SECURITY CLASSIFICATION OF THIS PAGE (When Data Entered)

REPORT DOCUMENTATION PAGE		READ INSTRUCTIONS BEFORE COMPLETING FORM
1. REPORT NUMBER NAVTRAEEQUIPCEN 76-C-0060	2. GOVT ACCESSION NO. <i>AD-A102 176</i>	3. RECIPIENT'S CATALOG NUMBER 176
4. TITLE (and Subtitle) Volume I Trainer Engineering Report (Final) for Miles CDRL Item A002 .	5. TYPE OF REPORT & PERIOD COVERED 29 May 1980 and Rev. 22 Apr 1981	
7. AUTHOR(s) Miles Technical Staff	6. PERFORMING ORG. REPORT NUMBER N61139-76-C-0060	
9. PERFORMING ORGANIZATION NAME AND ADDRESS Xerox Electro-Optical Systems 300 North Halstead Street Pasadena, CA 91107	10. PROGRAM ELEMENT, PROJECT, TASK AREA & WORK UNIT NUMBERS	
11. CONTROLLING OFFICE NAME AND ADDRESS Allen Herbeck, Project Engineer, Code 234 NAVTRAEEQUIPCEN, Orlando, FL 32813	12. REPORT DATE 22 Apr 1981	
14. MONITORING AGENCY NAME & ADDRESS (if different from Controlling Office)	13. NUMBER OF PAGES 248	
	15. SECURITY CLASS. (of this report) Unclassified	
	15a. DECLASSIFICATION/DOWNGRADING SCHEDULE	
16. DISTRIBUTION STATEMENT (of this Report) Approved for public release; distribution unlimited		
17. DISTRIBUTION STATEMENT (of the abstract entered in Block 20, if different from Report)		
18. SUPPLEMENTARY NOTES		
19. KEY WORDS (Continue on reverse side if necessary and identify by block number)		
20. ABSTRACT (Continue on reverse side if necessary and identify by block number) This document provides a detailed analysis of the MILES systems (Volume I) and a final hardware design disclosure (Volume II) of the 11 systems that comprise the current Engineering Development (ED) phase of MILES. The problem was to design and build a tactical training system for the U.S. Army that simulates the weapons, weapon characteristics, and weapon effects of a family of weapon systems including infantry, armor, and aircraft. The design of the initial 11 systems allows for expansion, flexibility, and compatibility with the total 1980 MILES family		

UNCLASSIFIED

SECURITY CLASSIFICATION OF THIS PAGE(When Data Entered)

of weapons.

The key elements of the systems are the low power pulsed laser transmitters used to simulate the weapons and the inexpensive silicon photodiode (solar cell) detectors used to receive the laser transmissions. Audio and visual indicators display the effects of weapon fire with kill, hit, and near-miss indications. The weapons of the infantryman or target vehicle are deactivated by the receipt of a kill signal.

UNCLASSIFIED

SECURITY CLASSIFICATION OF THIS PAGE(When Data Entered)

ABSTRACT

This document provides a detailed analysis of the MILES systems (Volume I) and a final hardware design disclosure (Volume II) of the 11 systems that comprise the current Engineering Development (ED) phase of MILES. The problem was to design and build a tactical training system for the U.S. Army that simulates the weapons, weapon characteristics, and weapon effects of a family of weapon systems including infantry, armor, and aircraft. The design of the initial 11 systems allows for expansion, flexibility, and compatibility with the total 1980 MILES family of weapons. Design reviews focused on the constraints of eye safety (power limited), design-to-unit-production cost (dollar limited) and ability to meet the performance criteria of weapon simulation while not causing countertraining situations.

Analysis and empirical data have established a data base which shows that the MILES systems meet the required performance constraints. The systems designs are such that capability is inherent for expansion to include all the weaponry planned for the MILES 1980 time frame.

The key elements of the systems are the low power pulsed laser transmitters used to simulate the weapons and the inexpensive silicon photodiode (solar cell) detectors used to receive the laser transmissions. Audio and visual indicators display the effects of weapon fire with kill, hit, and near-miss indications. The weapons of the infantryman or target vehicle are deactivated by the receipt of a kill signal.

From experience gained during the Advanced Development (feasibility) program and as a result of continued analysis and test, the laser transmitter/discrete detector approach to the simulation problem has proven to be effective from both a performance and cost standpoint.

XEOS has continued to improve on the state of the art while it developed a MILES system with the weaponry of the 1980s in mind. It can be concluded that growth and expansion of MILES in a timely manner is clearly attainable.

Accession For	NTIS CRA&I	<input checked="" type="checkbox"/>
DTIC TAB	Unannounced	<input type="checkbox"/>
Justification	_____	
Rv	_____	
Distributor/	_____	
Availability Status	Avail and/or Dist Special	
A		

FOREWORD

This volume establishes the analytical design data base for the MILES system. Information derived from the analysis was used as a basis for hardware implementation. The hardware implementation is presented in Volume II.

This volume is an update of the "Trainer Engineering Report-Preliminary" including the changes that occurred during the course of the engineering development program and further updated as a result of changes made based on OTII Operational Testing during the summer of 1978 and OTIII Operational Testing in the fall of 1979.

A large amount of analytical work, documented in design file memoranda, has been summarized herein. A few of the more critical DFSs are included in revised form as appendices, but no attempt was made to include them all due to the detailed and voluminous amount of material contained in them.

The objective of the MILES program is to provide the U.S. Army with a combat tactical training system that will closely simulate the effects of weapon engagement. Weapon simulation and casualty assessment are vital to the training system. To provide realistic training of the combat unit in taking cover and evasive action, weapon signature and the near-miss simulation of rounds are important. Human engineering factors are stressed to ensure that the simulators do not produce countertraining.

To achieve the stated goals, a system utilizing low power, eye safe, gallium arsenide (GaAs) laser transmitters to fire "rounds" and silicon solar cell photodiode detectors to record "hits," "kills," and "near misses" is employed. Weapon signatures are achieved by using blank rounds wherever possible and by using the antitank weapons effect signature simulator (ATWESS) to simulate missile firing. "Kills" and "near misses" are denoted by audio and visual signals that can be observed by controllers. "Kills" result in deactivation of the victims' weapon(s). In the case of vehicles, such as tanks, where a hit has a certain probability of kill, the electronics logic has the capability of making that decision based upon the code message of the attacking weapon. Thus, a hit on a tank may or may not be a disabling kill. Message codes are assigned to each weapon to provide a complete hierarchy of weapons and their kill/near miss effects.

The MILES design is simple, lightweight, and modular, with expansion capability inherent in the design so that it will accommodate not only the presently implemented weapon systems, but those of the 1980s. The present core system consists of a family of direct fire weapons including M16 rifles, M60 machine guns, armored personnel carriers (APCs), tank and antitank weaponry, and selected APC-mounted weapons.

The purpose of this document, Volumes I and II, is to establish a data baseline for the continued development of the MILES System and to provide a design disclosure of the ED Miles hardware. This document has been updated and is released as a Trainer Engineering Report (final) in accordance with the CDRL requirements. This final report with the engineering drawings and other contract documentation, completely describes the MILES for follow-on production phases.

This document is the culmination of six years of analysis, design, and testing of MILES systems. At the same time it forms the springboard for the development of future additions to the MILES.

Section 1 summarizes the method used to analyze the MILES systems, lists the analytical constraints, and summarizes the results of the analysis by listing the values of critical systems parameters. Section 2 contains the analysis of the MILES communication medium, the atmosphere, and its effects upon the transmission of laser messages over the required target ranges. Sections 3 and 4 analyze the MILES receiver and laser transmitter, respectively; and Section 5 contains an analysis of the MILES coding, decoding, and threshold setting required for optimum performance with minimum false alarms. Section 6 describes the results of parallel studies which resulted in the use of blank fire enablement of the MILES transmitter as well as the use of a single optical tube for both the kill and near miss beams. Appendices are included to preserve the totality of extensive analyses. The substance of the analyses is included in the body of the report in summary form.

CONTENTS

1.	SYSTEM DESIGN ANALYSIS	1-1
1.1	System Analysis Overview	1-1
1.1.1	Transmitter Design Approach	1-1
1.1.2	Channel Considerations	1-3
1.1.3	Receiver Design Approach	1-3
1.2	Theoretical Design Algorithm	1-3
1.2.1	Design Analysis Algorithm	1-6
1.2.2	Hit Probability Versus Range Algorithm	1-9
1.3	Analytical Constraints	1-10
1.3.1	Weapon Characteristics	1-15
1.3.2	Eye Safety Constraint	1-15
1.3.3	Beam Diameter	1-15 *
1.3.4	False Alarms	1-15 *
1.4	Critical Parameter Summary	1-15 *
2.	ATMOSPHERIC EFFECT UPON MILES PERFORMANCE	2-1
2.1	Introduction	2-1
2.2	Atmospheric Attenuation	2-1
2.2.1	Continuum Atmospheric Attenuation	2-1
2.2.2	Water Vapor Attenuation	2-5
2.3	Atmospheric Turbulence	2-10
2.3.1	Predictions of Log Variance	2-12
2.3.2	Saturated Scintillation	2-13
2.3.3	Fresnel Zone Size	2-15
2.3.4	Frequency of Atmospheric Scintillation	2-15
2.3.5	Effect of Multiple Detectors	2-19
2.3.6	Scintillation Effects on Probability of Detection	2-22
2.3.7	Scintillation Testing, Results, and Conclusions	2-23

CONTENTS (contd)

3.	RECEIVER ANALYSIS	3-1
3.1	Silicon Photodiode Characteristics	3-1
3.2	Background Irradiance	3-1
3.2.1	Photodiode Saturation	3-3
3.3	Noise Analysis	3-5
3.3.1	Shot Noise	3-7
3.3.2	Amplifier and Johnson Noise	3-8
3.3.3	Noise Equivalent Exposure	3-9
4.	TRANSMITTER ANALYSIS	4-1
4.1	GaAs Injection Laser Characteristics	4-1
4.1.1	GaAs Structure	4-1
4.1.2	Peak Emission Wavelength	4-1
4.1.3	Power Output Temperature Dependence	4-2
4.1.4	Temperature Compensation Requirements	4-4
4.2	Transmitter Parameters	4-4
4.2.1	Transmitter Optics	4-8
4.3	Beam Geometry	4-8
5.	CODING, DECODING, AND THRESHOLD SETTING ANALYSIS	5-1
5.1	Code Functions	5-1
5.2	Code Format	5-1
5.3	Code Set	5-5
5.4	Decoding Scheme	5-8
5.5	Kill Probabilities	5-13
5.6	Effect of Coding and Decoding on System False Alarm Rate	5-20
5.6.1	Theoretical Basis	5-20
5.6.2	Computer Model	5-21
5.6.3	Negative Effect of Multiple Word Receipt Requirements	5-26
5.6.4	Conclusion	5-26
5.7	Threshold-to-Noise Setting and False Alarm Rate	5-27

CONTENTS (contd)

6. PARALLEL STUDIES	6-1
6.1 Single Tube Transmitter	6-1
6.1.1 Introduction	6-1
6.1.2 Analysis	6-2
6.1.3 Conclusions from Analysis for VES	6-2
6.1.4 Conclusions from Analysis for TES	6-3
6.2 Blank Fire Detection	6-4
6.2.1 Testing	6-5
6.2.2 Conclusions	6-8
6.3 Blank Fire Enable	6-8
6.3.1 Multiple Detector Tests	6-8
6.3.2 Conclusions	6-10

APPENDIX A — MILES EYE SAFETY

APPENDIX B — ON THE CHARACTERISTICS OF A GAUSSIAN LASER BEAM
BEING DETECTED BY A FIXED THRESHOLD RECEIVER

APPENDIX C — VISIBILITY/RANGE CAPABILITY

APPENDIX D — UNION DECODING PROBABILITY ANALYSIS

APPENDIX E — SINGLE TUBE CONCEPT ANALYSIS

APPENDIX F — WEAPON SIMULATION (HIT PROBABILITY VERSUS RANGE)

APPENDIX G — GLOSSARY OF TERMS

APPENDIX H — REFERENCES

*
*
*

ILLUSTRATIONS

1-1	System Elements and Signal Flow	1-2
1-2	Algorithm for Analysis	1-4
1-3	First Design Iteration (Basic Feasibility)	1-7
1-4	Hardware Design/Tradeoff Algorithm	1-8
1-5	Algorithm for Probability of Hit versus Range	1-11
1-6	Kill Probability in Terms of Range for Centerline Beam Irradiance	1-12
1-7	MILES Mathematical Variable Analysis	1-14
1-8	Weapon Characteristics	1-16
*		
2-1	Atmospheric Transmittance	2-2
2-2	Gallium Arsenide Wavelength versus Temperature	2-6
2-3	Coefficient for Water Absorption as a Function of Wavelength	2-7
2-4	Precipitable cm of Water per Kilometer as a Function of Temperature and Relative Humidity	2-8
2-5	Variance in Log _e Intensity versus Range	2-14
2-6	Fresnel Zone Size versus Range	2-16
2-7	Fresnel Scintillation Frequency as a Function of Crosswind Velocity	2-17
2-8	Effect on Fluctuation Index Due to Aperture Averaging	2-20
2-9	Probability of Message Receipt versus Detector Quality	2-21
2-10	Probability versus Range, TES Laser	2-25
2-11	Probability versus Range, VES Laser	2-26
3-1	Photodiode Equivalent Circuit and Spectral Response	3-2
3-2	Spectral Response, RG 830 Filter	3-4
3-3	Schematic and Model for the MILES Detectors and Preamplifier	3-6
4-1	RCA Data for 0.003" Multiheterojunction Strep Geometry	4-3
4-2	Case I - Peak Current Just Above Threshold	4-5

4-3	Case II - Peak Current Much Greater Than the Laser Threshold Current	4-6
4-4	M16A1 Min/Max Energy Curves	4-9
5-1	Code Format	5-2
5-2	MILES Decoding Elements	5-9
5-3	Clock Frequency Error	5-11
5-4	Decoder Timing - Missile Tracker	5-14
5-5	Kill Probability Dependence on Range	5-17
5-6	Mean Number of Rounds to Kill	-18
5-7	False Alarm Probability - Man Decoder (Kill)	5-22
5-8	False Alarm Probability - Vehicle Decoder (Kill)	5-23
6-1	Acoustic Sound Levels, M60 Machine Gun	6-7

TABLES

1-1	Variables Affecting Hit Probability or Probability of Message Receipt	1-13
1-2	Critical Parameter Summary	1-18 *
2-1	GaAs Performance at $\lambda = 0.9 \mu\text{m}$	2-3
2-2	Representative Cases for TES (TES Range = 300 meters)	2-4
2-3	Representative Cases for VES (VES Range = 3 km)	2-5
4-1	Transmitter Parameters	4-7
5-1	MILES Code Parameters	5-4
5-2	MILES Weapon Code Assignment	5-6
5-3	MILES ED Target/Weapon Hierarchy	5-15
5-4	Vehicle Kill Probabilities	5-19
5-5	Man Near Miss	5-24
5-6	Man Kill	5-24
5-7	Vehicle Near Miss	5-25
5-8	Vehicle Hit	5-25
5-9	Allowable False Ones	5-27
6-1	Weapon Sound Levels	6-6

SECTION 1

SYSTEM DESIGN ANALYSIS

1.1 SYSTEM ANALYSIS OVERVIEW

MILES has been modeled as a pulse-code-modulation (PCM) optical communication system in which the communication medium is the atmosphere. A block diagram illustrating the major functional elements and showing the information flow from weapon fire to the decoded output is shown in figure 1-1. As with conventional optical communication systems, MILES will generate an encoded message, transmit the encoded message through varying atmospheric conditions, and decode the transmitted message to initiate required actions. The MILES differs from conventional communication systems in that the messages generated must simulate weapon firing characteristics, round dispersion patterns, and the probability of hit as a function of range for specific weapon systems.

1.1.1 TRANSMITTER DESIGN APPROACH

1.1.1.1 M16A1 Rifle and Machine Gun Laser Transmitters

A single tube laser transmitter scheme with a "kill" and "near-miss" message is used for all Miles weapons. With the initiation of trigger pull, a kill code message is generated in the encoder that "on-off" modulates the injection laser in the kill-transmitter. Upon completion of a kill message, a near-miss message is generated in the encoder which again on-off modulates the laser. The near-miss beam from the transmitter has a higher power than the kill beam and therefore transmits a larger effective beam diameter over an extended range. To further increase the near-miss beam diameter and range a larger number of words are sent out during the near-miss message (see Section 6). This greatly increases the probability of near-miss signal detection.

1.1.1.2 Tank Main Gun Transmitter

Tank main guns employ a single transmitter for kill and near-miss messages. To achieve the larger required near-miss beam diameter, higher power and many near-miss words are used in the near-miss message. This scheme was shown to be effective in field tests. Scintillation has a major influence in the realization of a larger near-miss zone relative to the central kill zone (see Section 6).

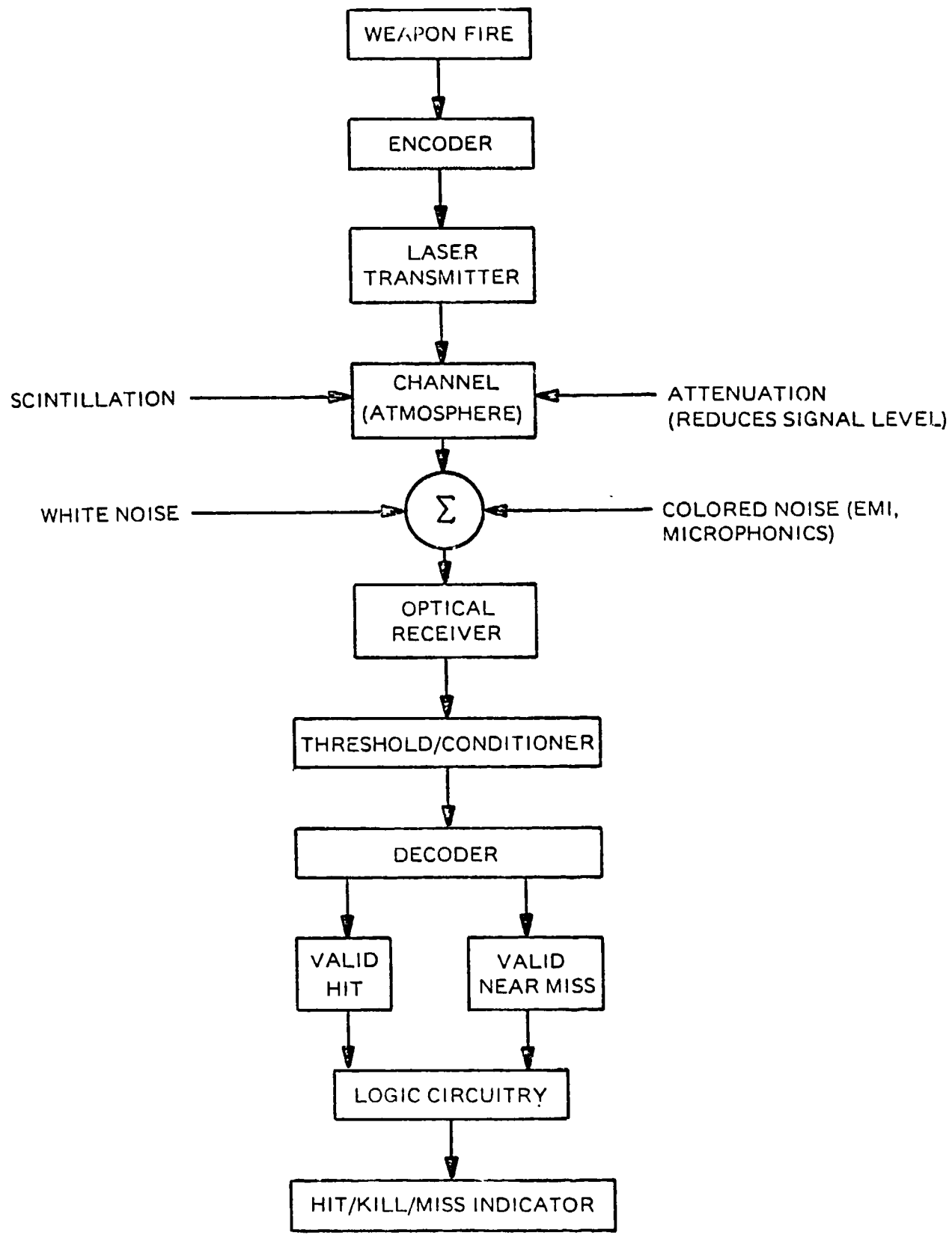


Figure 1-1. System Elements and Signal Flow

1.1.1.3 Missile Transmitter

Missile simulators employ a single transmitter. There is no separate near-miss beam generated in the simulation of missile fire. Correct tracking for the required time interval results in a hit and potential kill. Improper tracking in which the missile operator is not on target a sufficiently high percentage of the required time interval, is interpreted by the decoder as a near miss.

1.1.2 CHANNEL CONSIDERATIONS

The atmospheric channel through which the beam propagates generally contains molecules, aerosols, and turbulence, each of which can alter the spatial and temporal properties of the irradiance distribution. These variations, which include beam absorption, scattering, and scintillation, have the effect of producing long-term and short-term intensity fluctuations which in turn result in varying probability of detection of a given pulse code bit. A detailed discussion of the effects is presented in Section 2.

1.1.3 RECEIVER DESIGN APPROACH

The optical receiver is comprised of silicon solar cell photodiodes and an amplifier. The photodiodes convert incident optical energy in the channel to electrical signals. The number of detectors per amplifier and their placement are optimized for the man and vehicle systems. The receiver is subject to white noise due to background irradiance such as sun induced shot noise, thermally generated noise (Johnson noise) of the amplifier, and spurious noise such as that from microphonics or EMI.

Output of the optical receiver is analyzed by a threshold comparator which detects the presence of signals above a predetermined value. The output is conditioned for sampling by a continuous decoder. The decoder determines the presence of a valid kill or near-miss word and outputs the results to appropriate logic circuitry.

1.2 THEORETICAL DESIGN ALGORITHM

Because of the complexity and number of variables associated with the MILES communication system, a theoretical design algorithm, shown in figure 1-2, is used to obtain an optimum system design. The parameters used in the algorithm consist of uncontrollable parameters and variable parameters which the analyst can control. The critical parameters used in this algorithm are:

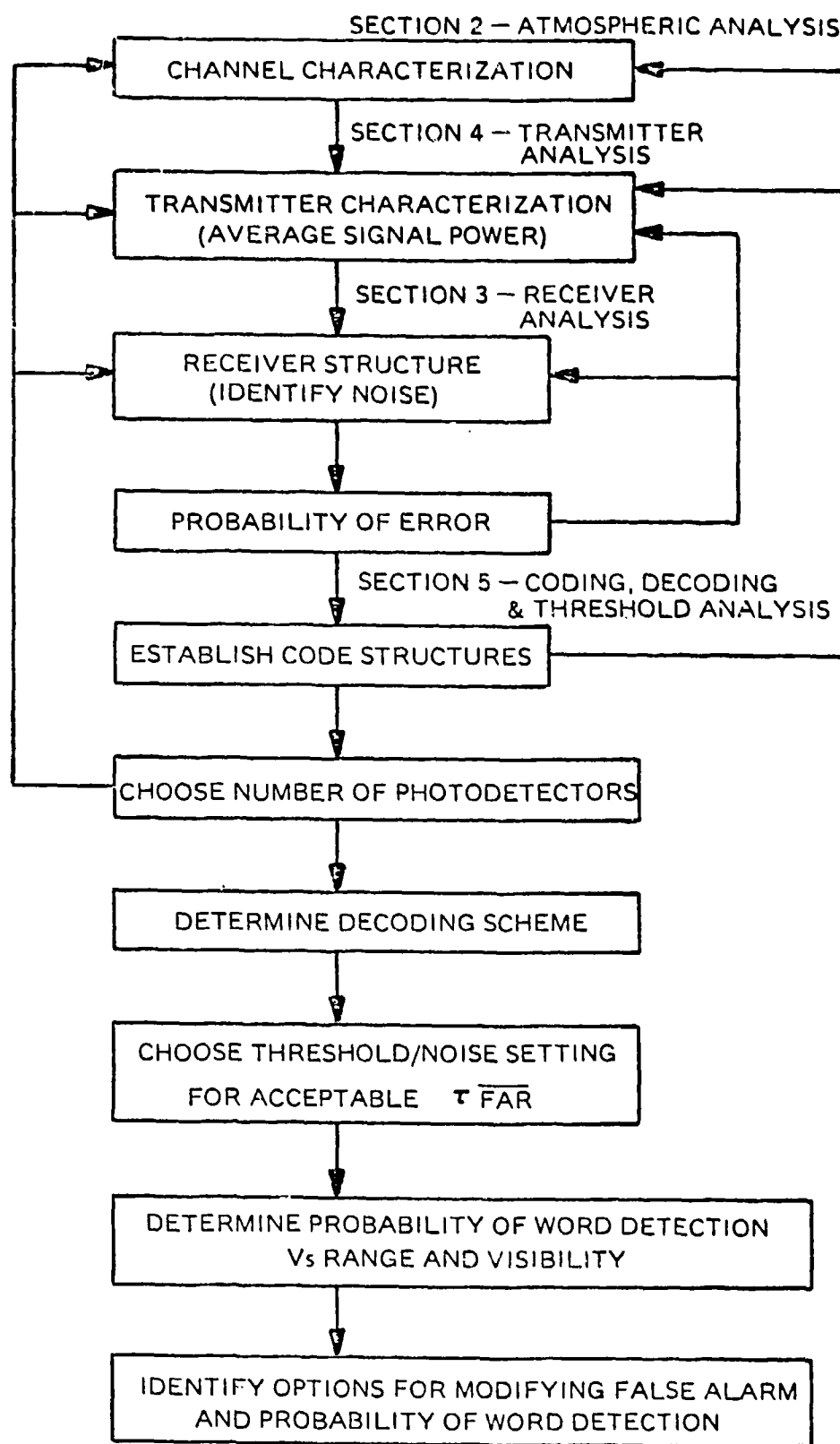


Figure 1-2. Algorithm for Analysis

a. Controllable Parameters

- o Transmitter power output
- o Beam divergence
- o Code type and code weight
- o Threshold-to-noise setting
- o Number of words transmitted
- o Receiver Geometry
- o Receiver threshold
- o Decoding scheme
- o Type of photodiodes (detectors)
- o Number and spacing of detectors
- o Number of words required to be received

b. Uncontrollable Parameters

- o Channel characterization (atmosphere)
- o Shot noise spectral density
- o Johnson noise spectral density
- o Maximum background irradiance
- o Maximum eye safe power output

Figure 1-2 depicts the analysis sequence described in the following sections:

- o Section 2 - Atmospheric Analysis (Channel Characterization)
- o Section 3 - Receiver Analysis
- o Section 4 - Transmitter Analysis
- o Section 5 - Coding, Decoding, and Threshold Analysis

1.2.1 DESIGN ANALYSIS ALGORITHM

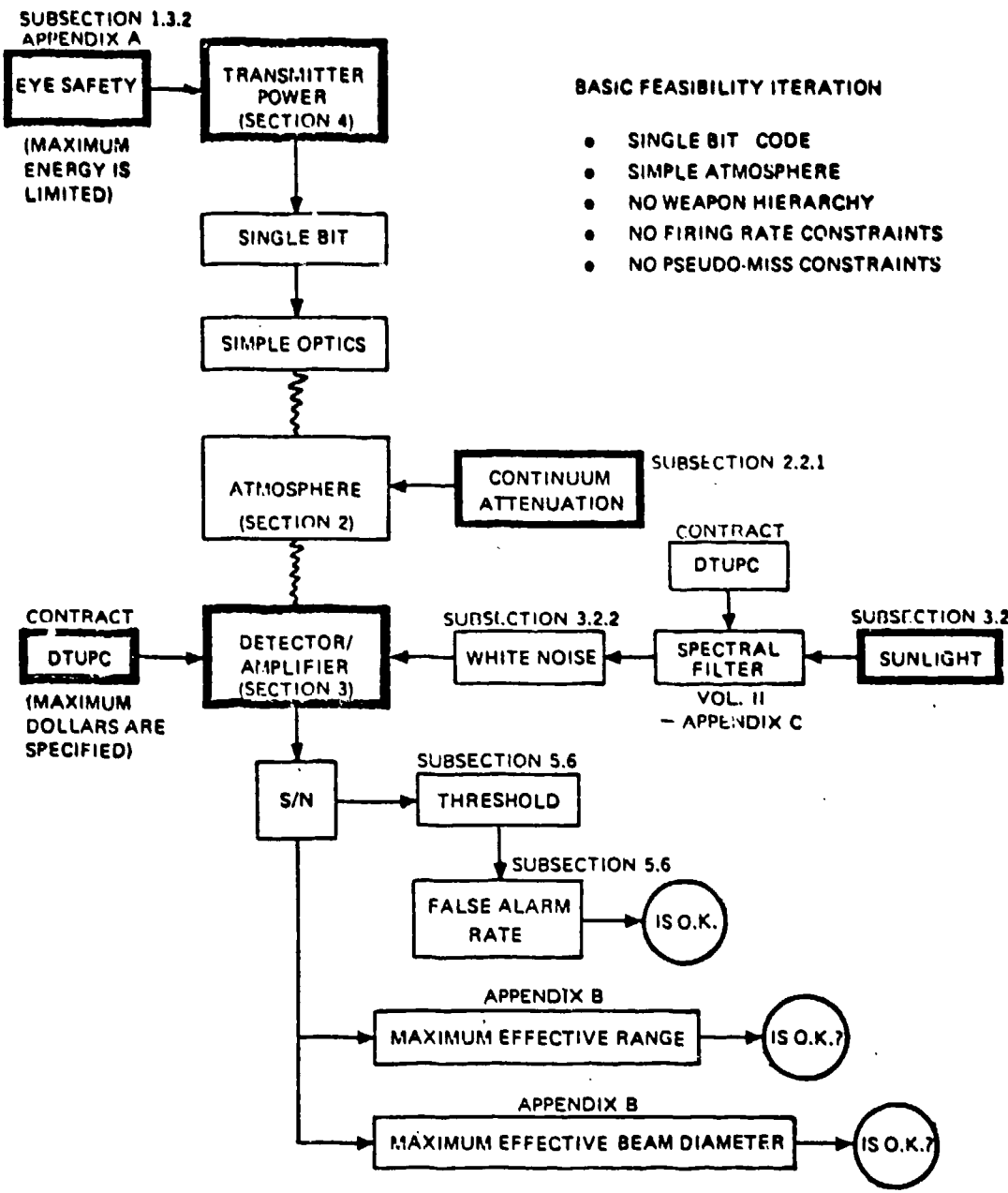
The algorithm for analysis, shown in figure 1-2, matches the analytical sections in this volume. The system analysis, however, cannot be performed without entering the hardware design constraints into the algorithm. Such things as Design-to-Unit-Production-Cost (DTUPC), problems of pseudo-miss at close range due to detector spacing, weapon hierarchy, firing rates, size, weight, and battery life must inherently be addressed in any conclusive analysis that leads to hardware development. These hardware tradeoffs are, of necessity, closely tied to the theoretical analysis, although not addressed in this summary analysis. The additional algorithm elements are therefore included to show in greater detail an algorithm which assures that the theoretical analysis does not overlook the practical problems of hardware design.

Figure 1-3 shows the first iteration starting with two basic hardware design constraints:

- o The device must be eye safe (maximum power constraint).
- o The device must meet DTUPC goals (minimum cost). For example, DTUPC constrains the "per/detection point" cost such that PIN detectors cannot be used. A simple silicon photodetector (solar cell) is the constraint at the detection end.

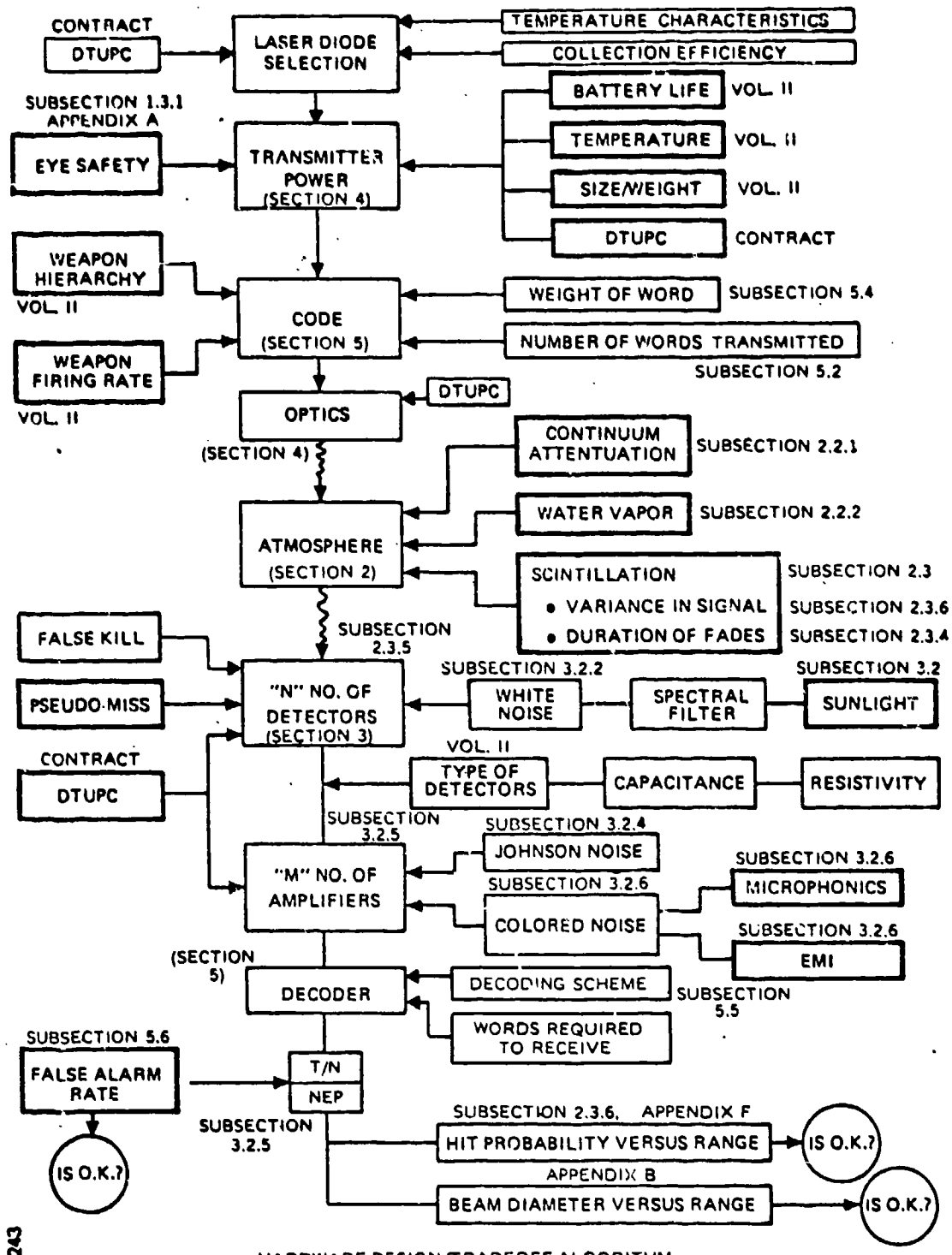
Using an eye safe laser output, single noncoded bits are transmitted out of a simple optics, through a simplified atmosphere affected only by continuum attenuation to a single silicon photodiode. Sunlight filtered through a spectral filter, chosen on the basis of DTUPC and spectral transmission characteristics, provides a shot-noise environment. With these criteria the signal-to-noise ratio, detection threshold, and maximum effective range and beam diameter can be determined. Signal-to-noise and threshold allow determination of an average false alarm rate (FAR). This is a basic feasibility iteration. When the parameters of FAR, maximum effective range, and maximum effective beam diameter all check out as satisfactory, the second iteration is performed.

Figure 1-4 depicts the second iteration. Hardware constraints on the transmitter are now shown. Battery life, environmental factors, including temperature, size, weight, and DTUPC constraints are considered. A code is added with its parameters of weight of word, number of words per message, and its constraints due to weapon hierarchy and weapon firing rates. The coded laser message is now sent through the worst case atmosphere which includes scintillation effects and water vapor attenuation in addition to the continuum attenuation.



58244

Figure 1-3. First Design Iteration (Basic Feasibility)



50243

HARDWARE DESIGN/TRADEOFF ALGORITHM

Figure 1-4. Hardware Design/Tradeoff Algorithm

Message receipt is now considered in the analysis by using multiple detectors. The problems of pseudo-miss, which could be solved by many detectors, must be traded off against DTUPC (less detectors to reduce cost). Detector selection is made at this point. Hardware performance, and cost tradeoffs must be made in order to select a detector whose characteristics can be used in the analysis. The use of multiple detectors requires a decision to be made on the number of amplifiers to be used. Ideally one amplifier per detector would be used, but DTUPC cost constraints must be traded off against performance so that the ratio of amplifiers to detectors can be selected. This ratio affects noise, S/N, FAR, hit probability versus range, and beam diameter versus range. A decoder and decoding scheme is added and the parameter of number of "words required to be received" is entered. This parameter and the decoding scheme affect the probability of hit versus range and FAR.

The algorithm shown as figure 1-4 is repeated while varying the many parameters and continuing the tradeoffs of cost versus performance until all constraints and performance criteria have been satisfied.

1.2.2 HIT PROBABILITY VERSUS RANGE (P_H vs R) ALGORITHM

No less than 17 variables shown or inherent in figure 1-4 affect the hit probability versus range. These include transmitter, atmosphere, and receiver variables.

To finally arrive at a theoretical hit probability versus range while at the same time satisfying all other system design constraints, it is most helpful to temporarily freeze certain variables as constants. Once this is done, a simplified algorithm can be drawn which shows those variables that directly affect the P_H vs R. Treated as constants are the following:

- a. Receiver responsivity is fixed. The receiver responsivity is maximized within the constraints of DTUPC.
- b. Laser powers are selected within the constraints of eye safety limits. Lasers are selected for temperature performance and DTUPC.
- c. The number of detectors and number of detectors per amplifier are fixed.
- d. False alarm rate is satisfied with adequate margin.
- e. Threshold-to-noise ratio is fixed.

With these parameters as constants and the other hardware constraints satisfied, the algorithm to achieve P_H vs R is shown in figure 1-5.

Figure 1-5 represents a unified detection theory using data supplied by the referenced McMillan and Barnes paper and by the equation for Message Detection Probability versus Bit Detection Probability (Appendix D). This equation is a function of the following variables:

- a. Number of code words transmitted (N)
- b. Weight of code word (W)
- c. Number of code word receipts required (M)
- d. Number of Boolean Unions (U)

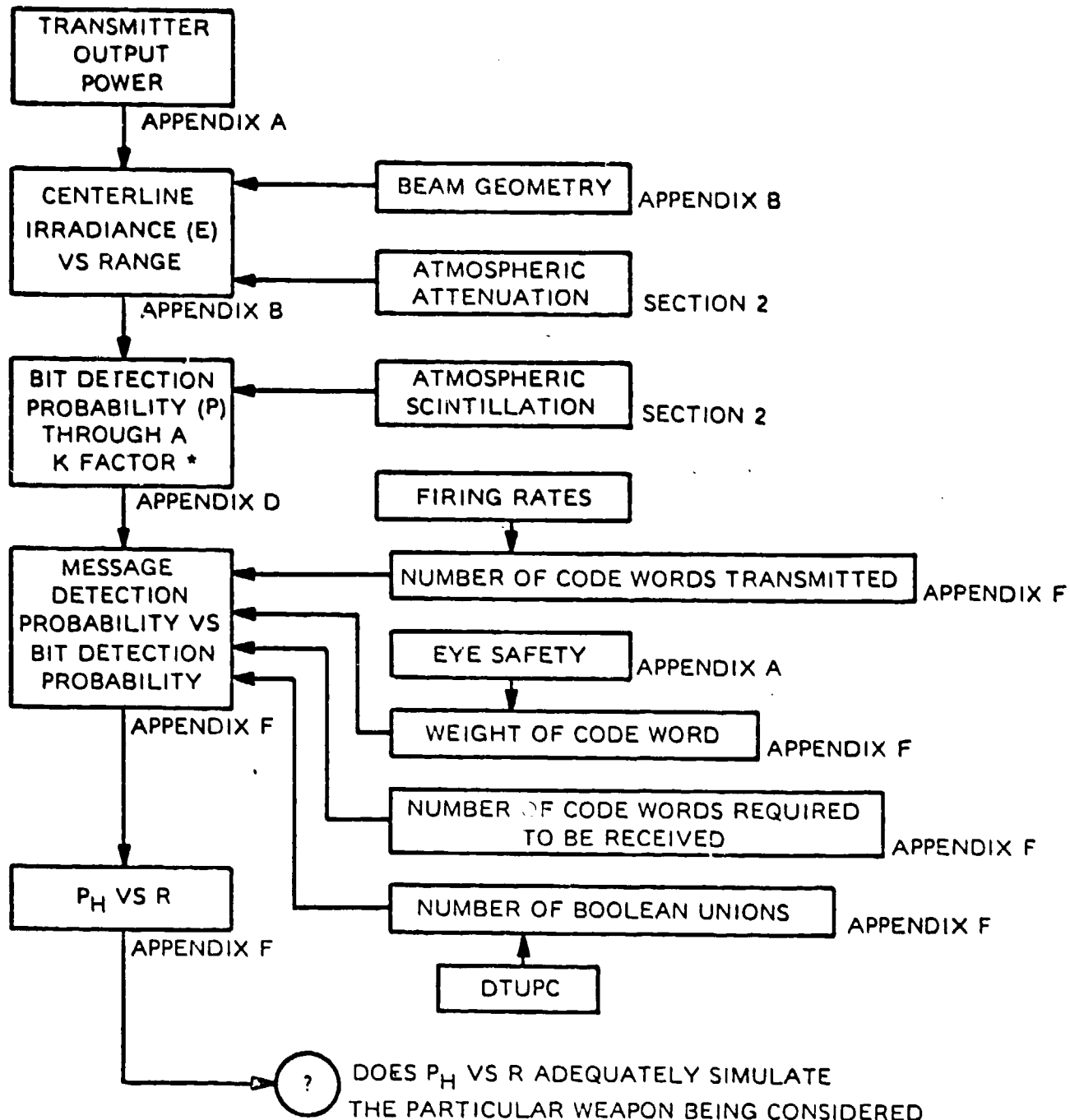
This analysis and theory is included as Appendix D and shows the effect of these variables on message detection probability. The algorithm is reiterated changing the variables to achieve optimum simulation of the various MILES weapons hit probabilities versus range. Figure 1-6 depicts a typical output of this algorithm for one set of the variables and plotted for four values of atmospheric attenuation. This figure is a computer printed output of the Detection Probability computer program discussed in Appendix F.

The 17 variables affecting P_H are listed in table 1-1 along with the constraints which affect or limit those variables. The manner in which the final iteration is performed on these 17 variables to determine P_H as a function of range and atmospheric extinction coefficient is shown in figure 1-7. Each of the 17 variables is systematically changed in value while all the others are held constant. This allows, in effect, the determination of the partial derivative of P_H with respect to that variable. After completing this sequence for all variables, and considering the system constraints on these variables, appropriate combinations are chosen for each weapon system by matching the optimized P_H curve as closely as possible to the desired value for the chosen weapon. At that point the selection is verified through actual field test.

1.3 ANALYTICAL CONSTRAINTS

In the MILES system there are a number of constraints which impact on the analysis. The more important constraints are: the weapon characteristics that are to be simulated; eye safety requirements on transmitter power; kill and near-miss beam diameter; and false alarm rates.

57279



*MCMILLAN AND BARNES, APPLIED OPTICS, OCTOBER 1976, PAGE 2501

Figure 1-5. Algorithm for Probability of Hit versus Range (P_H vs R)

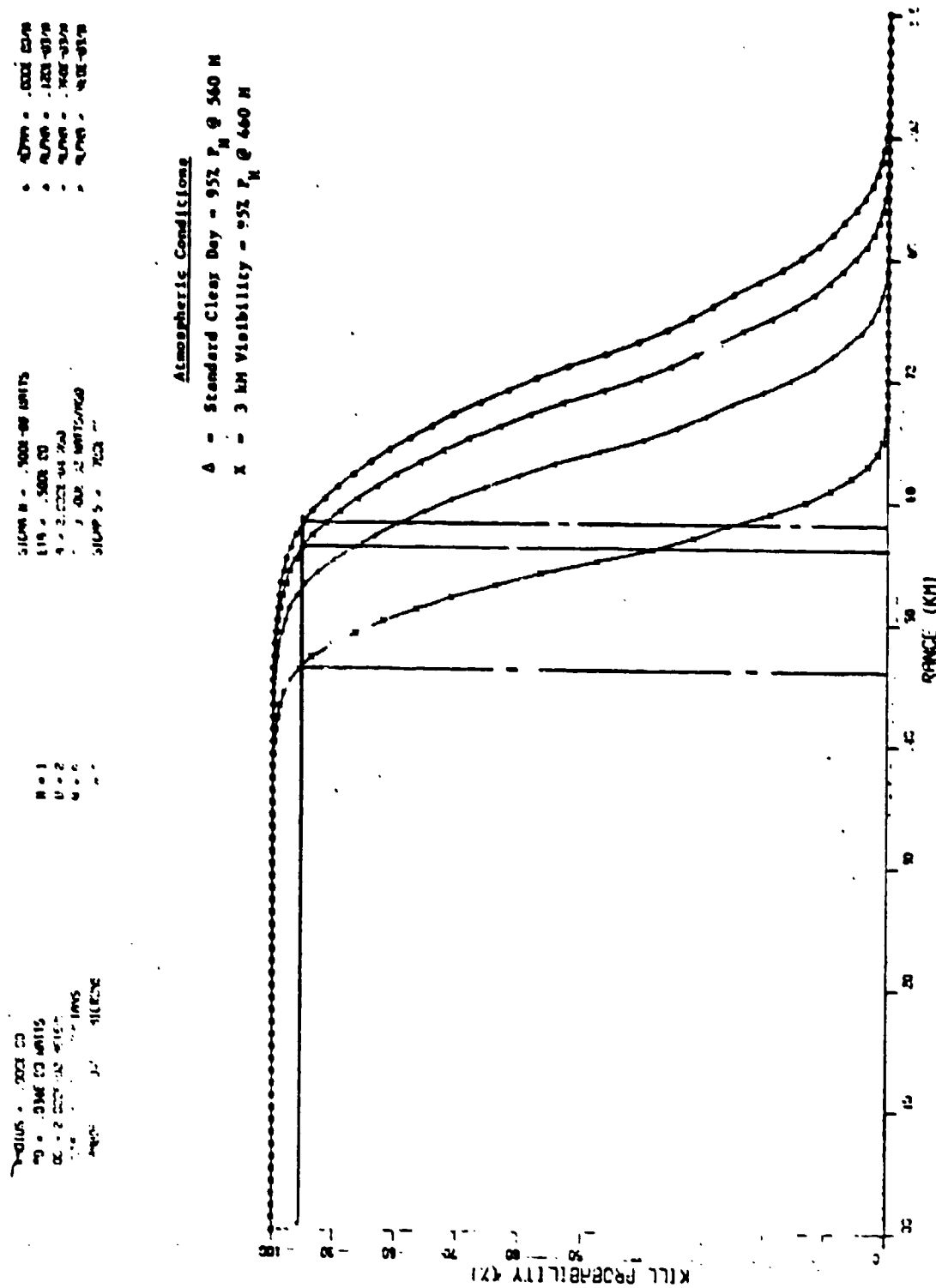
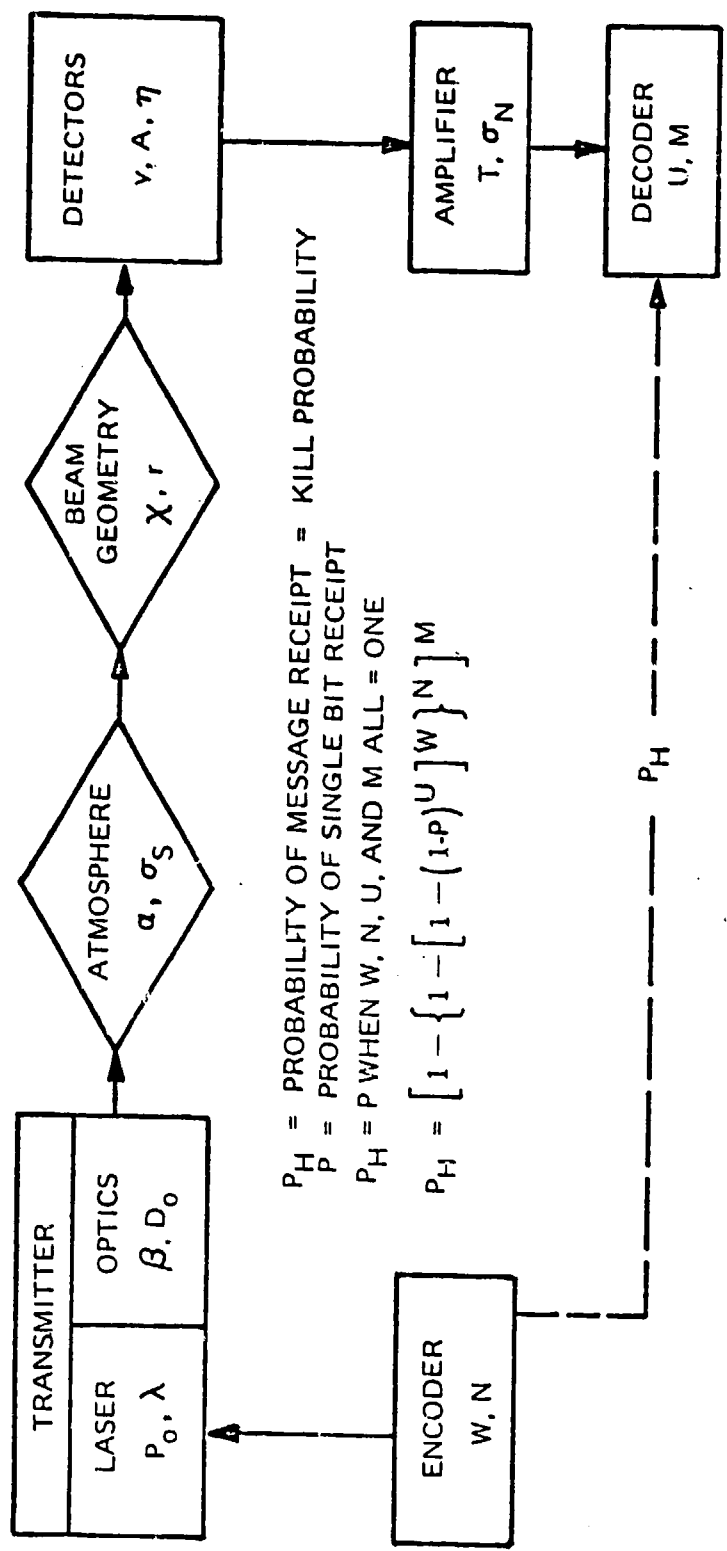


Figure 1-6. Kill Probability in Terms of Range for Centerline Beam Irradiance

TABLE 1-1
VARIABLES AFFECTING HIT PROBABILITY (P_H) OR
PROBABILITY OF MESSAGE RECEIPT

<u>Variable</u>	<u>Description of Variable</u>	<u>Constraints on the Variable</u>
W =	Weight of code word	Eye Safety, False Alarm Requirement, Maximum Laser PRF
N =	Number of code words transmitted	Eye Safety, Weapon Firing Rates, Blank Fire
D_o =	Transmitter aperture	Size, Weight, DTUPC
P_o =	Laser transmitter output power	Eye Safety, DTUPC, Availability, Tactical Fidelity
λ =	Wavelength of laser radiation	GaAs, DTUPC
β =	Beam spread	DTUPC, Maintainability, Reliability, Size, Weight
α =	Attenuation Coefficient	Field Environment, Tactical Fidelity
σ_s =	Square root of the variance due to scintillation	Field Environment, Tactical Fidelity
x =	Range	Tactical Fidelity
r =	Beam radius	Tactical Fidelity, Pseudo-miss
y =	Number of detectors within the beam	Pseudo-miss, DTUPC, Size, Weight
A =	Area of detectors	DTUPC, Size, Weight
η =	Detector collection efficiency	DTUPC, EMI, Field Environment (full sunlight)
T =	Detector threshold	DTUPC, EMI, Maintainability, Reliability, False Alarm Requirement
σ_N =	RMS noise equivalent power density	Field Environment, EMI, DTUPC
U =	Number of Boolean unions	DTUPC
M =	Number of word receipts required for a valid message	False Alarm Requirement, Tactical Fidelity

57278



Determination of Hit Probability (P_H), where:
 $P_H = F(W, N, P_o, \lambda, \beta, D_o, \alpha, \sigma_s, X, r, v, A, \eta, T, \sigma_N, U, M)$

Figure 1-7. MILES Mathematical Variable Analysis

1.3.1 WEAPON CHARACTERISTICS

Each weapon has an inherent probability of kill as a function of range for a specific target. These functions cannot be identically simulated with a laser beam. There are, however, design parameters which can be varied to permit the MILES system to approach weapon characteristics. These variables include beam shape, number of words transmitted per message, code length, and code weight. Figure 1-8 contains a plot of the desired probabilities of hit with respect to range for the MILES weapon fire simulators. The stated visibilities are for targets with contrast ratios of 100 percent.

1.3.2 EYE SAFETY CONSTRAINT

The subject of eye safety is discussed in detail in Appendix A.

*

1.3.3 BEAM DIAMETER

For good fidelity, the effective kill beam diameter is limited to dimensions comparable to the target size. The "effective kill beam diameter" is defined as that zone within which the irradiance is sufficiently above the detector threshold setting to be sensed and a valid kill code accepted by the detection system. Beam shaping, threshold setting, and coding and decoding schemes are all used to insure that the effective kill probability variation with range matches, as closely as possible, the actual kill probability vs range for an M-16 rifle against a man sized target. In addition to a kill beam, all weapons except missiles will have a near-miss beam to warn targets that they are under fire or that a near miss has occurred. This beam has a larger effective diameter and range compared to the kill beam. This is achieved primarily through the use of many repeated near-miss code words, and where applicable by the use of increased transmitter power output during the near miss message.

A summary beam geometry analysis is given in subsection 4.3 and in detail in Appendix B.

1.3.4 FALSE ALARMS

The MILES development specification required "not more than one false alarm per target system for 100 hours of field operation." However, this requirement appears to be much too lenient and could potentially cause distrust of the MILES system. XEOS therefore assumed that a false alarm rate of "not more than one false alarm per 100 hours of field operation per 100 TES (man-worn) systems or per 50 VES (vehicle) systems shall occur" was more reasonable. The design was based on this false alarm criterion.

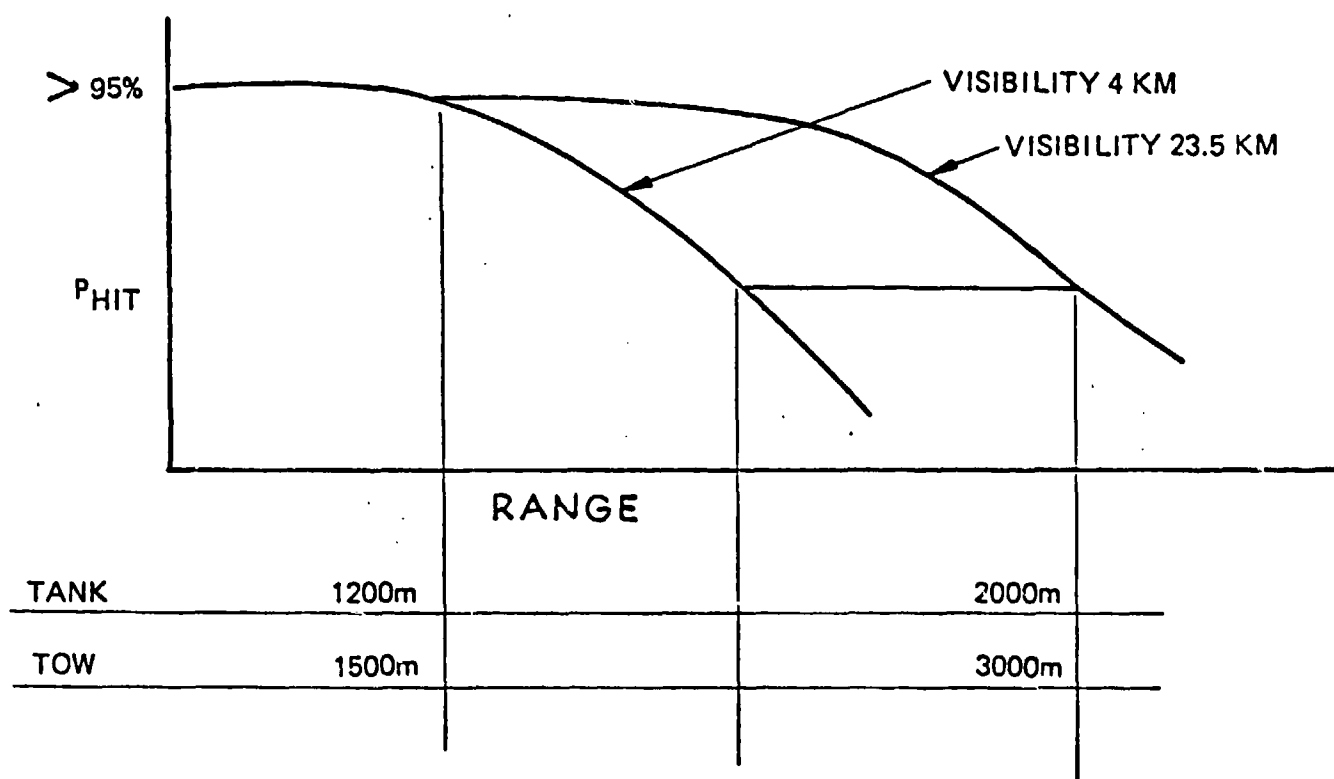
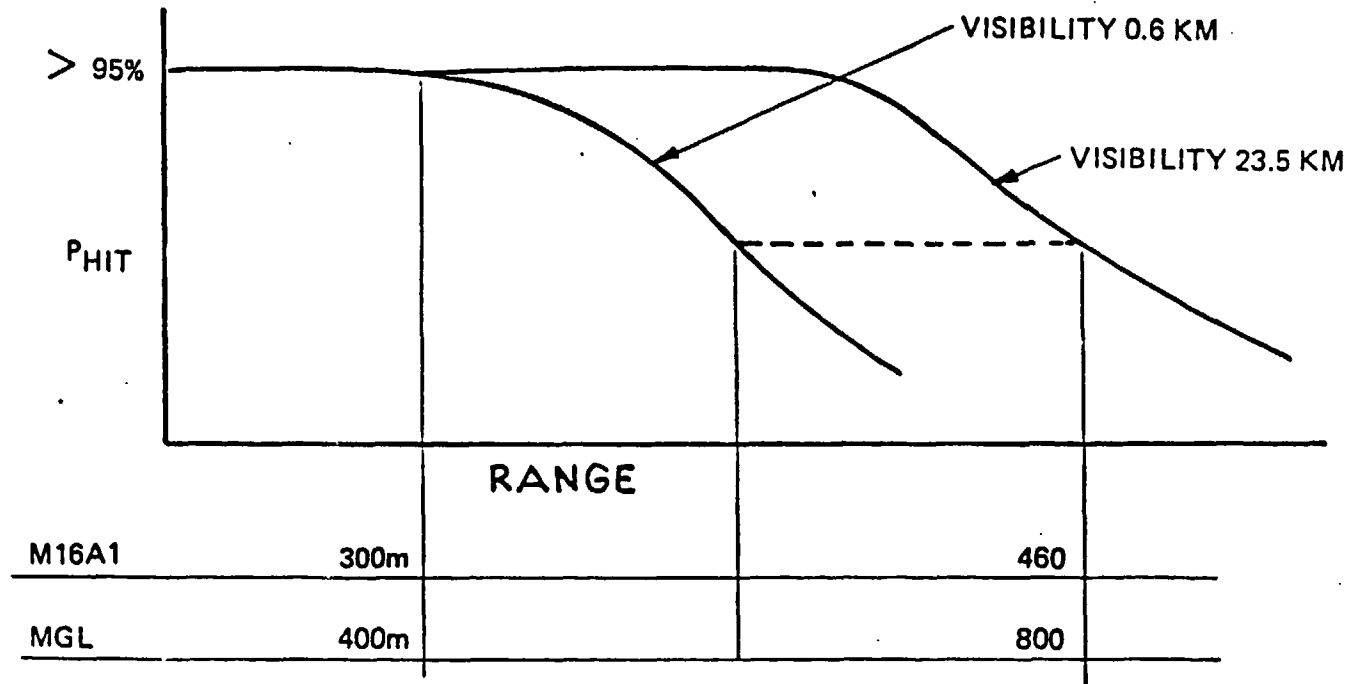


Figure 1-8. Weapon Characteristics

Since a combat vehicle laser detection system (CVLD) will have a maximum of eight threshold circuits, this requires an average false alarm rate per detector of $1/8 \times 1/100 \times 1/50 = 2.5 \times 10^{-5}$ false alarms per hour or 6.94×10^{-9} false alarms per second. The man worn laser detection system (MWLD) has a maximum of three threshold circuits. Thus, the maximum MWLD false alarm rate per detector will be $1/3 \times 1/100 \times 1/100 = 3.33 \times 10^{-5}$ false alarms per hour, or 9.25×10^{-9} false alarms per second.

1.4 CRITICAL PARAMETER SUMMARY

Table 1-2 summarizes the critical parameters that have been determined from the analysis that follows and from empirical data. These parameters along with system specifications form the basis for the hardware design constraints of Volume II of this document.

TABLE 1-2
CRITICAL PARAMETER SUMMARY

Parameter	Condition	Minimum	Nominal	Maximum	
Noise Equivalent Radiant Exposure	Sunlight and signal on 5 of 6 detectors			0.49 μ ergs/cm ²	*
Threshold/Noise Ratio	Full sun	4.5 (TES)	5.5	6.0	
Signal-to-Noise Ratio	(P _k = 90%)	7	7	11:1	
False Alarm Rate FAR	MWLD-full sun CVLD-full sun			3.33×10^{-5} /hr 2.50×10^{-5} /hr	
Irradiance (minimum required)		1.3 μ W/cm ²			
Peak Emission Wavelengths	-25°C to +62°C	8650Å 1 cm ² (1 detector)	9100Å	9311Å 8 cm ² (8 detectors)	*
Detector Area		100 kHz			
Shot Noise Bandwidth		500 kHz			*
Amplifier/Detector Bandwidth for Signal					
Johnson Noise Bandwidth					
Transmitter Power Output (with sun loading and barrel heating)	450M at 65°C 800M at 65°C 1000M at 65°C 2000M at 65°C 3000M at 65°C	0.3W 0.8W 0.9W 1.26W 1.55W	0.4W 0.9W 1.0W 1.5W 2.0W	0.5W 1.0W 1.2W 2.0W 2.5W	
Scintillation Signal Reduction	\geq 1000M 5 detectors	20%	35%	45%	
Optical Filter Sun Current Reduction	RG 830	70%	75%	80%	
Protective Cover Sun Current Reduction (Incremental Effect)	Optical filter already in place	17%	20%	23%	*
Optical Filter Laser Signal Reduction	RG 830 at 9040Å	10%	11%		
EMI Filter Signal Reduction		14%	16%		
Protective Cover Signal Reduction		9%	12%	14%	*
Code Weight		6	6	6	
Number of Word Repeats	Kill TES VES Near Miss TES VES		4 3 14 118		
Cosine and Off Axis Losses	45° off axis	30%	40%	50%	
Laser Transmitter	Present TB MED 279 Maximum Output Energy per Pulse = 0.32 erg			7.5 $\times 10^{-9}$ joules/cm ²	
	*Tentative LAIR eye safety conference ruling for MILES allows 5 ergs/pulse or 3.33 watts peak power output			*1.36 ergs/pulse *1.37 watts peak power	
ED Baseline	4.5 ergs/pulse maximum				

SECTION 2

ATMOSPHERIC EFFECTS UPON MILES PERFORMANCE

2.1 INTRODUCTION

This section discusses the effects of the atmospheric medium upon the MILES signal. Two main effects are considered; atmospheric attenuation and atmospheric turbulence. The analysis of attenuation effects is relatively straightforward, however, the subject of atmospheric turbulence, and especially scintillation, requires a more extensive discussion. Therefore, the major portion of this section is devoted to a discussion of atmospheric scintillation.

2.2 ATMOSPHERIC ATTENUATION

Basically, there are two different types of atmospheric attenuation that influence MILES performance. One type, continuum atmospheric attenuation, causes a reduction in radiant energy in the laser beam as the beam passes through the atmosphere. The second effect is discrete line absorption due to water vapor.

2.2.1 CONTINUUM ATMOSPHERIC ATTENUATION

Continuum atmospheric attenuation is caused by the inherent molecular and aerosol absorption and scattering phenomena present in the earth's atmosphere. The governing relationship for continuum atmospheric attenuation is Lambert's law stated as follows:

$$H(R) = H_0 e^{-\alpha R}$$

(2-1)

where:

$H(R)$ = irradiance of a plane parallel wave at range R

H_0 = irradiance of that wave at $R = 0$

α = continuum attenuation coefficient

e = 2.71828

With reference to figure 2-1 (excerpted from Reference 1), it can be determined that the values for sea level continuum attenuation coefficient (α) are a function of wavelength for various values of

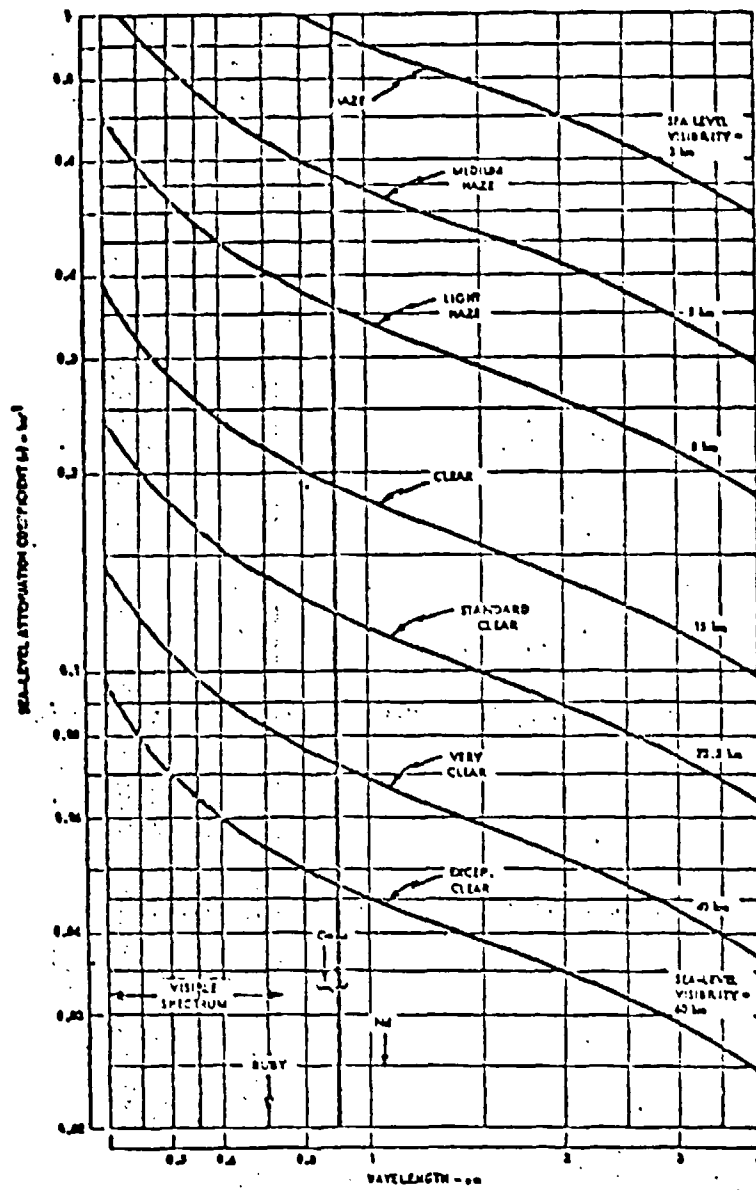


Figure 7-6.* Approximate variation of attenuation coefficient with wavelength at sea level for various atmospheric conditions. Neglects absorption by water vapor and carbon dioxide.

*RCA Electro-Optics Handbook

Figure 2-1. Atmospheric Transmittance

meteorological visibility. As shown on the graph, the curves slope downward with increased wavelength. This is an indication of the physical phenomena that longer wavelength radiation is less attenuated by the atmosphere than shorter wavelength radiation.

Since the MILES system will operate with laser temperatures from -25° to +62°C, the wavelength of interest is 9040A + 220A, -250A. The variation is the result of: (1) diode-to-diode variations in emitting wavelength; and (2) a wavelength shift of about 3 A/°C over the temperature range from -25° to +65°C. However, since the scale on figure 2-1 is 1000A per 4 mm, a 250A swing is only 1 mm, which is about the thickness of the heavy vertical line drawn at 0.9 μ wavelength. Table 2-1 lists typical values for the MILES GaAs laser diode taken from figure 2-1. α times V_M is calculated and listed for further use in deriving Eq. (2-2) which follows.

Note that at $\lambda = 0.9 \mu\text{m}$, the product of the continuum extinction coefficient (α) and the meteorological visibility (V_M) is very nearly constant. Taking the mean value it can be found that:

$$\boxed{\alpha_{\lambda=0.9\mu} = \frac{2.85}{V_M}} \quad (2-2)$$

TABLE 2-1

GaAs PERFORMANCE AT $\lambda = 0.9 \mu\text{m}$

Condition	Meteorological Visibility V_M (km)	α (Km ⁻¹)	αV_M
Exceptionally Clear	60	0.047	2.82
Very Clear	40	0.072	2.88
Standard Clear	23.5	0.120	2.82
Clear	15	0.190	2.85
Light Haze	8	0.36	2.88
Medium Haze	5	0.57	2.85
Haze	3	0.96	2.88

Thus, the simple relation $\alpha V_M = 2.85$ at $\lambda = 0.9 \mu\text{m}$ may be used for MILES. This relation is, in

effect, a near infrared version of Duntley's law which states that:

$$(\alpha V_M)_{\lambda} = 0.55 \mu = 3.912$$

The difference in the product of αV at $\lambda = 0.9 \mu\text{m}$ and $\lambda = 0.55 \mu\text{m}$ is due to reduced continuum atmospheric attenuation in the near IR relative to the visible.

Some representative cases calculated for the target engagement simulator (TES) and the vehicle engagement simulator (VES) are listed in tables 2-2 and 2-3. Starting with TES, the attenuation coefficient using Eq. (2-2) and then the attenuation using Lambert's law, Eq. (2-1) can be calculated for three representative cases as shown in table 2-2.

TABLE 2-2
REPRESENTATIVE CASES FOR TES (TES Range = 300 meters)

Condition	Meteorological Visibility (km)	$\alpha_{\lambda} = 0.9 \mu\text{m}$ (km ⁻¹)	Attenuation	Transmission
Standard Clear	23.5	0.120	0.04	0.96
Haze	8.0	0.36	0.09	0.91
Fog	0.6	4.75	0.76	0.24

Thus, a factor of about 4 degradation in TES irradiance at $R = 300$ meters* can be anticipated as the result of continuum atmospheric attenuation under minimum TES visibility conditions.

For representative cases calculated for VES (table 2-3) the results show that continuum atmospheric attenuation results in a degradation of the signal transmission by about a factor of nine for the VES situation at 3 km* under minimum VES visibility conditions.

TABLE 2-3
REPRESENTATIVE CASES FOR VES (VES Range = 3 km)

Condition	Meteorological Visibility (km)	$\alpha_\lambda = 0.9 \mu\text{m}$ (km^{-1})	Attenuation	Transmission
Standard Clear	23.5	0.12	0.30	0.70
Light Haze	8.0	0.36	0.62	0.38
Heavy Haze	4.0*	0.72	0.89	0.11

*Note the differences in table 2-2 and text of 0.6 km and 300 meters, and in table 2-3 and text of 4 km and 3 km. The lesser figure is the actual visibility apparent to the human eye of targets and target backgrounds whose contrast ratio is less than 100 percent. This subject is treated in detail and the latter figures derived in Appendix C, Visibility/Range Capability.

2.2.2 WATER VAPOR ATTENUATION

To this point we have considered atmospheric attenuation due to atomic and molecular scattering and particulate absorption and scattering under adverse visibility conditions. However, the current mode must also account for infrared absorption due to water vapor. This section presents the data, curves and equations necessary to determine the reduction in beam irradiance due to the absorption of GaAs radiation by water along the optical path from the transmitter to the target.

Since the spectral absorption coefficient K_ν depends upon wave-number ν , which depends upon wavelength ($\nu = c/\lambda = 1/\lambda$), and since the wavelength of a GaAs laser depends upon temperature, T , we must determine K_ν in two steps. Figure 2-2 is a plot of the gallium arsenide laser wavelength vs temperature. Knowing T , we can determine λ from Figure 2-2. Figure 2-3 is a plot of the spectral absorption coefficient for water K_ν , established using data from Reference 1. Knowing λ , we can determine K_ν . The quantity K_ν has the units of reciprocal centimeters. Figure 2-4 is a plot of precipitable cm of water per kilometer of path length as a function of temperature for various values of relative humidity. This figure was prepared using data taken from Reference 2. Note that the data in

61483

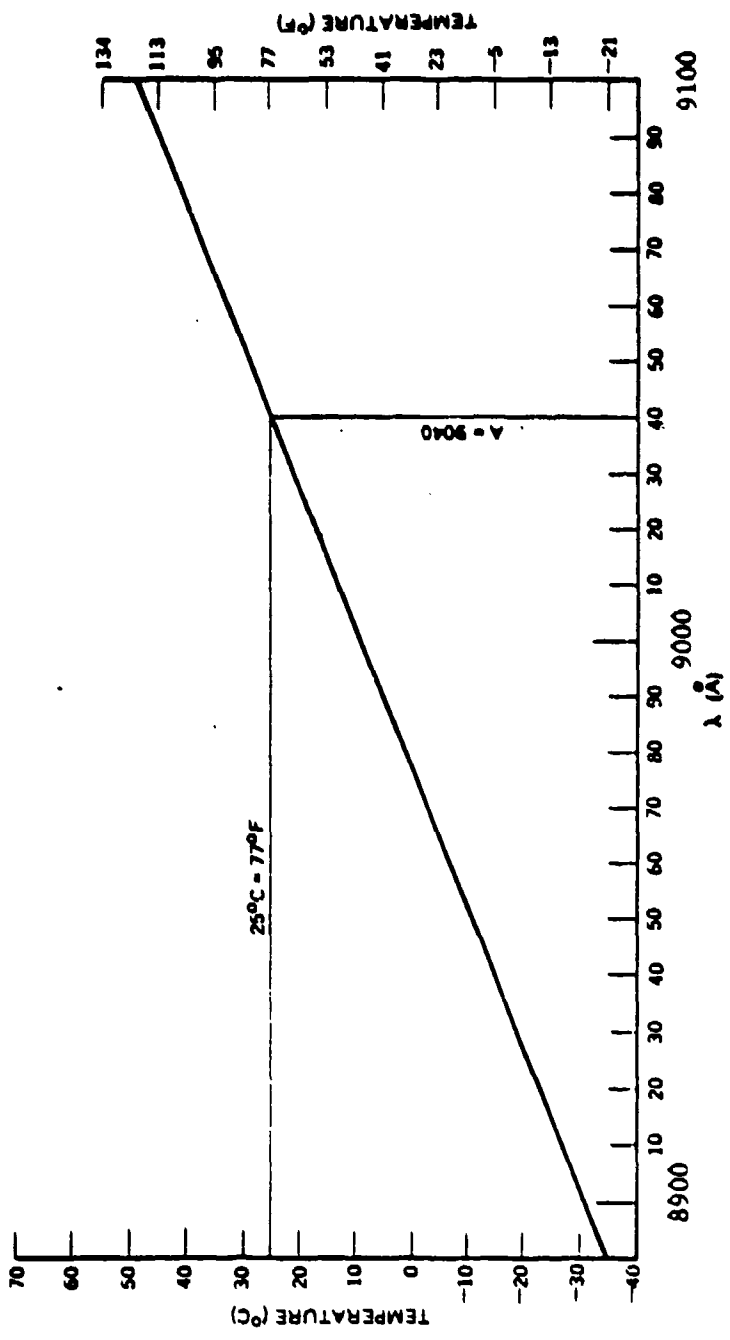


Figure 2-2. Gallium Arsenide Wavelength versus Temperature

62455

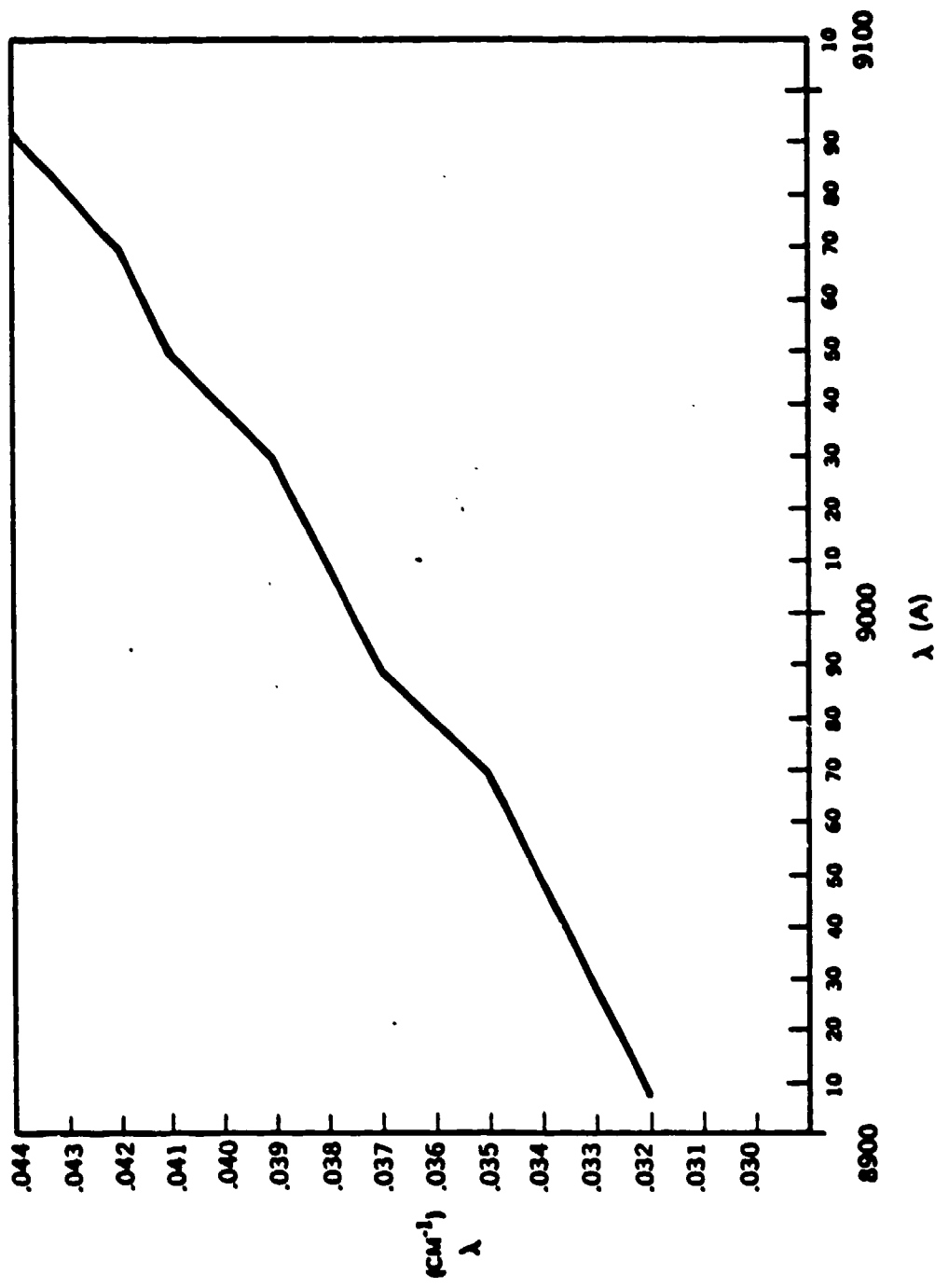


Figure 2-3. Coefficient for Water Absorption as a Function of Wavelength

62449

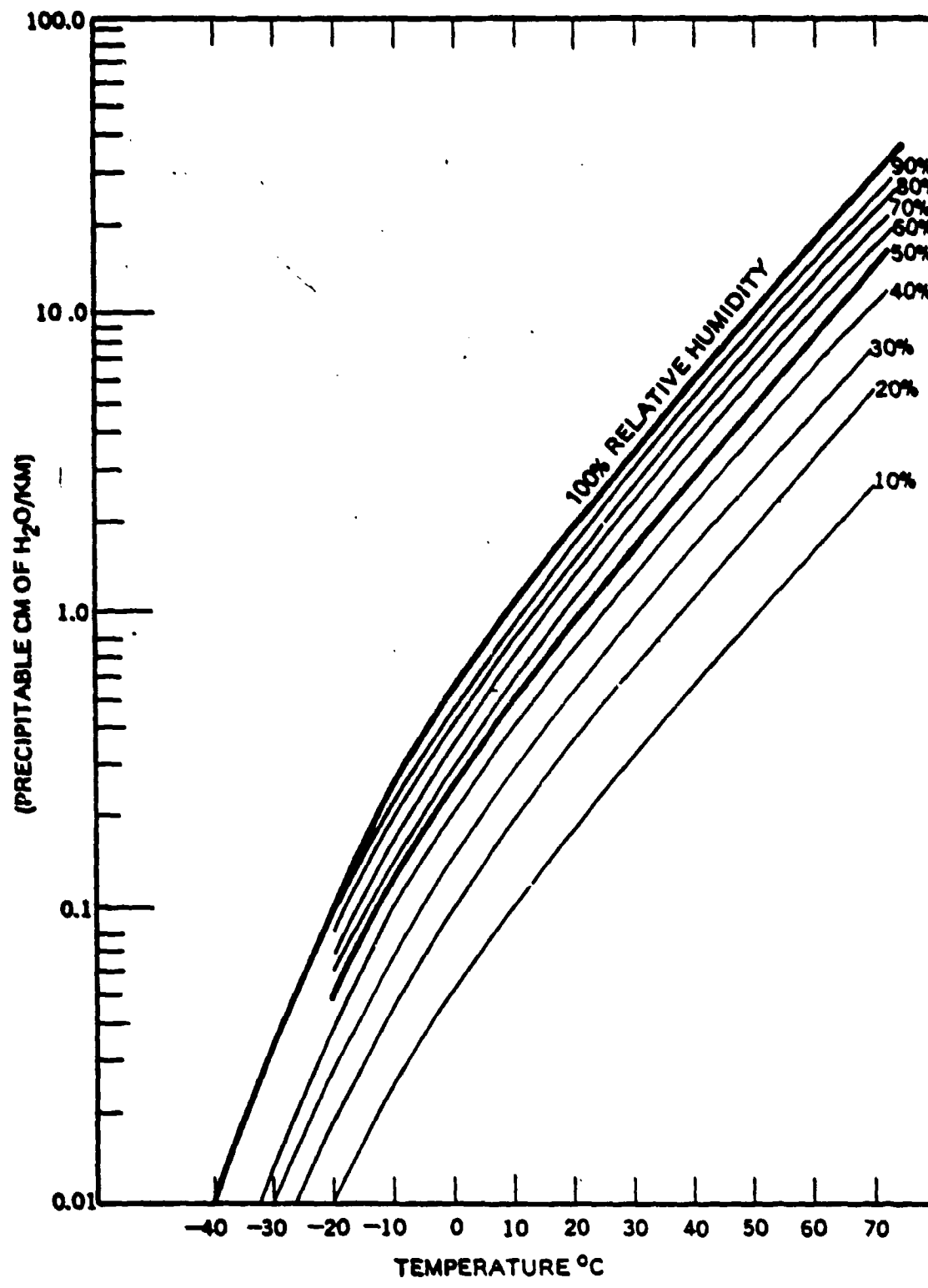


Figure 2-4. Precipitable cm of Water per Kilometer as a Function of Temperature and Relative Humidity

reference 2 are given in terms of vapor density, ρ_v^{sat} , in grams/M³, for saturated vapor (i.e., 100% relative humidity). Hence at any arbitrary relative humidity, Φ , the actual vapor density is simply:

$$\rho_v = \rho_v^{\text{sat}} \Phi \quad (2-3)$$

From the concept of precipitation, we know from conservation of matter that the mass of water, M, must be the same in the vapor and liquid phases, thus:

$$M = \rho_v V_v = \rho_L V_L \quad (2-4)$$

where V_v and V_L are the vapor and liquid volumes respectively, and ρ_L is the density of liquid water (1.00 gram/cm³). Starting with a volume of $V_v = 1 \text{ M}^3$ and letting $V_L = 1 \text{ M}^3 \times \Delta (\text{M}/\text{M})$ where Δ is the precipitable depth, we find:

$$\frac{\rho_v^{\text{sat}} \Phi \text{ grams}}{\text{M}^3} \times 1 \text{ M}^3 = \frac{1 \text{ gram}}{\text{cm}^3} \times 10^6 \text{ cm}^3 \times 1 \text{ M}^3 \times \Delta (\text{m}/\text{M})$$

$$\text{or } \Delta = 10^{-6} \rho_v^{\text{sat}} \Phi \text{ meters/meter}$$

$$\text{or } \Delta = 10^{-4} \rho_v^{\text{sat}} \Phi \text{ cm/meter}$$

$$\text{or } \Delta = 10^{-1} \rho_v^{\text{sat}} \Phi \text{ cm/kilometer} \quad (2-5)$$

Equation (2-5) in conjunction with the $\rho_v^{\text{sat}}(T)$ data from reference 2, forms the basis of Figure 2-4. Knowing T and Φ we can determine Δ . Since Δ is the precipitable cm of water per kilometer of path length, then the total precipitable cm of water, d, over a path of length L is simply:

$$d = \Delta L \quad (2-6)$$

Thus, knowing L we compute d from Equation (2-6). Finally the fraction of energy arriving at the detectors, relative to that which would have arrived in the absence of water vapor, F_{H_2O} is given by:

$$F_{H_2O} = e^{-K_v d} \quad (2-7)$$

Thus, by knowing T, Φ and L we can determine F_{H_2O} . As an example, the value of F_{H_2O} is calculated for the case of a test of the MILES system conducted at Big Dalton Wash on 26 September 1977. The analysis of this case is presented below.

$$T = 24^{\circ}C$$

$$\Phi = 65\%$$

$$L = 3.5 \text{ km}$$

Step 1: From Figure 2-2: for $T = 24^{\circ}C$

$$\text{find } \lambda = 9038 \text{ Å}$$

Step 2: From Figure 2-3: for $\lambda = 9038 \text{ Å}$

$$\text{find } K_v = .0399 \text{ cm}^{-1}$$

Step 3: From Figure 2-4: for $T = 24^{\circ}C, \Phi = 65\%$

$$\text{Find } \Delta = 1.5 \text{ cm/KM}$$

Step 4: From Equation 2-6 = ΔL , for $L = 3.5 \text{ km}$

$$\text{find } d = 1.5 \times 3.5 = 5.25 \text{ cm}$$

Step 5: From Equation 2-7 $H_2O = e^{-K_v d}$

$$\text{find } F_{H_2O} = e^{-0.0399 \times 5.25} = 0.811$$

Thus, for this case (i.e. $T = 24^{\circ} = 75.2^{\circ}\text{F}$, 65% relative humidity, and a path length of 3.5 km) we see that the decrease in irradiance due to water vapor absorption is only 19%.

Reference 2 points out that these values may be considered accurate to ± 5 percent. Thus, even at 100 percent relative humidity, at 90° F , and for a range of 3 km, it can be shown by these methods that the water vapor absorption can only decrease the irradiance by about 35 percent. It can be concluded that, for the MILES situation, water vapor absorption while not negligible is significantly less a problem than continuum atmospheric attenuation under adverse visibility conditions.

2.3 ATMOSPHERIC TURBULENCE

Now consider the critically important effects of atmospheric turbulence including scintillation. In propagating optical pulses through the atmosphere they are significantly perturbed by random fluctuations in the index of refraction caused by atmospheric turbulence. The effects of turbulence are:

- a. Wide variations in intensity from point-to-point within the beam (scintillation)
- b. Variations in the intensity at a given point in the beam with time (also scintillation)
- c. Movement of the beam centerline (beam wander)
- d. Variations in the overall diameter of the beam (beam breathing)
- e. Increase in the average spot diameter (beam spreading)

As a starting point, the previous work of Tatarski, Lawrence and Strohbehn, Fried, Hufnagel and Stanley, and Lutomirski (references 3 through 8 have been used.) Lutomirski (reference 8) shows that beam spreading due to diffraction is on the order of 18 microradians, which is negligible relative to the 1 to 2 milliradian divergence of the MILES beam. He also shows that beam spreading and beam wander due to turbulence are on the order of 0.2 milliradian under worst-case MILES conditions. Thus beam wander, beam breathing and beam spreading may be disregarded in the analysis of the effects of atmospheric turbulence on MILES performance. However, the effects of variations in intensity from point-to-point, and with time (scintillation) are far from negligible and are the subject of the major portion of this section.

Following the development of Lawrence and Strohbehn (reference 4), an examination is made of the theoretical expressions for the variations in intensity of the received wave resulting from the effects of atmospheric scintillation.

PLANE WAVE, HOMOGENEOUS MEDIUM

$$\sigma^2_{\ln I} = 1.23 C_n^2 k^{7/6} L^{11/6} \quad (2-8)$$

where:

- k = $2\pi/\lambda$ = wavenumber
- λ = wavelength
- C^2 = atmospheric refractive index structure parameter
- L = optical path length
- I = local irradiance
- $\sigma^2_{\ln I}$ = variance in the logarithm of the irradiance

SPHERICAL WAVE, HOMOGENEOUS MEDIUM

$$\sigma^2_{nl} = 0.50 c_n^2 k^{7/6} L^{11/6} \quad (2-9)$$

Thus, the dependence of the log variance upon C^2 , k , and L is identical in both the plane wave and spherical wave cases. The only difference lies in the multiplying factors 1.23 and 0.50, the log variance for spherical waves being about 40 percent of the plane wave values. However, for a divergent beam of 1 milliradian, reference 8 points out that the spherical wave theory is appropriate.

2.3.1 PREDICTIONS OF LOG VARIANCE

The problem of predicting values of the log variance in the received intensity over path lengths and atmospheric conditions appropriate to MILES is now considered. From Lawrence and Strohbehn (reference 4) and Hufnagel and Stanley (reference 7) we find the following:

- a. The highest values of C^2 occur nearest to the ground.
- b. The values of C^2 are lowest at dawn and dusk.
- c. The values of C^2 increase, relative to the dawn/dusk values at night, and increase further during the day time, reaching their peak near noon or in the early afternoon.

The following five cases are treated to allow the mathematical model to bracket the MILES cases.

- a. Dawn/dusk at a mean height above the ground, $\bar{H} = 10$ meters. For this case $C^2 = 3 \times 10^{-15} M^{-2/3}$. This probably corresponds to the least scintillation one could ever expect for MILES.
- b. Dawn/dusk $\bar{H} = 1$ meter, $C^2 = 1 \times 10^{-14} M^{-2/3}$. This would still represent a quite low level of atmospheric scintillation.
- c. Night, $\bar{H} = 1$ meter, $C^2 = 2 \times 10^{-13} M^{-2/3}$. A representative night-time value close to the ground.
- d. Daytime, $\bar{H} = 1$ meter, $C^2 = 4 \times 10^{-13} M^{-2/3}$. This is probably representative of an "average" sunny day.

e. Hot daytime. $H = 1$ meter, $C^2 = 10^{-12} M^{-2/3}$. This is typical of strong scintillation close to the ground on a hot, sunny day. It is probably representative of a worst case MILES situation.

Substitution can now be made for various values of C^2 corresponding to the cases discussed earlier, and various values of range, L , appropriate to MILES.

2.3.2 SATURATED SCINTILLATION

Lawrence and Strohbehn (reference 4) point out in considerable detail that "attempts at verifying experimentally (equations 2-8 and 2-9) have shown that for small values of σ there is good agreement between theory and experiment. However, when $V = \sigma_{\ln I}^2$ (the variance in the logarithm of the irradiance) is greater than about 2.5, as predicted by the preceding equations, the experimental values of $\sigma_{\ln I}^2$ appear to saturate and remain about constant."

Detailed mathematical evaluations of these equations are presented graphically in figure 2-5. The spherical calculations are used initially, and saturation is invoked whenever $\sigma_{\ln I}^2$ exceeds 2.5.

The most striking result of these curves is that except for the dawn/dusk cases all of the curves for daytime (and even nighttime) saturate before 1 kilometer.

Thus, beyond 1 km, for all practical MILES cases (day or night - except dawn/dusk), it may be assumed that scintillation is saturated.

Thus: $\sigma_{\ln I}^2 = 2.5 = \text{variance in } [\log_e(I)]$

$$\sqrt{\sigma_{\ln I}^2} = 1.58 = \text{standard deviation in } [\log_e I]$$

Hence, the standard deviation in the natural logarithm of the irradiance for all MILES cases beyond 1 km is 1.58. Detailed calculations by R. Lutomirski (reference 8) show that the maximum value for saturated scintillation is about $\sigma_{\ln I} = 1.6$ which is in excellent agreement with this result.

Lutomirski then integrates the general expression for cumulative probability and arrives at the following important results:

a. When $\sigma_{\ln I} = 1$ (almost saturated scintillation), the intensity 90 percent of the time will be equal to or greater than 17 percent of the unperturbed intensity for a single detector.

56196

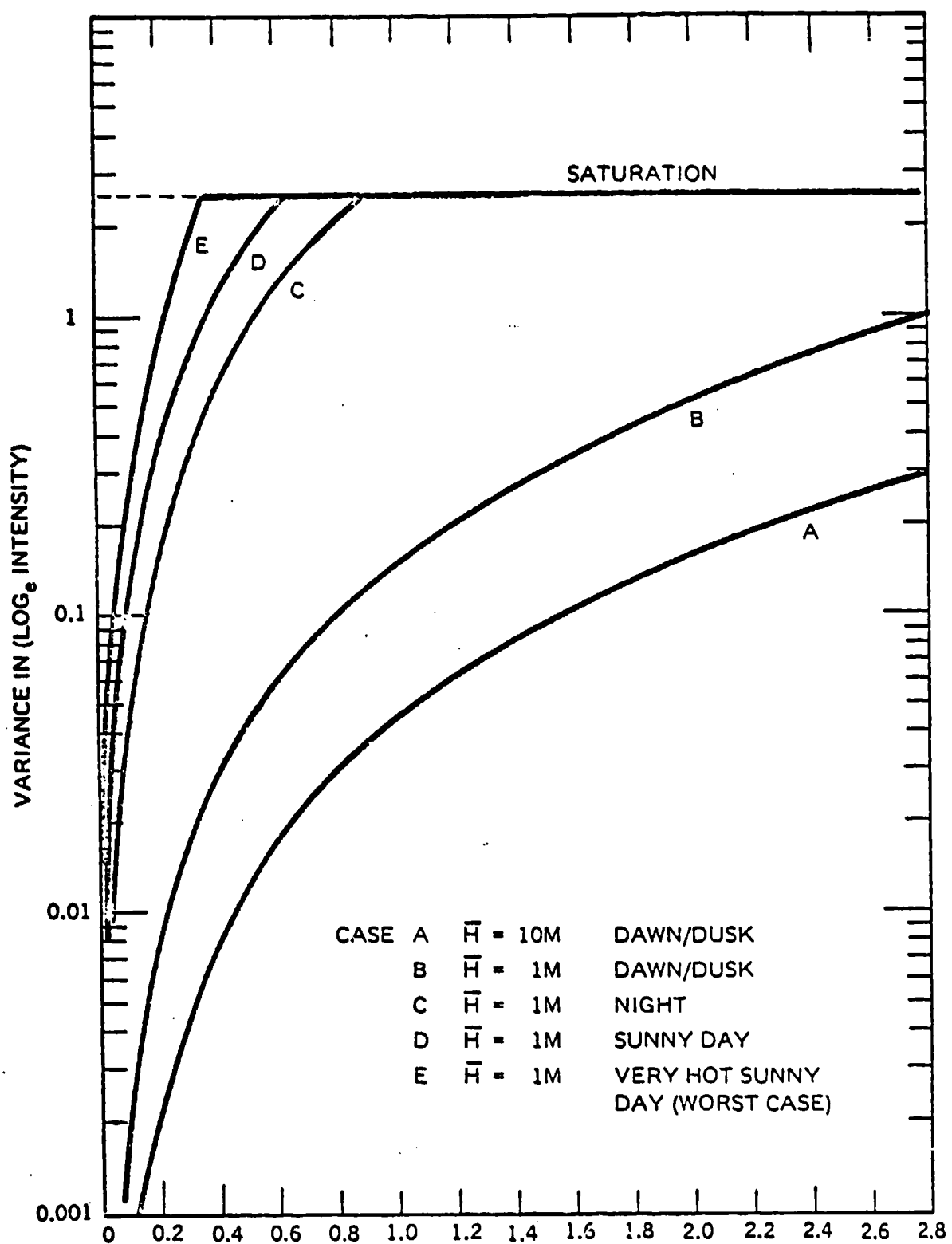


Figure 2-5. Variance in \log_e Intensity versus Range

b. When $\sigma_{\ln I} = 1.6$ (fully saturated scintillation), Lutomirski calculates that 90 percent of the time the intensity will exceed 4 percent of the unperturbed intensity for a single detector.

2.3.3 FRESNEL ZONE SIZE

As discussed by Lawrence and Strohbehn (reference 4) a key parameter in the analysis of atmospheric scintillation is the Fresnel zone size, ρ_F , defined by the relation

$$\rho_F = \sqrt{\lambda L} \quad (2-10)$$

For GaAs radiation, $\lambda = 0.904 \times 10^{-6}$ meter. Values of the Fresnel zone size, ρ_F , have been plotted for range values appropriate to MILES. (See figure 2-6.) Note that typical values of ρ_F are on the order of a few centimeters and at 3 km the value is about 5 cm. This is very important because the work of Fried (reference 5) shows that whenever any two points, separated by a distance ρ , are at least twice the characteristic length $4L/k$ apart, the signals received at these two points are essentially uncorrelated. Since:

$$\sqrt{4L/k} = \sqrt{16 \lambda L / 2\pi} = \sqrt{8/\pi} \rho_F = 1.596 \rho_F$$

then at a range of $L = 3$ kM we find:

$$\sqrt{4L/k} = 1.596 \times 5 = 8 \text{ cm}$$

Hence, if the MILES detectors are separated by more than about 8 cm they may be treated as independent. Since the detector separations will always exceed 8 cm, even on the TES system, and will generally be on the order of 50 to 80 cm on the VES system, the detectors can be treated as receiving independent signals.

2.3.4 FREQUENCY OF ATMOSPHERIC SCINTILLATION

Lawrence and Strohbehn (reference 4) state that "the predominant frequency is obtained by dividing the transverse wind velocity component by the Fresnel zone size."

$$F_F = V_{\perp}/\rho_F = V_{\perp}/(\lambda L)^{1/2} \quad (2-11)$$

Noting that 1 knot = 0.515 m/sec, the Fresnel scintillation frequency for $\lambda = 0.904 \mu\text{m}$ can be computed as a function of cross-wind velocity in m/sec or knots. This is shown in figure 2-7.

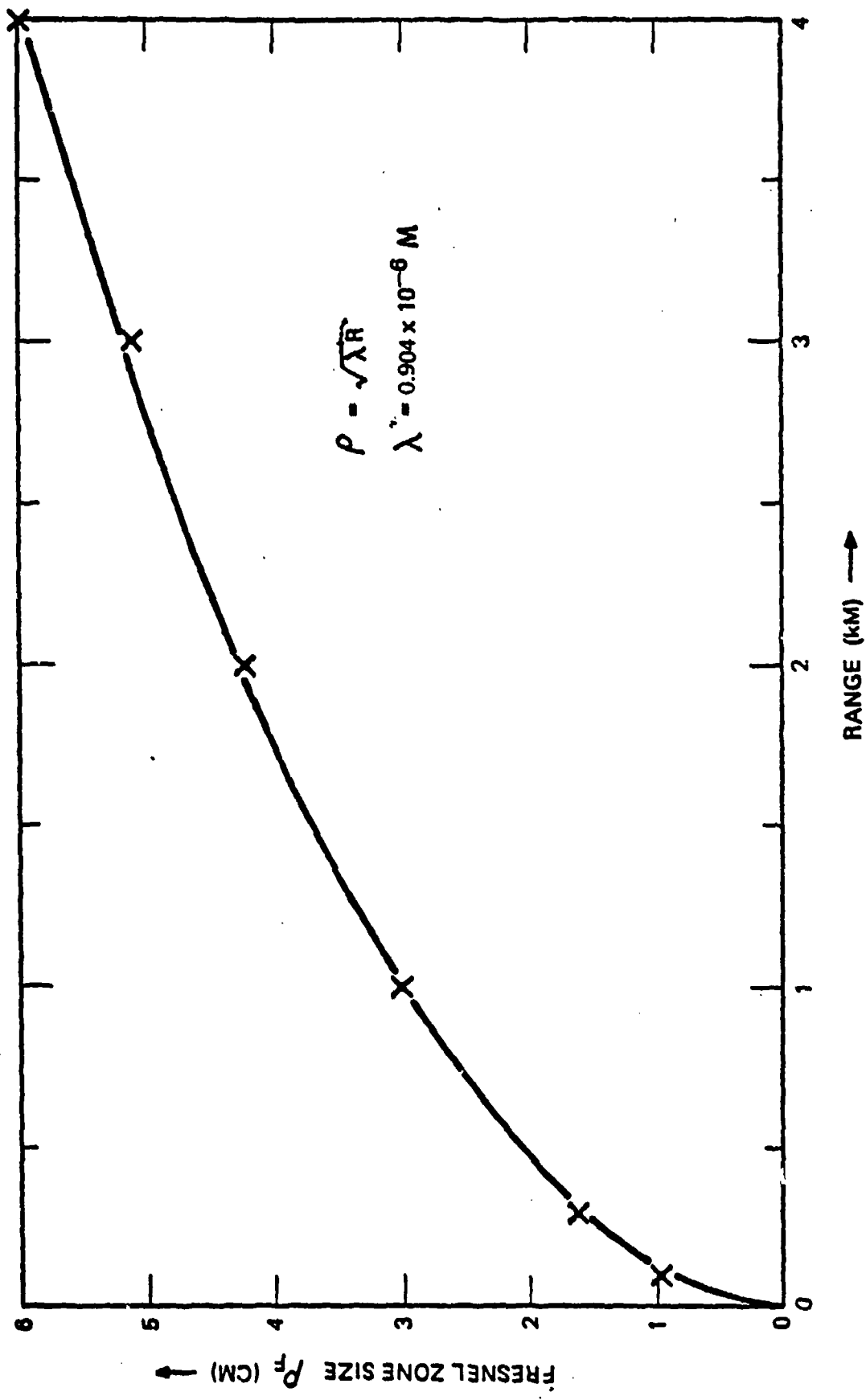


Figure 2-6. Fresnel Zone Size versus Range

56193

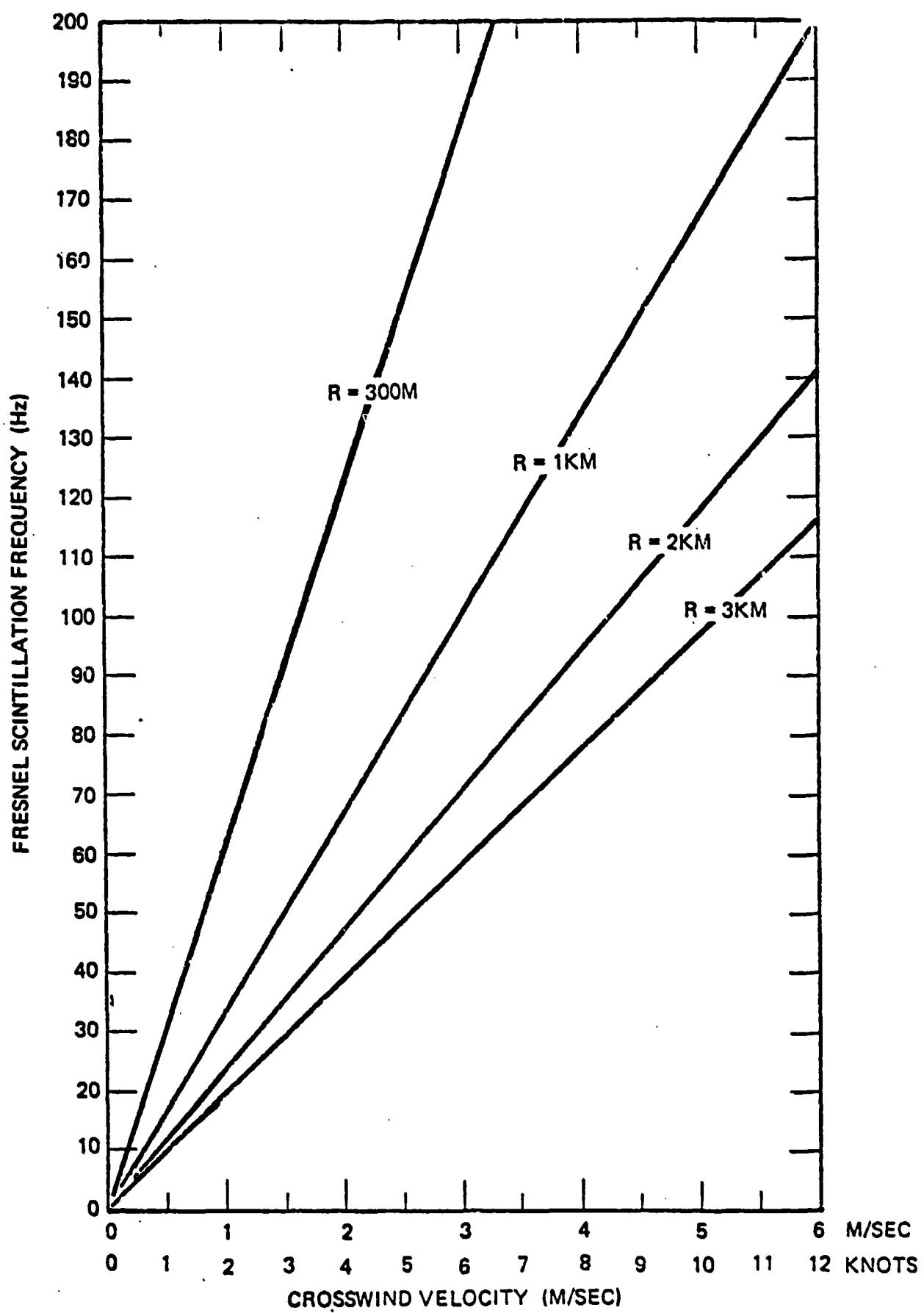


Figure 2-7. Fresnel Scintillation Frequency as a Function of Crosswind Velocity

Note:

1. The frequencies are higher for the short range TES requirements ($R \leq 300m$) than the long range VES ($R \leq 300m$).
2. Typical frequencies are on the order of about 50 Hz, with a range from 10 Hz to 200 Hz spanning most situations likely to be encountered by MILES.
3. Since the primary interpulse frequency for MILES is 3000 Hz, it would be anticipated, on theoretical grounds, that if a continuous stream of pulses were to be transmitted at 3000 Hz a group phenomena would be seen.

For example, if $F_F = 100$ Hz and the laser pulse rate frequency (PRF) is 3000 Hz, one would see "fades" of 30 or so pulses and then successful detection of a group of 30 or so pulses. This is important to MILES since it is the successful detection of words, not individual pulses, that is crucial to the communication channel. The dimensionless parameter may be defined as:

$$J = F_F \tau_p$$

Where:

$$F_F = \text{Fresnel frequency} = V_{\perp} / (\lambda L)^{1/2} \text{ (sec}^{-1}\text{)}$$

and:

$$\tau_p = \text{Interpulse period (sec)}$$

If $J \ll 1$ the pulses will exhibit a group scintillation phenomena while if $J \gg 1$ the pulses will be essentially independent. For MILES, typical values of J lie in the range 10^{-2} to 10^{-1} , hence a "group phenomena" can be anticipated.

It is worth noting that Lutomirski, reference 8, suggests that the characteristic scintillation frequency should be of the form $F = V_{\perp} / l$, where l is the so-called "correlation length." Since $l \ll \rho_F$ this would predict higher scintillation frequencies which could cause J to exceed unity. In this case independent rather than group fading would be observed. Since group fading is the more serious problem in the MILES communication channel, the Fresnel frequency analysis represents a worst case. Therefore, an assumption is made that group phenomena involving fades as long as 30 or so consecutive pulses may occur. Thus, the possibility exists for the occurrence of long and short duration fades. Multiple repetition of words are used to overcome long duration fades and the Boolean union decoding technique is used to overcome short duration fades. In this respect, the design is considered to be conservative because, for a very modest increase in electronics, both limitations have been overcome.

2.3.5 EFFECT OF MULTIPLE DETECTORS

The variance in received intensity due to atmospheric scintillation will be reduced as the number of independent samplings is increased. Figure 2 from Lawrence and Strohehn (reference 4) shows that the variance is a monotonically decreasing function of the parameter $(D/2)/(\lambda Z)^{1/4}$ where D is the effective diameter of N independent detectors. Provided the detectors are separated by a distance greater than the Fresnel zone size, $(\lambda Z)^{1/4}$, then $D^2 = Nd^2$ where d is the diameter of a single detector and n the number of detectors being irradiated. The value of the variance is normalized by the saturated value of 2.5.

For N independent detectors:

$$\sigma^2 \ln I = f(N^{1/4}d/2)/\lambda Z$$

This function is shown in figure 2-8

Let us now illustrate the effect of multiple detectors through a sample problem. Consider a machine gun system firing at a man target at a range $Z = 1.1 \times 10^3$ m with $\lambda = 0.904 \times 10^{-6}$ m. The Fresnel zone size is $(\lambda Z)^{1/4} = 3.16$ cm. Since the detectors are about 20 cm apart, they may be regarded as independent. Since the area of a MILES detector is 1 cm² its effective diameter is $\pi d^2/4 = 1$ cm² or $d = 1.13$ cm. Since $N = 4$, then $D = 4^{1/4}d = 2.26$ cm and $D/2 = 1.13$ cm. The abscissa of figure 2 is thus 1.13 cm/ 3.16 cm = 0.358. From figure 2 we obtain a value of $\sigma^2/2.5 = 0.48$ or $\sigma^2 = 1.2$, or $\sigma = 1.095$.

Thus we see that simply by increasing N from 1 to 4, σ is reduced from 1.58 to 1.095. In general, we find:

- a. Increasing the number of detectors within the beam, while maintaining them at separation distances large relative to the Fresnel zone size will improve the probability of detection.
- b. Theory predicts that the greatest marginal improvement occurs in going from one detector to two detectors.
- c. Beyond about $N = 4$ or $N = 5$, it is no longer cost effective to keep adding additional detectors in order to obtain small improvements in hit probability due to aperture averaging. This is a direct consequence of the asymptotic nature of the curve shown in Figure 2-9 for values of the abscissa greater than unity.

62453

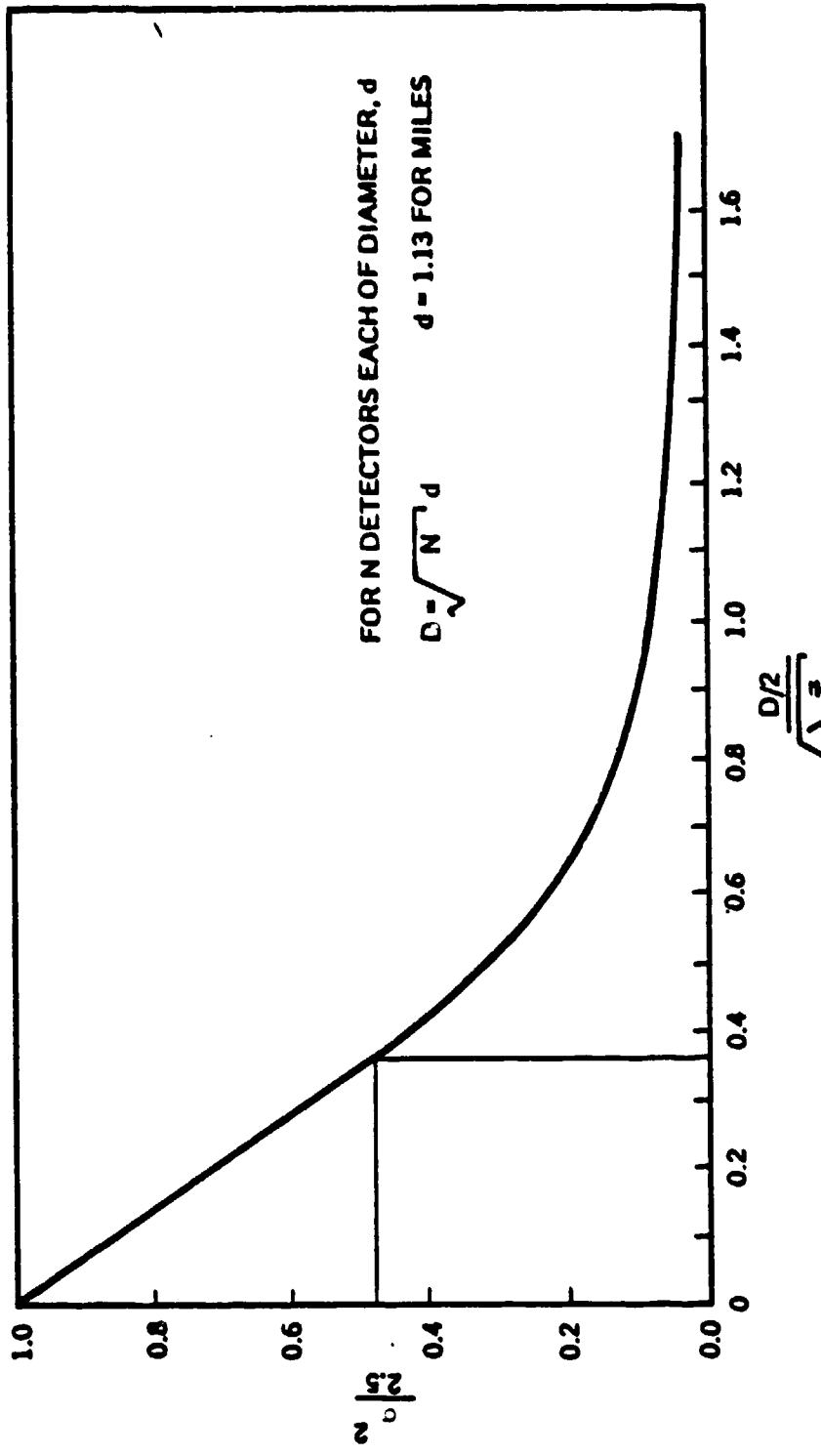
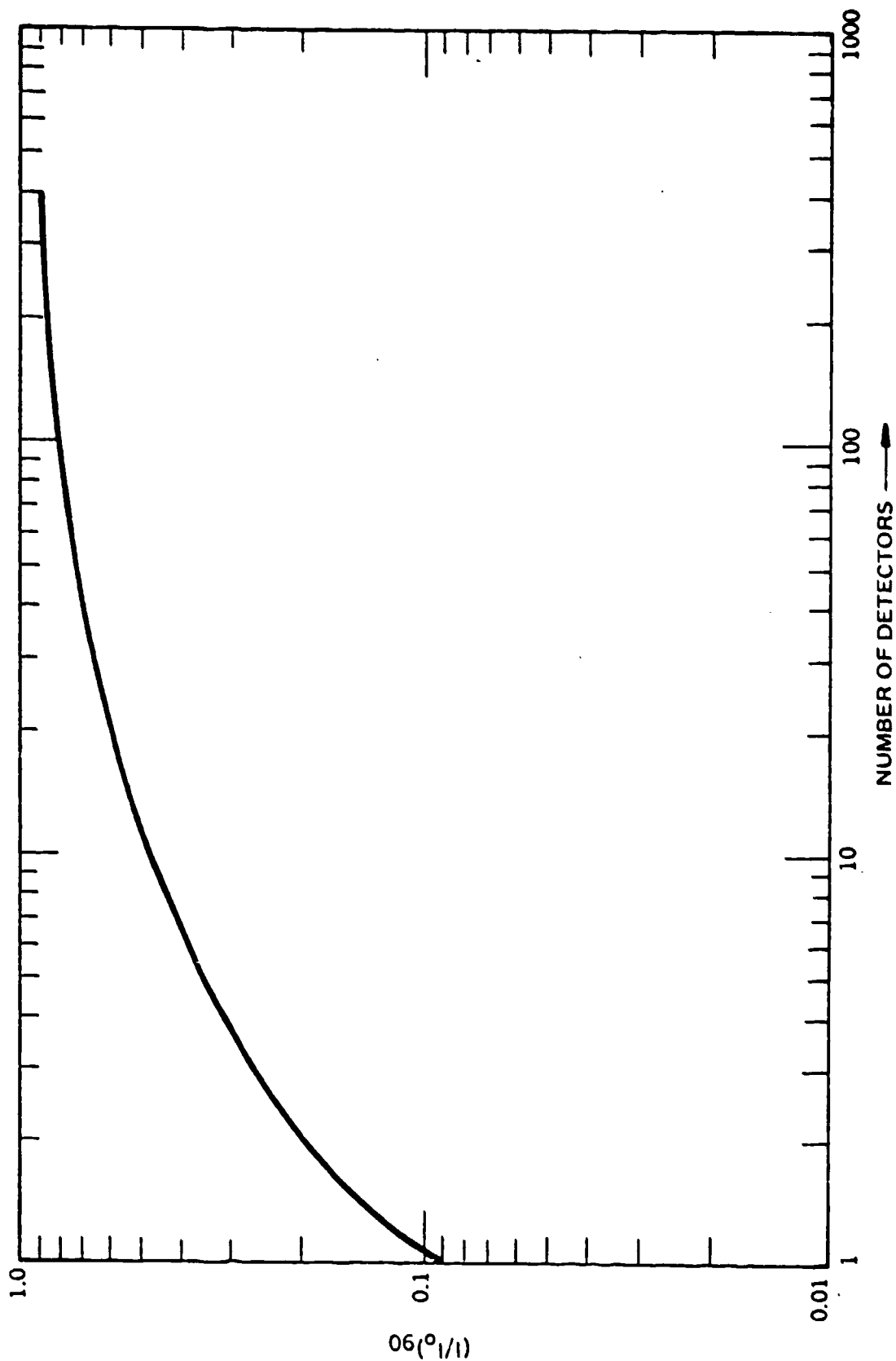


Figure 2-8. Effect on Fluctuation Index Due to Aperture Averaging

56194



2-21

Figure 2-9. Probability of Message Receipt versus Detector Quantity

2.3.6 SCINTILLATION EFFECTS ON PROBABILITY OF DETECTION

A computer program was written to determine detection probability of optical pulses in a scintillated atmosphere. (Ref. McMillan and Barnes). The data generated in the program was used to improve the hit probability vs range calculations.

2.3.6.1 COMPUTER ANALYSIS

The detection probability of optical pulses in a scintillated atmosphere is dependent upon the threshold to noise setting (T/N), the expected signal to noise (S/N), and the degree of scintillation σ_E ranging from $\sigma_E = 0$ (no turbulence) to $\sigma_E = 1.6$ (maximum observed scintillation). The results of McMillan and Barnes paper were incorporated into the MILES hit probability vs range analysis. The case T/N = 4, S/N = 7 and $\sigma_E = 0.7$ was used for these simulations. To improve fidelity of simulation, a computer program was written to generate appropriate detection probability curves for any value of σ_E . The inputs to the program are the threshold to noise setting of the receiver, the desired signal to noise and the value of σ_E .

The program was initially run for a number of cases given in the McMillan and Barnes paper. The results are in excellent agreement to those of McMillan and Barnes and thus there is a high confidence that the program is accurate.

The output data obtained can be used in the generation of hit probabilities vs range. This enables an accurate analysis of the MILES system, i.e., threshold/noise setting of 5.5 to 1 and the use of higher values of σ_E than given in the McMillan and Barnes paper.

A family of hit probability curves is shown for various values of σ_E (log Amplitude Fluctuation Index). This set of curves show that atmospheric scintillation has a significant effect on system performance. A discussion of aperture smoothing is included for man and vehicle standard target.

As discussed in Section 2.3.7, temperature effects alone could not account for the reduction in expected range experienced for the machine gun subsystem as tested at El Mirage. The M.G.'s energy output could not vary by more than 20% over the temperature ranges experienced. Comparison of the test results with the hit probability analysis dictated a reevaluation of aperture smoothing (averaging) effects on σ_E .

Previously, an aperture averaged value of $\sigma_E = .7$ was used for all MILES subsystem simulation. Results of El Mirage tests indicated that at ranges in excess of 600 m, scintillation effects are greater than the maximum given by McMillan and Barnes figures.

As a result of this, various cases were run on the computer for σ_E ranging from 0 to 1.6 (saturated scintillation for a point detector) with threshold/noise settings of 5.5:1 and signal to noise of 7:1.

Using this computer program a family of curves was run for the machine gun subsystem with the actual energy and beam spreads used in the El Mirage tests. Comparisons of actual data with computer simulation (see Figure 2-9) indicates that for the machine gun transmitter firing against a man target, the best fit is obtained when σ_E lies between $\sigma_E = 1$ and $\sigma_E = 1.2$. Aperture smoothing theory was then reviewed by P. Jacobs and R. Gammarino. The resulting figure from Lawrence and Strobehn has been replotted (expanded) and is included. A sample problem was done for the machine gun at a range of 1.1×10^3 m. Figure 2 gives a value of $\sigma_E^2/2.5$ of 0.48 for a value of $D/2(\lambda Z)^{1/2}$ of 0.36, corresponding to a value of σ_E of 1.095 at a range of 1100 m. This value is relatively constant from 900 to 1500 m ranging from $\sigma_E = 1$ to $\sigma_E = 1.16$. In long range systems the vehicle standard target is used. This target has 5 detectors. Calculations for σ_E for 2000 and 3000 m yields σ_E value of 1.18 and 1.28, respectively, for the vehicle standard target.

In all long range analysis, a value of $\sigma_E = 1.1$ will be used.

It is felt that this value of σ_E will give good fidelity when used in the generation of the hit probability vs range curves for moderately heavy scintillation. While it is important to analyze the worst case situation, it is not necessary to design for the assumption that the system will always be used under worst case scintillation. A value of $\sigma_E = 1.1$ will provide good correlation between computer simulation and actual field tests over a wide range of atmospheric conditions. When worst case scintillation is encountered a slower roll-off of hit probability vs range will be observed.

2.3.7 SCINTILLATION TESTING, RESULTS AND CONCLUSIONS

Testing was performed in Pasadena, California, and at El Mirage Dry Lake to verify the predicted analytical results. These tests were conducted over ranges from 25 to 4000 meters under widely varying conditions.

Test conditions, data, and analysis are included in XEOS reports. The test reports, identified by XEOS DFS documentation control numbers, were submitted to NTEC.

A summary of the El Mirage test results and conclusions drawn therefrom is provided in the following subsections.

2.3.7.1 Experimental Test Results

- a. The El Mirage scintillation test results (figures 2-10 and 2-11) are given in the form of "words" which were successfully detected, decoded, and counted. (A word consisted of six active bits in eleven allotted time slots). Ten words were transmitted per trigger pull with each bit at a frequency of 3.0 kHz. Hence, a single word required 3.667 msec and a 10 word sequence required 36.67 msec. The percentage of transmitted words which were successfully processed is labeled "word hit probability" on the graphs.

Data points identified by "X" were obtained by optimal aiming where the rifleman had feedback from the target to indicate where the laser beam was located.

Data points labeled " Δ " were obtained by simply aiming by means of the boresight telescope; that is, with no verbal feedback from the personnel at the target as to the optimality of the aiming.

Comparison of "X" and " Δ " data points on figures 2-10 and 2-11 can be interpreted to show the degradation of results when the man is inserted into the aiming and firing loop. Note that this still does not include the man having to hold the weapon steady since all data was taken with the laser on a tripod. Obviously, further degradation will occur when the soldier holds, aims, and fires the weapon. Therefore, the over-range hit probability will most likely be man-limited to reasonable range values.

- b. Figures 2-10 and 2-11 show that strong scintillation at El Mirage did not severely affect word detection probability at ranges up to one kilometer and that there was a quasi-saturation effect beyond one kilometer under hottest daytime conditions.

According to theory saturation should exist in all tests, except at dawn or dusk, for ranges beyond 0.5 kilometer. True saturation would manifest itself by word hit probability curves versus range (such as figure 2-11) being independent of environmental parameters. The fact that the daytime data lies in a narrow band despite considerable variations in wind velocity, wind direction, temperature, and time of day suggests that saturation, or at least quasi-saturation, does indeed occur.

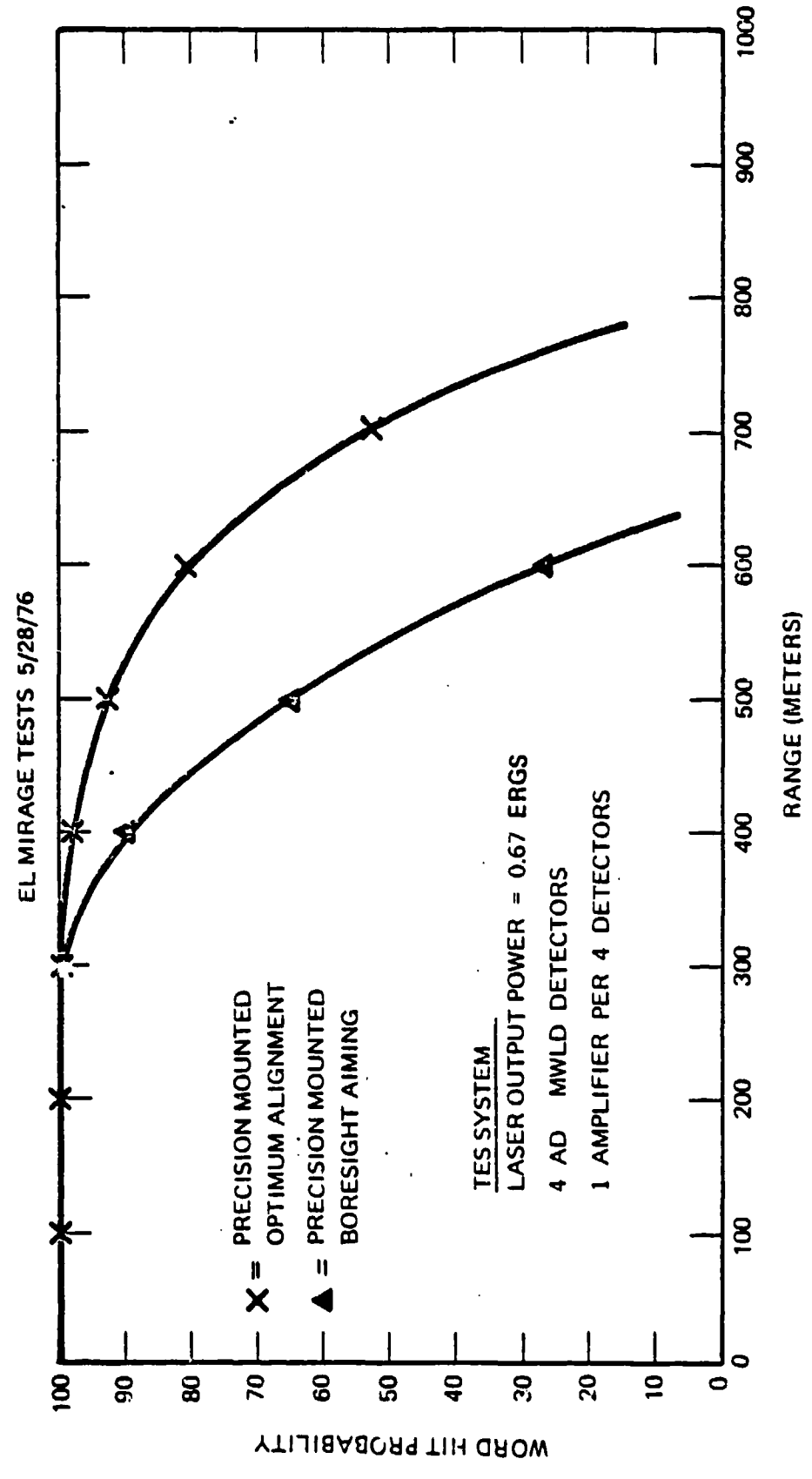


Figure 2-10. Probability versus Range, TES Laser

56197

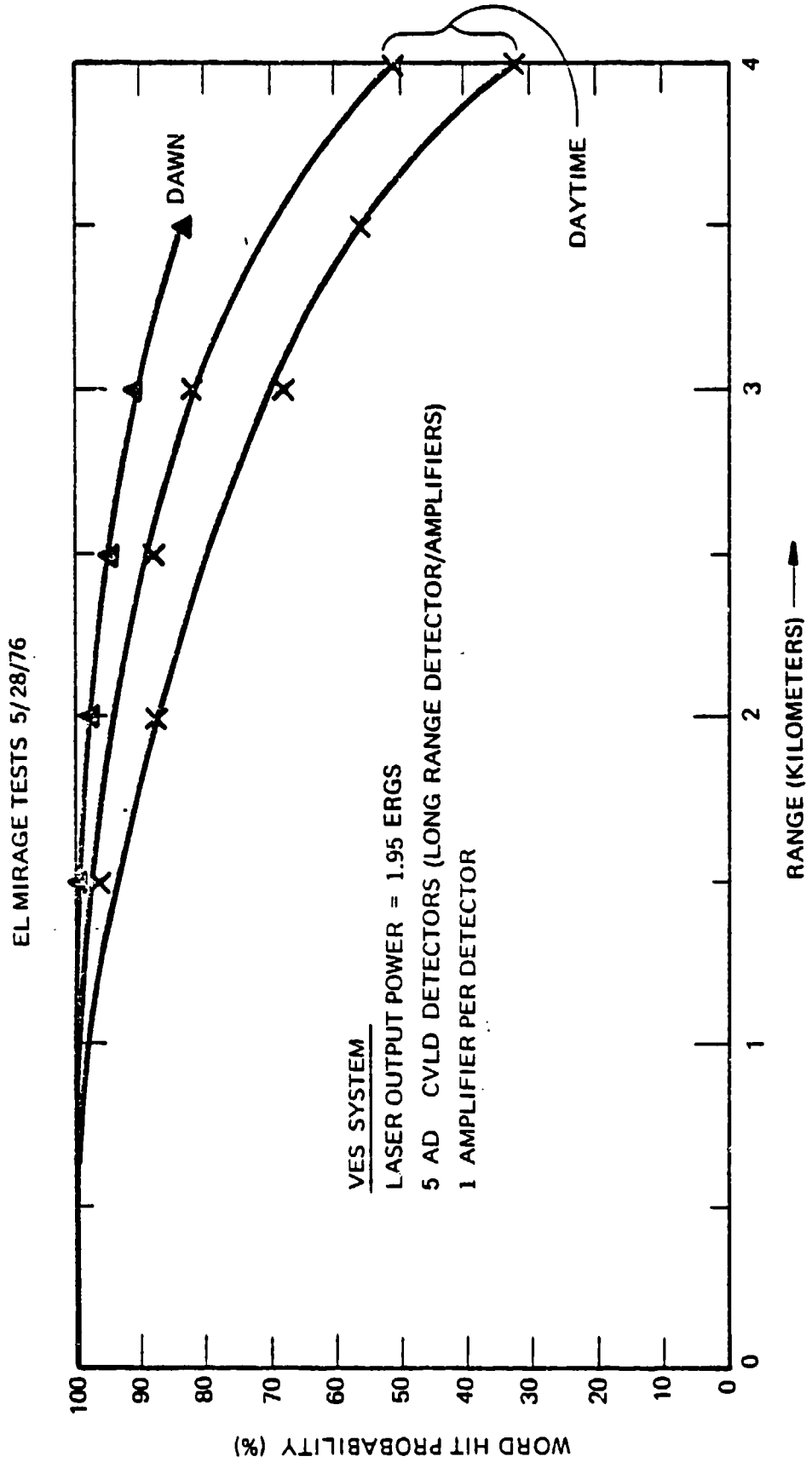


Figure 2-11. Probability versus Range, VES Laser

2.3.7.2 Conclusions

- a. Scintillation effects tend toward saturation beyond 0.5 kilometer and can therefore be handled in the analysis as a scintillation index having a range of $1.00 < \sigma_s < 1.60$ for a single detector in the VES portions of MILES. Assuming an array of four to nine detectors is illuminated and that the detectors are spaced greater than a Fresnel zone size apart, σ is inversely related to the number of detectors.**
- b. Hit probability at ranges beyond the specified device ranges (overkill) is reduced by atmospheric transmission factors including scintillation and will ultimately be man-limited due to holding, aiming, and firing degradations.**
- c. Scintillation effects are greatly reduced at dawn, relative to daytime or nighttime values.**

SECTION 3

RECEIVER ANALYSIS

3.1 SILICON PHOTODIODE CHARACTERISTICS

The optical detectors used on all MILES receivers employ silicon photodiodes (solar cell). Used in the photovoltaic mode (no externally applied bias), the p-n junction of the solar cell generates a current proportional to the incident optical radiation. The induced photocurrent divides between the diode internal junction resistance and the combination of its series resistance and external load. The flow of current produces a voltage with a polarity that will tend to forward bias the photodiode p-n junction. In the design of the system, special attention was taken to ensure that the receiver does not experience this saturation in the presence of full sunlight. See figure 3-1a for the diode equivalent circuit. Saturation effects are discussed in greater detail in subsection 3.2.1.

The spectral response of the photodiode is shown in figure 3-1b. It can be seen that the peak responsivity is near the peak emission of the GaAs injection lasers, giving an excellent design point.

3.2 BACKGROUND IRRADIANCE

A bare silicon photodiode of 1 cm^2 will produce 30 mA of dc current at a sun irradiance of 100 mW/cm^2 , corresponding to a standard clear day at the earth's surface over the entire wavelength regime. This high background irradiance can cause photodiode saturation and a high value of shot noise. To reduce these effects, an optical filter is employed. The choice of optical filter used in the receiver modules is a Schott RG 830, absorption glass. This filter has greater than 89 percent

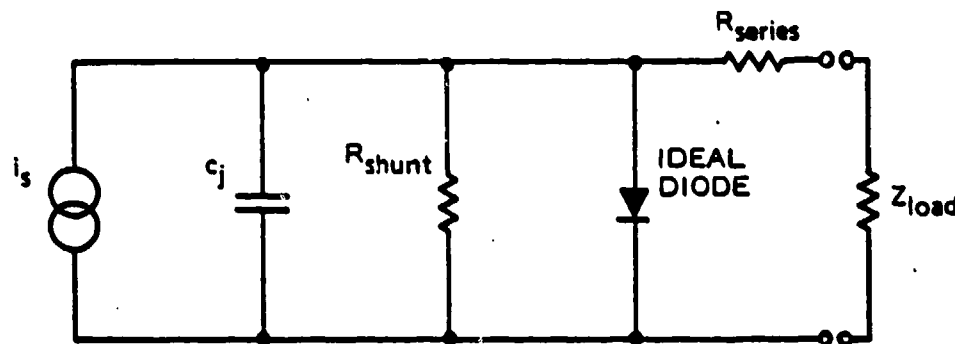


Figure 3-1a. Si Photodiode Equivalent Circuit

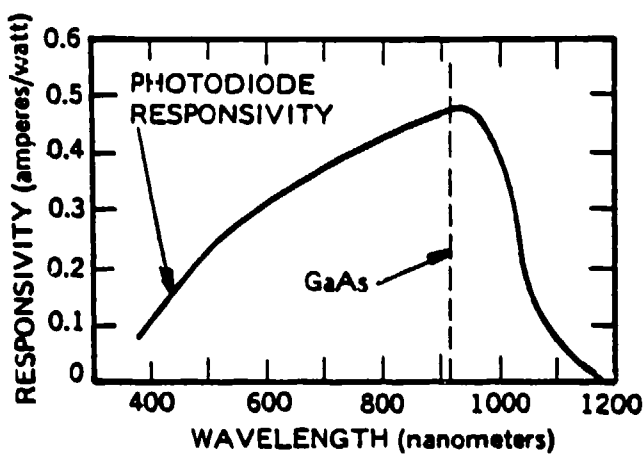


Figure 3-1b. Typical Responsivity versus Wavelength

Figure 3-1. Photodiode Equivalent Circuit and Spectral Response

transmission at the GaAs laser wavelength, and reduces the sun generated current to less than 9 mA. Narrow bandpass filters were considered. However, they are angle-dependent and cannot meet the off-angle detection requirements of MILES. A transmission plot of the RG 830 filter is shown in figure 3-2. The emission wavelength of the GaAs laser at + 25°C and -25°C is included to show that the transmission is satisfactory at the extreme low temperatures. At higher temperatures, the peak emission of the GaAs laser will shift to the right causing no potential problem. For additional analysis and tradeoffs on spectral filter selection, see Appendix C of Volume II.

In addition to the RG 830 filter, there are three sources of sun current and signal reduction. These are the EMI shield with a transmission of 80 percent, the package window with a transmission of 92 percent, and the protective cover, which incrementally achieves a sun current transmission of 80 percent, and a signal transmission of 88 percent. The RG 830 optical filter is bonded to the silicon photodiode in the detector module. This process reduces the Fresnel losses of one surface of the filter. The overall sun current produced from the photodiode module is thus:

$$\begin{aligned} I_{\text{sun}} &= 9 \text{ mA} \times {}^T \text{EMI} \times {}^T \text{window} \times {}^{\sigma} \text{surface} \times {}^T \text{cover} \\ &= 9 \text{ mA} \times 0.8 \times 0.92 \times 1.04 \times 0.8 \\ &= 5.5 \text{ mA} \end{aligned}$$

3.2.1 PHOTODIODE SATURATION

At the expected sun current value of 5.5 mA, the forward voltage developed across the photodiode series resistance may be shown to be 33 mV for a series resistance of 5 ohms and a transformer dc resistance of 1 ohm. This is clearly too small to sufficiently forward bias the photodiode to cause any shunting of signal current.

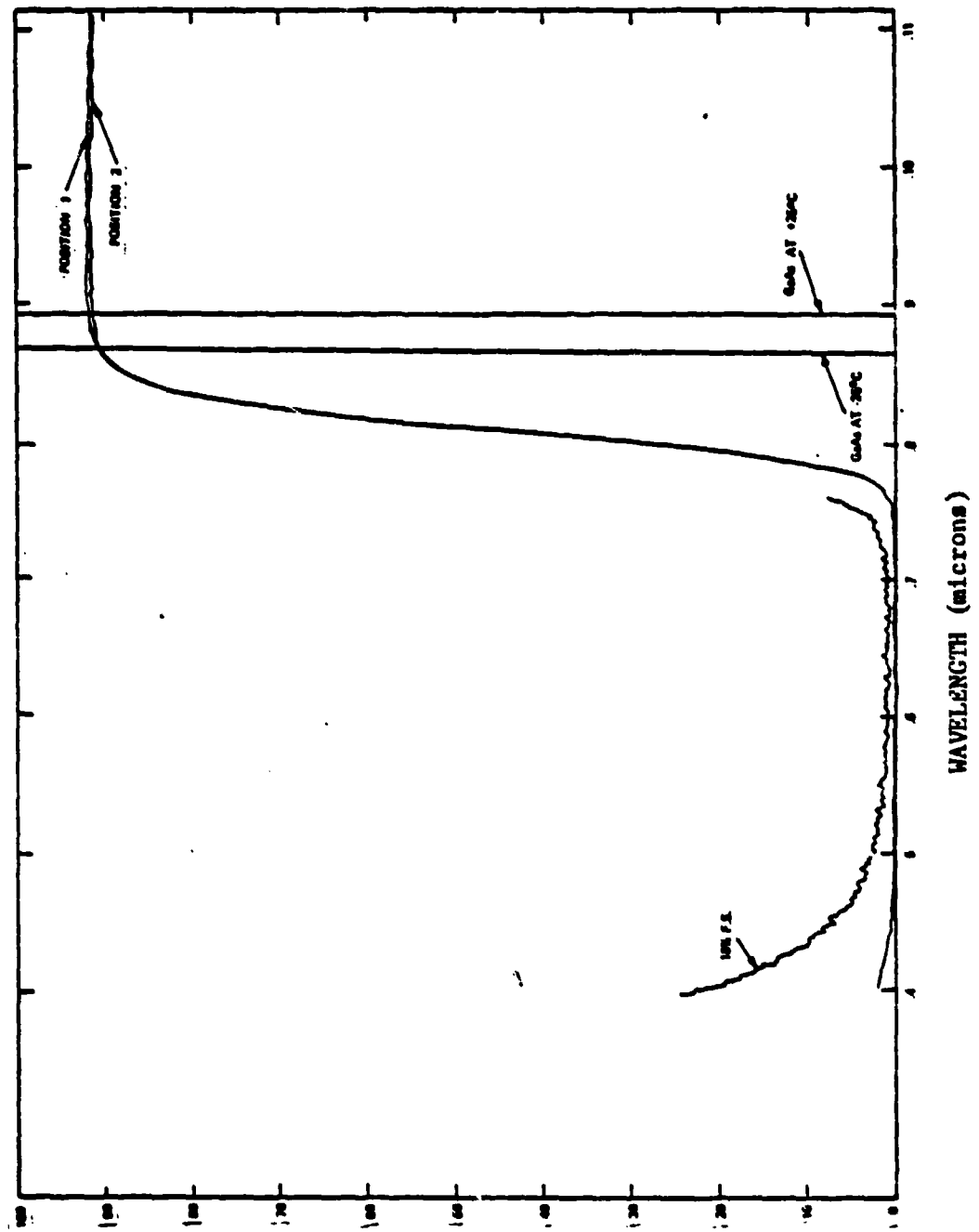


Figure 3-2. Spectral Response, RG 830 Filter

3.3 NOISE ANALYSIS

Four types of noise appear in the MILES receiver:

- a. Shot noise present in sun-induced dc current
- b. Johnson noise in the amplifier input resistor.
- c. Amplifier noise at the amplifier input
- d. Induced noise from EMI and microphonics

Induced noise is defeated by proper packaging, component design, and coding. Microphonics is defeated by frequency domain discrimination. This discussion treats shot noise, Johnson noise, and amplifier noise only.

Figure 3-3 shows the schematic and the model for the detector preamplifier. The following definitions apply:

V_a = amplifier noise = $4 \text{ nV}/\sqrt{\text{Hz}}$
 V_J = Johnson noise voltage in R_1 = $\sqrt{4 kT R_1} \text{ V}/\sqrt{\text{Hz}} = 2.36 \text{ nV}/\sqrt{\text{Hz}}$
 R_1 = 300Ω
 T = $65^\circ\text{C} = 338^\circ\text{K}$
 k = Boltzmann's constant = $1.38 \times 10^{-23} \text{ joules}/^\circ\text{K}$
 R_2 = $12 \text{ k}\Omega$
 C_2 = An artificial capacitance to simulate the roll-off of later stages at $1.2 \text{ MHz} = 11 \text{ pF}$
 C_1 = capacitance of a single photodiode = 4.5 nF
 N = transformer turns ratio = 2. (Actual turn ratio is 4:1 but the low permeability of the core material used to prevent microphonics gives an effective turn ratio of 2:1.)
 n = number of detectors connected to the amplifier
 q = number of detectors seeing the sun
 m = number of detectors seeing the laser beam
 I_s = shot noise from a single detector's worth of sun current = $\sqrt{2 eI} \text{ amp}/\sqrt{\text{Hz}}$
 e = electronic charge = $1.6 \times 10^{-19} \text{ coulombs}$

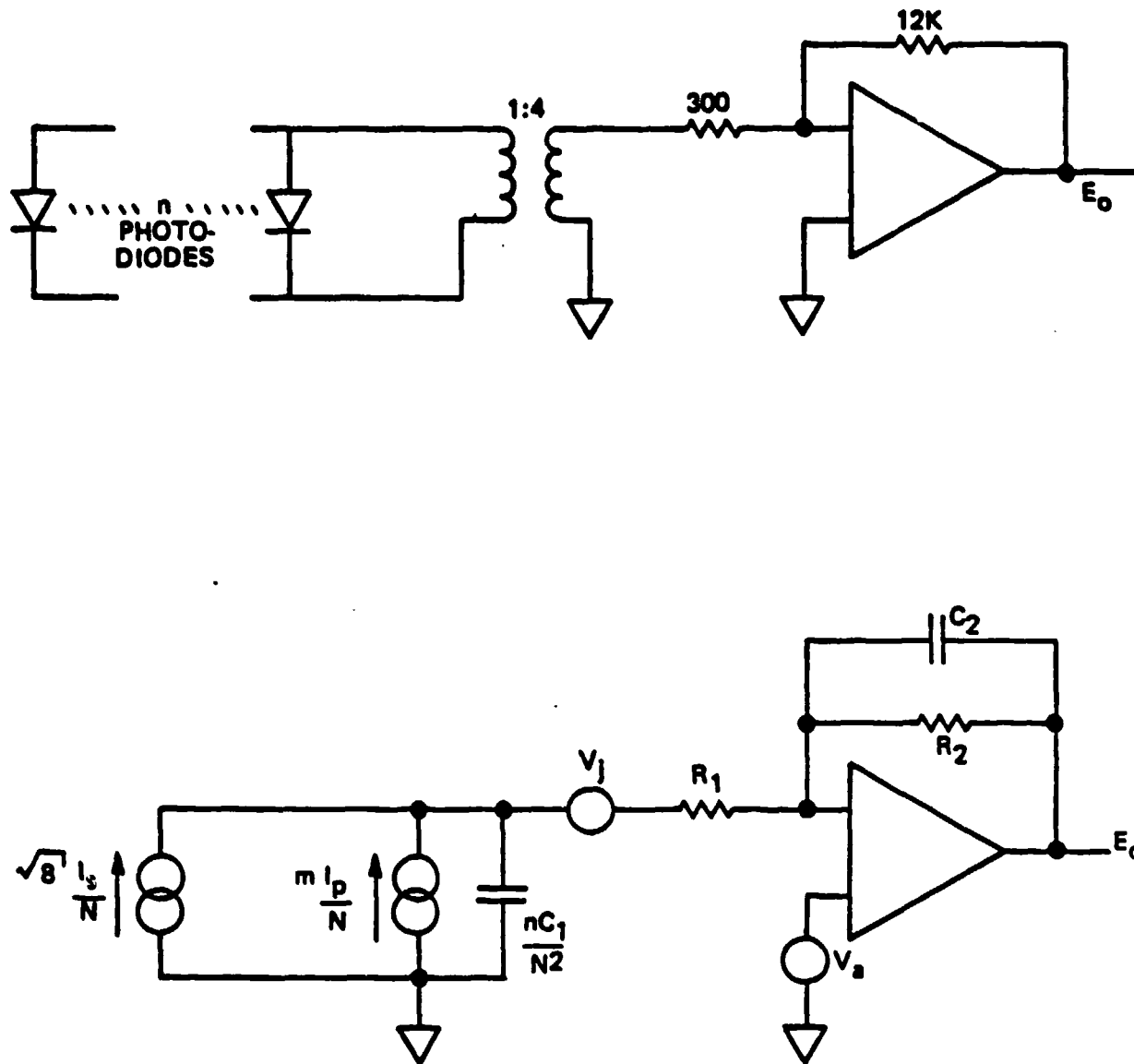


Figure 3-3. Schematic and Model for the MILES Detectors
and Preamplifier

62443

I = sun current = 7 milliamp

I_p = photo current from a single detector's worth of laser beam

The following assumptions and calculations apply to the analysis:

- a. High pass elements (transformer, coupling capacitors, etc.) are not significant since they cut off less than 20 percent of the system noise bandwidth.
- b. Low pass elements which ultimately cut off the high frequency response of the system at 1.2 MHz are modeled by an 11 pF capacitor (C_2) across the 12K preamplifier feedback resistor (R_2).
- c. It may be shown by evaluating the integral:

$$\int_0^{\infty} \frac{df}{1 + \left(\frac{f}{f_0}\right)^2} = f_0 \left(\frac{\pi}{2}\right) \text{ Hz}$$

that noise bandwidth is larger than the cutoff frequency of a low pass element by a factor of $\pi/2$.

- d. The time constant $\tau_1 = R_1 nC_1/N^2$ varies from 1.35 μs to 2.7 μs depending upon the number of detectors hooked to the amplifier. The time constant $\tau_2 = R_2 C_2 = 0.13 \mu\text{s}$. Therefore, $\tau_2 \ll \tau_1$.

3.3.1 SHOT NOISE

The shot noise spectral density at the photodiode is given by:

$$I_s = \sqrt{2 e I} \text{ amp}/\sqrt{\text{Hz}}$$

where:

I_s = shot noise of a single diode exposed to the sun

e = electronic charge = 1.6×10^{-19}

I = dc current from a single diode exposed to the sun = 7 mA

$$I_s = 4.73 \times 10^{-11} \text{ amp}/\sqrt{\text{Hz}}$$

The shot noise density at the amplifier output from q detectors illuminated by the sun is

$$R_2 \frac{\sqrt{q/2 eI}}{N} = \sqrt{q} \times 7.1 \times 10^{-9} \text{ volts}/\sqrt{\text{Hz}}$$

The shot noise bandwidth is controlled by the $nR_1 C_1/N^2$ low-pass filter characteristic and we may neglect further low-pass filtering, since $\tau_2 \ll \tau_1$. By assumption (c) in section 3.3 the noise bandwidth is:

$$BW_s = \left(\frac{\pi}{2}\right) \left(\frac{N^2}{2\pi R_1 nC_1}\right) = \begin{cases} 185 \text{ KHz (4 detectors)} \\ 98 \text{ KHz (8 detectors)} \end{cases}$$

Total shot noise at the amplifier output is:

$$\begin{aligned} E_o &= R_2 \frac{\sqrt{q/2 eI}}{N} \sqrt{\frac{N^2}{4 R_1 nC_1}} \\ &= \sqrt{\frac{q}{n}} \times 2.44 \times 10^{-4} \text{ V} \end{aligned}$$

Total shot noise then is proportional to the square root of the fraction, q/n , of detectors which see the sun.

3.3.2 AMPLIFIER AND JOHNSON NOISE

Examination of figure 3-3 yields a passband transfer function for both resistor Johnson noise, V_J , and amplifier noise, V_A . The low frequency cutoff is at

$$f_1 = \frac{N^2}{2\pi R_1 nC_1} = \begin{cases} 118 \text{ kHz (4 detectors)} \\ 60 \text{ kHz (8 detectors)} \end{cases}$$

The high frequency cutoff is at:

$$f_2 = \frac{1}{2\pi R_2} = 1.2 \text{ MHz}$$

The passband gain is

$$G = \begin{cases} \frac{R_2}{R_1} = 40 & \text{Johnson noise} \\ 1 + \frac{R_2}{R_1} = 41 & \text{Amplifier noise} \end{cases}$$

We may neglect the 10 percent effect of the low frequency cutoff and use a passband gain of 40 and a noise bandwidth of $\pi/2 \times 1.2 \text{ MHz} = 1.88 \text{ MHz}$.

The total amplifier and Johnson noise at the amplifier output is

$$\begin{aligned} E_N &= G \sqrt{(v_a^2 + v_J^2)(\pi/2) f_2} \\ &= 2.5 \times 10^{-4} \text{ V} \end{aligned}$$

Note that amplifier and Johnson noise are of the same order as shot noise in the sun background.

3.3.3 NOISE EQUIVALENT EXPOSURE

We shall now derive an expression for peak amplifier output voltage in terms of input signal exposure (ergs/cm^2). By solving for exposure required to give an output voltage just equal to the RMS noise, we obtain the noise equivalent exposure (NEE) for the MILES receiver.

The transfer function (in Laplace notation) from amplifier current input to amplifier output is:

$$\frac{E_p(s)}{I_p(s)} = \frac{R_2}{(1 + \tau_1 s)(1 + \tau_2 s)}$$

The signal is assumed to be a Dirac delta function, $\delta(t)$, of area Q_p , where Q_p is the total signal charge generated by the received pulse.

The assumption of such a narrow pulse is justified by the fact that both τ_1 and τ_2 are long compared with the pulselength of the signal received. τ_2 is the low-pass filter time constant in following stages.

The time response of a network to a delta impulse is the inverse transform of the network Laplace transfer function. For our transfer function, the response (from tables) is given by:

$$E_p(t) = \frac{R_2 Q_p}{(\tau_1 - \tau_2)} (e^{-t/\tau_1} - e^{-t/\tau_2})$$

To find the peak in this waveform, we need to set the derivative of $E_p(t)$ to 0, solve for t_p (the time when the peak occurs) and substitute this time into $E_p(t)$.

The derivative of $E_p(t)$ may be obtained by multiplying by s in the transform domain and inverting the transform. This gives (again from tables):

$$\dot{E}_p(t) = \frac{R_2 Q_p}{(\tau_2 - \tau_1)} \left(\frac{1}{\tau_1} e^{-t/\tau_1} - \frac{1}{\tau_2} e^{-t/\tau_2} \right)$$

Setting $E_p(t)$ to zero, and solving for t gives:

$$t_p = \tau_1 [\ln(K)] / \ln(K-1)$$

where $K = \tau_2/\tau_1$ and t_p is the time when the peak is reached.

Substituting t_p into $E_p(t)$ to obtain E_p gives:

$$E_p = \frac{R_2 Q_p}{\tau_1} K/(1-K) \quad (1)$$

For our system, τ_2 is about 0.133 μ sec. The input time constant depends upon n , the number of detectors, as follows:

$$\tau_1 = \frac{n C_1 R_1}{N^2} = \begin{cases} 1.35 \mu\text{sec} & (4 \text{ detectors}) \\ 2.7 \mu\text{sec} & (8 \text{ detectors}) \end{cases} \quad (2)$$

where:

C_1 = single detector capacitance = 4.5×10^{-9} f

R_1 = amplifier input resistance = 300 ohms

N = effective transformer turns ratio = 2

Thus K varies from $0.133/2.7 = 0.05$, to $0.133/1.35 = 0.1$. Peak signal voltage at the amplifier output therefore varies from $0.75 Q_p R_2/\tau_1$ to $0.82 Q_p R_2/\tau_1$. We shall use $E_p = 0.78 Q_p R_2/\tau_1$.

Now Q_p is the total photo-charge generated by the photodiode in response to an incoming optical pulse of collected energy E_p . Photo charge is related to exposure, E_x , as follows:

$$Q_p = E_x \times \eta_E \times \eta_W \times \sigma_S \times S \times A \times m \quad (3)$$

where:

E_x = incoming exposure in joules/cm²
 A = area of a single detector = 1 cm²
 η_E = transmission of EMI filter = 0.8
 η_W = transmission of window = 0.92
 σ_S = reduction in filter losses due to bonding it on the detector = 1.04
 S = photodiode sensitivity = 0.4 A/W
 m = number of detectors illuminated by the incoming signal.

So $Q_p = 0.306 m E_x$ and peak output voltage, E_p , is related to exposure by substitution of equations (2) and (3) into (1):

$$E_p = \frac{(0.78) R_2 N^2}{n R_1 C_1} \times 0.306 m E_x$$

Solving for E_x gives:

$$E_x = \left(\frac{n}{m}\right) 1.2 \times 10^{-10} E_p$$

Setting E_p equal to the RMS sum of shot, amplifier, and Johnson noise will give noise equivalent exposure in joules/cm²

$$\text{NEE} = \frac{n}{m} \frac{R_1 C_1}{(0.78)(R_2)(N^2)(0.306)} \sqrt{\frac{R_2^2}{N^2} \frac{2 q e I N^2}{4 R_1 n C_1}} \dots$$

$$\dots + \left(\frac{R_2}{R_1}\right)^2 \left(\frac{\pi}{2}\right) (1.2 \times 10^6) \left[(4 \times 10^{-9})^2 + (2.36 \times 10^{-9})^2 \right]$$

$$= 0.3 \mu\text{ergs}/\text{cm}^2 \times \left(\frac{n}{m}\right) \times \sqrt{1 + 1.06 \frac{q}{n}}$$

For a MWLD, $m/n = q/n = 0.5$ and

$$NEE_{MWLD} = 0.742 \mu\text{ergs/cm}^2$$

There are four square cm of detector exposed to laser illumination. If we multiply by four, we obtain the noise equivalent energy for the detection system. That energy is 3 μergs . If the threshold-to-noise ratio is set at 5.5, then the threshold equivalent energy (TEE) for the MWLD is:

$$\text{TEE} = 5.5 \times 4 \times NEE = 16.5 \mu\text{ergs}$$

This agrees closely with measurements on MILES MWLDs which had carefully been set at a TNR of 5.5. Those measurements ranged from 17 μergs to 24 μergs with four detectors in full sun.

SECTION 4

TRANSMITTER ANALYSIS

4.1 GaAs INJECTION LASER CHARACTERISTICS

The optical sources used in MILES transmitters are GaAs injection lasers. These lasers were chosen because they are lightweight, reliable, easily modulated, match the peak response of Si detectors and can operate in an eye safe mode. The emission regions of the injection lasers are sufficiently small, i.e., M16A1 laser junction is 0.003 by 0.0004 inch, to generate narrow (milliradian) beam spreads with inexpensive optics. These narrow beamspreads are required for good weapon simulation.

4.1.1 GaAs STRUCTURE

Transmitters which are mounted on hot gun barrels must employ multiheterostructure (MH) GaAs lasers because of their good high temperature characteristics. With these lasers usable power output can be obtained up to 85°C, which is the temperature an M16A1 rifle barrel can reach during automatic fire. Previously, the optical pulsedwidth of MH lasers was limited to 80 ns. Antireflection coatings used on MILES lasers permit operation of MH lasers at 150 ns with no damage. Far field laser beam spreads have been reduced since the initial devices were delivered and the MILES MH laser beam spreads approach that of single heterostructure (SH) lasers.

For long range systems, SH lasers can be used, but temperature compensation is more difficult, therefore, multiheterostructure lasers are used on all systems. These lasers have beam spreads which permit a collection efficiency of 50 percent when the MILES f/2.5 lens system is employed. This collection efficiency approaches that obtained previously only with SH lasers.

4.1.2 PEAK EMISSION WAVELENGTH

The peak emission wavelength (λ_p) at 25°C is specified at 900 ± 20 nm. This wavelength is temperature dependent and varies according to the following relationship.

$$\lambda_p = \lambda_{25^{\circ}\text{C}} \pm \beta \Delta T$$

where β varies from 2.5A/C° to 3A/C° , and ΔT is the temperature differential from 25°C . Thus, within the MILES temperature range (-25° to $+62^{\circ}\text{C}$), λ_p can vary from 8790\AA to 9260\AA .

4.1.3 POWER OUTPUT TEMPERATURE DEPENDENCE

GaAs laser output power varies greatly with temperature at fixed drive currents. This is due to threshold and differential slope efficiency variations with temperature. Threshold current increases with increasing temperatures and differential slope efficiency decreases with temperature. With fixed drive current, both of these factors tend to decrease the output power as temperature increases.

Plots of two RCA MH lasers fabricated with a 0.003 inch stripe contact are shown in figure 4-1. To get a feeling for the necessity of temperature compensation, let us look at laser 4464-1 in figure 4-1. If we were to operate this laser at 7 amps at -25°C the output power would be 2.7W. At 75°C the output power would be 0.2W. For training devices this power variation is not acceptable since system performance would vary greatly. Also, at low temperature, catastrophic damage to the laser may occur because the output power density of the laser diode can be exceeded when power output is set at room temperature.

The differential slope efficiency and threshold for diode 4464-1 at the temperature extremes are:

$$@ \quad T = -25^{\circ}\text{C}, \frac{\Delta P}{\Delta A} = 0.58 \text{ W/A}, I_{th} = 2.4\text{A}$$

$$@ \quad T = 75^{\circ}\text{C}, \frac{\Delta P}{\Delta A} = 0.35 \text{ W/A}, I_{th} = 6.3\text{A}$$

For laser 4464-2 they are:

$$\frac{\Delta P}{\Delta A}(-25^{\circ}\text{C}) = 0.53 \text{ W/A}, I_{th} = 2\text{A}$$

$$\frac{\Delta P}{\Delta A}(75^{\circ}\text{C}) = 0.3 \text{ W/A}, I_{th} = 6.9\text{A}$$

As we can see from these two typical MH lasers, threshold currents and differential slope efficiencies are slightly different. Requiring tight control on threshold current and differential slope efficiency is not feasible on devices which must be bought for less than \$15 each in high quantities to meet DTUPC goals. Data on laser production thus far has shown substantial variations in the above mentioned parameters. This requires extensive engineering analysis and design to permit operation of MILES lasers in systems which operate over wide temperature extremes.

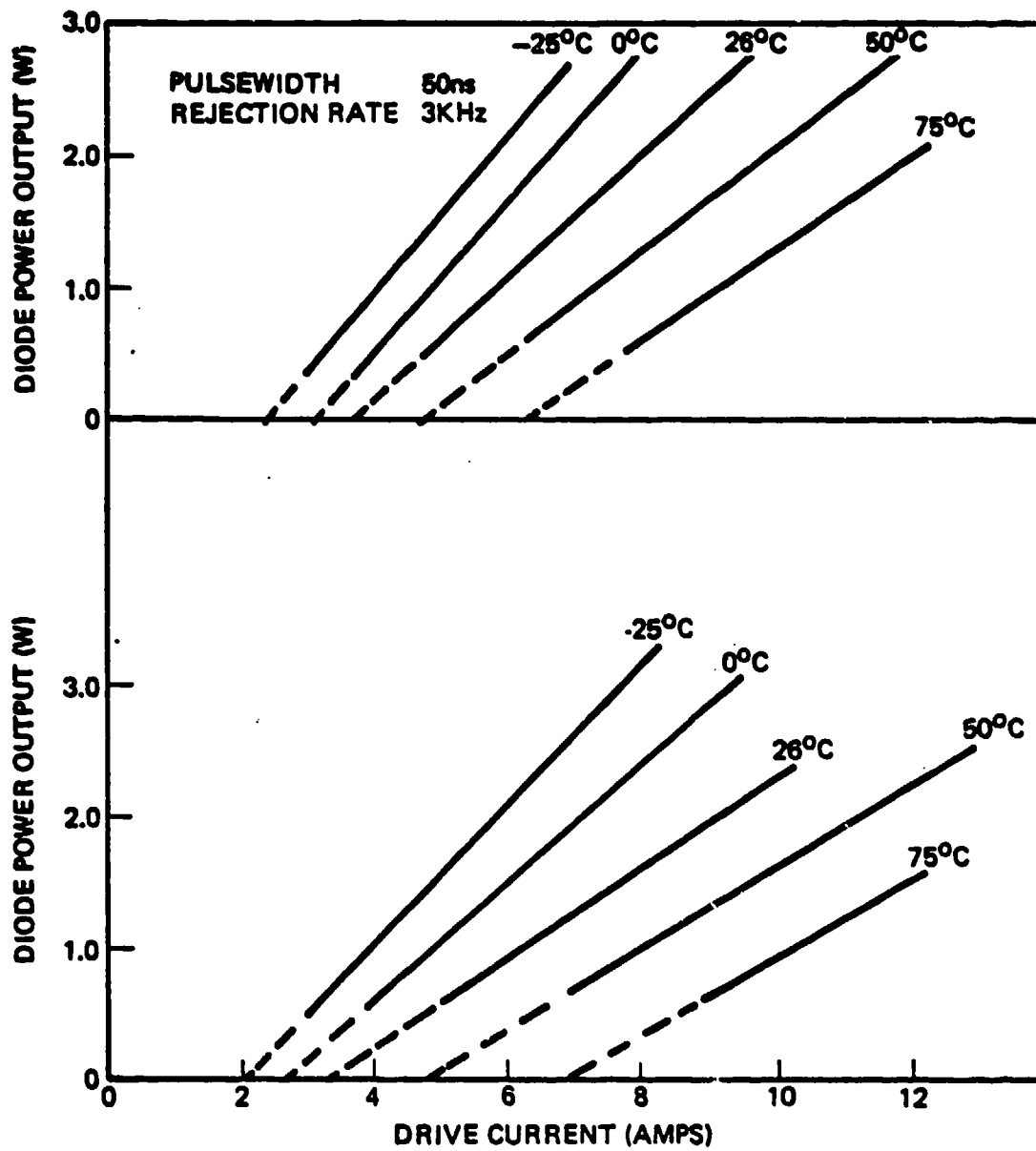


Figure 4-1. RCA Data for 0.003" Multiheterojunction Strip Geometry

62404

4.1.4 TEMPERATURE COMPENSATION REQUIREMENTS

The MILES design incorporates one temperature compensation network for MH lasers. This was decided upon because of cost limitations. Temperature compensation is simplified in MILES because the receivers are energy-dependent and not peak power-dependent. Energy varies faster than peak power because the current pulse is sinusoidal and the threshold current varies with temperature. Figures 4-2 and 4-3 show how peak power and energy output vary under worst case variations of threshold current and slope efficiency.

Comparing Cases I and II we see that for the same current shape pulse the power output ratio is $9/4 = 2.25$; whereas the energy output variation is $49.5/12 = 4.125$. Thus, since MILES receivers are energy dependent it is critical that energy output variations and not peak power output be controlled.

4.2 TRANSMITTER PARAMETERS

The MILES laser transmitters can be characterized for analysis by a few parameters. These are listed below.

- Weapon code
- Energy output
- Beam spread perpendicular to and parallel to laser junction
- Gaussian wings beam spread
- Saturated scintillation factor (anticipated over operating range) for the system
- Fraction of energy in primary beam

To minimize overall transmitter costs, all MILES transmitters employ the same lens. The size of the laser used, i.e., 0.003 or 0.006 inch, focusing and the energy output settings are the only controllable variables. The transmitter parameters used in the computer analysis are shown in table 4-1. Lines 1 to 9 contain transmitter information used in this analysis. Transmitter tubes are set up on an optical alignment bench to permit monitoring of the far field irradiance patterns. The laser position and the output energy are varied for each transmitter such that the far field pattern falls within the minimum/maximum curves required for each transmitter. This insures that each transmitter has the proper peak far field (50 m) irradiance and beam shape. This procedure insures that all transmitters of a specific

62456

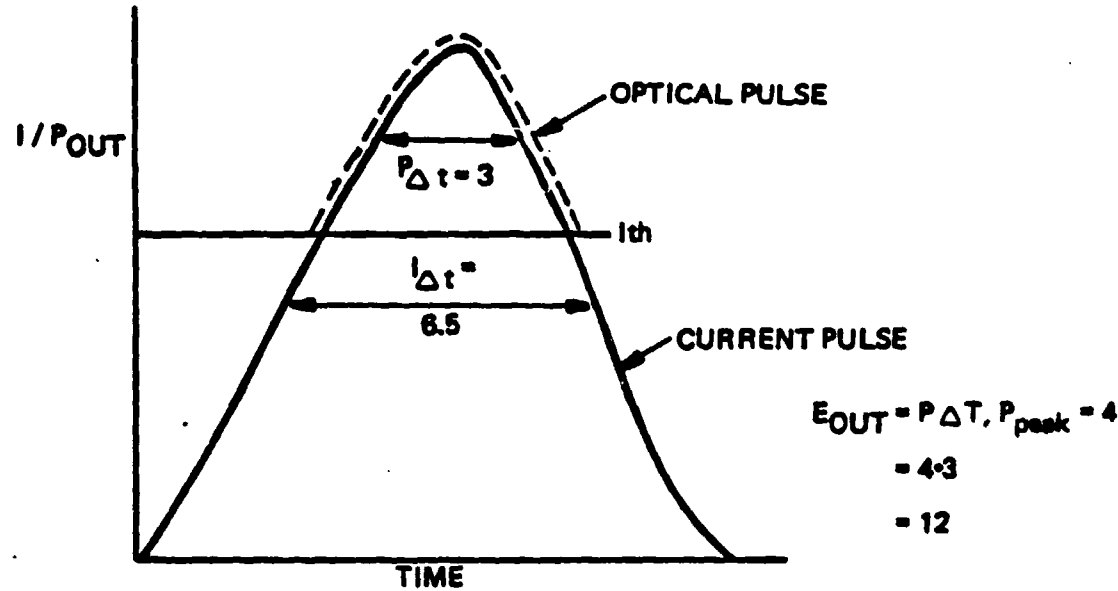


Figure 4-2. Case I - Peak Current Just Above Threshold

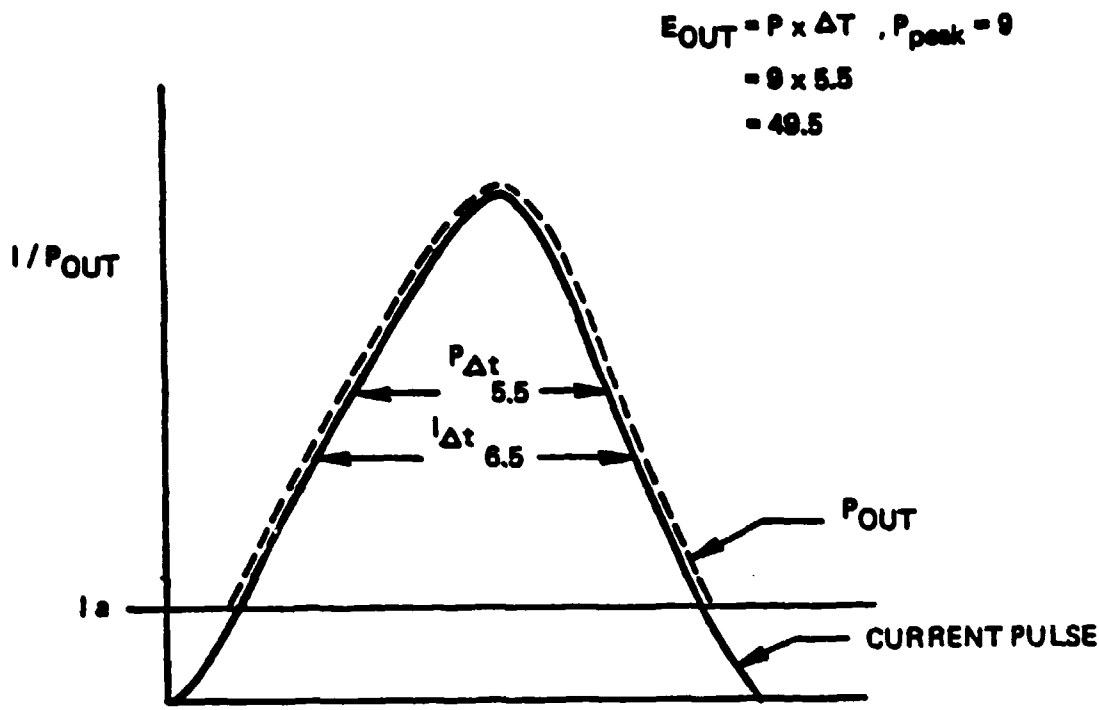


Figure 4-3. Case II - Peak Current Much Greater Than the Laser Threshold Current

62440

TABLE 4-1
TRANSMITTER PARAMETERS

WEAPON, E_0 , B_1 , B_2 , B_3	K FACTOR, RANGE, F
1.000 DRAGON .8 .0025 .0041 .007	1.44 100E2 .44
2.000 152MM(KILL) 1.17 .0036 .0013 .007 1.57 100E2 .44	
3.000 105MM(KILL) 1.94 .0036 .0013 .015 1.57 100E2 .44	
4.000 VIPER(KILL) .3 .005 .005 .007 1 25E2 .44	
5.000 MACHINE-GUNS(KILL) .32 .0012 .0016 .007 1.32 50E2 .44	
6.000 SHILLELAGH 1.8 .0032 .0012 .007 1.44 100E2 .44	
7.000 TOW 1.8 .0032 .0012 .007 1.44 100E2 .44	
8.000 M16(KILL) .2 5E-4 1.5E-3 .007 1.32 25E2 .44	
9.000 COAX(KILL-152MM) .36 .006 .006 .007 1.32 50E2 .44	
20.000 M60A1(SIDE) 7 -151 40 .4 -162 0 .2 -115 0 .8 -64 0 .9	
21.000 -10 0 1 48 0 1 107 0 1	
22.000 24E-6 400 200	
23.000 M60A1(FRONT) 5 44 40 .9 44 0 .94 90 0 .5 114 0 .3	
24.000 126 0 .05	
25.000 24E-6 400 200	
26.000 M60A1(REAR) 4 -79 0 .93 -80 0 .98 38 0 .98 98 0 .94	
27.000 24E-6 400 200	
28.000 M113(SIDE) 6 -148 0 1 -88 0 1 -30 0 1 30 0 1 88 0 1 148 0 1	
29.000 24E-6 400 200	
30.000 M113(FRONT) 4 -57 0 .7 -18 0 .7 18 0 .7 57 0 .7	
31.000 24E-6 400 200	-
32.000 M113(REAR) 4 -63 0 .98 -30 0 .98 0 0 .98 47 0 .98	
33.000 24E-6 400 200	
34.000 M551(SIDE) 7 -82 30 .5 -82 0 .17 -92 0 .68	
35.000 -36 0 1 27 0 .98 60 0 .86 100 0 0	
36.000 24E-6 400 200	
37.000 M551(FRONT) 3 50 30 1 70 0 1 113 0 .5	
38.000 24E-6 400 200	
39.000 M551(REAR) 1 -80 0 .7	
39.100 24E-6 400 200	
40.000 MAN(FRONT) 4 10 10 1 10 -10 1 -10 -10 1 -10 10 1	
41.000 24E-6 150 150	
--EOF HIT AFTER 41.	

E_0 = Energy Output

B_1 = Primary Gaussian Beam

B_2 = Primary Gaussian Beam

B_3 = Secondary Gaussian Beam

K Factor = Scintillation Effects on Detector Sensitivity

F = Ratio of Energy in the Primary Gaussians/Total Energy

type will have the same field performance. See figure 4-4 for the M16A1 minimum/maximum curves (perpendicular to laser junction).

4.2.1 TRANSMITTER OPTICS

A plano convex lens is used as the collimator for the laser emission in all transmitters. This lens has sufficient spherical aberration to produce a beam profile which gives a nearly constant kill zone independent of range. An asphere lens was designed and one sample fabricated. The improvement in performance was determined not to be sufficient to offset the cost of an asphere lens. Plastic aspheres are relatively inexpensive, however, index of refraction change over temperature would have to be compensated for if a plastic lens were used. Replicated aspheres, epoxy on glass substrates, would meet the temperature requirements. However, costs again were too high.

The plano convex lens used has a 50 mm focal length and 23 mm diameter. The material used is K5 Glass 522595 with an index of refraction at 903 nm of 1.514. The radius of the curved surface is 25.7 mm (convex), thickness is 6 mm. Beam divergence is achieved in the laser/optics assembly by defocusing the lens inside the paraxial focus.

4.3 BEAM GEOMETRY

A detailed theoretical analysis of the "Beam Geometry Equation" is included in Appendix B of this report. This work is an extension of the original work by P. Jacobs (Ref. 9). The analysis describes the nature of a Gaussian laser beam propagating through the atmosphere and being detected by fixed threshold receivers. The key results of this analysis may be summarized as follows:

- a. The maximum beam diameter is proportional to the square root of the laser output power divided by the detector threshold irradiance. Thus, increasing the laser output power or decreasing the detector threshold irradiance will increase the beam diameter.

$$D = K\sqrt{P/T}$$

- b. The maximum beam diameter is independent of the laser optics provided the beam distribution is Gaussian. The MILES laser beam distribution is essentially Gaussian, hence the maximum beam diameter does not depend upon the optical aperture, focal length, or beam divergence for the same transmitter power output.

62450

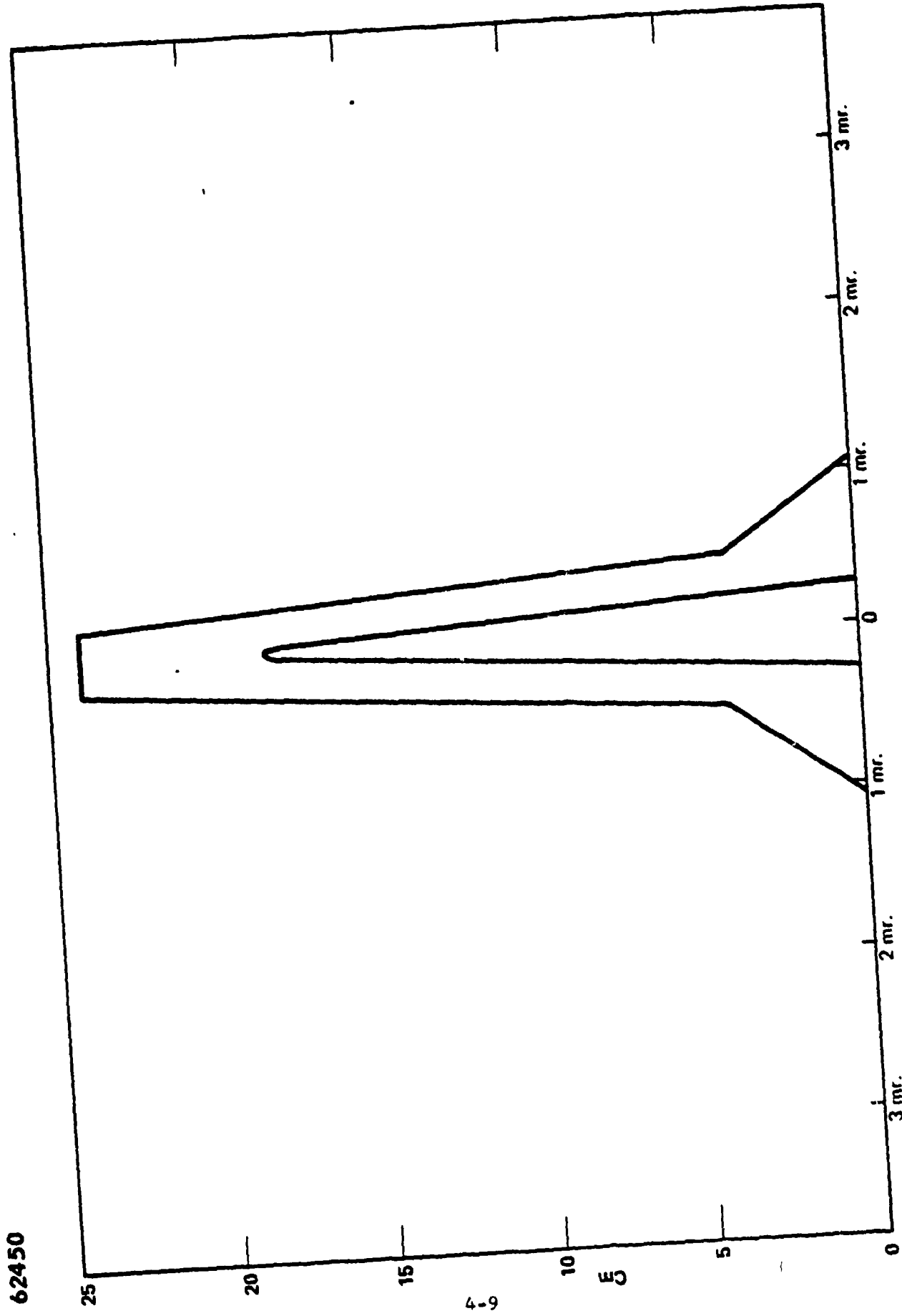


Figure 4-4. M16A1 Min/Max Energy Curves

c. The maximum beam diameter will decrease as the atmospheric attenuation coefficient increases.

Detailed calculations are presented in Appendix B for a range of conditions appropriate to MILES.

d. The maximum effective range also depends upon the square root of the laser output power divided by the detector threshold irradiance. However, in addition, the maximum range is inversely proportional to the beam divergence. Expressions for maximum range are derived in Appendix B.

$$R = \frac{K}{\beta} \sqrt{\frac{P}{T}}$$

e. The maximum effective range, and the range at which the beam achieves its maximum diameter, both decrease with increased atmospheric extinction coefficient. Detailed functional expressions are presented for both cases in Appendix B.

The results of this first order theory are theoretical relationships between maximum beam diameter, range to maximum beam diameter, and maximum range as a function of laser transmitter power, detector threshold, beam divergence, and atmospheric attenuation coefficient. An extended theory which is now programmed for the computer also treats the effects of:

- Atmospheric scintillation
- Multiple pulses (words, messages)
- Multiple detectors
- Electronics signal processing methods

The effects of atmospheric scintillation, multiple pulses, multiple detectors and electronics signal processing have been studied in considerable detail. For example, it is known that atmospheric scintillation will result in the loss of active bits in a code and, hence, multiple word repetition has been utilized to overcome this effect. It is also known that multiple detectors reduce the effects of scintillation and that electronics signal processing effects, such as a Boolean Union decoding scheme, improve signal detection probability in the event of high frequency scintillation. The Unified Detection Probability Analysis includes all these effects simultaneously (see Appendix D). Thus, a complete analysis of detection probability and the influence of transmitter related variables are given in Appendix F.

SECTION 5

CODING, DECODING, AND THRESHOLD SETTING ANALYSIS

5.1 CODE FUNCTIONS

MILES is a communication channel in which the ability to successfully transmit a message to an adversary simulates the ability to kill, hit or near-miss him.

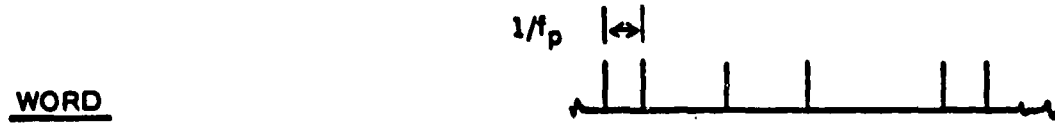
The ability to successfully complete the transmission of the message is significantly affected by the code set structure, message format, decoding method, and threshold setting of the detector. Conversely, the ability to avoid false message reception is affected by the same factors. This section then addresses these aspects of the MILES system design.

The functions of the MILES code are as follows:

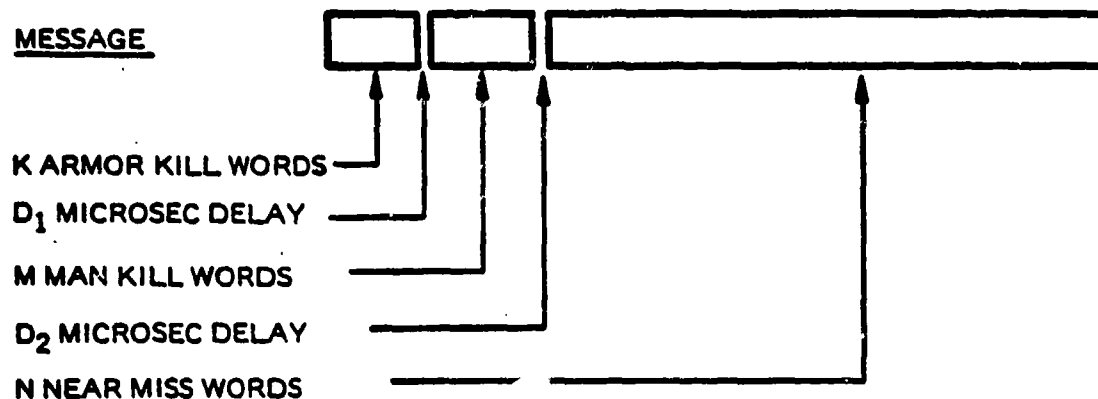
1. Discriminate between weapon types with high reliability;
2. Extend weapon simulator range in the presence of adverse atmospheric conditions;
3. Reject random false signals;
4. Simulate missile tracking requirements;
5. Shape the kill zone profile vs range to more accurately simulate weapon effectiveness.

5.2 CODE FORMAT

Figure 5-1 shows the code format. Each "word" is made up of eleven code slots containing six pulses and five empty slots. The word length is



6 BITS IN 11 TIME SLOTS
 $f_p = 3,000 \text{ KHz} \pm 0.015\%$
 PULSE WIDTH = 100 TO 200 nsec.



LIKE WORDS FOLLOW EACH OTHER WITHOUT DELAY

MISSILE SEQUENCE

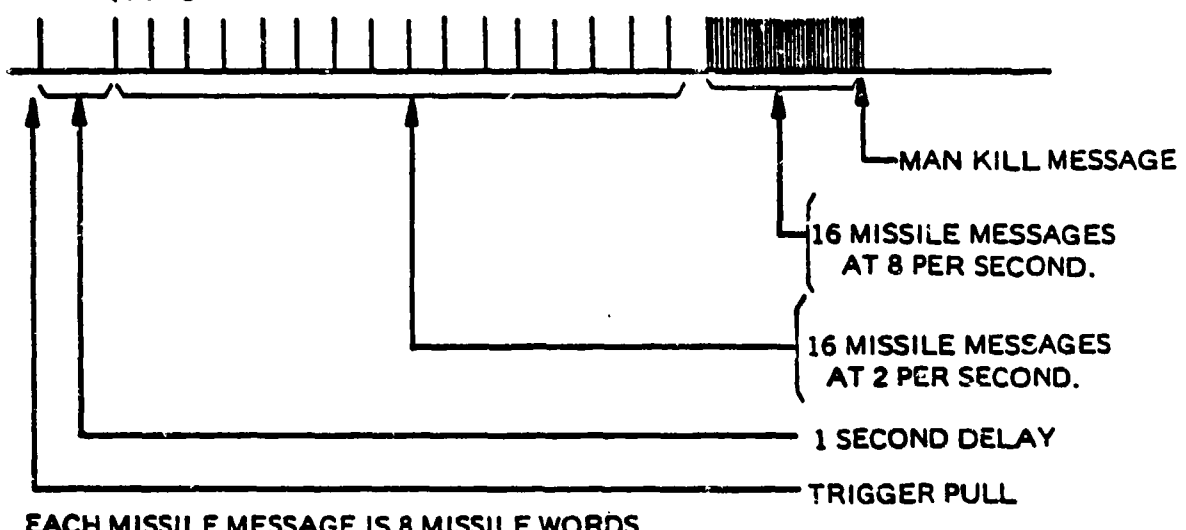


Figure 5-1. Code Format

defined as eleven and the word weight as six. The slots appear at a repetition rate of 3.0000 KHz $\pm 0.015\%$.

The accuracy of the transmission frequency is critical since the receivers are not synchronized, but are crystal controlled. Section 5.4 treats the accuracy requirement.

A "message" (simulating a single round in non-missile cases) is made up of K armor-kill words followed by M man-kill words followed by N near miss words. Table 5-1 shows values for code format parameters for various MILES weapons.

In many cases K, M, or N are zero. If the armor kill code is one of those decoded by the man-worn laser detector, there is no need for the M man-kill words. If the weapon kills men only and has zero armor effectively, then K is zero. In the case of missiles, near miss is detected by insufficient tracking time on the target; thus N is zero in each missile message. A separate man-kill message is then added after the regular missile sequence.

There are small delays between the groups of word types to avoid jamming in the Boolean union decoder (discussed in section 5.4). Within each group of like words, there is no delay required due to cyclic inequality of the code set (discussed in section 5.3).

TOW and Shillelagh missile tracking sequences are simulated by a sequence of 32 messages, 16 at 2 per second, followed by 16 at 8 per second. Dragon tracking sequences are 6 seconds long with 16 messages at 4 per second followed by 16 messages at 8 per second. The criterion for a target hit is the reception of at least 22 like missile codes in any 10-second interval. (This will be discussed in section 5.4.) The placement of half the pulses in the last 2 seconds simulates the requirements for accurate tracking during the terminal portion of missile flight in the actual system. A delay of 1 second after trigger pull is inserted prior to the beginning of this sequence.

TABLE 5-1. MILES CODE PARAMETERS

Weapon	Aeror Kill Code No.	Number of Aeror Kill Wards K	First Delay (μs)	Kill Code No.	Number of Aeror Kill Wards K	Second Delay (μs)	Near Miss Code No.	Number of Near Miss Mode			Basic Load Acc (Dry Fire Only)	Burst Limit Dry Fire Firing Rate (rps)
								Blank Fire Mode		Dry Fire Mode		
								Auto	Semi-Auto or Laser Auto Round	Auto		
Mle Ali	—	0	0	27	4	479-542*	29	≈ 20*	128	20	678	210
960	—	0	0	27	4	479-531*	29	≈ 20*	128	20	678	600
M2	—	0	0	24	4	479-531*	29	≈ 20*	128	20	678	1200
985	—	0	0	24	4	479-531*	29	≈ 20*	128	20	678	1200
Viper	15	8	479	27	128	510	28	—	—	128	6	4
60 mm	60	8	500	27	128	500	28	—	—	128	30	75
61 mm	64	8	500	27	128	500	28	—	—	128	12	99
4.2 inch	66	8	500	27	128	500	28	—	—	128	10	88
2.75 Rocket	14	8	500	27	128	500	28	—	—	4	116	76
105 mm (KMI)	12	8	500	27	128	500	28	—	—	128	12	60
90 mm	13	6	500	27	128	500	28	—	—	128	12	60
105 mm	12	8	500	27	128	500	28	—	—	128	12	60
120 mm	16	8	500	27	128	500	28	—	—	128	12	53
152 mm	13	8	500	27	128	500	28	—	—	128	6	20
120 mm (NM)	16	8	500	27	128	500	28	—	—	128	12	50
8 inch	18	8	500	27	128	500	28	—	—	128	2	99
105 Howitzer	18	8	500	27	128	500	28	—	—	128	3	99
Maverick	01	8	500	27	128	500	28	—	—	128	2	4
Chaparral	25	8	500	27	128	500	28	—	—	128	4	12
Gremlin (.0 mm)	19	24	500	27	128	500	28	—	—	8	100	99
Cobra (7.62 mm)	—	0	0	27	4	500 or 833	29	—	—	20	650	1800
Cobra (7.62 mm)	—	0	0	27	4	500 or 833	29	—	—	20	650	4900
Cobra (7.62 mm)	—	0	0	27	2	500 or 833	29	—	—	20	750	9900
7.62 mm Minigun	—	0	0	27	4	500 or 833	29	—	—	4	2000	2000
Bazooka (2.3 m.)	—	0	0	21	2	500 or 833	28	—	—	22	650	900
20 mm. Gatling	—	0	0	23	2	500 or 833	29	—	—	14	1000	1100
20 mm. Gatling	—	0	0	23	2	500 or 833	29	—	—	3	3100	1100
20 mm. Gatling	—	0	0	23	2	500 or 833	29	—	—	1	5400	1200
30 mm. Gatling	—	0	0	22	2	500 or 833	29	—	—	2	4000	1800
30 mm. Gatling	—	0	0	21	2	500 or 833	28	—	—	6	2000	1400
30 mm. (AH) Chaff	—	0	0	21	2	500 or 833	28	—	—	2	4000	1400
30 mm. (AH) Chaff	—	0	0	21	2	500 or 833	28	—	—	6	2000	600
Helldiver	02	—	—	27	128	0	—	—	—	4	16	12
Dew	07	Firing Sequence	27	128	0	—	—	—	—	4	4	9
Shillelagh	07	Refer to subsection 5.2, Code	27	128	0	—	—	—	—	4	4	4
Sub-Cr	03	Forces	27	128	0	—	—	—	—	4	4	4
Dragon	08	—	27	128	0	—	—	—	—	4	4	4

*Dependent upon operating mode

**Independent upon actual weapon firing rate

A message of 128 man-kill words follows the missile sequence to "kill" any men in the missile impact area. This message starts 121.3 milliseconds after start of the last missile message.

High rate of fire weapons which are triggered by blanks truncate the transmission of N near-miss words upon receiving an input from the blank fire microphone for the next round. K kill words are then transmitted followed by N more near-miss words unless truncated again. Should no microphone input be received (last round fired in a burst), N near miss words are transmitted.

In high rate of fire weapons operated without blank fire enablement, the number of near miss words is established by the desired firing rate and is identical on the last round of any burst.

5.3 CODE SET

The basic MILES code set is shown in Table 5-2. It is a set of 37 code words of length eleven and weight six. The codes in the set have the property of cyclic inequality. This property may be described as follows: Consider a field eleven bits wide containing any code word in the set. The code may be shifted to the right any number of bits, and the bits which are shifted out of the field to the right added sequentially to fill in the vacated spaces on the left side of the field. The resultant rotated code will not be equal to any other code in the set after any number of shifts. This property allows shift register decoding of repeated words without synch bits. It allows multiple multiple repetition of identical code words without gaps and decoding in a Boolean union decoder. This latter property is essential for reliable transmission through a turbulent atmosphere.

The codes in the MILES code set are of equal length and weight. This aids in error rejection since a bit must be dropped out and another bit added before one code is transformed to another.

TABLE 5-2
MILES WEAPON CODE ASSIGNMENT

- 37 Code Words - (Limited to 32 in any single vehicle type)
- 11 Bit Words
- 6 Weight Codes

DO	D1	D2	D3	D4	D5	D6	D7	D8	D9	D10	Code #	Weapon
1	1	0	1	0	1	0	1	1	0	0	15	* Viper Hit
1	1	0	1	0	1	1	0	0	1	0	12	* 105 mm Hit
1	1	0	1	0	1	1	0	1	0	0	8	* Dragon Hit
1	1	0	1	1	0	0	1	0	1	0	13	* 152 mm, 155 mm, 8 inch, 105 Howitzer Hit
1	1	0	1	1	0	0	0	1	0	0	21	GAU-8, AH (30 mm) Hit
1	1	0	1	1	0	1	0	1	0	0	7	* TOW, Shillelagh, Sagger, Hellfire (ASH) Hit
1	1	0	0	0	1	0	1	1	0	0	0	* Universal Hit, Controller Gun 100% Hit
1	1	0	0	0	1	1	0	1	0	1	2	TOW Shillelagh 100% Hit
1	1	0	1	0	0	1	0	0	1	1	1	Maverick Hit
1	1	0	1	1	0	0	0	1	0	1	20	Rockeye (Cluster Bomb) Hit
1	1	0	1	0	0	0	1	1	0	1	25	Roland II, Chaparral Hit
1	1	0	0	1	0	0	1	1	0	1	26	Stinger Hit
1	1	0	1	0	1	1	0	0	0	1	19	Grenade (40 mm) Hit
1	1	0	0	1	0	1	1	0	0	0	14	2.75 inch Rocket Hit
1	1	0	0	1	0	1	1	0	0	0	11	Claymore M81A1 and M16 Hit
1	1	0	0	1	0	0	1	0	1	1	10	M21 Antitank Hit
1	1	0	0	1	1	0	0	1	0	0	9	M202 Flame Hit
1	1	0	0	1	0	0	1	0	1	0	16	120 mm Hit
1	1	0	1	0	0	1	0	1	0	1	17	90 mm Hit
1	1	0	0	1	1	0	0	0	1	1	18	75 mm and 73 mm (Russian APC) Hit
1	1	0	0	1	1	0	0	1	0	1	6	105 mm 100% Hit
1	1	0	1	0	1	0	1	0	0	1	5	152 mm 100% Hit
1	1	0	0	1	0	1	0	0	1	1	4	Viper 100% Hit
1	1	0	0	0	1	0	1	0	1	1	3	Dragon 100% Hit
1	1	0	0	0	1	1	0	0	1	1	22	Bushmaster (25 mm), ZU23-4 (23 mm) Hit
1	1	0	1	0	0	1	1	0	0	1	Spare	
1	1	0	1	1	0	0	0	1	0	0	Spare	
1	1	0	1	1	0	0	0	0	1	1	Spare	
1	1	0	0	0	0	1	1	0	1	1	Spare	
1	1	0	1	1	0	1	0	0	0	1	31	Heavy Weapon Spare Miss
1	1	0	1	0	1	0	0	0	0	1	23	Vulcan (20 mm) Airborne (20 mm) Hit
1	1	0	1	0	0	0	0	1	0	1	24	* M2, M85 Machine Gun Hit
1	1	0	0	0	0	1	0	0	1	1	27	* M16 Rifle, M60 Machine Gun, Coax Hit
1	1	0	0	1	0	0	0	1	1	1	29	* M16 Rifle, M60 Machine Gun, Coax Miss
1	1	0	0	0	1	0	0	0	1	1	30	Light Weapon Spare Miss
1	1	0	0	0	0	0	0	1	1	1	28	* 152 mm, 105 mm, Viper Miss
1	1	0	1	1	1	0	0	0	0	1		* Bore sight Code Continuously Transmitted
1	0	0	0	0	0							

* Currently developed in ED MILES; all others programmed.

The number of ways in which one code may be transformed into a rotated version of another by the dropping of one bit, and adding of another is defined as the "error proclivity" between the two codes. The codes in Table 5-1 are arranged such that those near the top of the list have a small error proclivity with respect to those near the bottom. Thus it is relatively harder to transmute codes far apart on the list than those close together on the list. This property is useful in preventing light weapon codes being misinterpreted as heavy weapon codes.

It should be noted that Table 5-2 has spare codes and a boresight code. The boresight code is length five, weight one, and when repeated without gaps appears to be a 600 Hz pulse string. As its name implies, this code is used for boresighting and test. The low effective repetition rate precludes eye safety problems. The inherent difference between the boresight code and any real MILES code precludes its unauthorized use to kill targets.

Finally, the relatively high weight of the codes makes it difficult for noise to cause a false alarm.

The basic code has no explicit error correction capability and little error detection capability. However, the multiple copy transmission, the particular type of decoder, and the nature of the channel combine to make this code highly reliable.

To obtain error correction capability in the basic code would require a lengthening of the code and would require a more sophisticated decoder. This increase in complexity is not required and would tend to lower system reliability. The mechanisms used to achieve error correction are described in the following paragraphs.

5.4 DECODING SCHEME

Figure 5-2 shows those elements of the MILES receiver from the detector threshold to the decision outcome. They are described as follows:

- a. Threshold Circuit - The threshold circuit for MILES is adjustable and provides for simple threshold detection of photodiode output. A moderate amount of hysteresis is present in the threshold detector to avoid "chatter" should signals pass slowly through threshold.
- b. Flip-flop - The input to the shift register is provided by a flip-flop which is set by threshold output anywhere between clock pulse leading edges. The clock pulse clears the flip-flop and shifts the data into the register. Thus, no matter when a threshold output occurs, the data will go into the shift register. If the clock occurs in the middle of the incoming pulse, data occurs in two cells.
- c. Shift Registers (Boolean Union Decoder) - MILES decoders are always open and looking for a code to appear. Incoming signals are shifted through serial-in-serial-out shift registers. If, at any time, the ones and zeros appearing in the register match a valid code, a successful decode is achieved.

The system, as implemented, allows decoding in the presence of lost ones and rejection of pulses which do not fall exactly in a time slot.

Words are repeated multiple times to combat slow fades due to atmospheric variations. No gap is required between words due to the cyclic inequality property of the code set (see Section 5.3).

Repeating words on the same 3 KHz centers with no gap also allows Boolean Union decoding as follows:

The input to the second shift register is comprised of the Boolean Union of the present photodiode threshold output and the delayed output which occurred exactly one word time earlier. Delay is performed in the first shift register. The only way a bit may not appear in the second shift register is for it to have dropped out in two successive words.

The shift register clock is 48 KHz, 16 times higher than the code frequency. The shift registers each have $16 \times 11 = 176$ cells. Eleven decoding taps are provided at 16 bit intervals on the second register. Thus the decoder only sees incoming signals and noise through narrow time slots arranged precisely at the code spacing.

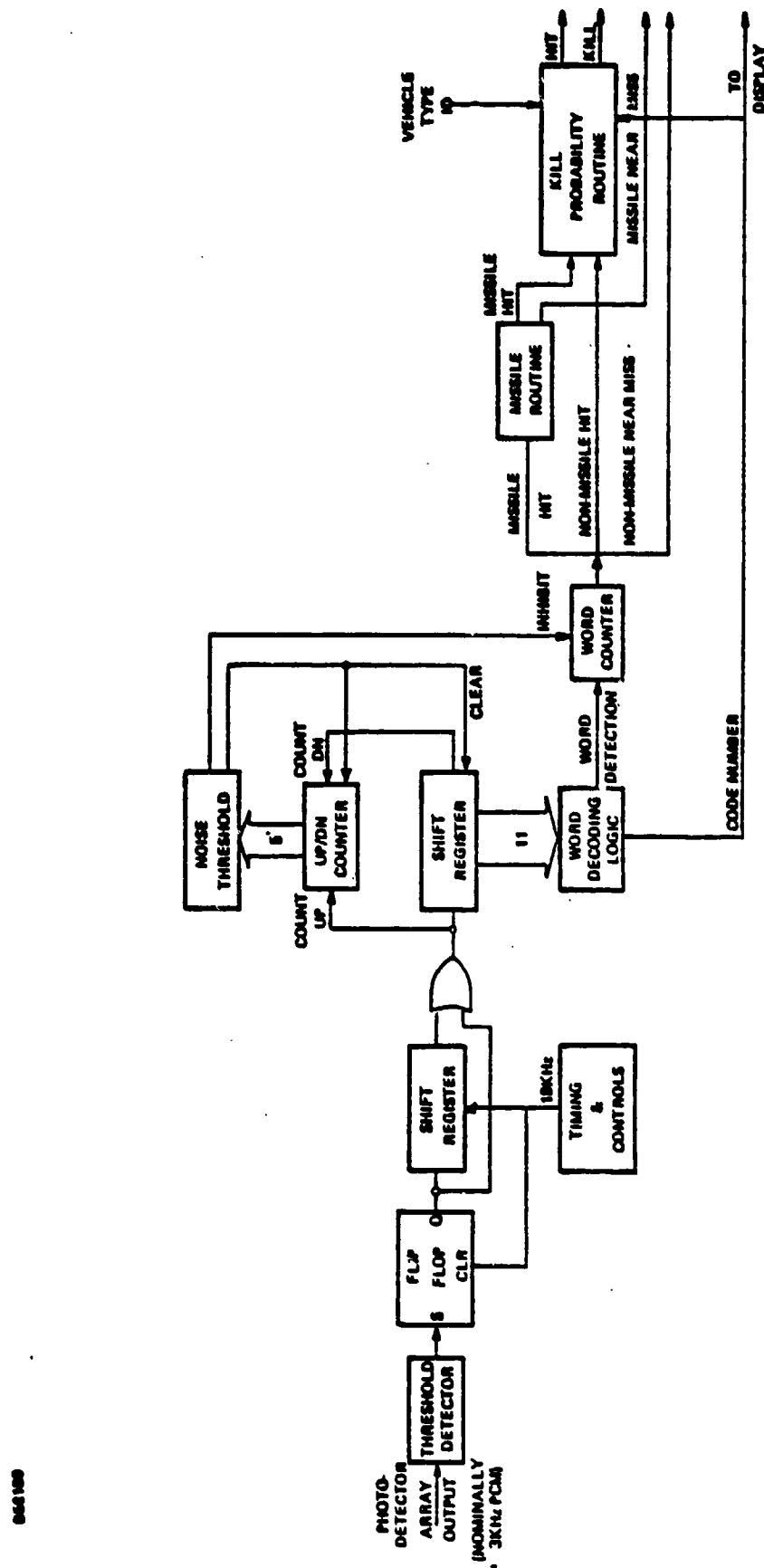


Figure 5-2. MILES Decoding Elements

The slots are 20.8 microseconds in width and at 333.3 microsecond intervals. Only noise falling into a given set of slots can be combined with actual code bits in that set of slots to jam reception.

The 48 KHz clock frequency must be near the 16th harmonic of the incoming code. If it is not, successive pulses might not appear in a single set of 3 KHz slots, and thus would not appear on the decoding taps at the same time.

Figure 5-3 shows the timing for a clock whose frequency is slightly off with respect to the incoming code. The minimum threshold output pulselwidth is five microseconds. In order to decode properly, code pulses must appear in shift register cells whose indices are multiples of 16. As can be seen, the 1st bit of the first word appears in only cell 16. Midway through the decoding sequence, the clock leading edge appears in the middle of the incoming pulse, such that the 12th bit (1st bit of 2nd word) appears both in cell 192 and 193. Finally, by the last bit of the 2nd word, the code appears in cell 337 rather than in cell 336 (16×21) and Boolean Union decoding may be inhibited.

The clock must drift at least five microseconds in 21 bit times (7 milliseconds) in order to cause misplacement of a bit. The relative crystal frequency difference between transmitter and decoder must be less than 5×10^{-6} sec/ 7×10^{-3} sec or .07%. Crystals procured for MILES are specified to $\pm 0.015\%$. Thus, even if transmitter and decoder are in error in opposite directions at the extreme of their tolerance, the total drift cannot misplace a bit.

The use of the Boolean Union decoder was prompted by the unsymmetrical nature of the binary communication channel, where scintillation causes bits to drop out more often than false bits are added. Simply lowering the threshold would cause the false alarm rate to go rapidly above specification. The Boolean Union decoder effectively combats high frequency scintillation while raising the false alarm rate only negligibly.

Section 2 of this report indicates that burst error length due to scintillation is unpredictable. The Boolean Union decoder represents an inexpensive approach to defeating high frequency components of scintillation in cases where these components exist. It also increases reception probability in fringe areas of the beam and tends to more sharply define the kill zone.

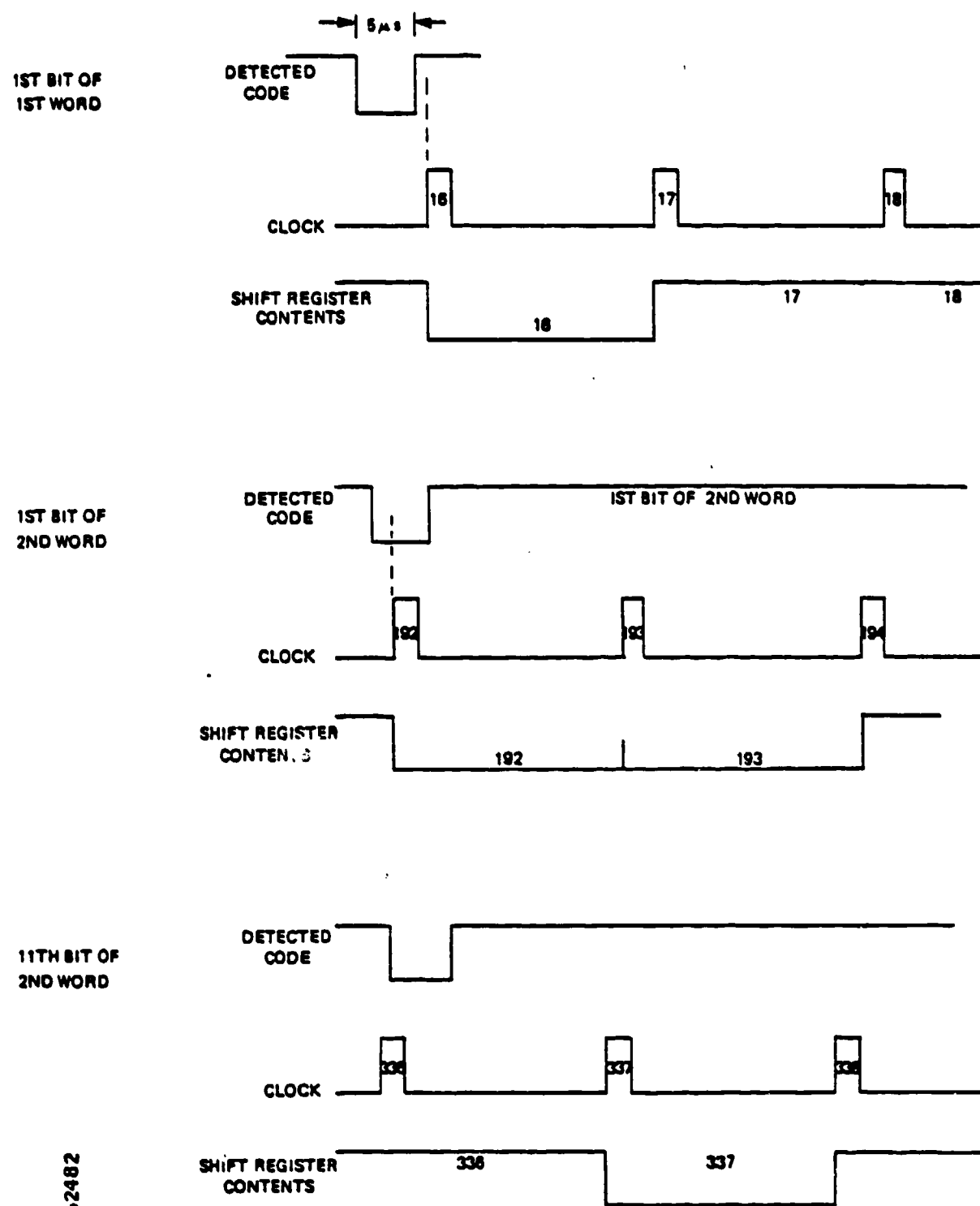


Figure 5-3. Clock Frequency Error

862482

d. Up/Down Counter and Noise Threshold - The second shift register in the decoder is monitored with an up-down counter, which always contains the count of the number of ones in the register. Since there are 16 times as many elements in the shift register as there are slots for a code, the total number of ones in the shift register provides a sensitive measure of the amount of noise in the system.

Whenever the count in the up-down counter exceeds 32, then the decoder is inhibited from operating on any codes until the count is reduced to a tolerable level. The threshold of 32 is high enough so that the system remains jam proof in the presence of non-lethal codes being fired at it. However, it is set low enough so as to effectively discriminate against high noise situations.

The ones counter constitutes the primary defense against unavoidable microphonics and EMI noise.

e. Word Counter - In vehicle systems, reception of two words within an 8 word time period are required to obtain a hit or near-miss. The man-worn laser detector (MWLD) requires only one. The reason for this is to provide false alarm protection in the vehicle decoders which are receptive to more codes (37) than the MWLD (6). (A two word requirement would be placed on the MWLD too, but small weapons are often capable of placing only one word on a target due to blank round recoil during the latter portion of the kill message.) Section 5.6 discusses quantitatively the merits of two vs one word decoding.

f. Word Decoder - The word decoder outputs a signal indicating a successful decode and the identification number of the successful code. This identifying number is used in the kill probability routine to apply appropriate kill probabilities to various weapon/ target pairs.

g. Kill Probability Routine - In the vehicle, a statistical routine is entered each time a hit is decoded to determine whether the hit caused a kill. (See Section 5.5).

h. Missile Routine - Upon detection of an initial tracking missile code word, the decoder internally initiates a ten second period representing the tracking interval (see Figure 5-4). Of the 32 code messages transmitted by the encoder during one tracking encounter, receipt of 22 or more code messages constitutes a vehicle kill, and receipt of

2 to 21 messages constitutes a near miss. For each of the 32 code messages, the encoder transmits eight copies of the missile kill code word ($32 \times 8 = 256$ code words).

The criterion for kill/near miss determination dictates that at most, one word detection per code message be allowed. Therefore, upon detection of a tracking missile kill code word, the decoder inhibits further code detection for a period equivalent to eight word transmission times (one message time) as shown in figure 5-4.

5.5 KILL PROBABILITIES

MILES vehicle systems have the capability of performing electronic statistical trials such that received hit messages may result in non-lethal "hits" rather than disabling kills. It is important to differentiate between kill probability, P_K , as it is traditionally used in weapon effect analysis, and the MILES probability of kill generator. The former is the probability of a kill given a round was fired. The MILES routine models the probability of a kill, given the round hit the armored vehicle target.

The target may be killed or hit based upon a hierarchy of weapons and targets. Table 5-3 shows the hierarchy for MILES ED weapons against five receiver types. Helicopters (Helo) and light vehicles (Truck/Jeep) are included as system expansion targets. The symbol, HK, in Table 5-3 indicates that the receiver-decoder on the target may generate either a hit or kill when a hit message is received.

The hit-kill decision statistics are based upon the number of kill words received and the weapon and target type involved. A random statistical decision is made electronically inside the target vehicle each time a successful message decode is achieved. A message decode occurs each time two hit words are received within an eight-word time interval.

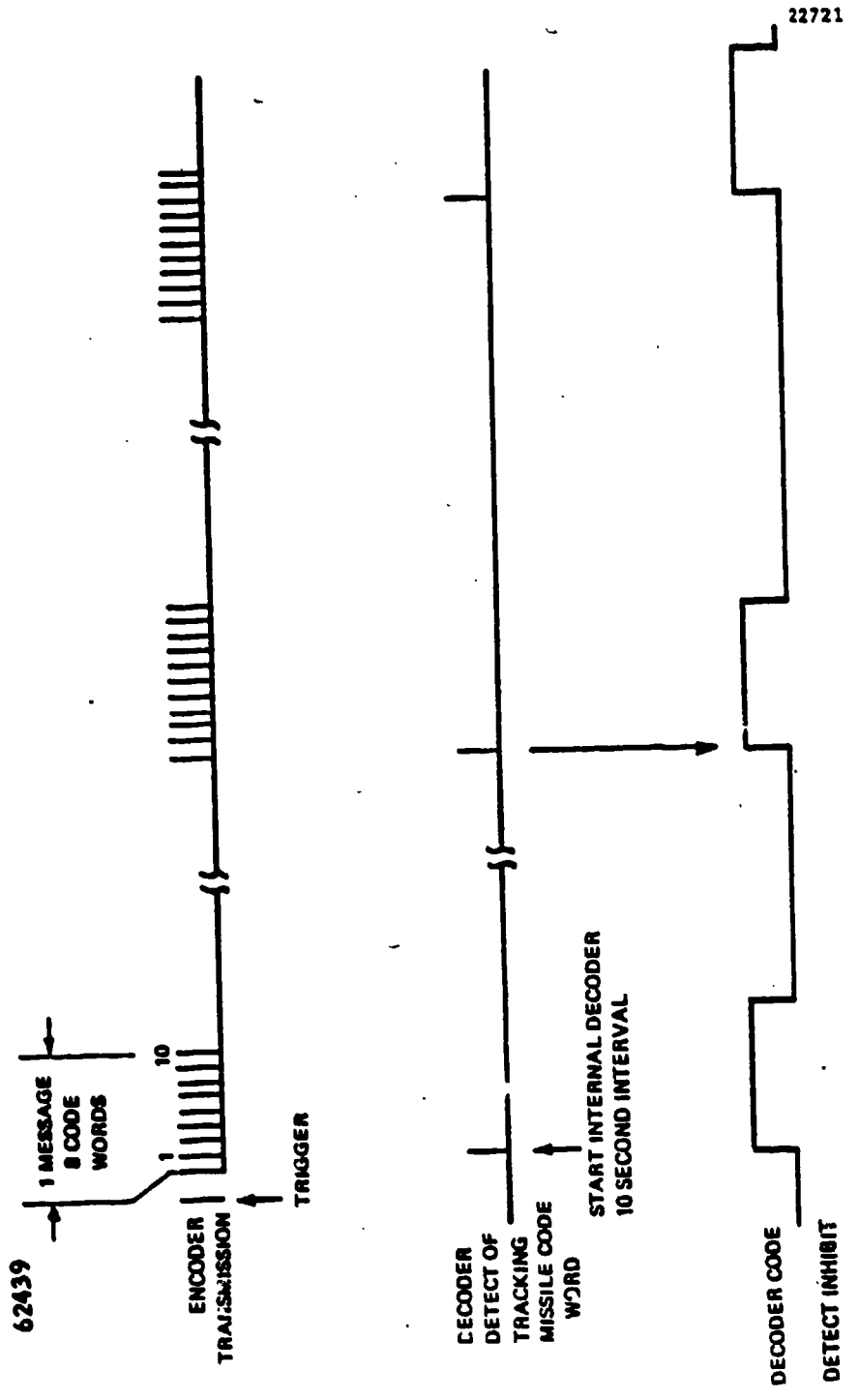


Figure 5-4. Decoder Timing - Missile Tracker

TABLE 5-3
MILES ED TARGET/WEAPON HIERARCHY

TARGET WEAPON	MVLD	CVLD			
		APC	TANK	AC/HELO	TRUCK & JEEP
M16 RIFLE	K,M	M	--	H,K,M	H,K,M
M60 MACHINE GUN	K,M	M	--	H,K,M	H,K,M
M85 MACHINE GUN	K,M	H,K,M	--	H,K,M	H,K,M
COAX MACHINE GUN	K,M	M	--	H,K,M	H,K,M
DRAGON MISSILE	K	H,K,M	H,K,M	K,M	K,M
VIPER	K	H,K,M	H,K,M	H,K,M	H,K,M
TOW MISSILE	K	K,M	H,K,M	H,K,M	K,M
SHILLELAGH MISSILE	K	K,M	H,K,M	H,K,M	K,M
105 mm GUN	K	H,K,M	H,K,M	K,M	H,K,M
152 mm GUN	K	K,M	H,K,M	K,M	H,K,M

K=Kill

H=Hit

M=Near Miss

There is a range dependency inherent in this implementation due to the fact that at close ranges, a single eight-word round will cause the routine to be entered four times; at long range, the routine will be entered fewer times owing to the probable reception of fewer than eight valid words.

Figures 5-5 and 5-6 show the range dependency of P_{Kill} and $1/P_{Kill}$ (mean number of rounds to kill) for the MILES technique. Note that the ordinate for figure 5-5 is probability per round, not per hit.

Since the routine is entered more than once at close range, the actual probability for each execution of the routine must be set substantially less than the desired single round close range kill probability. (One "kill" outcome from the multiple executions is sufficient to kill the vehicle.) In fact the equation relating the two probabilities is:

$$P_M = 1 - (1 - P_W)^D$$

where P_M = probability of kill given all words in the message were received (close range kill probability).

P_W = probability of kill given a single execution of the kill routine

D = number of executions of the kill routine given perfect message reception (D = two for a four-word message and four for an eight-word message.)

Table 5-4 gives close range kill probabilities for various weapon target pairs. MILES vehicles store data which yield these short range probabilities. Probabilities are all integral multiples of 1/32 (.03125) due to the use of a five-bit counter in the implementation.

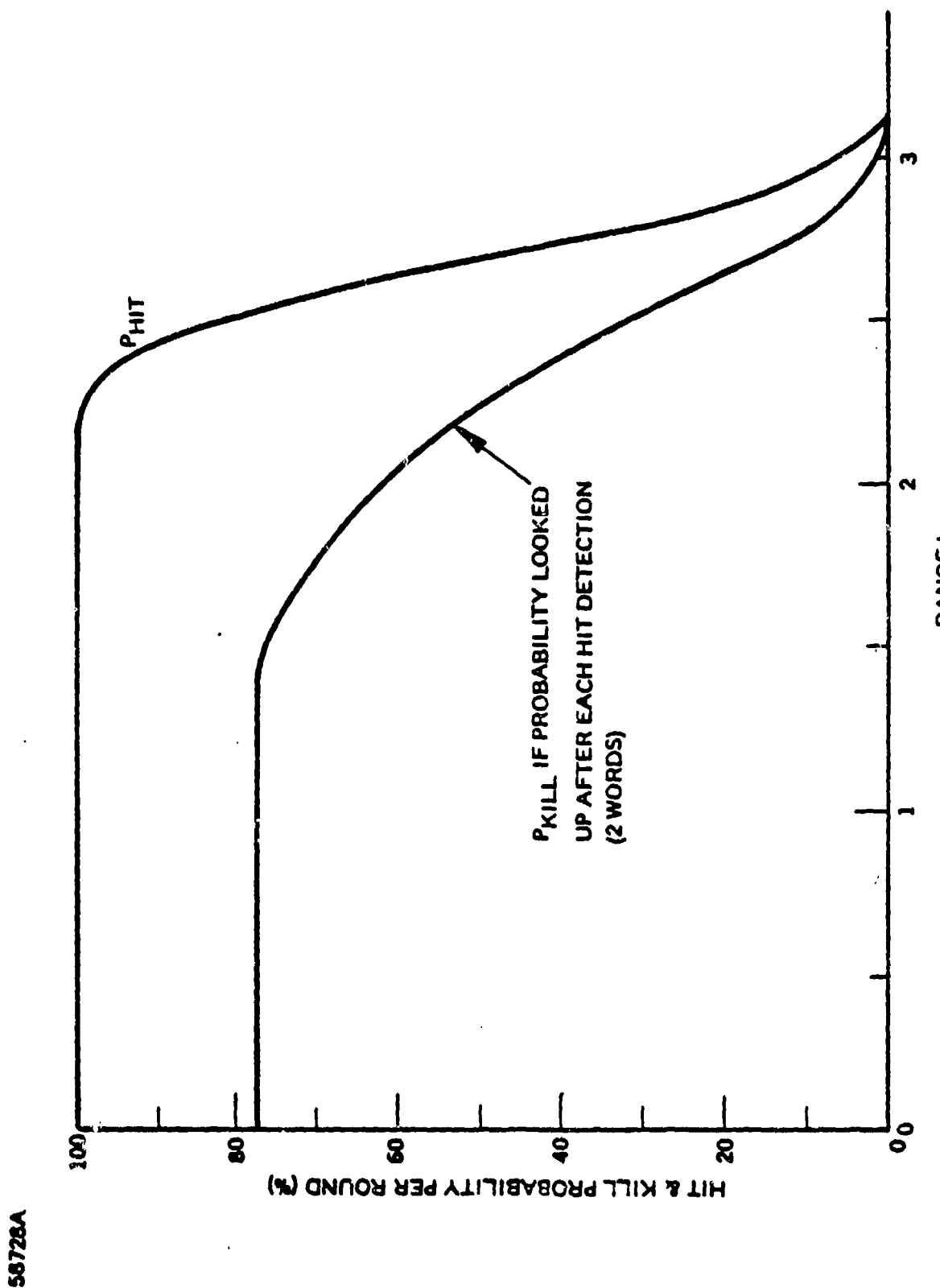


Figure 5-5. Kill Probability Dependence on Range

58727

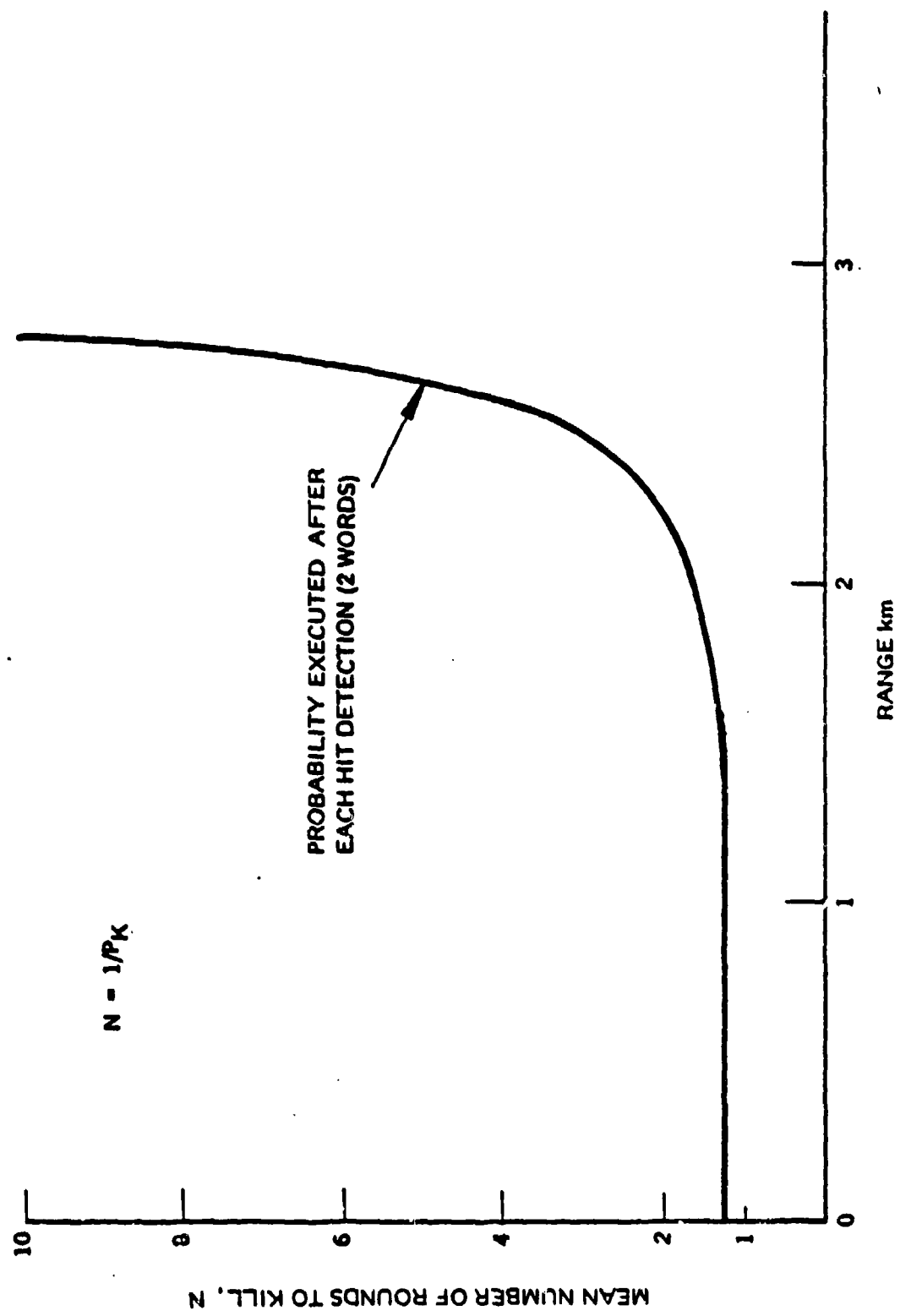


Figure 5-5. Mean Number Rounds to Kill

TABLE 5-4
VEHICLE KILL PROBABILITIES

CODE NO.	WEAPON	HIT WORDS PER ROUND	KILL PROBABILITY PER ROUND VEHICLE TYPE			
			TRUCK/JEEP	AC/HELICOPTER	APC	TANK
00	100% Univ. Kill	16	100.0%	100.0%	100.0%	100.0%
01	Maverick	8	100.0%	100.0%	100.0%	100.0%
02	Hellfire	N	100.0%	100.0%	100.0%	93.75
03	Sagger	N	100.0%	95.3125	98.4375	70.3125
04	60 mm, 81 mm, 6.2 inch	8	100.0%	100.0%	73.4375 28.125	1.5625 1.5625
05	M13A Mine (Track Cutter)	4	100.0%	100.0%	98.4375 87.5	98.4375 87.5
06	Weapon X	8	100.0%	100.0%	No Effect	No Effect
07	TOW, SHILLELAGH	N	100.0%	98.4375	100.0%	85.9375
08	DRAGON	N	100.0%	100.0%	98.4375	76.5625
09	H202 Flame	4	100.0%	100.0%	52.5 39.0625	78.125 53.125
10	H21 Anti-Tank	4	100.0%	100.0%	100.0%	79.6875 54.6875
11	Claymore M16A1 & M16	4	85.9375 62.5	78.125 53.125	No Effect	No Effect
12	105 mm	8	96.875 57.8125	100.0%	96.875 57.8125	87.5 40.625
13	152 mm	8	96.875 57.8125	100.0%	100.0%	78.125 51.125
14	2.75 in. Rocket	8	96.875 57.8125	92.1875 56.875	78.125 51.125	42.1875 12.5
15	VIPER	8	96.875 57.8125	92.1875 56.875	81.25 54.375	48.4375 15.625
16	120 mm	8	96.875 57.8125	100.0%	100.0%	93.75 50.0
17	90 mm	8	96.875 57.8125	100.0%	90.625 45.3125	34.375 0
18	8 Inch, 105 How., 120 mm, 155 mm	8	96.875 57.8125	100.0%	95.3125 53.125	1. 1.5625
19	Grenade (40 mm)	8	56.25 18.75	86.375 37.5	10.9375 3.125	4.6875 1.3625
20	Rockeye (CB)	2	81.25	81.25	15.625	20.3125
21	Bushmaster (25 mm), GAM-8, AH (30 mm)	2	84.375	43.75	9.375	6.25
22	ZUZ3-A	2	43.75	50.0	6.25	No Effect
23	Vulcan (20 mm)	2	43.75	23.4375	6.25	No Effect
24	H2, H85 (30 CAL)	4	37.5 20.3125	4.6875 3.125	4.6875 3.125	No Effect
25	Chaparral	8	No Effect	96.875 57.8125	No Effect	No Effect
26	Stinger	8	No Effect	92.1875 56.875	No Effect	No Effect
27	H16, H80, Coax (7.62 mm)	4	9.375 4.6875	3.125 1.5625	No Effect	No Effect
28	Heavy Weapon Mine	--	Miss	Miss	Miss	Miss
29	Light Weapon Mine	--	Miss	Miss	Miss	No Effect
30	Light Weapon Mine Spare	--	Miss	Miss	Miss	No Effect
31	Heavy Weapon Mine Spare	--	Miss	Miss	Miss	Miss

Code No. 0 thru 27=Mic Codon

N = Missiles

KILL Probability

Per Round

Per 2 Code Words Received

5.6 EFFECT OF CODING AND DECODING ON SYSTEM FALSE ALARM RATE

This section presents an expression relating the system false alarm rate to the single bit false alarm rate. From computer evaluations allowable false alarm rates are shown.

5.6.1 THEORETICAL BASIS

The probability of receiving a false alarm in 100 hours is:

$$P_{100} = 1 - (1 - P_W)^{1.73 \times 10^{10}}$$

where P_W is the probability of receiving a false word at any allowable decoding opportunity. (There are 1.73×10^{10} decoding opportunities in 100 hours, based upon 48,000 opportunities per second.)

The probability of decoding a false word at any decoding opportunity when only one word receipt is required is:

$$P_{W1} = I (1 - P)^{BN(1-W)} \left[1 - (1 - P)^{BN} \right]^W \quad (1)$$

where:
I = number of valid code words which can kill a man (e.g., M16,
M60, M6 etc.)
P = false bit probability
B = number of registers in the Boolean Union decoder
N = number of independent thresholds per unit (man or vehicle)
W = weight of code word

The probability of decoding a false word when M receipts are required is:

$$P_{WM} = K P_{W1}^M (1 - P_{W1})^{K-M} \quad (2)$$

where K = number of word periods during which the decoder will accept the second valid decoded word ($K = 2$ for man system and $K = 8$ for vehicle system). Equation (2) applies to both man worn laser detectors and vehicle detection belts where $M=2$. *

5.6.2 COMPUTER MODEL

A computer program was written which evaluated P_{100} as a function of P for various values of K , M , N , and I corresponding to the vehicle and the man system. Boolean union decoding was assumed throughout. Figures 5-7 and 5-8 plot the results of that program.

These figures are used as follows:

- a. Select the appropriate figure for the decoder (vehicle or man worn)
- b. Enter the graph on the left-hand side at the 100 hr false alarm probability (.01 on MILES).
- c. Using the appropriate word detection curve, find the single-bit false one probability

Note that the required single-bit probability is a strong function of the number of words required for receipt.

The initial model execution was followed by several (14) runs varying:

- a. Weight of miss code from 4 to 6
- b. Number of words required for detection
- c. Length of window in which the subsequent words were detected.

Tables 5-5 through 5-8 show the results. Note that:

- a. Window length has little effect on allowable single bit error probabilities.

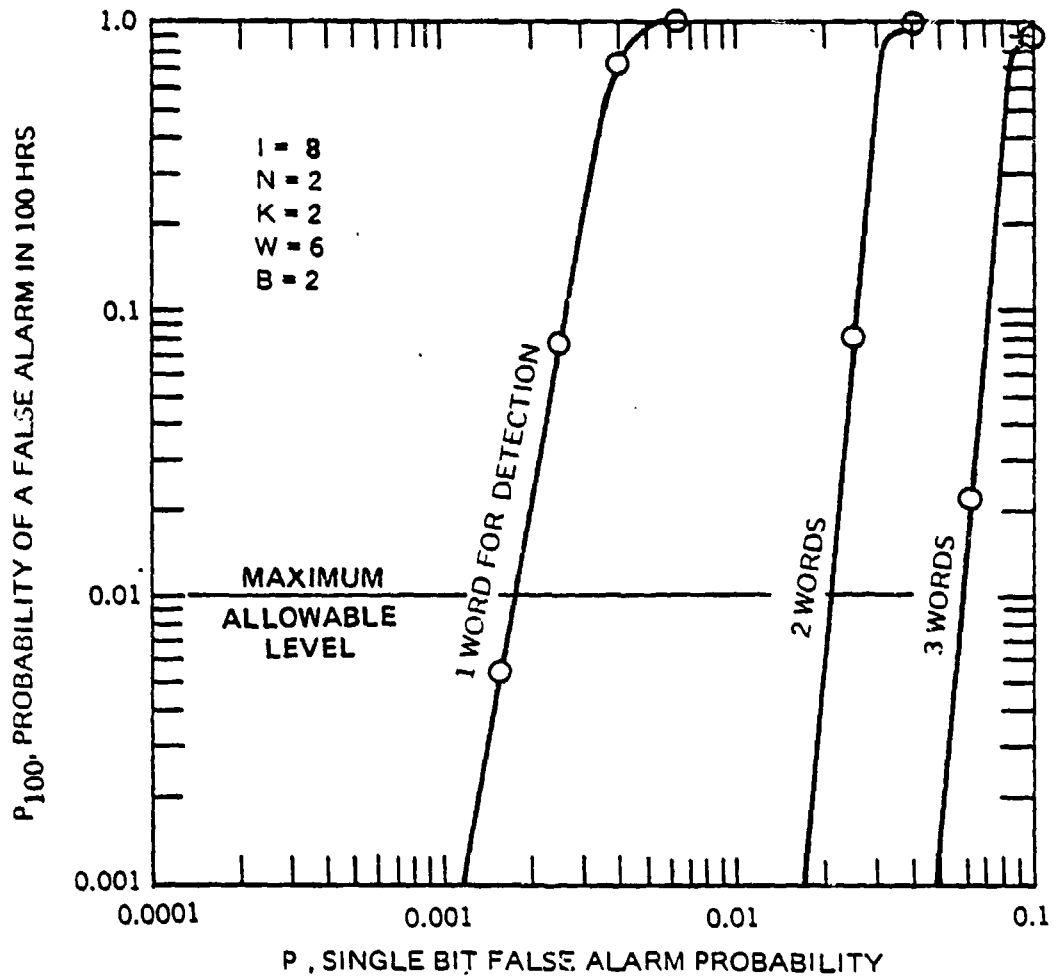


Figure 5-7. False Alarm Probability- Man Decoder (Kill)

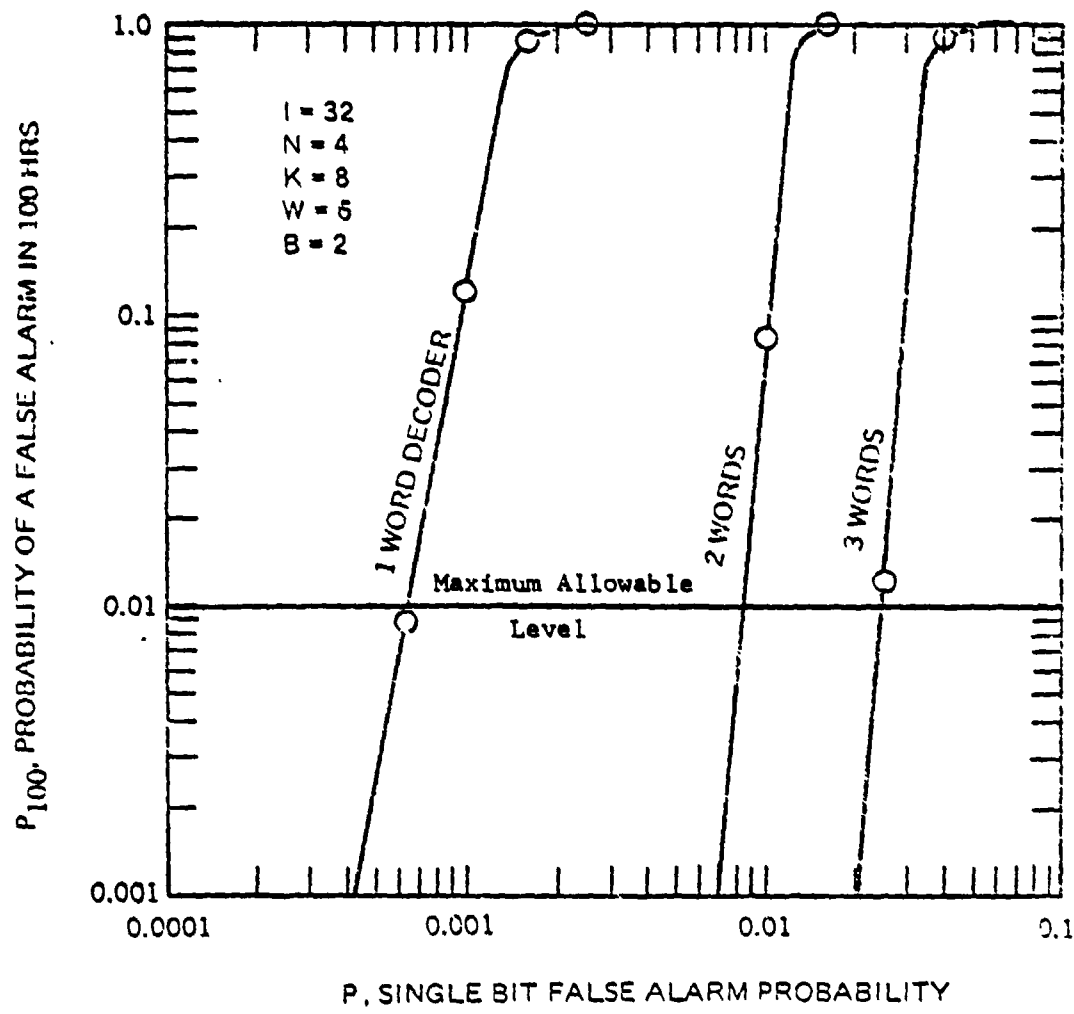


Figure 5-8. False Alarm Probability - Vehicle Decoder (Kill)

58724

TABLE 5-5
MAN NEAR MISS

M No. Reqd. Detect	W Code Weight	N Window Length	P, Single Bit False Alarm Probability which gives 100 hr False Alarm Prob, $P_{100} = 0.01$
1	4	24	0.0002
		4	0.0002
	6	24	0.0024
		4	0.0024
2	4	24	0.005
		4	0.007
	6	24	0.02
		4	0.024

TABLE 5-6
MAN KILL

M No. Reqd. Detect	W Code Weight	N Window Length	P, Single Bit False Alarm Probability which gives 100 hr False Alarm Prob, $P_{100} = 0.01$
1	6	24	0.0017
	6	4	0.0017
2	6	24	0.018
	6	24	0.020

TABLE 5-7
VEHICLE NEAR MISS

M No. Reqd. Detect	W Code Weight	N Window Length	P, Single Bit False Alarm Probability which gives 100 hr False Alarm Prob, $P_{100} = 0.01$
1	4	128	0.00008
		8	0.00008
	6	128	0.001
		8	0.001
2	4	128	0.002
		8	0.0025
	6	128	0.0075
		8	0.01

TABLE 5-8
VEHICLE HIT

M No. Reqd. Detect	W Code Weight	N Window Length	P, Single Bit False Alarm Probability which gives 100 hr False Alarm Prob, $P_{100} = 0.01$
1	6	128	0.00065
	6	8	0.00065
2	6	128	0.0065
	6	8	0.0085
3	6	128	0.02
4	6	128	0.042

- b. Changing code weight from 4 to 6 increases the allowable error probability by factors varying from 3.75 to 12.5.
- c. Going from one word to two word receipt increases the allowable error probability by factors varying from 5 to 35.

Going from one word to three or four word receipt on vehicle hit codes increases the allowable false one rate by 30.8 and 64, respectively.

5.6.3 NEGATIVE EFFECT OF MULTIPLE WORD RECEIPT REQUIREMENTS

System models have shown that the reduction in range by going between one word and three is undetectable for the 90% hit probability, 3KM visibility case. It was 7.8% for the 20% hit probability, 24KM visibility case. These are clearly unimportant magnitudes of change.

A two-word requirement on light weapon codes may be impractical due to the motion of the weapon. Hits or misses may be more difficult to achieve when two words are required on receivers whose primary function is receipt of hand-held weapon codes. *

5.6.4 CONCLUSION

The following Design decisions were made:

- a. All codes are 6-weight codes.
- b. Require only one word receipt on both kill and near-miss for the man decoder.
- c. Require two word receipts on both kill and miss for the vehicle decoder.

Allowable false one rates are shown in Table 5-9 below:

TABLE 5-9
ALLOWABLE FALSE ONES

Decoding System	Allowable False Ones Per Second
Man Kill	82
Man Miss	115
Vehicle Kill	312
Vehicle Miss	360

False one rate is obtained by multiplying the false one probability by the sampling frequency, 48KHz.

5.7 THRESHOLD-TO-NOISE SETTING AND FALSE ALARM RATE

The system false alarm rate requirement is a maximum of 1% in 100 hrs. Section 5.6 indicated a false bit rate of 82 per second or less was desired to satisfy this requirement for the man worn system. The threshold-to-RMS noise ratio which will meet the false bit rate requirement is derived below.

Rice (Reference 1) gives an equation for \overline{FAR} , the single bit false alarm rate, in terms of I_t/I_n , the threshold-to-noise ratio (TNR).

$$\overline{FAR} = \frac{1}{2\pi\sqrt{3}} \exp(-I_t^2/2I_n^2)$$

where $\frac{1}{2\pi}$ is the noise bandwidth of the system. If BW, the shot noise bandwidth developed in Subsection 3.2.3, is substituted for $1/2\pi$ and TNR for I_t/I_n , and this equation is solved for TNR, we have:

$$TNR = \sqrt{2\ln \left(\frac{BW}{\sqrt{3} \overline{FAR}} \right)}$$

Substituting the previously obtained values, $\overline{\text{FAR}} = 2$ and $\text{BW} = 333 \text{ KHz}$ (from Section 3.2.3), the desired formula is obtained for minimum threshold-to-noise ratio, TNR.

$$\text{TNR} = \sqrt{2 \ln \left(\frac{3.3 \times 10^5}{\sqrt{3} \cdot 82} \right)}$$

Evaluating the above expression gives a minimum allowable TNR of 3.94 for MILES.

In practice, the threshold-to-noise ratio is set in MILES receivers at manufacture by monitoring false one rates while simulating highest noise conditions (-35°C , full sunlight). The threshold is set such that the false one rate is about one per second under these conditions. Using the expression above for TNR, the TNR is approximately 5.0. At higher temperatures and out of the sun, the TNR is somewhat greater.

(It should be noted that the $\overline{\text{FAR}}$ is a fast function of the TNR; hence the safety margin on TNR.)

SECTION 6
PARALLEL STUDIES

At the beginning of the ED program several concepts that had not been done on the AD program seemed worthy of investigation and of potential use on the ED design. A single tube transmitter vs the two tube transmitter would conserve weight, volume and dollars. Blank fire enablement of the transmitter would provide realistic weapon simulation, eliminate the need for a rounds count display, and provide a 1:1 correspondence between blanks and laser rounds. These studies culminated in their successful application to the Engineering Development hardware.

6.1 SINGLE TUBE TRANSMITTER

6.1.1 INTRODUCTION

The original XEOS concept utilized on the LES Program in OTI for generating a near miss beam was a separate, circular near miss zone resulting from a separate near miss laser (i.e., two laser tubes). The reasoning proceeded as follows:

- a. The near miss zone should be larger than the kill zone.
- b. To provide a larger zone requires a greater beam divergence.
(It was originally believed that beam diameter was directly proportional to beam divergence.)
- c. To provide adequate detector irradiance the near miss laser output power must scale in direct proportion to the area of the beam.

However, this approach had a number of disadvantages.

- a. It would require two lasers, two optical assemblies and two drivers.
- b. It would increase the cost, weight, and size of the MILES transmitters.
- c. The two lasers must be aligned with great precision and must remain in precise alignment through field usage.
- d. Since the desired near miss beam diameter is about three times that of the kill beam its area is about nine times as great and, hence, the near miss beam would require almost an order of magnitude greater power level than the kill beam.
- e. The power requirements of the VES near miss beams were such as to exceed the current eye safety standards as stipulated in TB MED 279.
- f. OT-I Testing at Ft. Benning, Ga., indicated that the near miss beams of both VES and TES were not very effective and that beyond about 1.2 km no VES near miss zone could be detected.
- g. The binocular near miss/kill configurations would force the existence of four laser tubes in the 105 mm weapon barrel, and five laser tubes in the 152 mm weapon barrel. The mechanical and optical problems associated with space available and optical alignment would be formidable. The ED MILES system used the single tube transmitter for all laser transmitters.
- h. Mathematical analysis (see Appendix A), shows that the maximum beam diameter is independent of beam divergence. Thus, the original idea of utilizing two separate laser tubes, one with a narrow kill zone and one with a wide near miss zone was determined to be a nonoptimum approach to providing a near miss beam.

6.1.2 ANALYSIS

The analysis for the single tube concept is included as Appendix E.

6.1.3 CONCLUSIONS FROM ANALYSIS FOR VES

- a. For MILES, the single tube transmitter concept appeared to have considerable merit and was selected as a design baseline approach.

- b. Data taken at 1.8 km confirmed the reduction in detection probability with radial off-set from the aiming point.
- c. Analysis of an eight word kill message followed by a 128 word near miss message indicated that an effective kill beam diameter of about 1 meter and a concentric near miss zone having an effective diameter of about 3 meters, can be expected at a range of 1.8 km.
- d. Additional testing of the single tube VES kill/near-miss concept, utilizing the proposed ED MILES Boolean union decoding concept, was done to establish full technical feasibility. The cost, size, weight, reliability, simplicity, and eye safety advantages of the single tube VES concept were so significant that this approach was utilized after a test verification program.

6.1.3.1 Actions Taken

- a. Based on the results of the previous analysis and preliminary tests, a MILES breadboard transmitter/encoder and receiver/decoder pair were fabricated. This encoder and decoder generated the proposed ED codes and utilized the "Boolean Union" decoding scheme discussed in this report.
- b. The breadboard equipment was then used to develop experimental data on actual kill and near miss zone sizes and kill and near miss hit probabilities at ranges from 25 meters to 4 km.

6.1.4 CONCLUSIONS FROM ANALYSIS FOR TES

- a. The effects of human tremor for TES cause angular displacement of the aiming point by amounts between 3 and 10 milliradians.
- b. The use of a significantly greater number of near miss words, relative to kill words, has the effect of increasing the effective near miss zone size.
- c. For TES the effects of blank fire cause a further increase in the dispersion of the aiming point.
- d. Preliminary tests utilizing a TES 0.67 watt output power GaAs laser transmitter were performed using a 30 word (AD words) encoder and a non-binary union decoder. The decoder was required to successfully decode two words rather than one since two AD words more closely simulate

one ED word of weight 6. The transmitter was mounted on an M16A1 rifle and fired at a MWLD harness at a range of 300 meters. The rifle was hand-held in the standing position, and was fired with blanks 20 times. Nineteen successful near miss receipts were recorded. This test did not utilize the proposed kill and near miss codes, the 4 and 24 words per kill and near miss message, respectively, or the Boolean Union decoder. Thus, these results did not firmly establish the proof of feasibility of the single tube TES concept. However, they indicated a good chance for success. Further testing was performed to determine that the single laser tube would be used for the M16A1 Rifle.

6.1.4.1 Action Taken

- a. As with VES, a TES laser encoder employing the proposed kill and near miss codes and word count were fabricated and assembled. Furthermore, the TES decoder had the Boolean Union decoder capability.
- b. The above equipment was used to perform experimental tests from 5 to 500 meters to obtain kill and near miss zone size versus range as well as probability of hit and probability of near miss versus range. Cost, weight, size, reliability, ease of boresighting, and eye safety advantages of the single tube TES concept are so significant that this study was performed early in the MILES program so that the results of these tests were properly channeled into the MILES system design.
- c. As a result of the testing, the single tube concept was employed throughout the ED MILES system.

6.2 BLANK FIRE DETECTION

Detection of small weapon blank fire is a means by which realistic weapon simulation can be achieved. Blank fire detection in effect provides a trigger signal from the weapon to the laser transmitter. This weapon generated signal can be used to create accurate weapon character simulation.

Two functions for blank fire detection were considered, reset and enable. In the reset mode the laser is fired by a trigger overlay, the blank fire signal being used to reset the transmitter. In the enable mode the blank fire signal is used for direct laser firing.

6.2.1 TESTING

Two types of transducers were considered: an accelerometer switch which would sense the mechanical shock of the blank fire, and an acoustic pickup.

a. Accelerometer Sensor

Shock tests were performed on the M16 Rifle and M60 Machine Gun in order to define the accelerometer switch requirements. Accelerometers were mounted in each of the three major axes on the barrel of the weapon and response data were taken during the firing of blank ammunition. Three major transients occur for each blank fired. The first is caused by the firing of the round. The second occurs when the bolt hits its rearward stop and the third when the bolt returns to battery. The acceleration levels of the third transient are equal to or greater than the g levels of the blank fire. Manual bolt actuation also produced comparable g levels. The M60 machine gun response data is similar with two major transients occurring during the firing of the blank round and the bolt return to battery.

Spectral frequency analysis of the shock pulses did not indicate any singular or well defined point of resonance.

The conclusions of the shock tests were:

- (1) The shock associated with the bolt return to battery is equal in magnitude or greater than the shock associated with the blank fire.
- (2) It would be difficult to design a simple accelerometer switch that would respond to the blank fire shock pulse and not respond to the bolt return shock pulse.
- (3) The shock spectrum analysis does not indicate a unique frequency signature. The fact that the frequency content of the transient generated by manual bolt actuation is the same as that of blank fire indicates that a "tuned" accelerometer switch would not operate reliably.
- (4) The use of an accelerometer either as a switch or a sensor for blank fire detection does not appear feasible.

b. Acoustic Sensor

A series of tests were conducted to determine the suitability of an acoustic sensor for blank fire detection. A brief description of the tests and a summary of the results follows:

- (1) Feasibility - A Knowles Model BA-1501 sensor was used to determine if sufficient signal could be generated from the blast. Signal levels of ≈ 1.2 volts were measured. In addition the test indicated that the rifle blast could easily be differentiated from bolt noise. The blast generated an acoustic signal ≈ 6 times the level of bolt noise.
- (2) Acoustic mapping - Acoustic measurements were conducted on the M16 and M60 weapons. Table 6-1 summarizes the sound pressure levels obtained at the MILES transmitter location, and a representative curve is shown in figure 6-1.

TABLE 6-1
WEAPON SOUND LEVELS

	Sound Pressure Level (dB)		Major Frequency Component
	Min	Max	
M16	142	158	10 to 14 Hz
M60	128	137	10 to 14 Hz

It can be seen from this table that a transducer with a minimum sensitivity of 120 dB at 14 Hz will satisfy the minimum levels for both the M16 and M60 weapons.

In addition, the acoustic tests indicate that position of the blank fire adapter had little or no effect on the sound pressure levels, as long as it was close to the barrel.

- (3) Acoustic induced misfires - A test was conducted to determine the susceptibility of the acoustic detection system to misfires caused by adjacent shooters. The results indicate that no misfires occurred when two M16 shooters were separated by as little as 20 cm (8 inches).

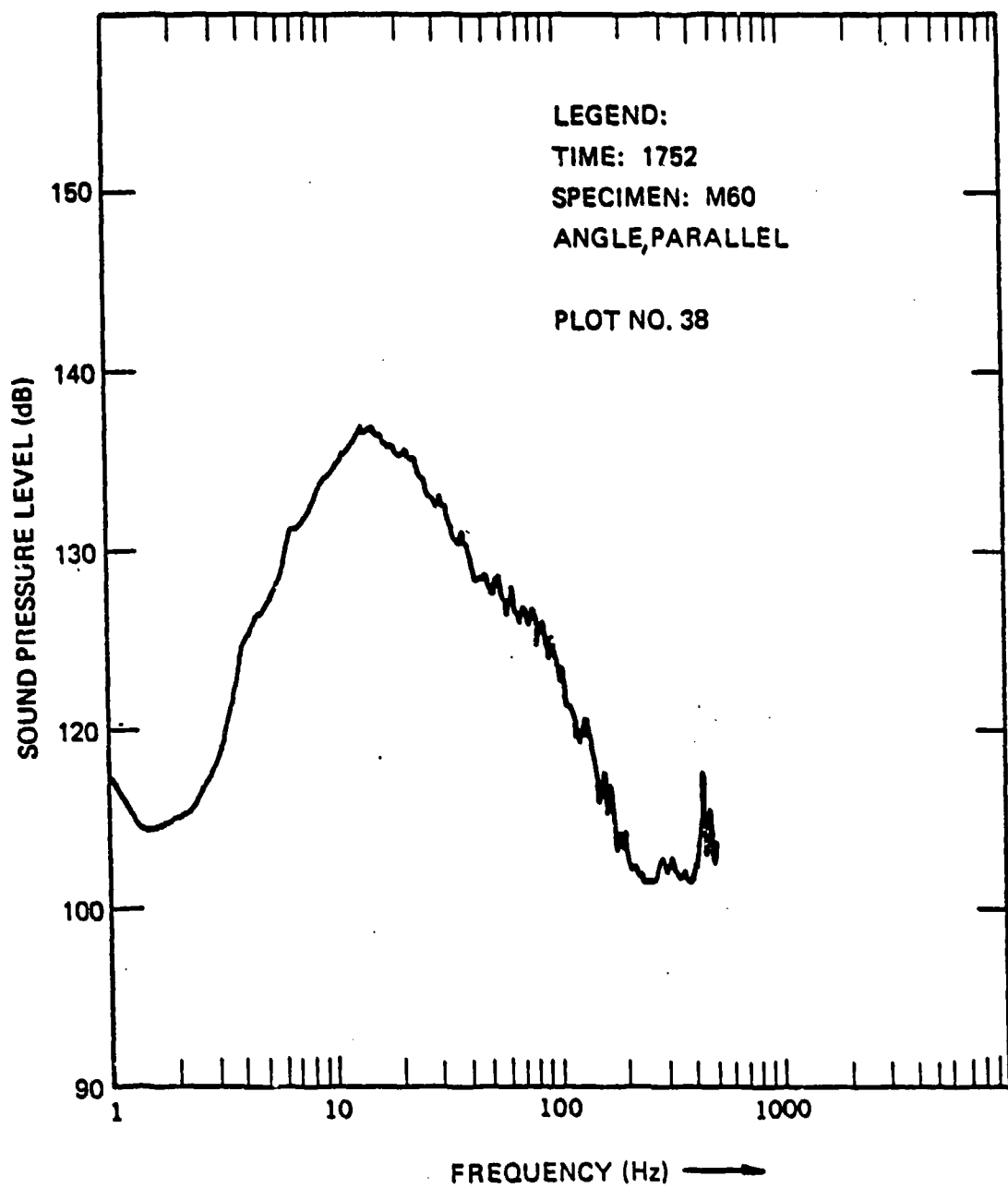


Figure 6-1. Acoustic Sound Levels, M60 Machine Gun

56258

6.2.2 CONCLUSIONS

- a. The signal generated by blank fire is sufficient for reliable performance.
- b. The blast can be separated from bolt travel noise.
- c. Sound pressure levels generated by the M16 and M60 are similar and the same sensor could be used for both weapons.
- d. The acoustic sensor is not susceptible to misfires caused by other nearby weapons being fired, provided they are more than 8 inches from the sensor.
- e. Blank fire reset should be feasible using the acoustic sensor to trigger the reset.

6.3 BLANK FIRE ENABLE

The principal problem anticipated with blank fire enable was the movement of the weapon after trigger squeeze and prior to laser fire.

Two test methods were devised to determine the angular deflection versus time of the M16 Rifle when using blank fire enable.

The first used two accelerometers, a_1 and a_2 , mounted on the forward end of the barrel separated by a distance L. The data taken during this test instead of being a typical half sine shock pulse was relatively high frequency sine waves which led to inconclusive results. Therefore, this method was abandoned.

6.3.1 MULTIPLE DETECTOR TESTS

The second test used five detectors connected to a strip chart recorder and a laser transmitter operating at a constant 1 kHz pulse rate. An acoustic pickup was mounted on the front face of the transmitter to sense the blank fire, thus establishing the instant of firing. The target was made up of five AD VES detectors mounted in an

"X" configuration with the four corner detectors forming a two foot square. Each detector output was connected to its own channel of a six channel strip chart recorder. The acoustic pick up mounted on the transmitter was connected to the sixth channel.

The data indicated a relatively stable period of ~ 10 msec immediately following blank fire. Based on this data some additional tests were conducted in which the laser transmitted four AD kill words at a 3.2 kHz bit rate. Since an AD word has five slots, a word required 1.56 milliseconds, plus 2.5 milliseconds blank interval between words or a total of 13.75 milliseconds for a four word, three interval message. An AD decoder was modified to accept the 3.2 kHz bit rate. The word requirement for a kill was made selectable at one, two, three or four words.

A detachable trigger overlay was also incorporated on the mockup laser so dry firing could be accomplished and a comparison base could be established for each shooter.

Three shooting positions were used in this test, standing, sitting, and prone. For each of the positions, 10 dry fire shots using the trigger overlay were recorded. Then 10 blank fire shots were recorded (four word requirement was used). For the 100 meter tests, good correlation between the dry fire and blank fire was achieved for every shooter.

6.3.2 CONCLUSIONS

- a. The electronics design was completed with allowance for either blank fire reset or blank fire enable as well as the dry fire capability.
- b. Further testing proved the blank fire enable concept to be workable and it was used for the ED MILES system with the alternative choice of dry fire. A trigger overlay switch was designed and included with the M16 and M60 laser transmitters to allow for the dry fire mode of operation.

APPENDIX A

MILES EYE SAFETY

2350-DFS-689

MILES

EYE SAFETY SUMMARY

FINAL REPORT

January 21, 1981

Dr. Paul F. Jacobs

INTRODUCTION

The subject of eye safety on the MILES Program has had a somewhat involved history. During the period from 1972 to 1975, Xerox/EOS was involved in the eye safety problem purely from an analytical standpoint; first on the LES proposal and then while completing the LES program itself. During this phase a number of events occurred:

- 1) XEOS personnel became more familiar with not only the existing standards (TB MED 279, BRH, ANSI-Z-136) but the rationale behind their adoption.
- 2) Calculations indicated that, based on existing eye safety criteria, the maximum range requirements of LES could not be achieved if one were to be simultaneously fully eye-safe and meet DTUPC requirements.
- 3) In a number of areas the standards were either unclear or incomplete when applied to pulse code modulated systems. Furthermore, little or no biological data existed for GaAs lasers.

During the next phase, from 1975 to 1978

- 4) XEOS personnel began to participate in biological testing at Letterman Army Institute of Research (LAIR) under direct support of PM-TRADE, to answer some of the questions regarding eye safety as applied directly to MILES.
- 5) XEOS completed R&D, fabrication and laboratory and field testing of MILES. As a result of numerous system improvements and innovations (more sensitive detectors, lower noise amplifiers, Boolean Union decoders, and redundant code transmission) it was possible to reliably achieve longer ranges with lower transmitter output radiant exposure, while satisfying performance and cost constraints.

- 6) Unfortunately, even under these "best" conditions it was still not possible to design a Class I exempt MILES system (i.e. completely eye safe under all conditions). Appendix A is the 1978/79 MILES eye safety study report (No. 25-42-0381-79) prepared by the U.S. Army Environmental Hygiene Agency.
- 7) Essentially, the M-16, machine gun and Dragon simulators were technically Class III-A and the remaining simulators were Class III-B. However, the hazards associated with interbeam viewing at close range with stabilized optics were considered very minimal in an engagement simulation scenario, and unaided eye hazards only existed under focused beam conditions between 1 and 6 meters from the exit aperture - which is not a hazard for the 105mm main gun due to barrel length. Furthermore, owing to their use with blanks the hazards for the M-16s and machine guns were considered minimal. In summary, MILES laser transmitters were slightly above suggested safety standards, but with allowance for the uncertainties within the biological data, the significant safety factors built into the protection standards, and the nature of the MILES scenario, the U.S.A.E.H.A. report stated:

"It was concluded that the MILES system did not present a personnel hazard in normal field use".

Thus, it was generally agreed, by XEOS, PM-TRADE and U.S.A.E.H.A. that MILES Engineering Development units were acceptable, but that the production units should not exceed the levels already tested for the Engineering Development models. Thus, put succinctly, the philosophy with respect to the production units was essentially;

"There is no practical way the MILES system can be Class I exempt. Since the ED models were Class III-A and III-B and these were acceptable to U.S.A.E.H.A., then let's not exceed these levels in production".

This now brings us to the final phase, from 1979 to the present.

- 8) XEOS enters the production phase of MILES. Detailed specifications are drawn up in many technical areas involving all aspects of MILES, including upper bounds on laser output energy, and the variations of these bounds with temperature. The maximum levels were intended to satisfy eye safety criteria.
- 9) Unfortunately, the eye safety criteria are written in terms of radiant exposure ($\text{Joules}/\text{cm}^2$), not energy (Joules). Thus, while well intentioned, the upper limits on laser output energy are not directly relevant to the eye safety problem.
- 10) Furthermore, in a somewhat ironic twist, the lasers supplied by RCA for production are actually more efficient than those supplied by RCA during the Engineering Development phase of the MILES program. As a result, at a given drive current, the production lasers emit more radiant power than the Engineering Development units. Therefore, it is necessary to utilize "select-in-test" resistors in the production MILES laser transmitters in order to reduce laser output. This reduction is necessary in order to comply with eye safety requirements which are discussed in detail in the remaining sections of this report.

Thus, we have the circumstance of production lasers with higher energy output, being accepted or rejected based on a maximum energy specification in an attempt to maintain "eye safety" levels, that already exceed the Class I exempt protection standards, which are based on a maximum radiant exposure criteria, and are therefore intrinsically different!

Obviously, this is not an ideal situation. However, neither is it as bad as one might think. As we shall see from the data included in this report, based on tests performed during June and July 1980 at XEOS by Mr. Wes Marshall, U.S.A.E.H.A., Dr. Paul Jacobs and Mr. Leo Taylor, XEOS, the results are in most cases quite similar to the E.D. test results. In the case of the M-16 and machine gun simulators, the production units exhibit almost exactly the same results as the E.D. versions.

- 1) The radiant exposure at the exit aperture of the transmitter is below the safety standard for the production units as it was for the E.D. units.
- 2) Due to focusing effects, the radiant exposure exactly on centerline from about 1 meter to 6 meters range exceeds the $.75 \text{ erg/cm}^2$ TB-MED-279 criteria for both the production and E.D. units. The production units are somewhat higher than the E.D. units but this difference has no material effect since a) both exceed TB-MED-279 levels and b) the range at which the radiant exposure falls below 0.75 erg/cm^2 is still about 6 meters. Since the M-16 simulators and the machine gun simulators normally require the firing of blanks in order to transmit laser energy*, and the safe zone for firing blanks at another trainee is comparable, the blank would constitute a greater safety hazard at close range. Beyond about 6 meters the radiant exposure drops below the 0.75 erg/cm^2 level, and the system is again Class I per TB-MED-279.

The only system which the recent tests indicated could present a possible problem was the 105mm main gun transmitter. Initial tests showed peak radiant exposure levels which were about 5.7 ergs/cm^2 at 1.4 meters range, on centerline, for focused production units, compared with about 3.6 ergs/cm^2 at 1.6m for the E.D. units.

* Blanks are employed to generate acoustic firing signals for the M-16 transmitter in the "Blank Fire Enable" mode. The transmitters may also be operated in a dry fire mode for boresighting or indoor training. In this mode, blanks are not used.

As a result, small, inexpensive, apertures were placed within the optical tube of the 105mm transmitters. This aperture has the effect of blocking some of the radiation which would otherwise exit the transmitter. With such apertures in place the radiant exposure levels returned to the measured values for the E.D. units, within experimental error (estimated to be \pm 15% repeatability, \pm 25% absolute accuracy).

SUMMARY

The detailed results of the June/July 1980 eye safety tests will soon be released in a comprehensive eye safety document by Wes Marshall, U.S.A.E.H.A. Based upon preliminary evaluation of a portion of this data (see section II, Results), the following conclusions are appropriate.

- 1) For the M-16 rifle simulators and the machine gun simulators no change in the present XEOS MILES specifications are recommended. The measured radiant exposure levels are slightly higher than the E.D. versions, but the increases will have no practical significance for the following reasons:
 - a) The systems will still be Classs III A systems anyway.
 - b) The very small increase in radiant exposure will not change the conclusion of report 25-42-0381-79 "Instruct troops using MILES not to aim their weapons at an individuals eyes at close range (5-10m)". This is true because, as described earlier, the radiant exposure levels for the production units of these simulators are below the protection standard at about 6m anyway.
 - c) The units tested represented "mean value" and "worst case" situations. Based on XEOS testing of a large number of production transmitters, a transmitter was selected for eye safety testing which most closely matched the mean-value energy output of the distribution and a second was tested which was the highest output transmitter allowed by the existing contract

specifications. The impact upon peak radiant exposure and maximum safe range was relatively small between these two cases and, again, had no significant effect upon the aforementioned conclusion from study 25-42-0381-79.

- 2) For the large weapon transmitters (e.g. the 105mm main tank gun simulator) it is recommended that rather than change the existing contract specifications (which are not directly appropriate to the eye safety problem) a better approach would be to allow for inclusion of an aperture in the optical tube which would have the effect of reducing the total radiated energy per pulse and also reducing the maximum radiant exposure to earlier E.D. levels. Thus, the recommended procedure would be as follows:
 - a) Use the existing contract specifications to limit maximum energy per pulse.
 - b) Evaluate that value of energy/pulse which produces maximum radiant exposure levels equal to the E.D. levels of study 25042-0381-79.
 - c) For those units which have output levels less than the maximum allowable values of the specification, but greater than the level determined in step b), incorporate an aperture to limit radiant exposure to E.D. levels.
 - d) For those units having output levels below this value, no aperture is necessary.

It is believed that these conclusions and recommendations will be the most practical, cost-effective method of insuring that production units of MILES comply with the results of the U.S. Army Environmental Health Agency report 25-42-0381-79 and the recommendations set forth therein.

RESULTS

A considerable amount of MILES radiant exposure data was obtained during June and July 1980 at XEOS by both XEOS and U.S.A.E.H.A. personnel. This data is summarized in Figures 2, 3, 4* and are plotted on the same scales as the original data for the E.D. devices. Let us examine the data in some detail.

Figure (2) plots radiant exposure per pulse (Joules/cm^2) vs viewing distance (meters), for the "Small Weapon MILES Transmitters" (i.e. the M-16 Rifle simulator and the various machine gun simulators). The data shown on Figure 2 is the maximum possible radiant exposure which could be measured through a 7mm aperture corresponding to the diameter of a fully dark adapted human pupil. The aperture and detector were moved up and down, right and left and rotated in all possible directions (i.e. "pitch", "roll", and "yaw") until the absolute maximum reading is achieved at a given range. The range values are then varied systematically, and occasional points, at random, are "repeated blind" (i.e. repeated by different personnel not aware of the previously measured values). From this procedure we have determined that the repeatability of the measurements (e.g. how close are two "independent" readings of the same point) is about $\pm 15\%$. The absolute accuracy (in the sense of tracability to National Bureau of Standards values) is estimated at $\pm 25\%$. This is typical of radiometric measurements of this type.

*Note that the figure numbers correspond to those of report U.S.A.E.H.A. 25-42-0381-79 to allow direct comparison. These are the first three, and only, figures of this report other than those within appendix.

Nonionizing Radn Prot Sp Study No. 25-42-0381-78, Aug-Dec 78

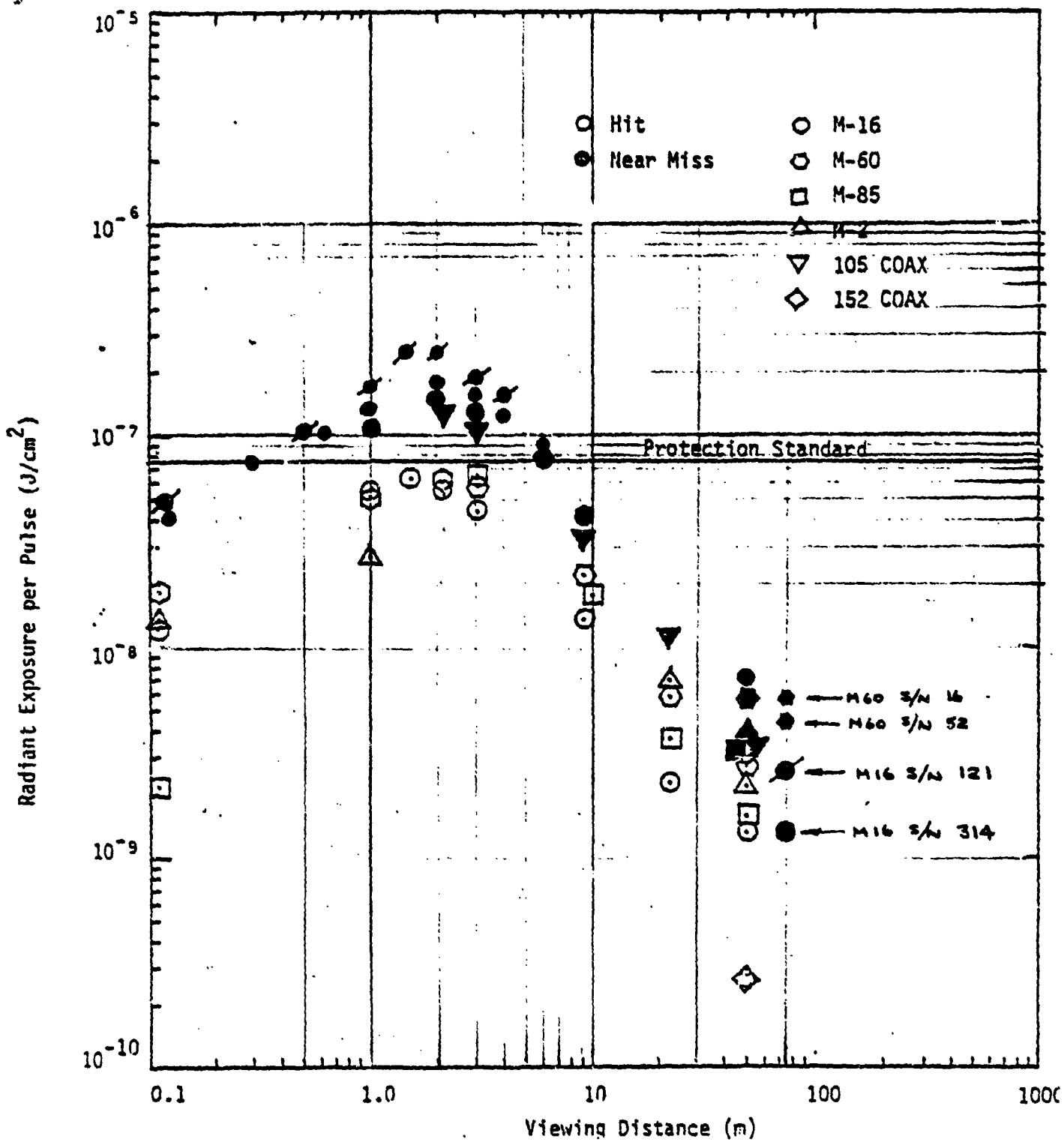


Figure 2. Radiant Exposure Versus Viewing Distance as Measured Through
a 7-mm Aperture for the Small Weapons MILES Transmitters.

Nonionizing Radn Prot Sp Study No. 25-42-0381-79, Aug-Dec 78

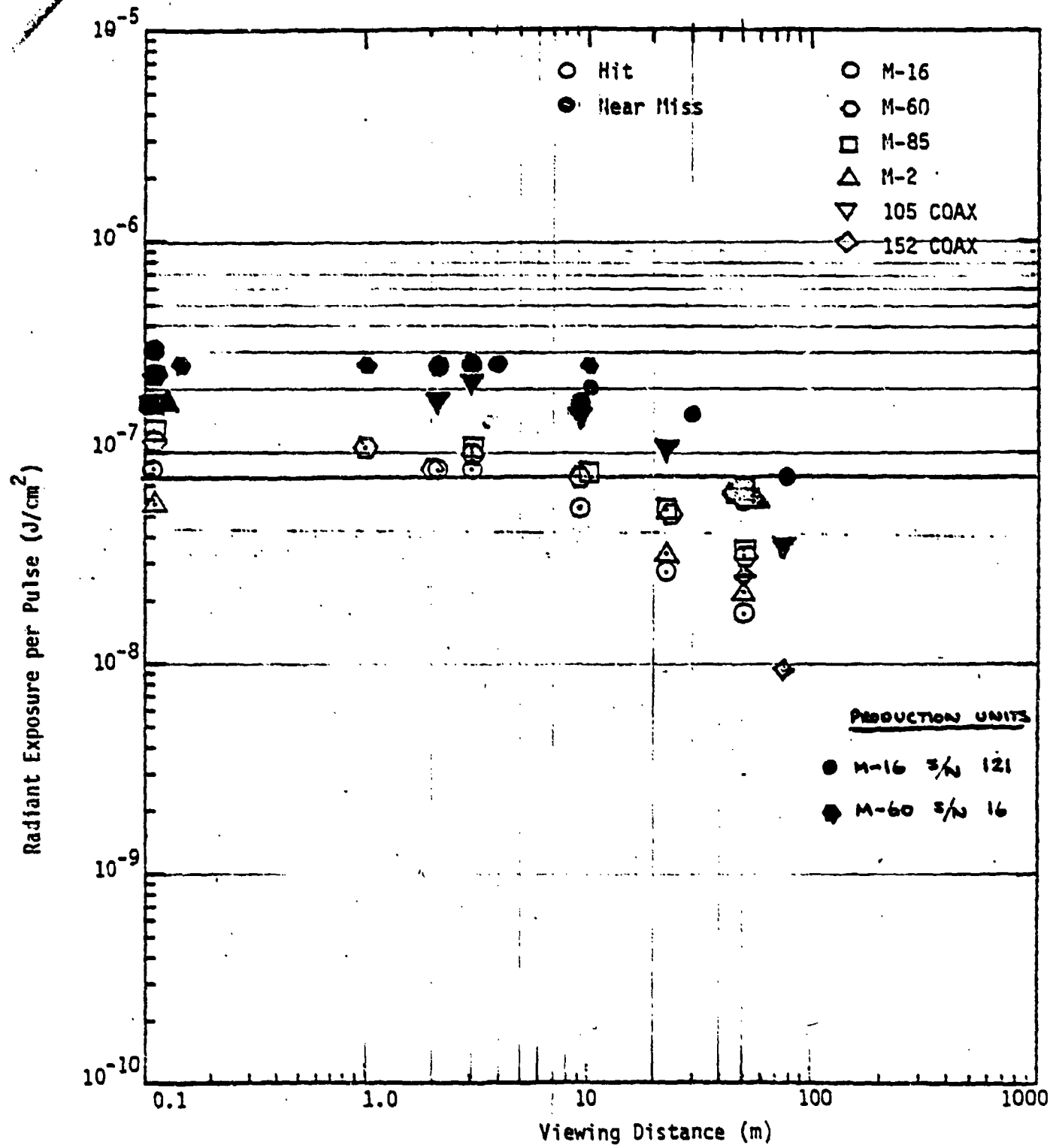


Figure 3. Radiant Exposure Versus Viewing Distance as Measured Through a 8-cm Aperture and Focussed to 7-mm for the Small MILES Transmitters.

Nonionizing Radn Prot Sp Study No. 25-42-0381-79, Aug-Dec 78

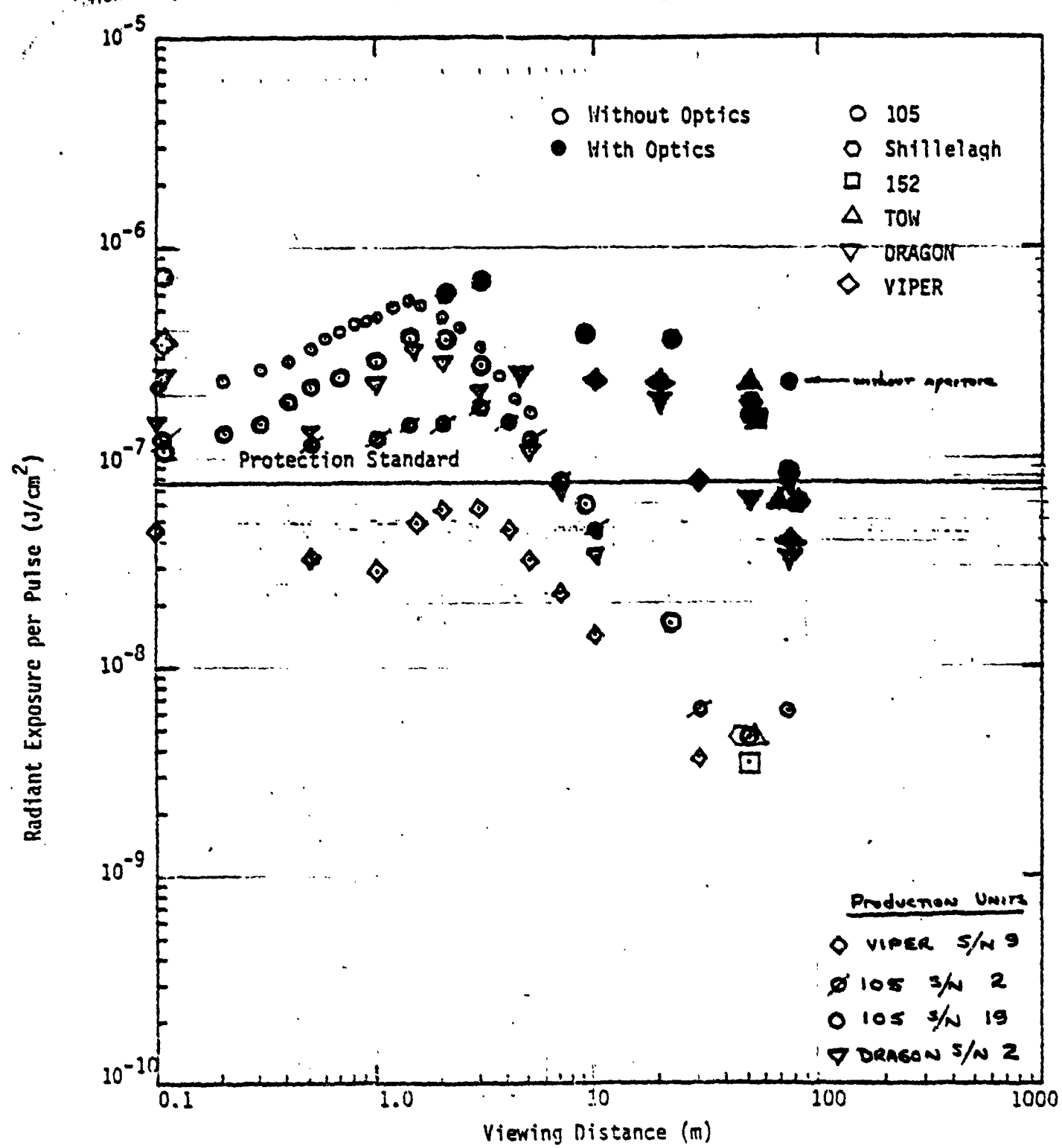


Figure 4. Radiant Exposure Versus Viewing Distance Through a 7-mm Aperture for Unaided and Optically Aided Viewing of the Large gun transmitters.

Figure 2 taken from U.S.A.E.H.A. study 25-42-0381-79, August - December 1978* shows the original MILES E.D. test data. Superimposed on this plot is the data taken on MILES production units during June - July 1980. The following observations are appropriate:

- 1) The data for the production units is generally quite close to that for the E.D. units.
- 2) The spread in the data between "mean value" units (e.g. M-16 S/N 314) and "upper limit" units (e.g. M-16 S/N 121) is really not very great when plotted in terms of radiant exposure.
- 3) The original E.D. units exceeded the protection standard out to about 6 meters. The production units are almost identical, perhaps extending this value to 7 meters, but still less than the 10 meter value described earlier in the U.S.A.E.H.A. report summary.
- 4) The same type of data spread appears for the M-60 transmitters.
- 5) In summary, the small weapon MILES production transmitters, which are being evaluated per production specifications based upon energy output, are not substantially different from the E.D. units when evaluated on the basis of radiant exposure levels appropriate to T.B. MED 279 eye safety standards. For this reason it is recommended that the present specifications for these transmitters, while technically not directly relevant to the eye safety question, may be retained because they, in effect, result in acceptable radiant exposure values.

*The data was taken during 1978, but the report was released and dated during 1979.

Figure 3 shows the data for the production units, relative to the E.D. units, for the M-16 and M-60 MILES transmitters measured through an 80mm lens and focused within a 7mm aperture simulating a fully dark adapted human pupil. This is the TB MED 279 test for stabilized optics. Only the worst case (i.e. maximum allowable energy per the MILES specifications) transmitters were tested. The values, again, are somewhat higher than the E.D. values, and do not cross the protection standard until about 75m. Thus, there is no significant change from the E.D. units except perhaps a slight increase in the safe range for viewing with stabilized optics.

Rather than recommend a change in the specifications it is recommended, as has been recommended in prior XEOS eye safety reports, and also in U.S.A.E.H.A. study 25-42-0381-79, all stabilized sights used in MILES should employ KG-3 optical filters which would completely eliminate all eye safety problems with respect to the stabilized optical intrabeam viewing of any MILES laser. All viewing optics on the XM-1 tank already have built-in laser protection in the form of KG-3 filters. In the event that cost implications negate inclusion of KG-3 filters for the M-60 tank or M-115 APC viewing optics, the next best recommendation would be to utilize the existing clip-on sunlight filters - which have a 20% transmission at the GaAs wavelength. The use of this existing filter would result in all MILES transmitters being safe for viewing by stabilized optics at any range. In the event that both of these recommendations are not followed, the system will require warning labels advising against intrabeam viewing with stabilized optics out from about 50 - 100 meters.

Finally, we turn to Figure 4. Here we have plotted the data for the viper, 105mm main gun and dragon transmitters. The data for the 105 shows values for two separate production units (S/N 2 and S/N 19) to show the spread which can occur between median and maximum acceptable total energy per existing production specifications.

Basically, the data is, again, not very different from the E.D. values except that the data for the "maximum level" 105 MILES transmitter is beginning to show potential problems for the stabilized optics intrabeam viewing case. Again, adopting the use of KG-3 filters would completely solve this problem, and even the use of sunlight filters would essentially alleviate the difficulty. Failing these recommended actions, the only practical recourse is to insert optical apertures within the optical housings of those large weapon transmitters which exceed the median value of the production units.

The fact that the radiant exposure levels without optics exceed the protection standard out to about 7m is not really a significant problem (the E.D. units had the same difficulty) because the barrel of the 105mm main tank gun is nearly this long, so one could not, even accidentally, position ones eye at a point any closer to the transmitter. However, the problem of the intrabeam viewing with stabilized optics, of a worst case high power MILES transmitter is potentially more serious, and it is recommended that filters be considered for all MILES stabilized optics.

RECOMMENDATIONS

The following are recommendations based upon the results of tests performed at XEOS during June/July 1980 to measure the radiant exposure levels characteristic of MILES production laser transmitters.

- 1) As discussed in Sections I and II of this report, it is recommended that no changes be made to MILES production specifications. The existing specifications relevant to MILES production laser transmitter output set an upper bound on laser output energy per pulse. The T.B. MED 279 eye protection standards are written in terms of radiant exposure (energy per unit area). Thus, reducing the numerical value of the maximum allowable peak energy per pulse would not insure eye safety. Furthermore, altering the specifications to prescribe upper limits on radiant exposure would not be practical as it would require completely new measurements and measurement equipment late in a production program.
- 2) The small weapon (i.e. M-16, M-60, M-85 and M-2) simulators will be Class III-A regardless of production specifications. Thus, it is recommended that no changes be made to the production specifications for these transmitters.
- 3) The large weapon transmitters (105mm, 152mm, TOW, SHILLELAGH and DRAGON) will be Class III-B. This was the case for the MILES E.D. transmitters. Therefore, it is recommended that KG-3 filters be used on all stabilized viewing optics employed in MILES. This will eliminate any potential hazard associated with viewing a MILES laser through such optical systems.

- 4) As a back up, it is recommended that radiation restricting apertures be used in the optical tubes of those large weapon transmitters whose output energy is above the E.D. levels*. This will have the result of causing the radiant exposure levels of the production MILES units to remain equal to or below the E.D. levels. Since the E.D. levels were determined by U.S.A.E.H.A. to be acceptable, the production units would then achieve this status.
- 5) If neither recommendations 3 or 4 are adopted it is likely that warning labels will be required to avoid intrabeam exposure with stabilized optics for ranges to about 100 meters. Since this is not desirable, it is strongly suggested that both recommendations 3 and 4 be implemented. The former is in concert with Army philosophy. All optics on the XM-1 tank already have permanent KG-3 filters to avoid laser hazards to personnel from Nd:YAG laser rangefinders or laser target designators. These filters are also very effective at GaAs wavelengths. Finally, the latter recommendation has already been implemented, on a test basis, by XEOS.

* This recommendation has already been implemented.



2150-OR 1-46 2
DEPARTMENT OF THE ARMY
U. S. ARMY ENVIRONMENTAL HYGIENE AGENCY
ABERDEEN PROVING GROUND, MARYLAND 21010

Mr. Marshall/cw/584-3932

HSE-RL/WP

SUBJECT: Nonionizing Radiation Protection Special Study No. 25-42-0381-79,
Final Hazard Evaluation of the Engineering Development Model of the
Multiple Integrated Laser Engagement Simulator, August - December
1978

Project Manager for Training Devices
Naval Training Equipment Center
Orlando, Florida 32813

A summary of the pertinent findings and recommendations of the inclosed report follows:

a. A laser radiation protection special study was performed on the Engineering Development version of the Multiple Integrated Laser Engagement System (MILES). Laser simulators using Ga-As lasers designed for use with rifles, machine guns, tank weapons, and missiles were evaluated.

b. The rifle, machine-gun, and Dragon Simulators were technically Class IIIa Laser Systems according to present Army standards. Nevertheless, these units would not present a real hazard during normal field use. Since the beam radiant exposure exceeded protection standards at the beam waist (approximately 2.5 m in front of the laser), intrabeam viewing within 6 m was not advised. The other systems were Class IIIb systems and the beam fell below Army protection standards also at about 6 to 9 m. Current protection standards appear to have a built-in safety margin of 12 below an actual retinal burn threshold based on the work performed at Letterman Army Institute of Research.

c. It was concluded that even though protection standards were slightly exceeded, the actual risk is minimal. This would certainly be true if those persons using the simulators are instructed not to point the devices at the face and eyes of another individual at very close range. Blank ammunition would normally be fired with the transmitter and such precautions would therefore be necessary anyway.

HSE-RL/WP

SUBJECT: Nonionizing Radiation Protection Special Study No. 25-42-0381-79,
Final Hazard Evaluation of the Engineering Development Model of the
Multiple Integrated Laser Engagement Simulator, August - December
1978

d. It was recommended that warnings be placed in the MILES manuals instructing personnel not to stare into the laser transmitter or at close range with optics, that tank optics not be used within 75 m without protective filters, that an exemption label be attached to the device or shipping container and that troops using the MILES be instructed not to point the MILES transmitters at the eyes or face of another individual at very close range.

1 Incl
as (5 cy)

GORDON M. LODDE
LTC, MSC
Director, Radiation and
Environmental Sciences

CF:

HQDA (DASG-PSP)
HQDA (DAMA-CSS-D) (3 cy)
Cdr, DARCOM (DRCSG) (10 cy)
Cdr, HSC (HSPA-P)
Cdr, TRADOC (ATPR-HR-S)
Cdr, TRADOC (ATMD)
Cdr, USAMRDC (SGRD-OP)
Cdr, LAIR (SGRD-WB-NR) (3 cy)



DEPARTMENT OF THE ARMY
U. S. ARMY ENVIRONMENTAL HYGIENE AGENCY
ABERDEEN PROVING GROUND, MARYLAND 21010

HSE-RL/WP

NONIONIZING RADIATION PROTECTION SPECIAL STUDY NO. 25-42-0381-79
FINAL HAZARD EVALUATION OF THE ENGINEERING
DEVELOPMENT MODEL OF THE MULTIPLE INTEGRATED
LASER ENGAGEMENT SIMULATOR
AUGUST - DECEMBER 1978

1. AUTHORITY. Letter, DRCPM-TND-SE, Office of the Project Manager for Training Devices, 4 October 1978, subject: Request for Reevaluation of the Multiple Integrated Laser Engagement System (MILES), and indorsement thereto.

2. REFERENCES. A list of references is provided in Appendix A.

3. PURPOSE. To evaluate the potential health hazards associated with the use of the Engineering Development (ED) version of the Multiple Integrated Laser Engagement Simulator (MILES) by measuring ED models before and after Operational Testing, Phase II, and to make recommendations regarding the design and use of this equipment to avoid exposure of personnel to potentially hazardous laser radiation from this device.

4. GENERAL.

a. Advanced Development Version. A hazard evaluation was performed on the Advanced Development (AD) version of the MILES system during September and October 1974 (reference 7, Appendix A). This version used nominal 5-watt and nominal 1-watt gallium-arsenide (Ga-As) single-junction laser diodes. It was concluded in that study that these devices did not present a retinal burn hazard under normal operating conditions, although the lasers did slightly exceed conservative, "point source," laser protection standards and did not qualify as Class I laser systems. Although optically-aided viewing was considered potentially hazardous at close viewing distances from the laser, it was concluded that hand-held binoculars did not pose a significant risk due to the instability of both the binoculars and the laser transmitters at the normal target engagement ranges that are used in most training exercises.

b. Theoretical ED Version. A preliminary theoretical hazard evaluation was made of the ED model during January-February 1976 (reference 8, Appendix A). A 10-watt and a 20-watt laser combination was originally planned for this version. It was concluded from theoretical calculations that this system would present a potential personnel hazard within 20 m for unaided viewing or within 500 m for optically aided viewing. It was recommended

Distribution limited to US Government agencies only:
test and evaluation; Jan 79. Other requests for this
document must be referred to Project Manager for Training
Devices (US Army), Naval Training Equipment Center,
Orlando, FL 32813.

Nonionizing Radn Prot Sp Study No. 25-42-0381-79, Aug-Dec 78

that the system be modified, if at all feasible, to either use less power or to use an extended source laser to reduce personnel hazards. It was further concluded that biological data were lacking concerning hazards of pulsed Ga-As lasers and that it was necessary to determine what degree of eye safety was required.

c. Early ED Version. A study of early models of the MILES was conducted during February and March 1977 (reference 9, Appendix A). Field usable models of the MILES systems were not available at the time of this study. Measurements were made on a general purpose unit which used the actual laser diodes and lens configuration of the ED system but used a physically larger version of the pulse coding electronics which could be varied to represent the various transmitters. A sample of an attenuator was also measured for transmission. This attenuator would be installed in the beam path of the M-16 rifle transmitters if necessary.

d. Revised Study of the ED Version. A revised study of the MILES ED version was conducted during May 1978 (reference 10, Appendix A). Simulators for the rifle, machine-gun, Dragon and Shillelagh missiles, and 105-mm and 152-mm main guns were measured. It was found that the Dragon, rifle, and machine-gun simulators were Class IIIa. All other systems were Class IIIb. In addition, the beams for all systems were found to shrink in size at approximately 2.5 m from the laser before again expanding. On most of the simulators (except for the Dragon), nearly all the beam would pass through a 7-mm aperture at this distance. It was therefore recommended that a warning be placed in the MILES manuals that personnel not stare into the beam at very close range or use unfiltered tank optics at less than 75 m. It was concluded, however, that the MILES system did not present a personnel hazard in normal field use.

e. Biological Studies. After the preliminary hazard evaluation and throughout the development of the MILES ED system, several meetings were held with representatives of the Letterman Army Institute of Research (LAIR), San Francisco, CA; Xerox Electro-Optical Systems (EOS), Pasadena, CA (Engineering Development Manufacturer); Office of the Project Manager for Training Devices (PM TRADE), Orlando, FL; and this Agency for the purpose of discussing the assessment of the potential eye hazards of MILES. Research with Rhesus monkeys was initiated concerning the effect of pulse additivity on coded pulses and the necessary protection standard for Ga-As devices. Pulse additivity studies on 1, 2, 3, and 6 pulses at the MILES clock rate and a neighboring wavelength (1064 nm) had been completed. Also, monkeys had been exposed to actual coded Ga-As pulses similar to the present MILES code. An Erbium laser was used to verify the presently used single-pulse protection standard at 850 nm (a wavelength very close to Ga-As, 905 nm), however, no repetitive-pulse data from this laser were available at the time of this study. A very brief summary of the LAIR studies is presented in Appendix B.

Nonionizing Radn Prot Sp Study No. 25-42-0381-79, Aug-Dec 78

f. Inventory. At the time of this study, ED simulators for the following weapons had been manufactured:

- (1) M-16 rifle - 120 each
- (2) M-60 machine gun - 12 each
- (3) M-2 machine gun - 29 each
- (4) M-85 machine gun - 18 each
- (5) 105 mm tank gun - 18 each
- (6) 152 mm tank gun - 8 each
- (7) Dragon missile - 12 each
- (8) Shillelagh missile - 8 each
- (9) TOW missile - 8 each
- (10) Viper missile - 23 each

g. Abbreviations. A table of radiometric abbreviations and units is provided as Appendix C.

h. Laser System Operation. The MILES system was developed to provide two-sided, real-time simulation of infantry small arms, tank and missile engagement without the use of live ammunition. The present version of the ED MILES system consisted of one laser per transmitter rather than two lasers per transmitter as originally conceived. The two beam-spreads for the "hit" and "near-miss" were accomplished through pulse coding and computer interpretation rather than through the use of two actual laser beams with differing beam divergences. The "hit" pulses were formed by operating the same laser diode at a lower peak power than the "near-miss" pulses. The completed MILES ED system is illustrated in Figure 1.

i. Laser Pulse Coding. The laser pulses from each type of weapon simulated were coded to distinguish between weapons and to realistically simulate the duration and frequency of firing. A series of subgroups called "words" were emitted by all transmitters. Each "kill" word consisted of six laser pulses in 11 time slots. Each "near-miss" word also consisted of six laser pulses in 11 time slots. Time slots were spaced 333 μ s apart. Each round fired consisted of "kill" words followed by "near-miss" words. Normal firing rates were used for each weapon. Part of the "near-miss" words may necessarily be terminated on rapid-fire systems. Pulse coding for the various systems is listed in Table 1. Some of the weapon systems which may

Nonionizing Radn Prot Sp Study No. 42-0376-78, May 78

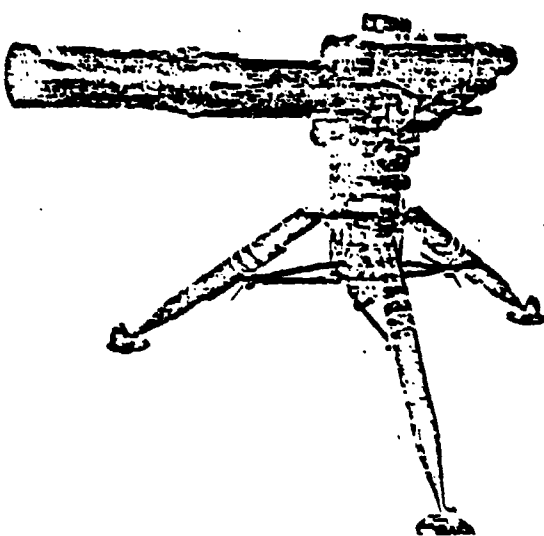
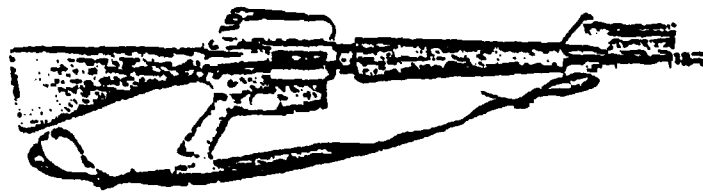


Figure 1. Photograph of the Nominal 2-Watt MILES ED Transmitter Mounted on an M-16 Rifle (Upper) and a Nominal 5-Watt Transmitter Mounted on a Missile Launcher (Lower)

Nonionizing Radn Prot Sp Study No. 25-42-0381-79, Aug-Dec 78

be fired either with or without blanks have different coding for each condition.

TABLE 1. PULSE CODING FOR THE VARIOUS MILES SYSTEMS. CODES FOR THE INDIVIDUAL "KILL" AND "MISS" WORDS ARE NOT LISTED

Weapon	Transmitted Code and Sequence Per Round
M-16 Rifle	
Dry Fire	4 Hit Words, 20 Miss Words, Automatic
Dry Fire	4 Hit Words, 128 Miss Words, if Semi-Automatic
Blank Fire	4 Hit Words, 128 Miss Words or Less, Dependent Upon the Starting of the Next Round
M-2, M-85, M-60 Machine Gun	
Dry Fire	4 Hit Words, 20 Miss Words
Blank Fire	4 Hit Words, 128 Miss Words or Less, Dependent Upon the Starting of the Next Round
Coax Machine Gun	4 Hit Words, 20 Miss Words, for Either Dry or Blank Fire
Viper, 105-mm Main Gun, and 152-mm Main Gun	8 Hit Words, 8 Man Hit Words, 128 Miss Words
Shillelagh Missile	32 Messages, 8 Hit Words/Message in 10 Second Track Period, 8 Man-Hit Words Short Range Inhibit for 1st 16 Messages - Complement of Missile-Hit Words, Front Coax Hit Laser
Dragon Missile and Tow Missile	32 Messages, 8 Hit Words/Message in 10 Second Track Period, 8 Man-Hit Words
Controller Gun	
Univ. Kill	16 Kill Words
Miss	8 Heavy Miss Words, 18 Light Miss Words

5. FINDINGS.

a. Laser Output Energy. Extensive downrange measurements were taken on a few MILES devices prior to Operational Test II (OTII). Output energy measurements on a number of devices were performed on the devices after OT II. In addition, Xerox personnel had taken output energy measurements on a number of devices before OT II. A summary of the average output energy measurements is provided in Table 2. A more complete listing is provided in Appendix D.

Nonionizing Radn Prot Sp Study No. 25-42-0381-79, Aug-Dec 78

TABLE 2. AVERAGE LASER OUTPUT PARAMETERS

Device	Mode	Energy Per Pulse (nJ)		Before OT II*
		After OT II	Before OT II	
M-16	Hit	23.3 \pm 7		27.3 \pm 8.4
	Miss	91.7 \pm 25		102 \pm 17
Controller	Both	30.9 \pm 12.7		37.8 \pm 12.1
M-2, M-85, M-60 Machine Gun	Hit	31.1 \pm 13.9		40 \pm 15
	Miss	107 \pm 34.4		108 \pm 34
105 and 152 Main Gun	Hit	233 \pm 61		250 \pm 113
	Miss	281 \pm 89		316 \pm 112
105 and 152 Coax Machine Gun	Hit	40.5 \pm 25		59.9 \pm 23
	Miss	82.9 \pm 13		118 \pm 33
Shillelagh and Tow Missile	Hit	244 \pm 45		260 \pm 55

* As measured by Xerox on units listed in Appendix D.

b. Irradiance Versus Range. Figures 2 through 4 illustrate the theoretical corneal beam radiant exposure produced when viewing through various optical instruments and by the unaided eye at various viewing distances. Radiant exposure values are given for a 7-mm exit aperture. Laser beam divergence was not easily defined for the MILES transmitters. Formulas derived for a gaussian type output would not provide an accurate determination of corneal radiant exposure at various distances unless measurements were taken at those distances; however, the central portion of the beam on most of the transmitters had a divergence between 1 and 2 mrad. In addition, 20 percent of the laser energy diverged very rapidly at the laser exit. This portion of the beam originated from an extended source and should not enter into safety calculations. Figure 5 is an infrared photograph of one of the MILES transmitters projected on a flat surface 22 m away.

c. Beam Waist. The output beam from all the MILES simulators, except for the Dragon, narrowed to a small diameter beam waist approximately 2 m from the laser. Due to this narrowing of the beam the energy passing through

Nonionizing Radn Prot Sp Study No. 25-42-0381-79, Aug-Dec 78

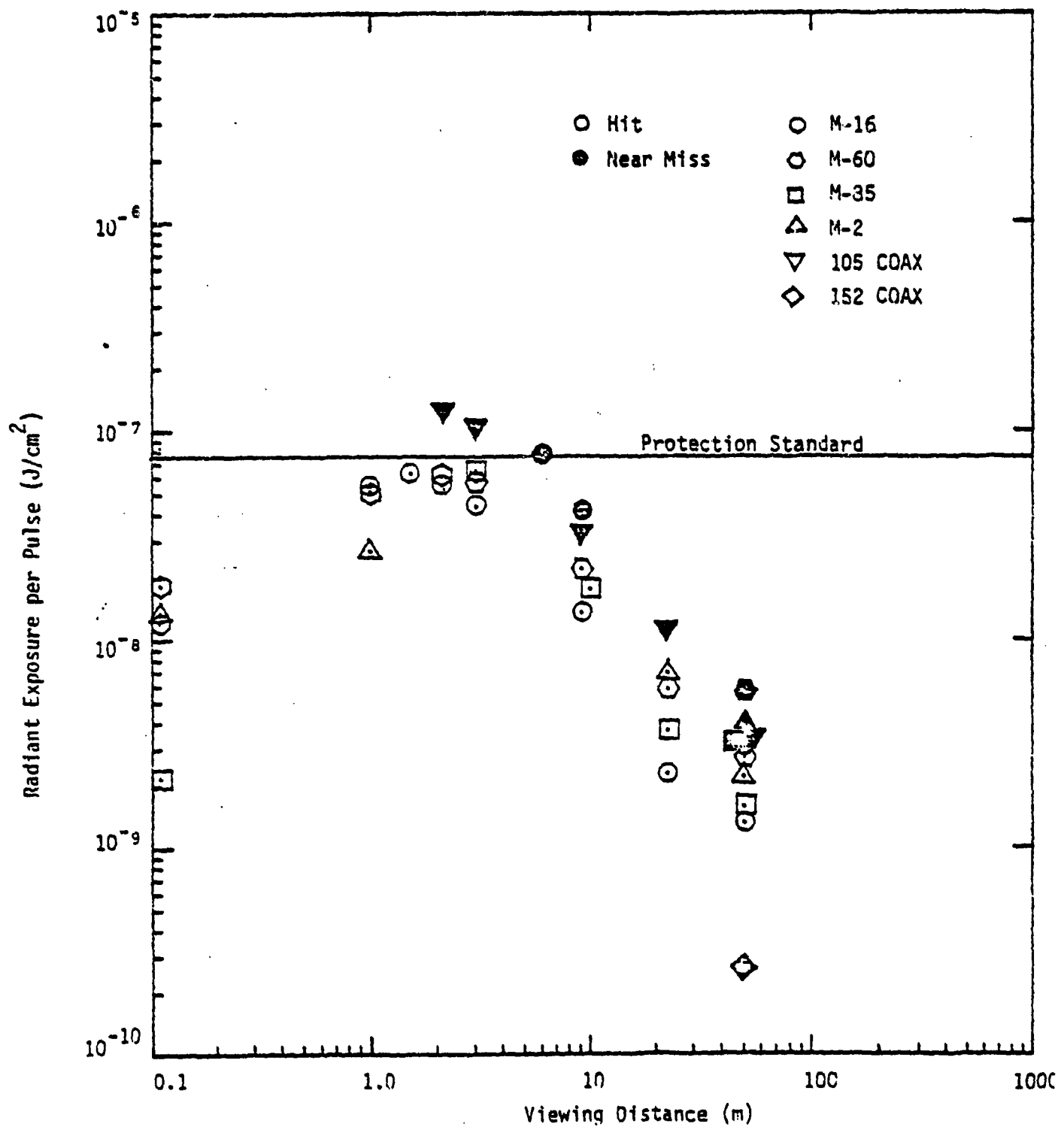


Figure 2. Radiant Exposure Versus Viewing Distance as Measured Through a 7-mm Aperture for the Small Weapons MILES Transmitters.

Nonionizing Radn Prot Sp Study No. 25-42-0381-79, Aug-Dec 78

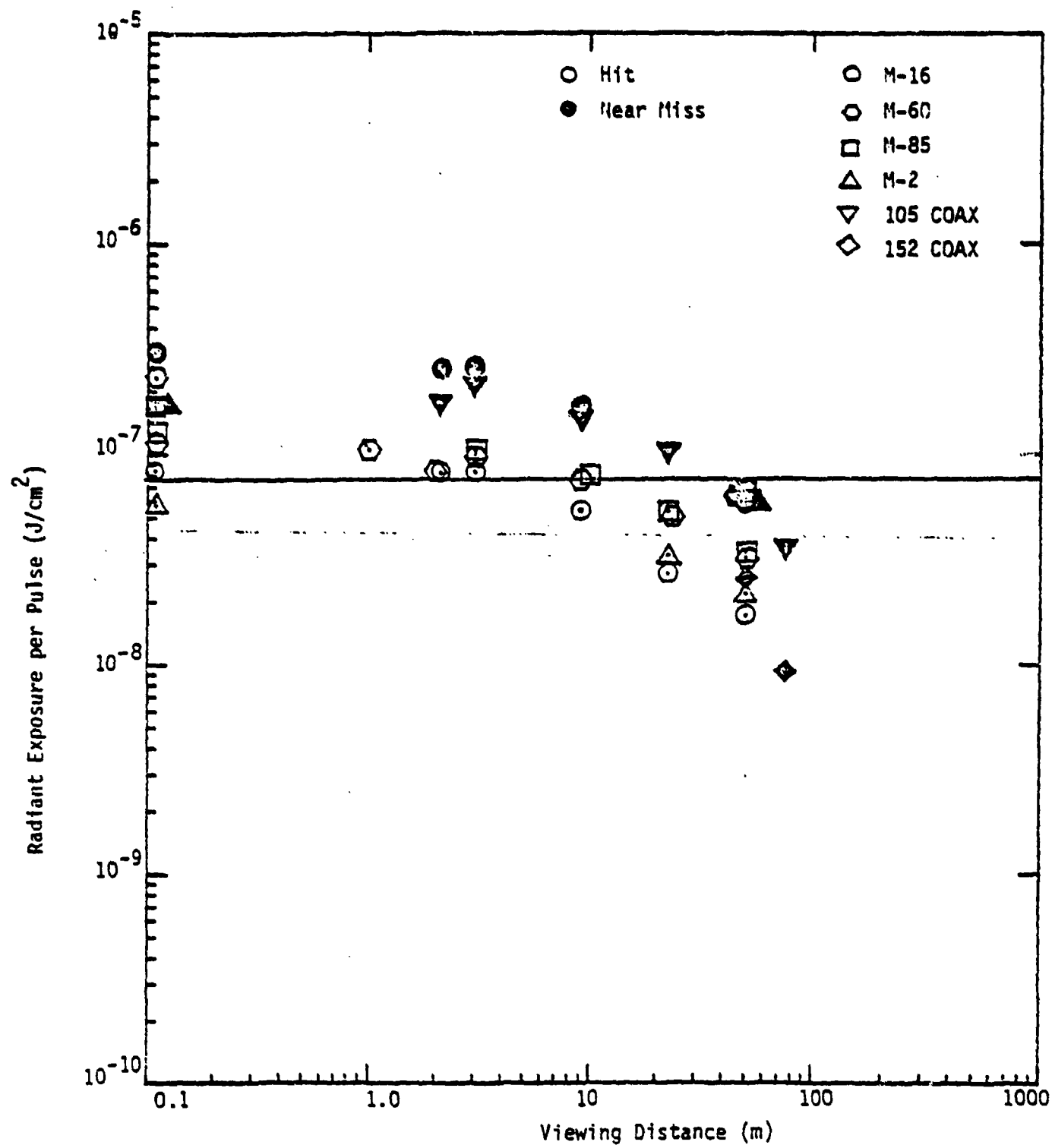


Figure 3. Radiant Exposure Versus Viewing Distance as Measured Through a 3-cm Aperture and Focussed to 7-mm for the Small MILES Transmitters.

Nonionizing Radn Prot Sp Study No. 25-42-0381-79, Aug-Dec 78

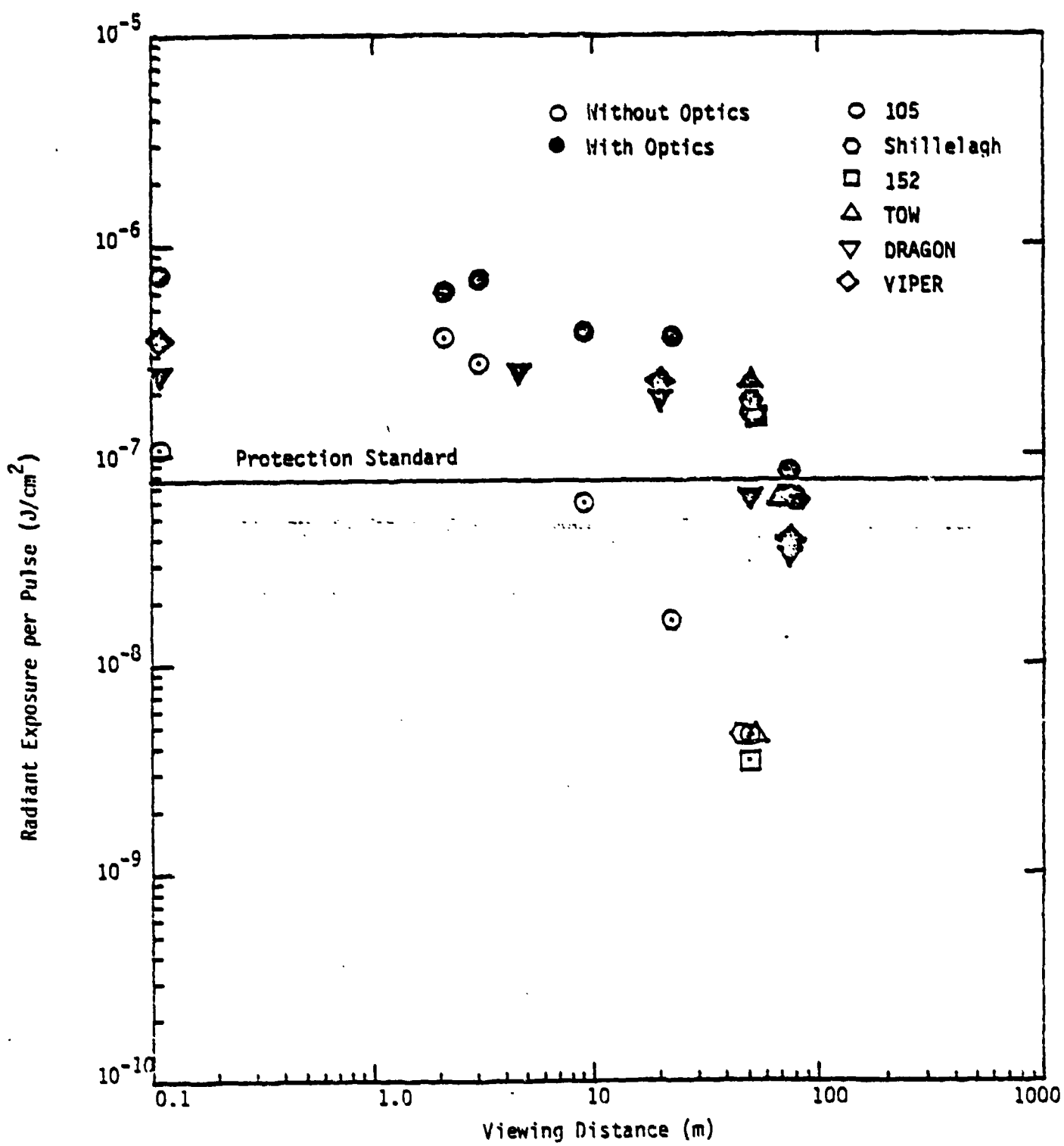


Figure 4. Radiant Exposure Versus Viewing Distance Through a 7-mm Aperture for Unaided and Optically Aided Viewing of the Large gun transmitters.

Nonionizing Radn Prot Sp Study No. 25-42-0381-79, Aug-Dec 78

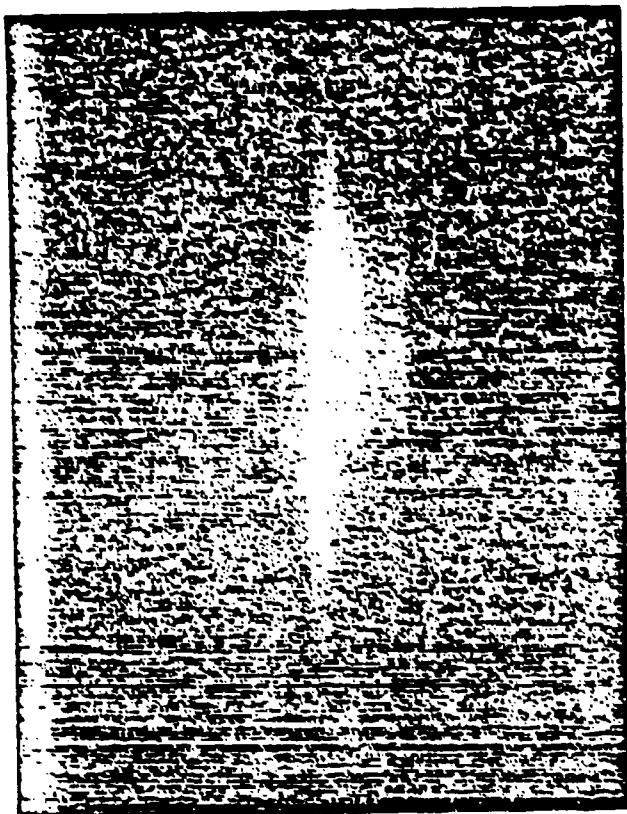


Figure 5. Downrange Photograph of the MILES Transmitter Beam Projected on a Flat Surface 22 m From the Transmitter.

Nonionizing Radn Prot Sp Study No. 25-42-0381-79, Aug-Dec 78

a 7-mm aperture exceeded protection standards for a localized area within 6 m to 9 m for all MILES transmitters except the Dragon unit. Therefore, operating the MILES transmitters while pointed at an individual's eye at close range (6-9 m) presents a theoretical hazard to the eye. Of course the likelihood of a 7-mm beam being pointed at a 7-mm pupil is very low. For the machine-gun or rifle simulators, this possibility of a hazardous exposure is still more remote because protection standards are exceeded only slightly for these devices.

d. Transmission of Optical Sights.

(1) Transmission measurements were taken on one set of M60 tank optics using a MILES transmitter as a source. The M105D telescope had a transmission of 38 percent. The M-36 commander's periscope had a transmission of 45 percent with unity power and 26 percent through the magnifying portion. The gunner's periscope had 11-percent transmission on unity power and 13-percent transmission through the magnifying portion. A clip-on sunlight filter had a measured transmission of 20 percent. The use of the Sunlight filter in conjunction with any of the optics in this tank provided complete protection against any of the MILES transmitters at any distance. However, measurements taken on one set of optics should not be applied to magnifying optics in all vehicles until more measurements are taken.

(2) All viewing optics on the XM-1 tank have built-in laser protection (KG-3 in all sights or viewing ports). Therefore, no hazard exists from viewing the MILES transmitters through these optics.

(3) On the M-551 Sheridan Vehicle, the commander's telescope is equipped with a built-in filter (12.5-mm, BG-38) which has an incredibly high density at 905 nm(OD=27). The gunner's telescope has a filter(2.5 mm of BG-18) in the filter wheel which also has a very high density at the MILES wavelength.

(4) The DRAGON Tracker Eyepiece has a laser protective coating which has a transmission of approximately 15-percent at 905 nm. Attenuation in the rest of the optical train would most likely reduce the transmission to acceptable levels.

(5) The TOW optics have a transmission of about 5-percent at the Ga-As wavelength which is sufficient protection for any of the MILES simulators.

e. Ocular Image Characteristics.

(1) For Ga-As lasers, the retinal image (produced at close viewing distances when the laser beam is collimated) is not a diffraction-limited circular image as can be attained most nearly by gas discharge lasers. Instead, the retinal image created by these simulators is a line image or, in some cases for similar devices, a group of line images; one for each laser

Nonionizing Radn Prot Sp Study No. 25-42-0381-79, Aug-Dec 78

diode junction. Therefore, the application of corneal maximum permissible exposure criteria derived for gas lasers may be overly conservative at close viewing distances. Extended source hazard criteria may not be used because these sources do not subtend a viewing angle in excess of a min (3.7 mrad). Any attempt to use extended source hazard criteria for these small sources will result in more conservative results than point-source hazard criteria. Extended-source hazard criteria are overly conservative even for sources slightly above a min since these standards were derived for very large retinal image sizes (1 mm) and do not allow for additional microscopic retinal cooling effects for smaller sources.

(2) The retinal image produced at short viewing distances when the laser beam is focused is larger than for the collimated situation. The retinal image size depends on the size of the laser diode junction, the characteristics of the laser optics, and the distance between the laser and observer. Since the laser beam may be focused, it is possible for the eye to collect nearly all of the radiant power available from the laser. Due to the fact that the laser diode in this device is extremely small, intrabeam viewing levels of the laser beam in the focused mode would be above current protection standards.

6. DISCUSSION.

a. Direct Viewing of the Collimated Beam.

(1) The hazard from the laser systems discussed in this report are limited to the unprotected eyes of individuals viewing the laser system from within the direct or specularly reflected laser beam at close range. The laser protection standards for intrabeam viewing of a Ga-As laser with a pulse duration of 100 ns for both a single pulse and for multiple pulses are shown in Figures 2 through 4. Viewing multiple pulses is considered more hazardous than viewing single pulses even if the time interval is sufficient to allow for thermal cooling. The LAIR studies bear this out. However, the use of the normal C_p repetitive-pulse correction factor may be overly conservative since only a maximum of six pulses are emitted in succession for these laser transmitters and the original biological data for repetitive pulses upon which the protection standard was based were taken for 0.5-s pulse trains.

(2) From a composite study of presently available repetitive-pulse biologic data, it was determined that a safety margin of at least 10 existed between present standards and the level known to cause chorioretinal burns in rhesus monkeys at the MILES repetition rate. It is desired, however, that this margin of safety be maintained in protection standards for all lasers due to a variety of conditions which may reduce this margin (measurement error, hot spots, sensitive individuals, etc.). Further, not all biologic data are in complete agreement.

Nonionizing Radn Prot Sp Study No. 25-42-0381-79, Aug-Dec 78

(3) Retinal injury data collected under an Air Force Contract (reference 12, Appendix A) by Technology Incorporated using 10- μ s Argon and 700-ns Neodymium laser pulses show that pulsed exposures separated by approximately 1 second were almost linearly additive, but if separated by 1 ms there was very little additivity for a train of six pulses. In the face of much apparently conflicting threshold data for repetitive pulses there had been no serious effort to update present laser exposure limits for these types of lasers before the recent work at LAIR. It is unlikely that there will be any changes made in national consensus standards or Federal safety standards until more corroborative data are published.

b. Viewing with Optical Instruments.

(1) Viewing with optical instruments is generally considered more hazardous than viewing with the unaided eye since more of the energy may enter the eye. However, several effects tend to reduce this added hazard as listed below:

(a) The telescopic optics attenuate a certain percentage of the incident radiation due principally to reflection losses at the lens surfaces.

(b) Part of the incident radiation may not enter the eye due to possible mismatching of the viewer's pupil size with the exit pupil diameter of the device.

(c) The laser source is increased in size (actually slightly reducing the retinal irradiance) possibly to an extent that the laser diode becomes an extended source at close range.

(d) The hand-held MILES transmitters cause the beam to draw a figure eight in space due to the blank firing. Anyone located within the beam would receive less of a laser exposure due to this effect.

(e) The effective beam divergence was measured with a 7-mm aperture. Due to irregularities in the laser output irradiance distribution, the effective divergence with optics is somewhat larger.

(2) Although these effects are known to exist, quantitative values may not now be assigned to all these effects unless a considerable number of measurements are taken on each optical sighting device used, unless further bioeffects data are obtained, and unless measurements are made of the actual Ga-As laser transmitters used in a particular application. Theoretically, these missile and tank simulator lasers may present an optical viewing hazard to a distance of 100_r for stabilized viewing through 80-mm optics [corresponding to high-power (e.g., 13X) viewing]. The term "stabilized viewing" as used here refers to viewing through optics mounted on a firm mount such as a tripod, optical bench, or a stationary tank. However, even

the best optics designed for visible transmission would not be expected to transmit over 80-percent of 905-mm radiation. However, from preliminary studies of the transmission of tank optics, viewing any of the MILES transmitters within 75 m with tank optics may not be hazardous. Until further studies of tank optics can verify or disprove these early measurements, optically aided viewing with stabilized optics should be considered hazardous within 75 m.

(3) The use of infrared absorbing filters which normally protect against Ruby or Neodymium lasers would provide sufficient protection against these Ga-As lasers. For instance, a 3-mm thickness of Schott KG-3 glass which provides an optical density of 5 at the neodymium wavelength would provide an optical density greater than 2 at the Ga-As wavelength. This density would provide adequate protection against any of the MILES lasers at any distance through any size optics. Clip-on filters may be used on stabilized optics if a built-in filter is not available and the distance restrictions (75 m) cannot be met. Since the XM-1 and M551 vehicle have built-in laser filters for the infrared, no hazards exists from the use of these optics.

c. Laser Hazard Classification Systems.

(1) A guide to the present Army system of laser classification is provided in Appendix E. All of the MILES laser systems are on the borderline between a Class I "eye-safe" laser and a Class III medium power laser (Class II is reserved for visible lasers). The Dragon-missile, rifle, and machine-gun simulators are Class IIIa laser systems "restricted eye-safe" since none of these systems exceed protection standards at the laser exit through a 7-mm aperture. However, the rifle and machine gun simulators do exceed protection standards through 7 mm at 2.5 m away due to focussed outputs. A new revision to STANAG 3606, the NATO Laser Regulation, refers to these lasers as "Restricted Eye-Safe Laser Systems" (reference 5, Appendix A). The simulators for the other missiles and the tank gun simulators are Class IIIb systems since their output may be as high as 16 times the Class I emission limit.

(2) However, the Class I limit was established with a sizable margin of safety since: (a) gas lasers and other solid-state lasers may have a significant fluctuation in output; (b) the Class I limit is used to calculate the degree of eye protection required, and eye protection may vary in optical density from sample to sample; and (c) some error is allowed in laser measurement. Due to the multiplicity of errors possible in prescribing safety measurements for most types of lasers, a sizable margin of safety has been deemed necessary in classifying a laser system.

Nonionizing Radn Prot Sp Study No. 25-42-0381-79, Aug-Dec 78

(3) For the Ga-As laser, however, the output is more stable. A large fluctuation upward in output energy may destroy the diode in a very few pulses. Safety goggles are not normally required for such a low-power device; therefore, no errors may result from optical density calculations. Careful measurement of a number of identical diodes will establish the maximum output precisely, due to the uniformity of these types of solid-state devices.

(4) Therefore, a deviation of the output power by twofold or threefold from the limit essentially means a reduction in a "safety factor" from perhaps 30 to 15 or to 10. Therefore, the room-temperature, injection-diode laser should not be considered very dangerous if the Class I criteria are exceeded slightly. The present ED version presents no more of a hazard than did the AO version. USAEHA calculations indicate that a safety margin of approximately 12 exists between protection standards and a 50-percent probability of retinal injury. However, higher power diodes (greater than 5-6 watts) when installed in a laser lens arrangement, or cooled diodes of an even lower peak power, when operated at a high duty cycle should still be considered potentially hazardous.

d. Federal Performance Standard Requirements.

(1) A Federal [Food and Drug Administration (FDA)] standard for laser products applies to all laser products manufactured after 1 August 1976 unless the DOD exemption for tactical laser devices is utilized (references 2 and 6, Appendix A). The Class I accessible emission limit for lasers operating for various exposure durations, and the maximum MILES output levels are listed in Table 3. It appears that the MILES lasers, except for the machine gun operated in one mode, already meet the Class I emission limits of the Federal standard. (The machine-gun simulator would have to be fired with single shots spaced at half-second intervals while firing blanks for nearly the full 200 round belt in order to exceed the standard.) Both DA policy (reference 2, Appendix A) and DOD policy (reference 6, Appendix A) require that the system developer try to meet the Federal standard and have the laser manufacturer certify the laser's compliance with the standard where feasible. Inasmuch as some of the production MILES units may well emit levels sufficiently below the Federal standard to be certified as always meeting the standard, those versions would have to be certified. Other versions such as the machine gun may have to make use of the exemption because the BRH requirements for emission indicators, labeling, etc. would interfere with the intended tactical training use.

Nonionizing Radn Prot Sp Study No. 25-42-0381-79, Aug-Dec 78

TABLE 3. TOTAL ENERGY EMITTED FROM THE MILES SYSTEM COMPARED TO FEDERAL PERFORMANCE STANDARDS FOR VARIOUS TIMES

Exposure Time	Federal Standard	Shillelagh Missile	MILES Systems	
			Machine Gun	M16 Rifle
10 μ s	0.49 μ J	0.32 μ J	0.11 μ J	0.074 μ J
0.5 s	1.0 mJ	61 μ J	88 μ J	57 μ J
2.0 s	2.9 mJ	244 μ J	352 μ J	228 μ J
10 s	9.6 mJ	490 μ J	1.2 mJ	1.1 mJ
100 s	9.5 mJ	4.9 mJ	DF* 9.0 mJ BF† 17.6 mJ	7.2 mJ
<100 s	95 μ W	49 μ W	DF 9 μ W BF 160 μ W	72 μ W

* DF - Dry Fire

† BF - Blank Fire

(2) Since the ED version, MILES lasers were exempt under the DOD exemption a warning label should have been installed either on the device housing (or shipping carton if room was unavailable on the housing) which read:

CAUTION

This electronic product has been exempted from FDA radiation safety performance standards prescribed in the Code of Federal Regulations, Title 21, Chapter I, Subchapter J, pursuant to Exemption No. 76 FL-01 DCD issued on 26 July 1976. This product should not be used without adequate protective devices or procedures.

(3) Since it appears that the MILES systems, except for the machine gun, may meet all the requirements and since DOD policy and Army policy dictate that laser systems should comply with the FDA performance standard where practicable, production units should be certified by the manufacturer with the Bureau of Radiological Health, if the machine gun simulator is modified or if the other units are found to meet this standard. In this case a

Nonionizing Radn Prot Sp Study No. 25-42-0381-79, Aug-Dec 78

different label would have to be permanently attached to the device housing indicating nomenclature, name and address of manufacturer, month of manufacture, place of manufacture, and a statement that the device meets the Federal Performance Standard 21 CFR 1040.

e. Eye Examinations. Not required.

f. Outlook. There are clearly many advantages to developing MILES laser transmitters that are not hazardous under any viewing condition, i.e., Class I laser systems. Future biologic research may even show that the present designs are truly not hazardous, and future Army standards could be relaxed to include these designs as Class I systems. Apparently the general present design has achieved the greatest possible range with the lowest possible power for a reasonably priced system. Any further reduction in power would result in either a decrease in range or an astronomical increase in price. As the present system now stands, the most hazardous piece of hardware is safe to view within 6-9 m by present Army standards (which presently appear to incorporate a substantial safety factor below an actual retinal burn threshold). Even at the beam waist (the most hazardous distance in front of the laser) the protection standard levels are exceeded by no more than a factor of 5 (and the actual output is still suspected to be below a true threshold of injury). Viewing with optical instruments is theoretically a hazard; however, an individual usually does not require the use of binoculars or higher power optical instruments within a 75-m viewing distance. Further measurements on the transmission of tank optics may show that these optics may be used at any distance. Optics such as in the M-551 vehicle, the Dragon sight and the XM-1 tank and other systems equipped with laser protective filters may be used without risk.

g. Risk of Exposure. In normal use in simulated combat, an individual will not place his eye close to the output of the laser device since blanks will be fired in conjunction with the laser. The laser in this situation presents less of a hazard to the eye than does the blast from the blank. Optical-devices placed near the laser output must be carefully aligned and focused to maximize the hazard. Even if the alignment and focusing were accomplished either intentionally or accidentally, the possibility for injury is still extremely remote. One-time field exposures from these devices should not be considered as serious as would be repeated exposures of long duration that could be expected in a laboratory environment.

7. CONCLUSIONS.

a. Field Use. Based upon the best available present knowledge of laser hazards and the intended use of the MILES equipment, these laser transmitters do not pose an actual optical radiation hazard in normal field use. Intentional misuse of some of the MILES transmitters by deliberately directing the beam into the eye at very close range (e.g., at 6-9 m) may be

hazardous, and continued staring into a continuously pulsing laser is clearly not advisable. Inasmuch as the MILES laser transmitters are mounted on weapons and most devices will not transmit unless a blank is fired, the normal precautions followed with the firing of blank ammunition and the pointing of weapons should preclude any hazardous exposure. With the present output characteristics of the MILES, except for telescopic viewing from within the beam, actual exposure of the eyes of target personnel will be far below exposure limits during field use. In actuality, even the viewing of the laser through telescopic weapon sights within 75 m may in many cases be completely safe due to filtration in the sights. As time passes, more sights such as those of the XM-1 tank, the Dragon system, the M-551 Sheridan vehicle will have built-in safety filters.

b. LAIR Studies. The biologic studies performed by LAIR in support of the MILES effort have clearly shown that there is a substantial margin of safety between actual retinal injury levels and exposure limits for the short exposures that would occur during field use. However, the LAIR studies also showed that such a margin of safety did not exist for lengthy (e.g., 30-s) fixed exposures to a stable retina at very close range. Fortunately such lengthy exposures at very close range are totally out of context (if not impossible by design) in the MILES system.

c. Maintenance. Precautions are necessary during any continuous operations that could occur during servicing.

8. RECOMMENDATIONS.

a. Insure that a warning is placed in the MILES manuals to instruct personnel to avoid staring into the laser transmitter with optical instruments or at close range (less than 6 m) (paragraph 1-4b, AR 40-46).

b. Avoid using tank optics at close engagement ranges (less than 75 m) unless protective filters are installed in the optical system or until further measurements of each optical system prove that sufficient attenuation is already present [paragraph 5-38b(5), AR 40-5].

c. Install a label on the device housing or shipping container of ED models similar to the one described in paragraph 6d(2) of this report; production models will require a label as discussed in paragraph 6d [paragraph 1-5d(4), AR 40-46].

Nonionizing Radn Prot Sp Study No. 25-42-0381-79, Aug-Dec 78

d. Instruct troops using the MILES not to aim their weapons (with any of the MILES transmitters) at an individual's eyes at close range (5-10 m).

Wesley J. Marshall

WESLEY J. MARSHALL
Physicist
Laser Microwave Division

David L. Jenkins

DAVID L. JENKINS
2LT, MSC
Nuclear Medical Science Officer
Laser Microwave Division

APPROVED:

GARY W. GASTON
MAJ, MSC
Chief, Laser Microwave Division

APPENDIX A

REFERENCES

1. Paragraph 2-35a(7), AR 10-5, Organization and Functions, Department of the Army, 1 April 1975.
2. AR 40-46, Control of Health Hazards from Lasers and Other High Intensity Optical Sources, 6 February 1974 with Change 1, 15 November 1978.
3. TB MED 279, Control of Hazards to Health from Laser Radiation, 30 May 1975.
4. Title 21, Code of Federal Regulations (CFR), 1977 ed., Part 1040, Performance Standards for Light-Emitting Products.
5. Standardization Agreement, Evaluation and Control of Laser Hazards, STANAG 3606 LAS, Edition No. 3 in circulation for revision.
6. DOD Instruction 6050.6, Exemption for Military Laser Products, 1 May 1978.
7. Report, USAEHA-RL, this Agency, Radiation Protection Special Study No. 42-097-75, Electro-Optical Systems Version of the Ga-As Laser Weapon Simulators Used with the Multiple Integrated Laser Engagement and Scoring System, September-October 1974 (Defense Documentation Center No. ADB001151L).
8. Report, HSE-RL/WP, this Agency, Nonionizing Radiation Protection Special Study No. 42-068-76, Preliminary Theoretical Hazard Evaluation of the Engineering Development Model (ED) of the Multiple Integrated Laser Engagement Simulator (MILES), January-February 1976 (Defense Documentation Center No. ADB010421L).
9. Report, HSE-RL/WP, this Agency, Nonionizing Radiation Protection Special Study No. 42-0313-77, Hazard Evaluation of the Engineering Development Model of the Multiple Integrated Laser Engagement Simulator, February-March 1977 (Defense Documentation Center No. ADB019109L).
10. Report, HSE-RL/WP, this Agency, Nonionizing Radiation Protection Special Study No. 42-0376-78, Revised Hazard Evaluation of the Engineering Development Model of the Multiple Integrated Laser Engagement Simulator, May 1978.
11. Report, HSE-RL/WP, this Agency, Nonionizing Radiation Protection Special Study No. 42-303-76, Exemption from New Federal Laser Performance Standards for Tactical Army Laser Systems and Field Training Lasers, July 1976 (Defense Documentation Center No. ADA029453).
12. Report, SAM-TR-78-20, USAF School of Aerospace Medicine, Ocular Hazards of Picosecond and Repetitive-Pulsed Lasers, Volume I: ND:YAG Laser (1064 nm), Volume II: Argon-Ion Laser (514.5 nm), April 1978.

APPENDIX B

RELEVANT BIOLOGIC INVESTIGATIONS BY LAIR

The biological research performed at LAIR primarily for the MILES project on pulse additivity of coded pulses and threshold damage levels for Gallium-Arsenide lasers had not all been published at the time of this study. However, preliminary findings were furnished to this Agency.

a. Pulse Additivity. For 1064-nm laser pulses spaced 300 μ s apart, pulses were found to be directly additive for a series of up to three pulses. For six pulses at this rate or 1000 pulses spaced at 1 ms apart, the additivity values were found to be 93 percent. Therefore, the Cp value used in the MILES hazard analysis (1.0-additivity) was retained at 0.06 as specified in TB MED 279 (reference 3, Appendix A).

b. Damage Threshold. Monkeys were exposed to 1-watt and 10-watt Ga-As lasers and MILES simulators for 30-second exposures. Although no lasting effect was observed (>24 hours) a retinal change did occur during some of the exposures lasting for several seconds. These changes were visible to an observer during the exposure and could be photographed afterward. Whether this effect was harmful was not yet known at the time of this report. No retinal burns were produced during any of these tests. An actual retinal burn threshold for repeated exposures at this wavelength ($900 \text{ nm} \pm 100 \text{ nm}$) still needs to be established. The equipment needed to do this research had been delivered to LAIR at the time of this study.

ISEPIL CIF: RADIOPHOTIC AND PHOTOMETRIC TERMS AND UNITS^{1,2}

PHOTOMETRIC					
Term	Symbol	SI Unit and Abbreviation Defining Equation	Term	Symbol	Definition Equation
Radiant Energy	Q_e	Joule (J)	Quantity of Light	I_v	$I_v = \int_{\lambda_1}^{\lambda_2} \nu dI_v$
Radiant Energy Density	W_e	Joule per cubic meter ($J \cdot m^{-3}$)	Luminous Energy Density	N_v	$N_v = \frac{dI_v}{d\nu}$
Radiant Power (Radiant Flux)	Φ_e	Watt (W)	Luminous Flux	Φ_v	$\Phi_v = \cos \theta \int_{\lambda_1}^{\lambda_2} N_v d\lambda$
Radiant Exitance	N_a	$\frac{d\Phi_e}{d\lambda} = \int L_e \cdot \cos \theta d\lambda$ Watt per square meter ($W \cdot m^{-2}$)	Luminous Exitance	N_v	$N_v = \frac{d\Phi_v}{d\lambda} = \int L_v \cdot \cos \theta d\lambda$
Irradiance or Radiant Flux Density (those Rate in Photobiology)	E_e	$E_e = \frac{d\Phi_e}{dA}$ Watt per square meter ($W \cdot m^{-2}$)	Irradiance (luminous flux density)	E_v	$E_v = \frac{dN_v}{d\lambda}$
Radiant Intensity	I_e	$\frac{d\Phi_e}{d\Omega}$ Watt per steradian ($W \cdot sr^{-1}$)	Luminous Intensity (candlepower)	I_v	$I_v = \frac{dN_v}{d\Omega}$
Radiance	L_e	$L_e = \frac{d^2\Phi_e}{d\Omega dA \cdot \cos \theta}$ Watt per steradian and per square meter ($W \cdot sr^{-1} \cdot m^{-2}$)	Luminance	L_v	$L_v = \frac{d^2N_v}{d\Omega dA \cdot \cos \theta}$
Radiant Exposure (those in Photobiology)	H_e	$H_e = \frac{d\Phi_e}{dA}$ Joule per square meter ($J \cdot m^{-2}$)	Light Exposure	N_v	$N_v = \frac{dI_v}{dA} = \int I_v d\lambda$
Radiant Efficiency ³ (of a source)	η_e	$\eta_e = \frac{P}{P_i}$	Luminous Efficacy (of radiation)	K	$K = \frac{I_v}{N_v}$
Optical Density ⁴	ρ_e	$\rho_e = -\log_{10} \nu$	Luminous Efficiency (of broad band radiation)	$V(\nu)$	$V(\nu) = \frac{I_v}{N_v} = \frac{K}{680}$
			Luminous Efficiency (of a source)	η_v	$\eta_v = \frac{I_v}{P_i}$
			Optical Density ⁵	ρ_v	$\rho_v = -\log_{10} \nu$
				F_t	$F_t = \frac{I_v}{S_b}$
					irradiated (ν) lumens in cm^{-2} times m^{-2} area in m^2

1. The units may be altered to refer to narrow spectral bands in which case the term is preceded by the word *spectral*, and the unit is then per wavelength interval and the symbol has a subscript A. For example, spectral irradiance has units of $W \cdot m^{-2} \cdot nm^{-1}$ or more often, $W \cdot cm^{-2} \cdot nm^{-1}$.

2. While the meter is the preferred unit of length, the centimeter is still the most commonly used unit of length for many of the above terms and the m or cm are most commonly used to express wavelength.

3. At the source $I = \frac{dI}{d\lambda \cdot \cos \theta}$ and at a receptor $I = \frac{dI}{d\lambda}$.

4. ν is the transmission.

5. P_i is electrical input power in watts.

APPENDIX B

**ON THE CHARACTERISTICS OF A
GAUSSIAN LASER BEAM BEING DETECTED
BY A FIXED THRESHOLD RECEIVER**

INTRODUCTION

An important aspect of MILES tactical fidelity is the matter of beam geometry. The actual beam shape, maximum beam diameter and maximum theoretical range are all parameters which must be understood in order to properly design the MILES transmitters and receivers.

ANALYSIS

The total power output of the transmitter, P_o , is given by the integral of the irradiance over the exit aperture. Thus

$$P_o = \int_A H(x, r) dA \quad (1)$$

The irradiance function, $H(x, r)$ is assumed to be Gaussian in the radial coordinate, r , and to fall off as the inverse square of the range, x , in the axial direction. We shall initially neglect atmospheric attenuation for the sake of simplicity. Thus, the range and beam diameter values obtained will represent maximum theoretical values. Under actual meteorological conditions these parameters will be reduced. With these assumptions, the irradiance may be written as

$$H(x, r) = \frac{H_0}{\left[1 + \frac{r^2}{D_o^2}\right]^2} e^{-x^2/2\sigma^2} \quad (2)$$

where H_0 is the maximum centerline irradiance at $x = 0$ and $r = 0$, θ is the total beam divergence (i.e., full-angle between 10 percent points), D_o is the aperture diameter, and σ is the standard deviation of the diverging Gaussian beam distribution, given by

$$\sigma(x) = k \left[\frac{D_o}{2} + \frac{\theta}{2} \right] \quad (3)$$

Thus, equations (2) and (3) have two undetermined constants, H_0 and k . These are determined by the following boundary conditions:

1. At the exit plane ($x = 0$), and at the edge of the aperture ($r = D_0/2$) the irradiance is 10% of the centerline value. That is, we shall define the Gaussian in terms of the 10% points. Thus, mathematically, we may write $H(0, D_0/2) = 0.10 H_0$. Setting $x = 0$ and $r_0 = D_0/2$ and $r^2/2\sigma^2 = D_0^2/8\sigma_0^2$ we obtain

$$H(0, D_0/2) = 0.10 H_0 = H_0 e^{-D_0^2/8\sigma_0^2}$$

where $\sigma_0 = \sigma(x = 0) = \frac{kD_0}{2}$

Thus $D_0^2/8\sigma_0^2 = \frac{1}{2k^2}$ (4)

and hence $0.10 = e^{-\frac{1}{2k^2}}$

or $\frac{1}{2k^2} = \ln e(10) = 2.30259$

or $k^2 = \frac{1}{2 \times 2.30259}$

or $k = 0.466$ (5)

Substituting equation (5) into equation (3) we obtain
 $\sigma(x) = 0.233(D_0 + x\beta)$

or $2\sigma^2 = 0.108(D_0 + x\beta)^2$ (6)

2. Having determined k and σ we may now substitute equation (6) into equation (2) obtaining

$$H(x_1 r) = \frac{H_0}{\left[1 + \frac{x_1 r}{D_0}\right]^2} e^{-r^2/.108(D_0+x_1 r)^2} \quad (7)$$

We may now integrate, per equation (1), to solve for H_0 as a function of P_0 . Noting that $dA = 2\pi r dr$ we find, at $x = 0$, the second boundary condition:

$$P_0 = \pi H_0 \int_{r=0}^{r=D_0/2} e^{-r^2/.108 D_0^2} 2r dr \quad (8)$$

$$\text{Let } u = r^2/.108 D_0^2$$

$$\text{Then } 2r dr = .108 D_0^2 du$$

and

$$P_0 = 0.34109 D_0^2 H_0 \int_{r=0}^{r=D_0/2} e^{-u} du \\ = 0.34109 D_0^2 H_0 \left[1 - e^{-D_0^2/4(.108 D_0^2)} \right]$$

$$\text{or } P_0 = 0.34109 D_0^2 H_0 (1 - 0.100) = 0.30698 D_0^2 H_0$$

$$\text{or } H_0 = 3.2575 \frac{P_0}{D_0^2} \quad (9)$$

Note that the average irradiance, \bar{H} , would normally be defined by

$$\bar{H} = \frac{P_0}{\pi D_0^2/4} = 1.2732 \frac{P_0}{D_0^2}$$

Hence the peak centerline irradiance of the Gaussian distribution exceeds the average irradiance by a factor of about 2.56. Substituting equation (9) into equation (7) we obtain the expression for the irradiance

$$H(x_1 r) = \frac{3.2575 P_0}{(D_0 + \chi\beta)^2} e^{-r^2/0.108 (D_0 + \chi\beta)^2} \quad (10)$$

Equation (10) gives the irradiance over the x, r field. If we now assume that the detectors have a fixed irradiance threshold, T , when $H(x_1 r) = T$ we know from Reference 1 that the detection probability is 50%. Hence when $H = T$, $r = r_{50}$ or $D = D_{50} = 2r_{50}$ where D_{50} is the 50% detection probability beam diameter. Thus, setting $r = D_{50}/2$ when $H = T$ in equation (10) we obtain

$$e^{D_{50}^2 / .434(D_0 + \chi\beta)^2} = \frac{3.2575 P_0}{T} \times \frac{1}{(D_0 + \chi\beta)^2}$$

or

$$\frac{D_{50}^2}{.434(D_0 + \chi\beta)^2} = \ln_e \left[\frac{3.2575 P_0}{T} \times \frac{1}{(D_0 + \chi\beta)^2} \right]$$

or

$$D_{50} = 0.659 (D_0 + \chi\beta) \left[\ln_e \left(\frac{3.2575 P_0}{T} \times \frac{1}{(D_0 + \chi\beta)^2} \right) \right]^{1/2}$$

Let us now define the characteristic length

$$L^2 = \frac{3.2575 P_0}{T}$$

or

$$L = 1.8049 \sqrt{\frac{P_0}{T}}$$

(11)

NOTE: $1.8049\dots = \frac{2}{3} \sqrt{\frac{10 \ln_e(10)}{\pi}}$

Upon substitution we obtain

$$D_{50} = 0.659 (D_0 + X\beta) \left[\ln_e \left(\frac{L}{D_0 + X\beta} \right)^2 \right]^{1/2}$$

or

$$\underline{\underline{D_{50} = 0.932 (D_0 + X\beta) \left[\ln_e \left(\frac{L}{D_0 + X\beta} \right) \right]^{1/2}}} \quad (12)$$

We note that this function initially increases with range X , reaches a maximum value, decreases, and finally goes to zero. The range $X = X_{50}^{\max}$ at which $D_{50} = 0$ is the maximum effective 50% hit detection probability range and may be determined from equation (12) when $D_{50} = 0$.

Thus $.932 (D_0 + X_{50}^{\max} \beta) \left[\ln_e \frac{L}{D_0 + X_{50}^{\max} \beta} \right]^{1/2} = 0$

or $\ln_e \left(\frac{L}{D_0 + X_{50}^{\max} \beta} \right) = 0 \quad (13)$

or $\frac{L}{D_0 + X_{50}^{\max} \beta} = e^0 = 1$

or $\underline{\underline{X_{50}^{\max} = \frac{L - D_0}{\beta}}} \quad (14)$

Substituting the expression for L (equation 11) into equation (14) we obtain the expression for the maximum 50% detection probability range in the absence of atmospheric effects

$$\boxed{X_{50}^{\max} = \frac{1.8049 \sqrt{\frac{P_0}{T}} - D_0}{\beta}} \quad (15)$$

For the MILES VES system $P_o = 1.95$ watts, $T = 7 \times 10^{-6}$ w/cm², $\beta = 2.4 \times 10^{-3}$ radian and $D_o = 2$ cm. Thus

$$\begin{aligned} X_{50 \text{ VES}}^{\max} &= \frac{1.8049 \sqrt{1.95/7 \times 10^{-6}} - 2.0}{2.4 \times 10^{-3}} \text{ cm} \\ &= \frac{952 - 2}{2.4 \times 10^{-3}} \text{ cm} \end{aligned}$$

or $X_{50 \text{ VES}}^{\max} = 3960$ meters = max 50% detection probability range neglecting atmospheric effects.

This value will be reduced by atmospheric effects. Similarly for the TES system, where $P_o = 0.67$ watts, $T = 27 \times 10^{-6}$ w/cm², $\beta = 2.4 \times 10^{-3}$ and $D = 2$ cm we find

$$\begin{aligned} X_{50 \text{ TES}}^{\max} &= \frac{1.8049 \sqrt{0.67/27 \times 10^{-6}} - 2}{2.4 \times 10^{-3}} \\ &= \frac{285 - 2}{2.4 \times 10^{-3}} \text{ cm} \\ &= \frac{2.83}{2.40} \times 10^3 \text{ m} \end{aligned}$$

or $X_{50 \text{ TES}}^{\max} = 1180$ meters

Since atmospheric attenuation under worst case conditions (i.e., where the target is just visible at maximum range) will reduce the power level to 10% of the above values then since $L \gg D_o$ the maximum range is proportional to the square root of P_o and under worst case conditions we find $(X_{50 \text{ TES}}^{\max})_{\text{worst case}} = 373$ meters, for 50% detection probability.

Returning to equation (12), we may differentiate the expression for $D_{50}(x)$, noting that

$$\frac{dD_{50}}{dx} = 0 \text{ at } D_{50} = D_{50}^{\max}$$

which will occur at some value $x = x^*$. Differentiating,

$$\begin{aligned} \frac{dD_{50}}{dx} = 0 = 0.932 & \left\{ (D_0 + x^* \beta) \times \frac{1}{2} \left[\ln_e \left(\frac{L}{D_0 + x^* \beta} \right) \right]^{-1/2} \left(\frac{D_0 + x^* \beta}{L} \right) \left[\frac{-L\beta}{(D_0 + x^* \beta)^2} \right] \right. \\ & \left. + \left[\ln_e \left(\frac{L}{D_0 + x^* \beta} \right) \right]^{1/2} \beta \right\} \end{aligned}$$

or

$$-\frac{1}{2} \beta \left[\ln_e \left(\frac{L}{D_0 + x^* \beta} \right) \right]^{-1/2} + \beta \left[\ln_e \left(\frac{L}{D_0 + x^* \beta} \right) \right]^{1/2} = 0$$

or

$$\ln_e \left(\frac{L}{D_0 + x^* \beta} \right) = \frac{1}{2} = \ln_e [e^{1/2}]$$

Thus

$$\frac{L}{D_0 + x^* \beta} = e^{1/2}$$

or

$$D_0 + x^* \beta = \frac{L}{e^{1/2}} \quad (16)$$

or

$$x^* = \frac{L/e^{1/2} - D_0}{\beta} \quad (17)$$

Thus we see that for $L \gg D_0$

$$x^* \approx x_{50}^{\max} / \sqrt{e} = .607 x_{50}^{\max}$$

Hence the maximum beam diameter will occur at a range which is about 61% of the maximum range, in the absence of atmospheric attenuation.

Substituting equation (16) into equation (12) we may now solve for D_{50}^{\max}

$$D_{50}^{\max} = 0.932 \frac{L}{\sqrt{e}} \left[\ln_e \left(\frac{L}{L/\sqrt{e}} \right) \right]^{1/2}$$

$$= \frac{0.932}{\sqrt{e}} L \left(\frac{1}{2} \right)^{1/2}$$

$$= \frac{0.932}{\sqrt{2e}} L$$

or

$$\underline{\underline{D_{50}^{\max} = 0.3997 L}} \quad (18)$$

Finally, substituting equation (11) into equation (18) we obtain

$$\boxed{D_{50}^{\max} = 0.7214 \sqrt{\frac{P_o}{T}}}$$

(19)

Thus we see from Equations (15, (17) and (19):

1. The maximum beam diameter is proportional to the square root of the laser output power to detector threshold irradiance ratio.

2. The maximum beam diameter is independent of the beam divergence as well as the aperture diameter, and is therefore completely independent of the optical design.

3. The maximum range is also proportional to the square root of the laser output power to detector threshold ratio, but is inversely proportional to the beam divergence.

Thus a "narrow" beam will produce a long range detection capability while a "wide" beam will reduce the maximum range, but neither will have any influence upon beam diameter. This is the reason the two-tube near-miss concept on the AD VES system was not effective. Increasing the beam divergence of the near-miss beam did not produce a wider beam, it only tended to shorten the maximum range of the near-miss beam. The miss beam on the AD TES was effective since the miss laser power was 5 times that of the kill laser.

Finally, let us compute theoretical maximum values of D_{50}^{\max} for TES and VES.

For TES $P_o = 0.5$ watts $T = 25 \times 10^{-6}$ w/cm²

Thus

$$D_{50 \text{ TES}}^{\max} = 0.721 \sqrt{\frac{0.5}{25 \times 10^{-6}}} \text{ cm}$$
$$= 1.02 \text{ meters}$$

Thus the maximum beam diameter for TES is about 1 meter. Under actual meteorological conditions it will be somewhat smaller.

For VES $P_o = 1.95$ watts $T = 7 \times 10^{-6}$ w/cm²

Thus

$$D_{50 \text{ VES}}^{\max} = 0.721 \sqrt{\frac{1.95}{7.0}} \times 10^3 \text{ cm}$$
$$= 3.81 \text{ meters}$$

Hence the maximum beam diameter of the VES system will be about 4 meters.

NOTE: $0.7214\dots = \frac{2}{3} \sqrt{\frac{10}{\pi e}}$ B-9

ATMOSPHERIC EXTINCTION

We may now generalize these results to include the effects of atmospheric extinction. Utilizing Lambert's Law and equation (10) we obtain

$$H(x_1 r) = \frac{3.2575 P_0}{(D_0 + X\beta)^2} e^{-\left[\frac{4 \ln_e(10) r^2}{(D_0 + X\beta)^2} + \alpha X \right]} \quad (20)$$

where α = continuum atmospheric attenuation coefficient

$$3.2575\dots = \frac{40 \ln_e(10)}{9 \pi}$$

Note that at $X = 0$, $r = 0$ equation (20) still reduces to equation (9).

We now apply the 50% detection probability criteria

$$H(x, D_{50}) = T \quad \text{when } D = D_{50}$$

After some algebra we obtain

$$\underline{\underline{D_{50} = \frac{D_0 + X\beta}{\sqrt{\ln_e(10)}} \left[2 \ln_e \left(\frac{L}{D_0 + X\beta} \right) - \alpha X \right]^{1/2}}} \quad (21)$$

Since $\left[\frac{1}{\ln_e(10)} \right]^{\frac{1}{2}} = 0.659\dots$ the reader will observe the similarity between equations (21) and (12); the only difference being the atmospheric extinction term, $-\alpha X$.

Again, applying our earlier criteria that $X = X_{50}^{\max}$ when $D_{50} = 0$, we find

$$2 \ln_e \left(\frac{L}{D_0 + X_{50}^{\max} \beta} \right) = \alpha X_{50}^{\max}$$

or

$$\frac{L}{D_0 + x_{50}^{\max}} = e^{-\frac{1}{2} \alpha x_{50}^{\max}}$$

or

$$D_0 + x_{50}^{\max} = L e^{-\frac{1}{2} \alpha x_{50}^{\max}}$$

or

$$x_{50}^{\max} = \frac{L e^{-\frac{1}{2} \alpha x_{50}^{\max}} - D_0}{\beta}$$

(22)

The reader will again note that when $\alpha = 0$ equation (22) reduces to equation (14). When $\alpha > 0$ equation (22) is a transcendental equation which may be solved iteratively. Let us consider the VES case. Here $P_0 = 1.95$ watts, $T = 7 \times 10^{-6}$ w/cm² and $\beta = 2.4 \times 10^{-3}$ radian. We shall take $\alpha = 1.2 \times 10^{-4}$ M⁻¹ (standard clear visibility, at 9040Å wavelength). We see from equation (11)

$$L = 1.80 \sqrt{\frac{1.95 \times 10^6}{7}} \text{ cm}$$

or

$$L = 9.5 \text{ meters}$$

$$D_0 = 0.02 \text{ meters}$$

A zero order approximation to x_{50}^{\max} occurs when we set $\alpha = 0$ in equation (22) and obtain the vacuum result

$$(x_{50}^{\max})_0 = \frac{L - D_0}{\beta}$$

We may now use $(x_{50}^{\max})_0$ to determine $(x_{50}^{\max})_1$.

Proceeding with an iterative scheme of the form

$$(x_{50}^{\max})_N = \frac{L e^{-\frac{1}{2} \alpha (x_{50}^{\max})_{N-1}} - D_0}{\beta}$$

we obtain

$$(x_{50}^{\max})_0 = 3960 \text{ meters}$$

$$(x_{50}^{\max})_1 = 3121 \text{ meters}$$

$$(x_{50}^{\max})_2 = 3282 \text{ meters}$$

$$(x_{50}^{\max})_3 = 3250 \text{ meters}$$

$$(x_{50}^{\max})_4 = 3257 \text{ meters}$$

$$(x_{50}^{\max})_5 = 3255 \text{ meters}$$

and $(x_{50}^{\max})_6 = 3256 \text{ meters}$

Hence, after six iterations the method has converged to within 1 part per thousand and we find that the maximum predicted VES MILES 50% detection probability range, under standard clear conditions is

$$x_{50\%}^{\max} = 3256 \text{ meters}$$

(NEGLECTING SCINTILLATION)

We now return to equation (21). Noting that D_{50} will reach its maximum value when $dD_{50}/dx = 0$ we may solve for the range at which this occurs, x^* .

$$\begin{aligned} \frac{dD_x}{dx} = 0 &= \frac{D_0 + x^{*B}}{\sqrt{\ln_e(10)}} \left\{ \frac{1}{2} \left[2 \ln_e \left(\frac{L}{D_0 + x^{*B}} \right) - \gamma x \right]^{-1/2} \left[2 \left(\frac{D_0 + x^{*B}}{L} \right) \left(\frac{-L\beta}{(D_0 + x^{*B})^2} \right) - \alpha \right] \right\} \\ &+ \left[2 \ln_e \left(\frac{L}{D_0 + x^{*B}} \right) - \gamma x \right]^{1/2} \left[\frac{\beta}{(\ln_e(10))^{1/2}} \right] \end{aligned}$$

or

$$\left[2 \ln_e \left(\frac{L}{D_0 + X^* B} \right) - \alpha X^* \right] = 1 + \frac{\alpha D_0}{2B} + \frac{\alpha X^*}{2}$$

or

$$\ln_e \left(\frac{L}{D_0 + X^* B} \right) = \frac{1}{2} + \frac{\alpha D_0}{4B} + \frac{3\alpha X^*}{4}$$

or

$$\frac{L}{D_0 + X^* B} = e^{\left[\frac{1}{2} + \frac{\alpha D_0}{4B} + \frac{3\alpha X^*}{4} \right]}$$

or

$$Y^* = \frac{L e^{-\frac{1}{2} \left[1 + \frac{\alpha D_0}{2B} + \frac{3\alpha X^*}{2} \right]}}{D_0} \quad (23)$$

The reader will again note that for $\alpha = 0$ equation (23) reduces to equation (19).

It is also of interest to consider the three terms in the bracket. The first term is unity. The second term is of order

$$\frac{\alpha D_0}{2B} \approx \frac{1.2 \times 10^{-4} \text{ M}^{-1} \times 2 \times 10^{-2} \text{ M}}{2.4 \times 10^{-3}} \approx 10^{-3}$$

The third term is of order

$$\frac{3\alpha X^*}{2B} \approx \frac{3\alpha L}{2\sqrt{e} B} \approx \frac{3 \times 1.2 \times 10^{-4} \text{ M}^{-1} \times 12.2 \text{ M}}{2 \times 1.6 \times 2.4 \times 10^{-3}} \approx .57$$

Hence, the third term is comparable to the first term. Thus the effects of atmospheric attenuation will be to cause the range at which the beam reaches its maximum diameter to decrease. For the case $\alpha = 0$, $L \gg D_0$ we found $X^*_{\max} = 1/\sqrt{e}$. For the case $\alpha < 1$, $L \gg D_0$ we find

$$\frac{x_{50}^*}{x_{50}^{\max}} = \frac{\frac{L}{s} e^{-\frac{1}{2}} e^{-\frac{3}{4} \alpha x}}{\frac{L}{s} e^{-1/2 \alpha x}} = \frac{e^{-\frac{1}{4} \alpha x}}{\sqrt{e}}$$

Thus we see that when $\alpha > 0$ the range at which $D_{50} = D_{50}^{\max}$ will be a smaller proportion of the maximum range than when $\alpha = 0$. For the VES case of interest we see that

$$\begin{aligned}\frac{x_{50}^*}{x_{50}^{\max}} &= \frac{-\frac{1}{4} \times 1.2 \times 10^{-4} \times 4 \times 10^3}{e^{-1/2}} \\ &= 0.6065 \times 0.8869 \\ &= 0.5379\end{aligned}$$

Thus we find that under standard clear conditions the range at which the beam reaches its maximum diameter will be about 54% of the maximum range.
Thus atmospheric attenuation will have the dual effect of:

1. Reducing the maximum range.
2. Causing the beam to even more closely approximate a "tube".

Substituting equation (23) into equation (21) and defining

$$y = 1 + \frac{\alpha D_0}{2s} + \frac{3\alpha x^*}{2}$$

$$\text{Then } D_{50}^{\max} = \frac{L e^{-1/2y}}{\sqrt{I_{\infty}(10)}} (y - \alpha x^*) \quad (24)$$

$$\text{but } y - \alpha x^* = 1 + \frac{\alpha D_0}{2s} + \frac{3\alpha x^*}{2} - \alpha x^*$$

$$= 1 + \frac{\alpha D_0}{2s} + \frac{\alpha x^*}{2}$$

Thus

$$D_{50}^{\max} = \frac{L}{\sqrt{\epsilon \ln_e(10)}} \left\{ e^{-\frac{\alpha D_0}{4B}} + \frac{3}{4} \alpha x^* \left(1 + \frac{\alpha D_0}{2B} + \frac{\alpha x^*}{2} \right)^{1/2} \right\}$$

Since we have shown that $\frac{\alpha D_0}{4B} \ll \frac{3}{4} \alpha x^*$ and $x^* \approx \frac{1}{2} x_{50}^{\max} \approx \frac{1}{2} \frac{L}{3}$

then

$$D_{50}^{\max} \approx \frac{L}{\sqrt{\epsilon \ln_e(10)}} \left\{ e^{-\frac{3}{2} \frac{\alpha L}{4B}} \left(1 + \frac{\alpha L}{4B} \right)^{1/2} \right\} \quad (25)$$

The reader will again note that for $\gamma = 0$ equation (25) reduces to equation (18).

For the VES case $P_0 = 1.95$ watts, $T = 7 \times 10^{-6}$ w/cm², $\theta = 2.4 \times 10^{-3}$ radians, $\alpha = 1.2 \times 10^{-4}$ M⁻¹, $L = 9.5$ meters we find

$$\begin{aligned} D_{50}^{\max} &= 0.3997 \times 9.5 \left\{ e^{-\frac{3}{8} \times 1.2 \times 10^{-4} \times 9.5 / 2.4 \times 10^{-3}} \right. \\ &\quad \left. \times \left(1 + \frac{1.2 \times 10^{-4} \times 9.5}{4 \times 2.4 \times 10^{-3}} \right)^{1/2} \right\} \\ &= 3.79 \left\{ 0.8368 \times 1.1188 \right\} \end{aligned}$$

or $D_{50}^{\max} = 3.55$ meters

Thus we see that the key parameter which defines the effects of atmospheric attenuation is the dimensionless group

$$J = \frac{\alpha L}{4B} = \frac{1}{6} \sqrt{\frac{10 \ln_e(10)}{\pi}} \frac{g}{s} \left(\frac{P_0}{T} \right)^{1/2}$$

or
$$J = 0.4512 \frac{g}{s} \left(\frac{P_0}{T} \right)^{1/2} \quad (26)$$

Thus we see that the maximum beam diameter for 50% detection probability,
 D_{50}^{\max} is given by

$$D_{50}^{\max} = 0.7124 \sqrt{\frac{P_0}{T}} F(J) \quad (27)$$

where

$$F(J) = \frac{\sqrt{1+J}}{\frac{3}{2} J} \quad (28)$$

We may tabulate the function F(J)

<u>J</u>	<u>F(J)</u>
0	1.0000
.1	0.9027
.2	0.8115
.3	0.7270
.4	0.6493
.5	0.5786
.6	0.5142
.7	0.4562
.8	0.4040
.9	0.3573
1.0	0.3155
1.5	0.1666
2.0	0.0862
2.5	0.0440
3.0	0.0222
3.5	0.0111
4.0	0.0055
4.5	0.0027
5.0	0.00135
5.5	0.00066
6.0	0.00033

This function is plotted in Figure 5-1. Since

$$D_{50}^{\max} \approx 0 = 0.7214 \sqrt{\frac{P_0}{T}}$$

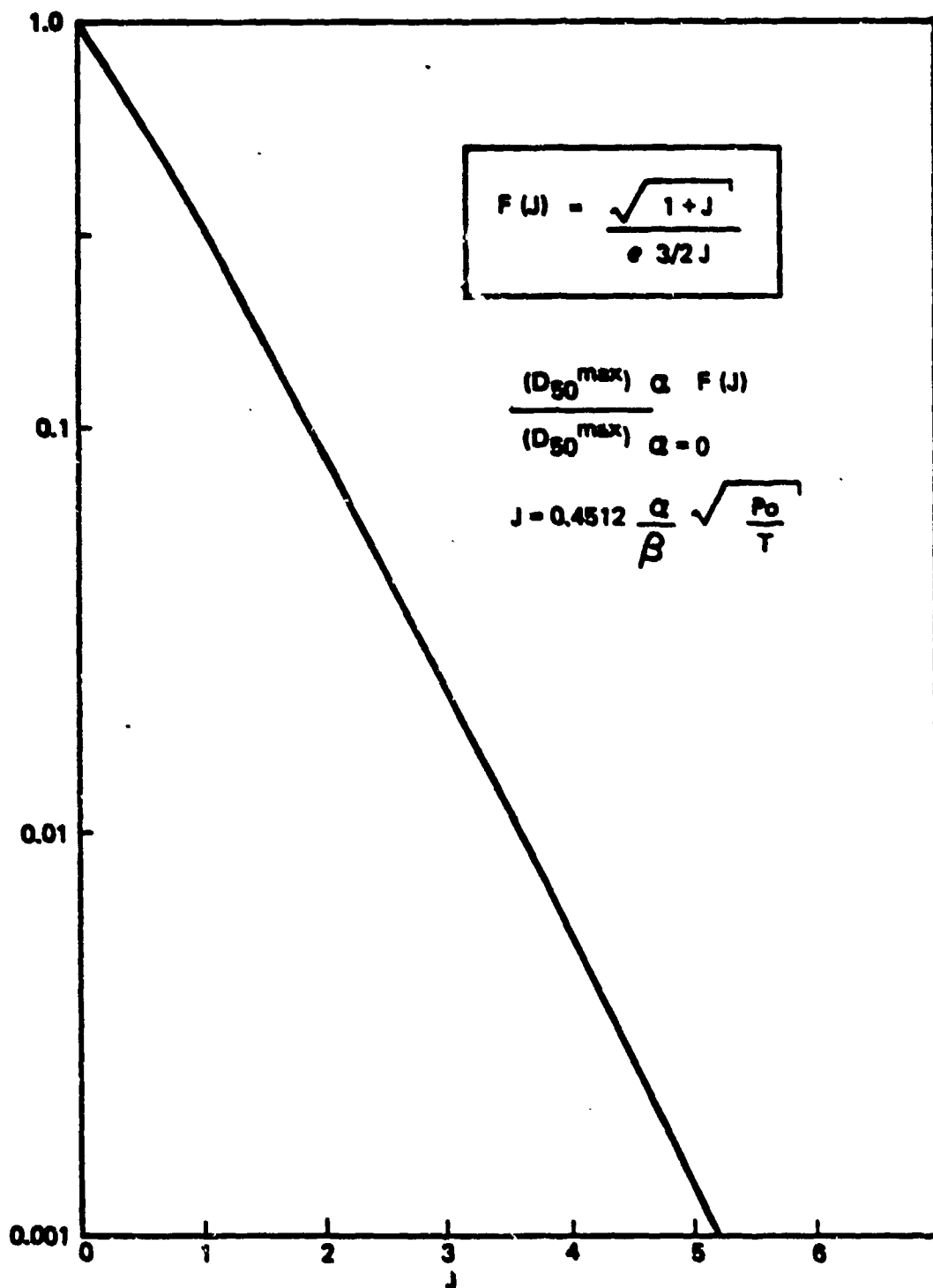


Figure B-1. Extinction Function $F(J)$ as a Function of the Extinction Parameter J

62454

Then

$$F(J) = \frac{(D_{50}^{\max})_a}{(D_{50}^{\max})_{a=0}} \quad (29)$$

Hence $F(J)$ is the ratio of the maximum beam diameter for an atmosphere having a mean continuum attenuation coefficient a , relative to the maximum beam diameter in vacuum, as given by equation (26). For the VES case under standard clear conditions

$$\begin{aligned} a &= 1.2 \times 10^{-4} \text{ M} \\ P_o &= 1.95 \text{ watt} \\ T &= 7 \times 10^{-6} \text{ watt/cm}^2 \\ \theta &= 2.4 \times 10^{-3} \text{ radian} \end{aligned}$$

we find

$$J = 0.1191$$

from which $F(J) = 0.809$

and since, for these parameters $(D_{50}^{\max})_{a=0} = 3.81 \text{ M}$ we find, as before,

$D_{50}^{\max} = 3.55 \text{ meters}$. We may now tabulate

<u>Visibility</u>	<u>$(a).94$</u>	<u>J</u>	<u>$F(J)$</u>
23.5 KM	0.12 KM^{-1}	0.1537	0.85
15 KM	0.19 KM^{-1}	0.2436	0.76
10 KM	0.29 KM^{-1}	0.3714	0.67
8 KM	0.36 KM^{-1}	0.4611	0.60
5 KM	0.57 KM^{-1}	0.7300	0.43
4 KM	0.71 KM^{-1}	0.9094	0.35
3 KM	0.95 KM^{-1}	1.2168	0.24

Since the maximum MILES range is 3 KM then at visibilities less than 3 KM it will not be possible to see the target. This constraint is shown in Figure 2 which plots D_{50}^{\max} vs visibility over the entire range of MILES conditions. The reader will note that D_{50}^{\max} lies between 1.2 meters and 4.2 meters over the entire range of MILES conditions. In all cases D_{50}^{\max} is sufficiently large as to insure against pseudo-miss, since the VES detectors are only 30 inches (0.76 meter) apart.

CONCLUSIONS

1. The maximum beam diameter for a Gaussian laser beam being detected by a fixed threshold receiver is proportional to the square root of the laser output power to detector threshold irradiance ratio.
2. The maximum beam diameter is completely independent of the laser optics provided the beam distribution is Gaussian.
3. The maximum beam diameter will decrease as the atmospheric attenuation increases. The function which defines the reduction in beam diameter has been uniquely determined as a function of a dimensionless parameter, J, which, itself, is a function of the laser output power, the laser beam divergence, the detector threshold irradiance and the atmospheric attenuation coefficient.
4. The maximum effective range is a function of the laser optics. Specifically, the maximum range for 50% detection probability is inversely proportional to the beam divergence. Theoretical calculations for typical VES parameters suggest a maximum 50% detection probability range of about 4 KM. This is in good agreement with experimental test results obtained at El Mirage Dry Lake.
5. The maximum effective range and the range at which the beam achieves maximum diameter both decrease with increased atmospheric attenuation. Detailed functional relationships are presented for both cases. A typical plot of these functions is shown in figure B-2.

62454

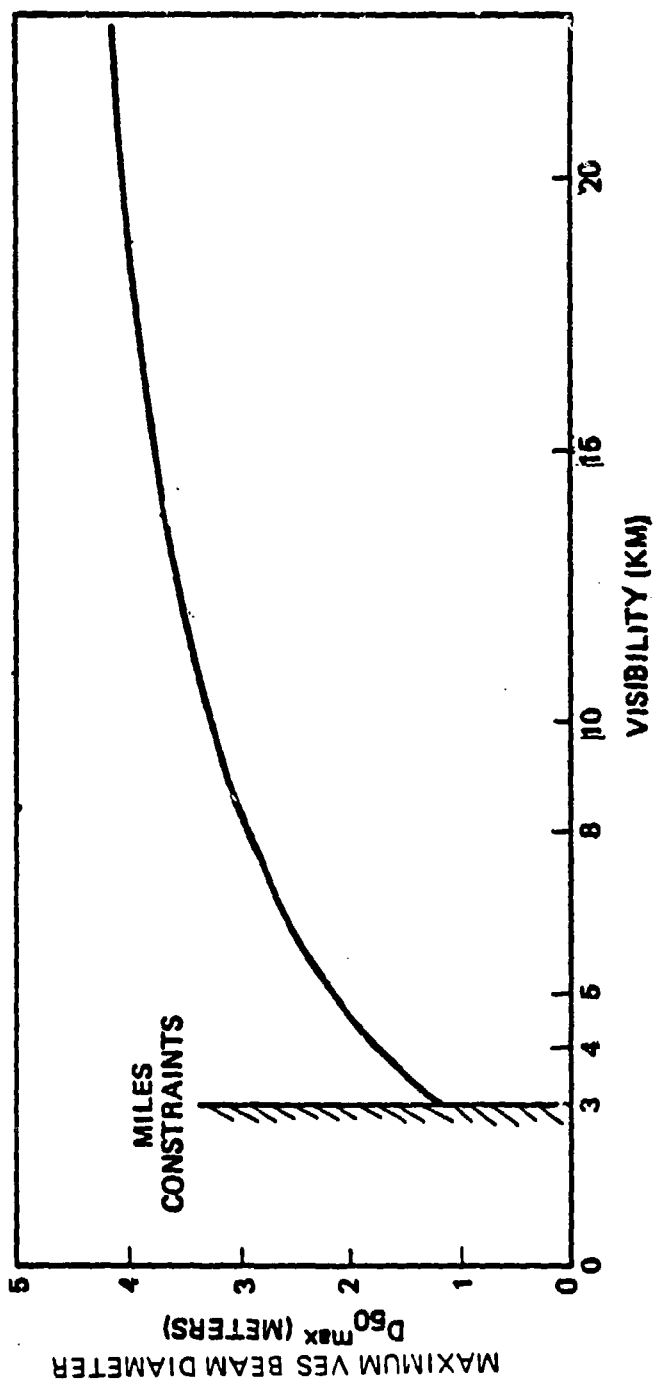


Figure B-2. Maximum VES Beam Diameter For 50% Hit Probability
vs Visibility

APPENDIX C

VISIBILITY/RANGE CAPABILITY

APPENDIX C
VISIBILITY/RANGE CAPABILITY

C.1 INTRODUCTION

Lambert's law states that if the intrinsic contrast of an object with respect to its background is C_o , then the contrast at a range, R, as viewed through an atmosphere having an extinction coefficient α is given by

$$C = C_o e^{-\alpha R}$$

where C is the contrast as seen at range R and C_o is the contrast as seen at zero range (i.e., the intrinsic contrast). Strictly speaking this equation is only valid for monochromatic radiation since C_o and α depend upon wavelength. Nonetheless, we shall treat the visible portion of the spectrum as if it were concentrated at 5550Å, the peak response of the human eye.

Furthermore, Duntley's law (see references 1, 2, and 3) states that $R = V$ when $C = 0.02$. Thus, the definition of the "visibility range" V, is that range at which the contrast of an object, relative to its background, has been reduced to two percent. This stems from the physiological/psychological fact that the human eye/brain combination cannot reliably detect contrast differences of less than two percent.

C.2 APPROACH

From reference 4, the reflectivity P of typical backgrounds at $\lambda = 5550\text{\AA}$ is tabulated in table C-1.

TABLE C-1
REFLECTIVITY OF VARIOUS BACKGROUNDS

<u>Background</u>	<u>Reflectivity @ $\lambda = .555\mu$</u>
Straw	20%
Evergreens	8%
Grass	14%
Sand (Dry)	33%
Loam	7%

We shall consider the reflectivity of U.S. Army fatigue pants to be representative of typical man targets and olive drab paint to be representative of vehicle targets. The reflectivities of these objects at $\lambda = .555\mu$ are 25 percent and 16 percent, respectively. We define the intrinsic contrast, C_o , in terms of the target and background reflectivities P_T and P_B respectively, by the relation

$$C_o = \left| \frac{P_T - P_B}{P_T + P_B} \right| \quad 0 \leq C_o \leq 1$$

Thus, the intrinsic contrasts may now be tabulated for man and vehicle targets against various natural backgrounds. These are listed in table C-2.

TABLE C-2
INTRINSIC CONTRASTS

<u>Background</u>	<u>(C_n) Man</u>	<u>(C_n) Vehicle</u>
Straw	0.11	0.11
Evergreens	0.51	0.33
Grass	0.28	0.07
Sand	0.14	0.35
Loam	0.56	0.39

Now, utilizing Duntley's law and Lambert's law, we may calculate the visibility range.

$$\text{Since } C = C_0 e^{-\alpha R}$$

$$\text{and } C = 0.02 \text{ when } R = V$$

$$\text{Then } 0.02 = C_0 e^{-\alpha V}$$

$$\text{or, } \alpha V = \ln_e \left[\frac{C_0}{0.02} \right]$$

It is worth noting that if C_0 were 1.00 (i.e., white on black) then $\alpha V = \ln_e(50) = 3.912$ which is the usual relationship between the atmospheric extinction coefficient and the visibility range. However, for reduced intrinsic contrast targets, the visibility range is also reduced.

The values of αV are now listed in table C-3.

TABLE C-3

EXTINCTION COEFFICIENTS

<u>Background</u>	<u>Man</u>	<u>Vehicle</u>
Straw	$\alpha V = 1.70$	$\alpha V = 1.70$
Evergreens	$= 3.23$	$= 2.80$
Grass	$= 2.64$	$= 1.25$
Sand	$= 1.94$	$= 2.86$
Loam	$= 3.33$	$= 2.97$

The meteorological visibility, which, for purposes of clarity we shall refer to as V_M (the subscript "M" referring to "meteorological") is defined in terms of a very high intrinsic contrast target, while the actual visibility range of a low contrast target shall be referred to as V_T (the subscript "T" referring to "target"). Thus, we may now compute the ratio V_T/V_M . This quantity is simply the ratio of the actual range at which a particular target can be just barely seen against a given background relative to the meteorological visibility. These values are listed in table C-4.

TABLE C-4

RANGE RATIOS

<u>Background</u>	<u>Man</u>	<u>Vehicle</u>
Straw	$V_T/V_M = 0.43$	$V_T/V_M = 0.43$
Evergreens	$= 0.83$	$= 0.72$
Grass	$= 0.68$	$= 0.32$
Sand	$= 0.50$	$= 0.73$
Loam	$= 0.85$	$= 0.76$

Thus, a man wearing olive drab fatigues can only be seen against a sand background at half the meteorological visibility range. Hence, if the meteorological visibility were 600 meters the man in olive drab fatigues against a sand background would only be visible at an actual range of $600 \times 0.5 = 300$ meters. Similarly a tank against sand would only be visible at about 2200 meters when the meteorological visibility is 3000 meters.

C.3 CONCLUSIONS

Since a goal of the MILES design is "if you can see it, you can hit it," and since the maximum range of the VES is 3000 meters, this would seem to imply that one should design the VES system for a value of atmospheric extinction coefficient corresponding to a visibility of 3 KM. However, due to the fact that the intrinsic contrast of real targets against real backgrounds is always less than unity, then the actual range at which the target can be seen will always be less than the meteorological visibility. The approach taken was to design for a minimum 4000 meter visibility for the VES case, and then recognize that a tank will only be visible for about 3000 meters against a sand background when the meteorological visibility is 4000 meters. Similarly, for the TES case we designed for a minimum 600 meter meteorological visibility since this is the worst visibility in which a man wearing olive drab fatigues would be barely visible at 300 meters against a sand background.

APPENDIX D

UNION DECODING PROBABILITY ANALYSIS

APPENDIX D
UNION DECODING PROBABILITY ANALYSIS

D.1 INTRODUCTION

A Union Decoding Probability analysis was presented as appendix D of the Trainer Engineering Report (Preliminary), XEOS document No. 22639. The analysis in the Preliminary report was essentially a first order approximation. This analysis is an update of the Preliminary document and is an exact analysis of kill probabilities for the MILES system employing Boolean Union decoding.

D.2 MATHEMATICAL DERIVATION OF KILL PROBABILITY AS A FUNCTION OF BIT PROBABILITY AND CODE STRUCTURE

The MILES decoding scheme involves the use of "Boolean Union Decoding." In this technique the corresponding bits of two successive words are logically or^{ed}. Pictorially, Boolean Union Decoding may be represented as follows:

WORD A	WORD B
[0 1 1 0 1 0 1 0]	[0 1 1 0 1 0 1 0]
BOOLEAN UNION OF THE FIRST BIT IN EACH WORD	

In Boolean union decoding, there are $N + 1$ decoding opportunities when N words are sent in a message. The kill probability when N words are sent is:

$$P_k = \sum_{k=2}^{N+1} P_{\text{Tot}}(k) P_{\text{Seq}}(k) \quad (1)$$

where:

$P_{Tot}(k)$ = probability that exactly k words were decoded out of a sequence of N words

$P_{Seq}(k)$ = probability of kill given exactly k words were decoded
(k determines how many times the kill probability routine is entered)

N = Number of words in the message

k = Number of words decoded in a message

There are $N - 1$ Boolean Union decoding opportunities, and 2 non-Boolean Union decoding opportunities in receiving an N -word message. There are three ways of receiving k words in a message:

1. k Boolean Union and 0 non-Boolean Union
2. $k-1$ Boolean Union and 1 non-Boolean Union
3. $k-2$ Boolean Union and 2 non-Boolean Union

$$\text{Thus } P_{Tot}(k) = \sum_{n=0}^2 P_1(k-n) P_2(n) \quad (2)$$

where:

$P_1(k)$ = probability of decoding exactly k Boolean Union words in $N-1$ opportunities.

$$P_1(k) = \frac{(N-1)!}{(N-1-k)! k!} \left[1 - (1-p)^2 \right]^{6k} \left\{ 1 - \left[1 - (1-p)^2 \right]^6 \right\}^{N-1-k} \quad (3)$$

p = single bit reception probability

$P_2(k)$ = probability of decoding exactly k words in the two non-Boolean Union opportunities.

$$P_2(k) = \frac{2!}{k! (2-k)!} p^{6k} (1-p^6)^{2-k} \quad (4)$$

The exponents 2 and 6 in equations (3) and (4) are due to the two registers in the Boolean Union decoder, and to the weight, six, of the code words.

$$\text{Finally, } P_{\text{Seq}}(k) = 1 - (1-P_w)^{\lceil k/M \rceil} \quad (5)$$

where: P_w = The probability that is returned by receiver kill probability routine for a single execution
 $\lceil k/M \rceil$ = k/M rounded down to nearest integer. (We are assuming the routine is entered each time M words are decoded).
 M = number of words required for a hit decode.

Thus the equation for kill probability, P_k , vs single bit probability, P , may be obtained by substitution of equations (3) and (4) into equation (2), and subsequently, substitution of equations (2) and (5) into (1). This resulting equation is shown in figure D-1 with a block diagram showing its derivation and definition of the terms of the equation.

D.3 COMPUTER ANALYSIS

This final Mathematical model was computer programmed so that the probability of kill could be plotted as a function of:

P = single bit detection probability

P_w = The probability that is returned by receiver kill probability routine for a single execution

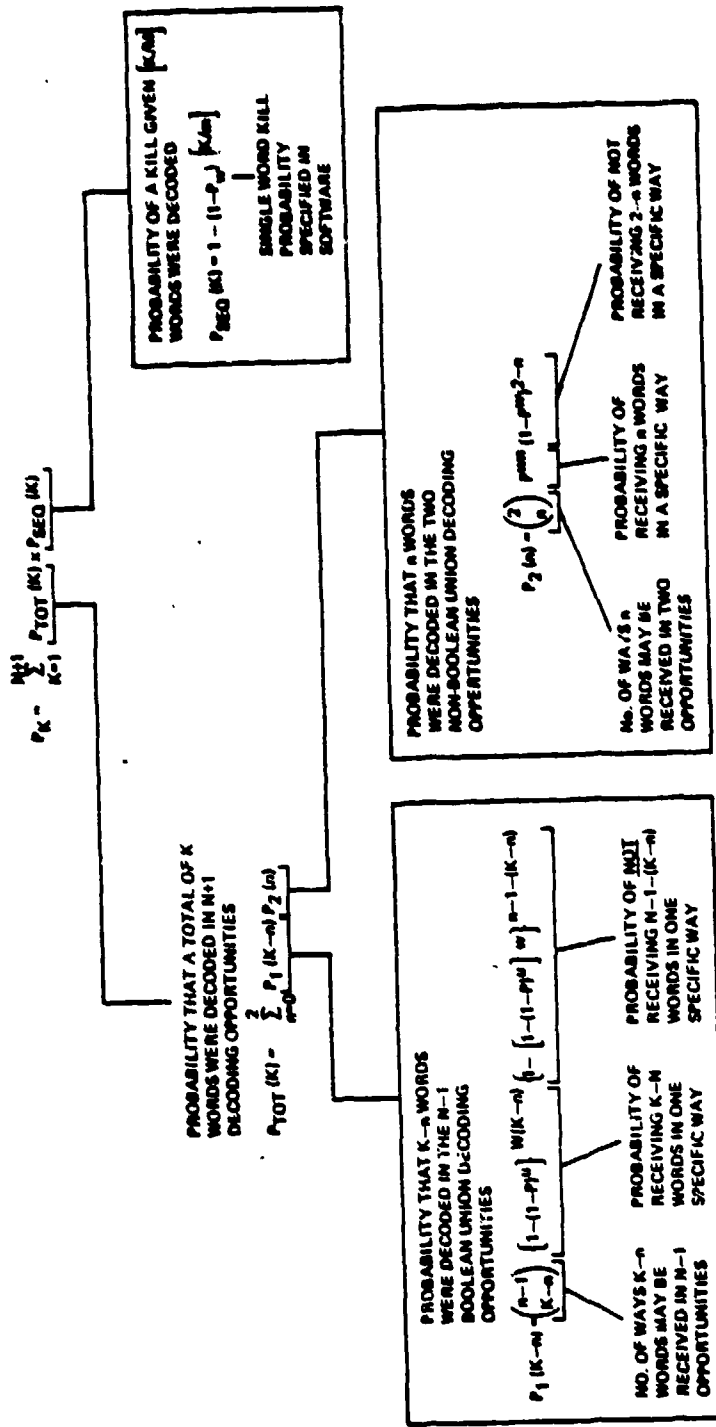
N = number of words transmitted per message

M = number of word receipts required to be successfully decoded per message

U = number of unions (2 for all MILES systems)

W = weight of code word (6 for all MILES systems)

For MILES, the code weight was established at $W=6$. Two-register Boolean Union decoding was selected and therefore $U=2$. The number of words sent per message (N) is used as a variable from weapon to weapon and is a valuable tool for manipulating this probability of kill. Figure D-2 shows the effect of the number of words sent (N) on this kill probability (P_k). Note the increase in P_k as N varies from 2 words to 256 words.



P = SINGLE BIT DETECTION PROBABILITY IVARIES WITH RANGE, ATMOSPHERE, POWER.
 T = THRESHOLD, NOISE, ETC.
 W=2 = NO. OF REGISTERS IN BOOLEAN UNION DECODER.
 W=1 = WEIGHT OF KILL WORDS.
 N=2 = NO. OF KILL WORDS TRANSMITTED TO SIMULATE ONE ROUND.
 P_W = SINGLE WORD KILL PROBABILITY AS SPECIFIED IN SOFTWARE.

Figure D-1. Derivation of Kill Probability Equation if Program Executed After Each Word Receipt

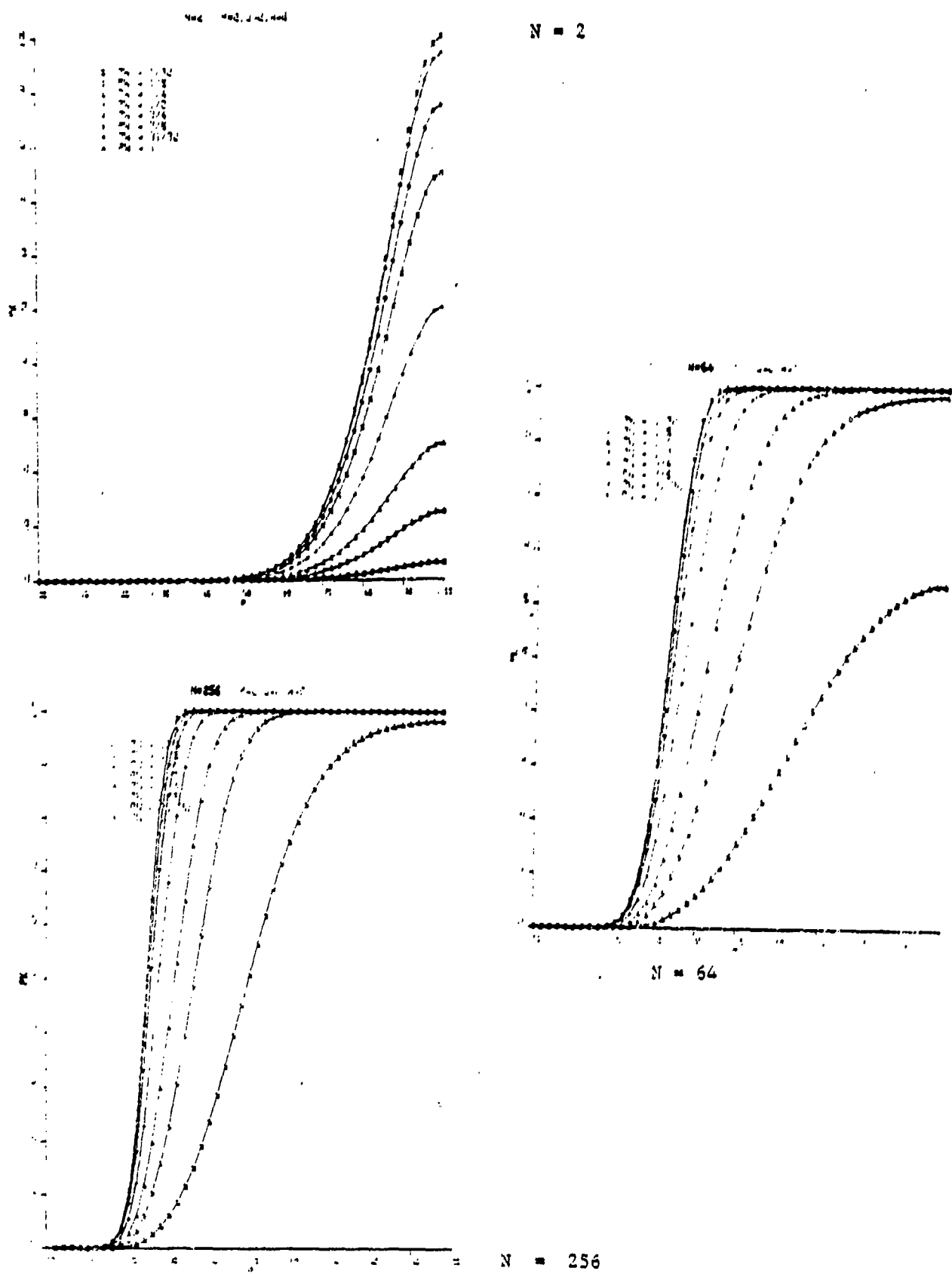


Figure D-2. P_K vs. P - Effect of Varying Number of Words Transmitted (N)

Figure D-3 shows the effect of Boolean union decoding on the kill probability. Notice the increase in P_k from non-union decoding to two-register Boolean union decoding. A lesser increase occurs when going from two to three register union decoding.

Figure D-4, D-5 and D-6 show P_k vs P for the various MILES weapon codes in their use against vehicles where, $M=2$ and against infantrymen where $M=1$.

CONCLUSIONS:

Inspection of figures D-2 through D-5 leads to the following conclusions, in the light of figures 1, 2, and 3 taken from McMillan and Barnes "Detection of Optical Pulses: The Effect of Atmospheric Scintillation", Applied Optics, October 1976, p. 4901.

- A. For any values of M , U , W , increasing W reduces the value of P necessary to achieve a given P_k .
This may be briefly condensed to
"more words improve detection probability."
- B. Two-register Boolean Union decoding improves detection probability, relative to Non-Union decoding, in all cases studied.
- C. Three-register Boolean Union Decoding also improves detection probability, relative to two-register Boolean Union decoding.
- D. Since the cost, size, weight, and complexity of three-register Boolean decoding is considerably greater than comparable values for two-register Boolean Union decoding, while the increase in performance is relatively small, we concluded that two-register decoding was definitely justified, but three-register decoding was not justified.
- E. From an eye safety standpoint, the worst MILES problem was the long range near-miss situation since this involved the highest laser transmitter peak pulse power level. It was thus important

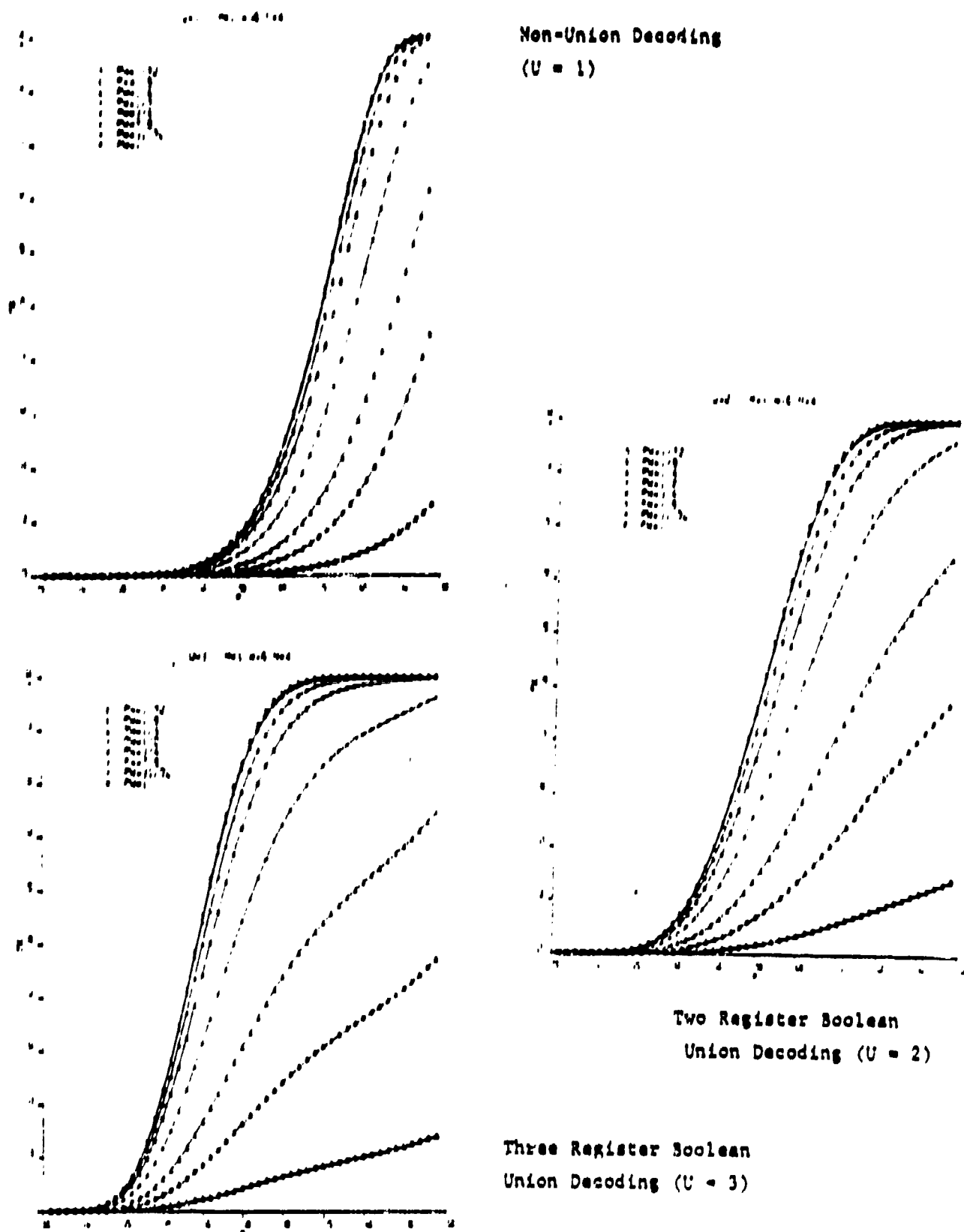
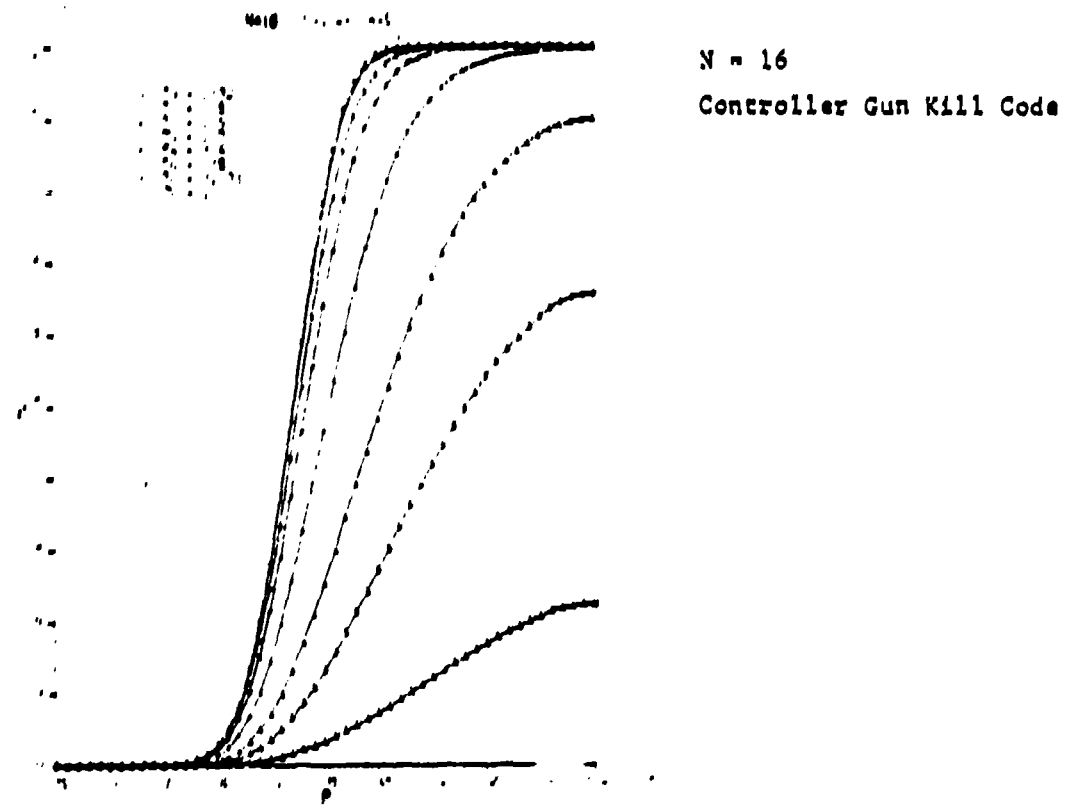


Figure D-3. Effects of Number of Unions on P_K vs. P_W



N = 4
Controller Gun Near Miss
Codes (Four Distinct Near
Miss Codes)

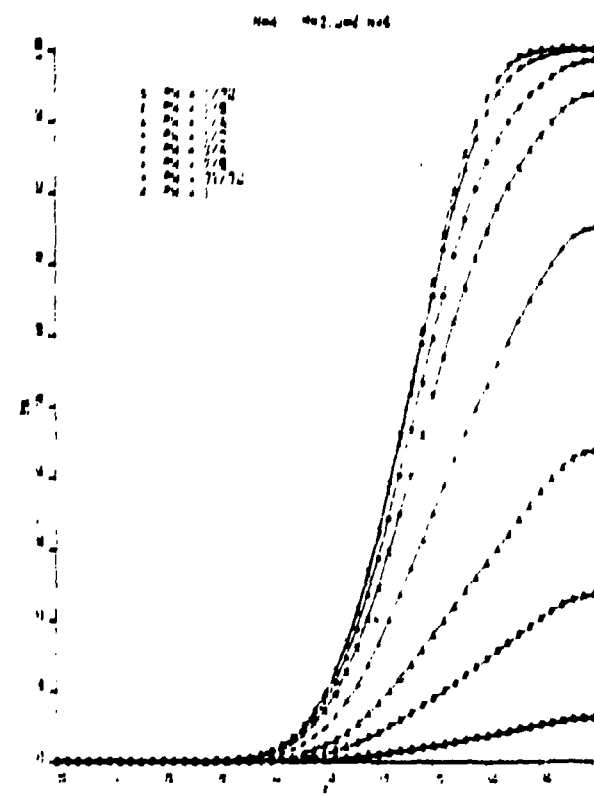


Figure D-4. P_K vs. P for $M = 2$, $U = 2$, and $W = 6$ - Varying N and P_W

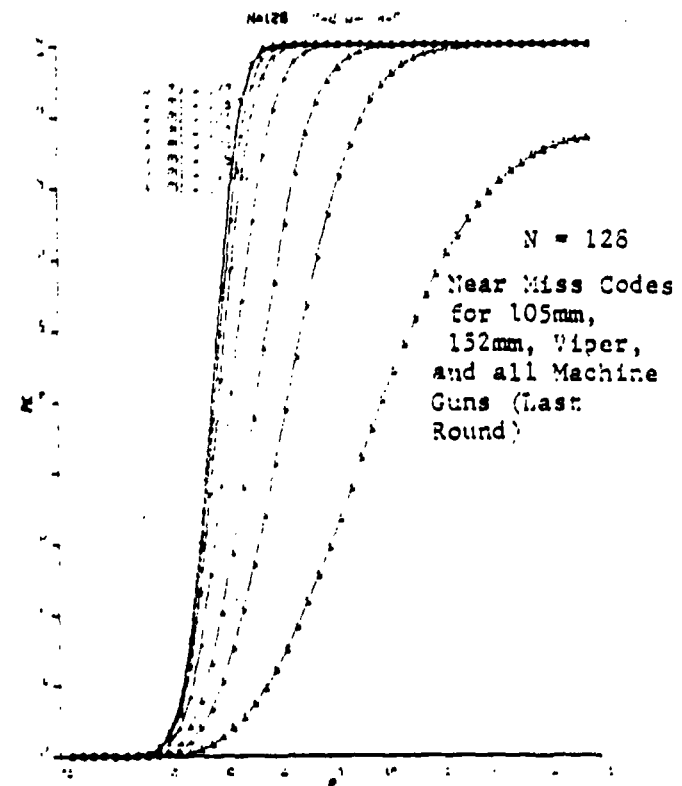
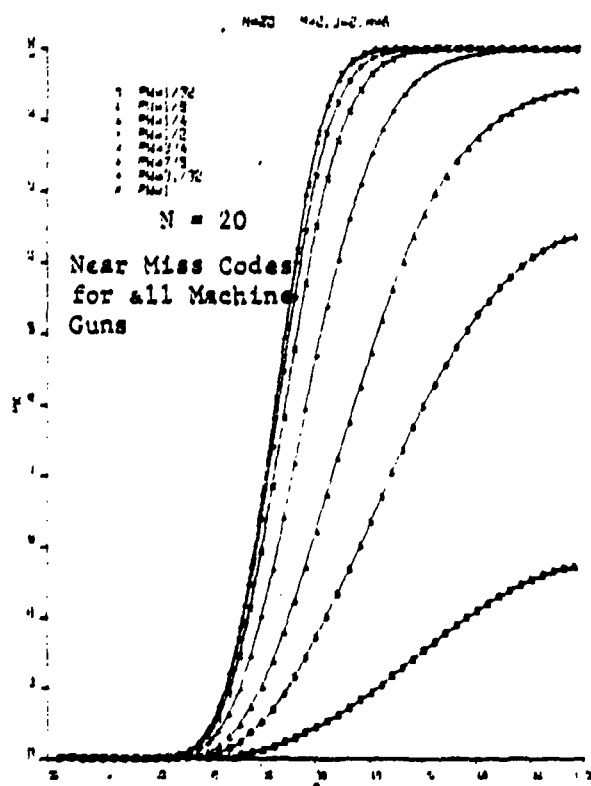
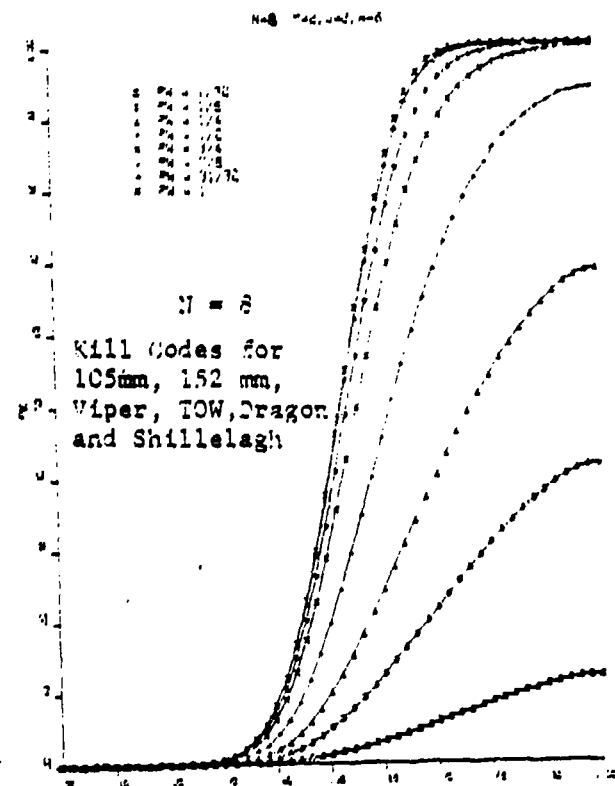
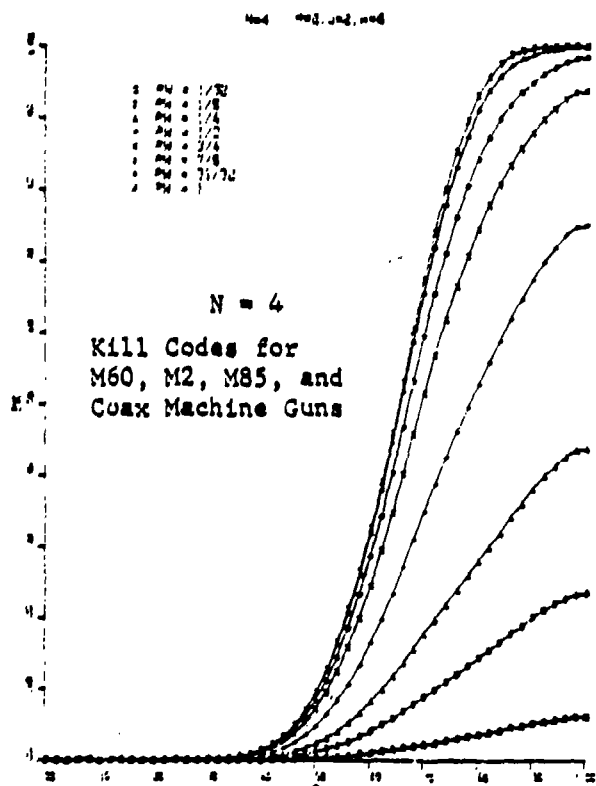


Figure D-5. P_K vs. P for $M = 2$, $U = 2$, $W = 6$ - Varying N and P_W

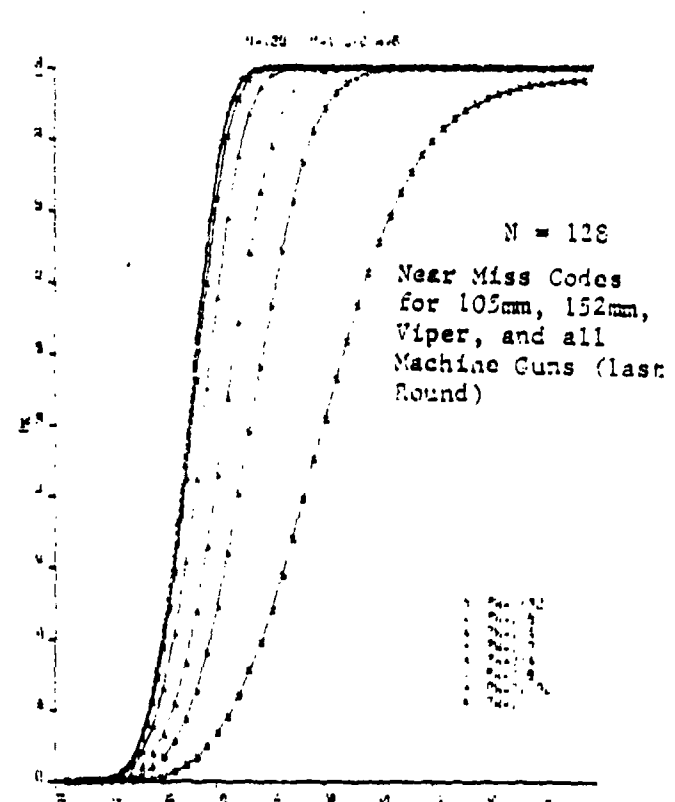
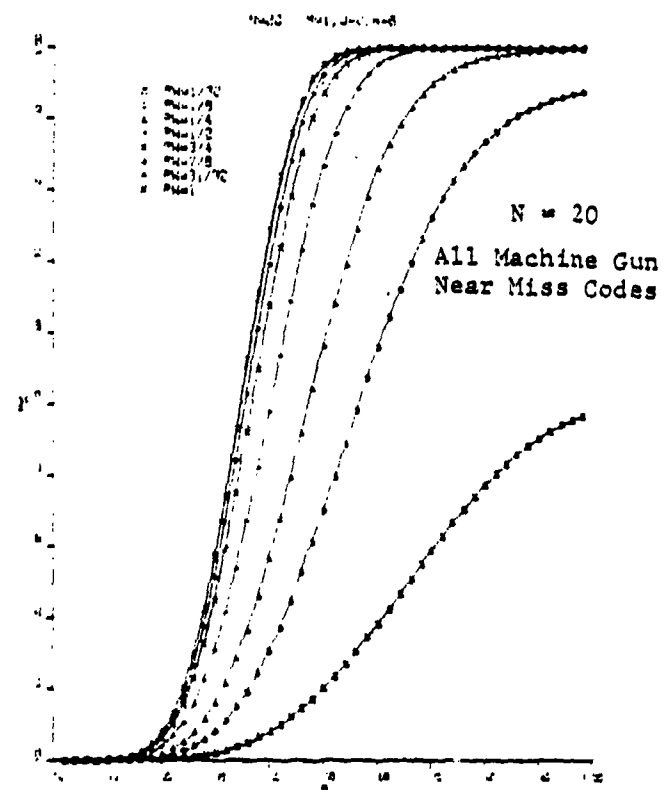
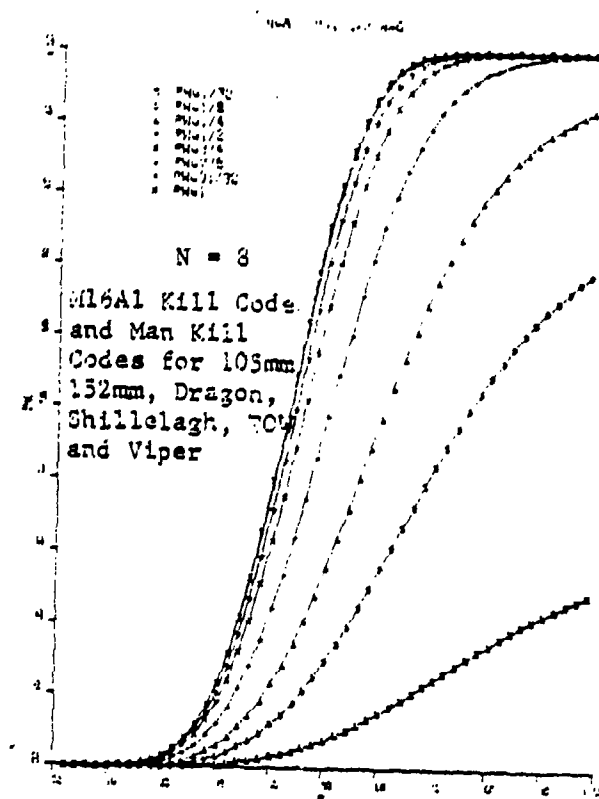
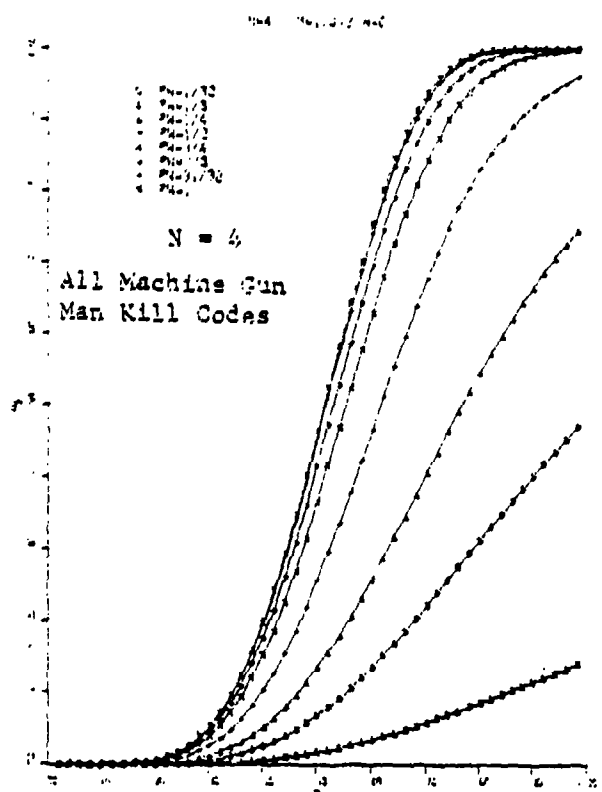


Figure D-6. P_K vs. P for $M = 1$, $U = 2$, and $W = 6 = \text{varying } N \text{ and } P_W$

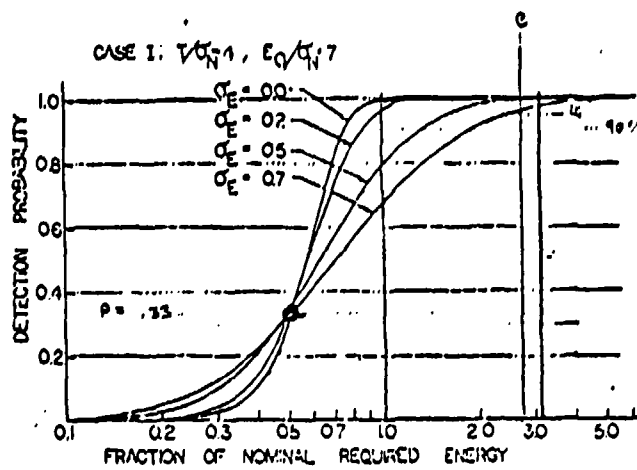


Fig. 1. Detection probability of an optical pulse in the presence of scintillation as a function of transmitted energy for a system designed with a threshold-to-noise ratio of 4 and requiring a SNR of 7 to give 99.9% detection probability. Degree of scintillation ranging from $\sigma_E = 0$ (no turbulence) to $\sigma_E = 0.7$ (heavy turbulence) is plotted as a parameter.

of rms value σ_N and the integrand of the first integral as the probability of achieving energy between E and $E + dE$ on the receiver. The over-all miss probability is then the sum of this product over all energies resulting in Eq. (2).

In the second integral, let

$$X = (T - E)/[(2)^{1/2}\sigma_N], \quad (3)$$

then $d\tau = (2)^{1/2}\sigma_N dX$ and $X = (T - E)/[(2)^{1/2}\sigma_N]$ at $T = \tau$. The second integral then becomes

$$\frac{1}{(\pi)^{1/2}} \int_{-\infty}^{T-E/(2)^{1/2}\sigma_N} \exp(-X^2) dX = \frac{1}{2} \left[1 + \text{erf} \left(\frac{T - E}{(2)^{1/2}\sigma_N} \right) \right], \quad (4)$$

where the error function is defined as

$$\text{erf}(x) = \frac{2}{(\pi)^{1/2}} \int_0^x \exp(-t^2) dt. \quad (5)$$

In the first integral, let

$$(\ln E - \ln E^*)/(\sigma_E) = W, \quad (6)$$

then $\sigma_E dW = d \ln E$ and $W = -\infty$ at $E = 0$. The first integral is then

$$\frac{1}{(2)^{1/2}} \int_{-\infty}^{-\infty} \exp(-W^2/2) dW. \quad (7)$$

The miss probability is therefore

$$P_M = \frac{1}{(2\pi)^{1/2}} \int_{-\infty}^{-\infty} \exp(-W^2/2) \left(\frac{1}{2} \left[1 + \text{erf} \left(\frac{T - E}{(2)^{1/2}\sigma_N} \right) \right] \right) dW. \quad (8)$$

Solving Eq. (6) for E gives

$$E = E^* \exp(\sigma_E W). \quad (9)$$

Hald⁷ shows that the constant E^* is given by

$$E^* = \bar{E} \exp(-\sigma_E^2/2), \quad (10)$$

where \bar{E} is the average value of E . Now let $\bar{E} = KE_0$, where K is a constant equal to the fraction of the nominal energy E_0 received. Substituting these results into the error function argument of Eq. (8) gives

$$\frac{T - E}{(2)^{1/2}\sigma_N} = \frac{T - KE_0 \exp(-\sigma_E^2/2 + \sigma_E W)}{(2)^{1/2}\sigma_N}, \quad (11)$$

The quantities T/σ_N and E_0/σ_N are the receiver threshold-to-noise ratio and signal-to-noise ratio, respectively, which are chosen during receiver design to give a desired false alarm rate and detection probability in the absence of turbulence. The integrand of the integral (8) has been expressed entirely as a function of W , and, although it cannot be integrated in closed form, it is not difficult to integrate numerically on the computer. In performing this integration, the multiplier K is used as a parameter to determine the energy that must be transmitted to realize an acceptable single pulse detection probability.

III. Calculations

Equation (8) was numerically integrated for several cases of interest using values of σ_E corresponding to light, medium, and heavy turbulence as parameters. The detection probability for zero turbulence ($\sigma_E = 0$) is plotted for reference. The threshold-to-noise ratio T/σ_N was determined from the equations⁸

$$\frac{T}{\sigma_N} = \left[2 \ln \left[\frac{1}{2(3)^{1/2} \tau F(A)} \right] \right]^{1/2}, \quad (12)$$

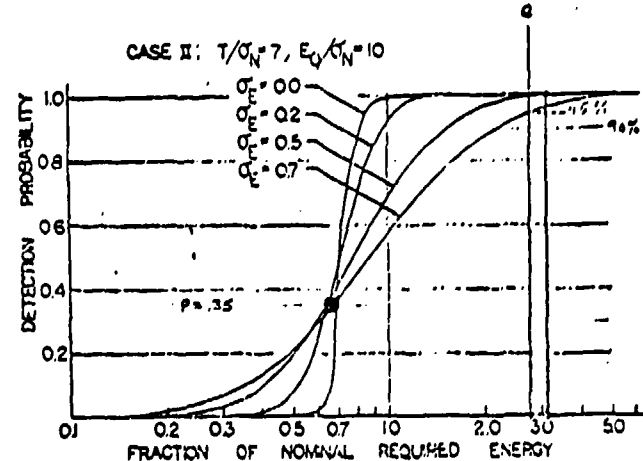


Fig. 2. Same as Fig. 1 except the threshold-to-noise ratio is 7 and the SNR is 10.

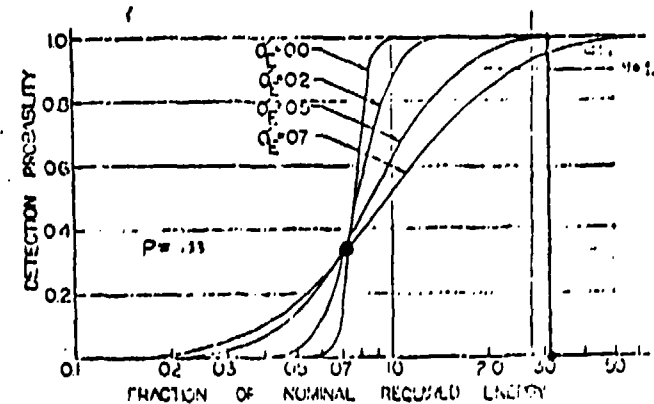


Fig. 3. Same as Fig. 1 except the threshold-to-noise ratio is 10 and the SNR is 13.

to simultaneously:

- reduce near miss peak power
- reduce near miss average power
- reduce near miss inter-pulse frequency
(to increase retinal relaxation)

This was accomplished by utilizing large values of N. For N = 128, M = 1, U = 2, W = 6 we find P = .32 in order to achieve $P_k = .95$. From figure 1 of McMillan & Barnes a value of P = .32 requires K = .5 (interestingly enough, this value is invariant; being true for all values of the log variance, γE , resulting from scintillation). Here K is the fraction of nominal required energy; E_0 , to effect a given P. Thus we need only 0.5 E_0 to achieve 95 percent overall detection probability, instead of 2.0 E_0 had we used only N = 4 words per message. Thus, using larger N reduces peak power for the same performance.

APPENDIX E

SINGLE TUBE CONCEPT ANALYSIS

APPENDIX E
SINGLE TUBE CONCEPT ANALYSIS

E.1 SINGLE TUBE VERSUS TWO TUBE TRANSMITTER

The original XEOS concept for the generation of a near miss beam was a separate, circular near miss zone resulting from a separate near miss laser (i.e., two laser tubes). The reasoning proceeded as follows:

- a. The near miss zone should be larger than the kill zone.
- b. To provide a larger zone requires a greater beam divergence. (It was originally believed that beam diameter was directly proportional to beam divergence.)
- c. To provide adequate detector irradiance the near miss laser output power must scale in direct proportion to the area of the beam.

However, this approach had a number of disadvantages.

- a. It requires two lasers, two optical assemblies and two drivers.
- b. It increases the cost, weight, size of the MILES transmitters.
- c. The two lasers must be aligned with great precision, and must remain in precise alignment through field usage.
- d. Since the desired near miss beam diameter is about three times that of the kill beam its area is about nine times as great and, hence, the near miss beam would require almost an order of magnitude greater power level than the kill beam.
- e. The power requirements of the VES near miss beam were such as to exceed the current eye safety standards as stipulated in TB-MED-279.
- f. OT-1 Testing at Ft. Benning, Ga., indicated that the near miss beams of both VES and TES were not very effective and that beyond about 1.2 KM no VES near miss zone could be detected.
- g. The binocular near miss/kill configurations would force the existence of four laser tubes in the 105 mm weapon barrel, and

five laser tubes in the 152 mm weapon barrel. The mechanical and optical problems associated with space available and optical alignment would be formidable. (The ED baseline assumed use of the single tube transmitter for the VES and TES systems.)

- h. Mathematical analysis (see Appendix B) shows that the maximum beam diameter is independent of beam divergence.

E.1.1 THE VES SINGLE TUBE CONCEPT

The MILES near miss concept was a direct offspring of the El Mirage Dry Lake Scintillation Testing. While the XEOS team was performing atmospheric tests at El Mirage Dry Lake, CA., a number of new and significant insights into the physics of GaAs laser beam propagation through the atmosphere became apparent. The results of the scintillation work were presented to NTEC in memos 2350-DFS-028 and 2350-DFS-046, and need not be repeated in full here. The key ideas are briefly summarized below:

- a. At each range the beam diameter was measured with a detector. The detector was an AD MILES VES detector which was modified by the inclusion of a visual indicator (light bulb). Receipt of any laser pulse exceeding threshold would light the bulb.
- b. As we measured the beam diameter at any range (e.g., 1 KM) it was observed that a central zone existed. That is, there was a region, typically of the order of 1-2 meters diameter, in which the indicator would remain on almost continuously when the laser was transmitting a continuous stream of pulses directed at a fixed aiming point.
- c. Outside the central zone, the detector did not go out immediately. As one moved radially away from this central zone the percentage of time that the indicator was "on" would decrease. As one moved further outward, the indicator would flicker until gradually it would seldom come on.
- d. This type of behavior was observed at all ranges tested, although the very large increase in the diameter of the "flicker zone" relative to the central zone did not manifest itself until the range was in excess of 400 meters.

At this point the idea of a new type of near miss concept began to take shape. It was apparent that what was happening was as follows:

- a. In the central portion of the beam, especially at ranges less than 2 KM for the VES transmitter, the local irradiance was sufficiently great that even with saturated scintillation, the signals still exceeded threshold nearly all of the time. This is shown in figure E-1 by the portion of the lower band of scintillated signals which remain above threshold despite saturated scintillation. This is the central zone of radius, r_i .
- b. However, as one proceeds outward radially from the center, a domain is entered into in which only some fraction of the time is the signal above threshold. As one proceeds radially outward, the fraction of the time that signals exceed threshold is continuously decreasing. This is the "flicker zone," extending from r_i out to r_o .
- c. Eventually as one proceeds sufficiently far out from the center of the beam, even the upper limits of signal irradiance cannot achieve threshold and the detector light will be essentially off beyond r_o . Occasional super-irradiant pulses, resulting from local scintillation "hot spots" may trigger a pulse now and then, but the beam is essentially dead beyond radius r_o .

The key idea is fraction of the time. Since the signals within the central zone ($0 < r < r_i$) exceed the threshold a very high fraction of the time, this is an obvious kill zone. In the annular zone, referred to as the "flicker zone," the fraction of the time the signals exceed threshold is decreasing. Previously, we had attempted to overcome this with more laser power in a larger beam. The key, however, is clearly to overcome this by simply sending more words. Since the VES systems have relatively low firing rates (10 per minute), the time interval between firings is quite long (i.e., 6 seconds). One could send 8 total kill messages in about 25 milliseconds and then have literally thousands of milliseconds available for near miss codes. Even if less than one second were used, at the MILES pulse repetition frequency of 3 KHz with a 11 total bit word (6 active bits) with no spaces in between, a coded word would require 3.67 milliseconds and we could fire 8 kill words in 29.33 milliseconds and another 128 near-miss words in an additional 469 milliseconds.

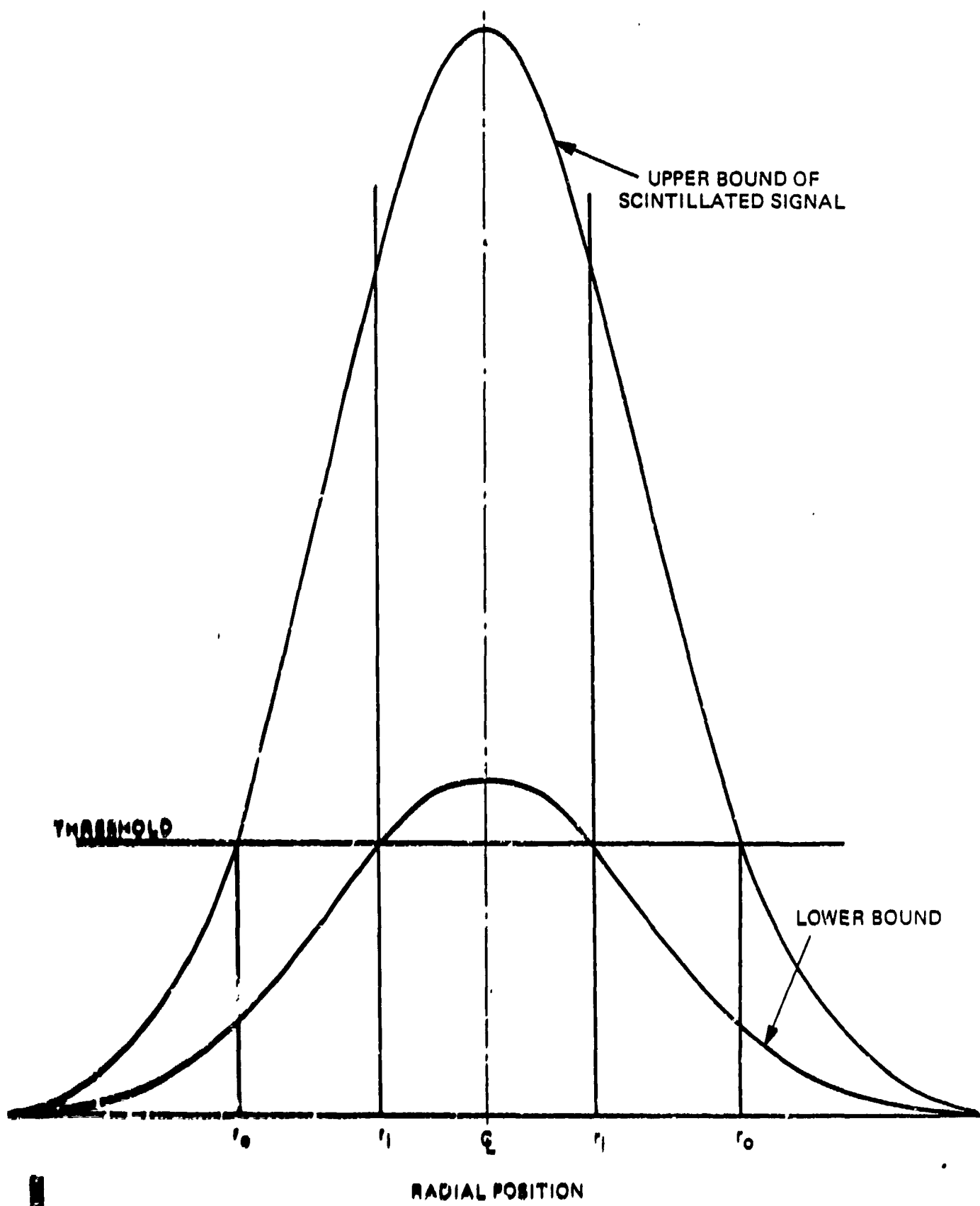


Figure 8-1 Scintillated Signal versus Threshold
E=4

The choices of 8 and 128 are somewhat arbitrary, but they are convenient from a binary logic standpoint, present no total time difficulty, and have a ratio of slightly more than a factor of 10.

The idea of having at least 10 (in this case 16) times as many near miss words is to utilize the fact that the outer edges of the measured beams in the El Mirage tests had the light on at least 10 percent of the time. Thus, if we transmit 10 times as many near miss messages as kill messages, the probabilities of receipt of a miss word in the annular "flicker zone" and a kill word in the central zone should be roughly equal. This concept is confirmed by the data presented in the following section.

E.1.2 EXPERIMENTAL METHOD

A special experiment was devised to test the single tube concept. A MILES transmitter was set up on building roofs in Pasadena and operated over a range of 1.8 km. The laser was mounted on a heavy, stable platform, and was turned on in the continuous code word mode (i.e., sending a continuous stream of 100 code words without requiring reset or re-triggering). A panel of 5 detectors, configured in the ED tank geometric pattern, was positioned so as to maximize the word detection probability.

Next, the laser was turned off, the target positioned at the optimum location and 100 code words were transmitted in 10 bursts of 10 words each. The total number of words received, decoded and counted on a numerical counter was recorded. The detector array was then moved 0.5 meters perpendicular (i.e., radially) with respect to the laser beam, and the entire sequence was repeated. The same procedure was performed at 1.0, 1.5, 2.0, 2.5, 3.0, 3.5 and 4.0 meter radial offsets, both off the right and left of center line.

E.1.3 RESULTS AND ANALYSIS

The results of these tests are presented in figure E-2. This figure plots the word detection probability as a function of radial offset for the situation described above. The reader will note that out to about 1 meter radius, the word detection probability exceeds 70 percent. Hence, if we transmit 8 words the overall hit probability would be:

$$P_{\text{hit}}_{\text{message}} = 1 - P_{\text{miss}}_{\text{message}}$$

and

$$P_{\text{miss}}_{\text{message}} = \left(P_{\text{miss}}_{\text{word}} \right)^N = \left(1 - P_{\text{hit}}_{\text{word}} \right)^N$$

Where N is the number of words per message, which we have tentatively chosen to be 8. Thus, the probability of missing a single word is $1 - 0.7 = 0.3$, and the probability of missing all eight words in a message is $(0.3)^8 = 6.5 \times 10^{-5}$. Thus the probability of receiving at least one hit word out of eight transmitted when the probability of receiving any one word is 70 percent is:

$$P_{\text{hit}} = 1 - 6.5 \times 10^{-5} = 99.994 \text{ percent}$$

Hence, the kill zone will exceed one meter radius at 2 KM, and the hit probability will exceed 99 percent.

However, at 2 meters radial offset, the individual word detection probability is only 15 percent. Thus, at 2 meters radial offset:

$$P_{\text{hit}} = 1 - (1 - 0.15)^8 = 1 - 0.273 = 72.7 \text{ percent}$$

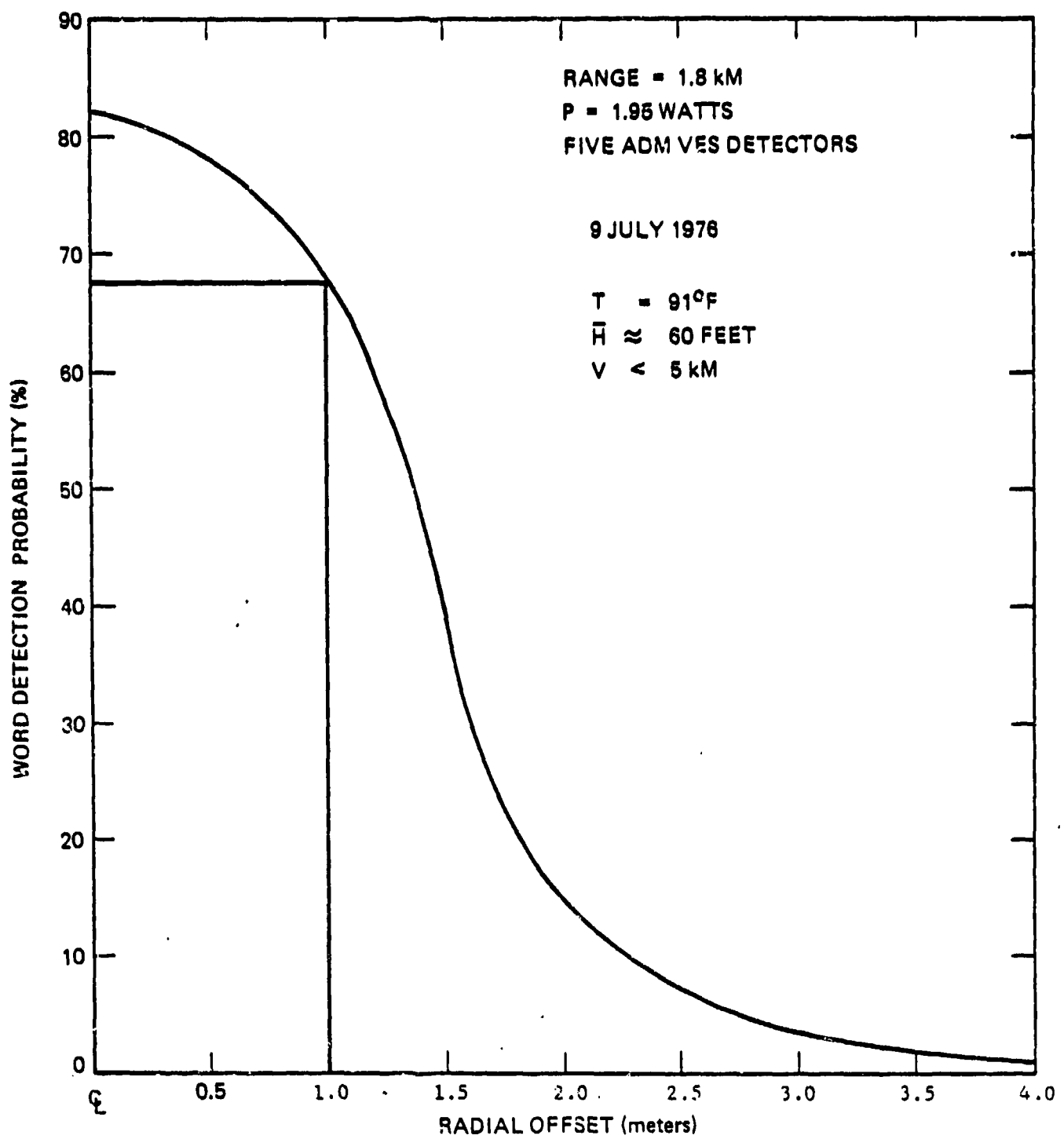


Figure E-2. Word Detection Probability versus Radial Offset

56261

E-7

While this is still quite good, we note that the overall hit probability is beginning to decrease. At $r = 3$ meters, we find:

$$P_{\text{hit}} = 1 - (1 - 0.035)^3 = 24 \text{ percent}$$

While at $r = 4$ meters:

$$P_{\text{hit}} = 1 - (1 - 0.01)^8 = 7.7 \text{ percent}$$

Thus we see that the probability of successfully receiving a single word out of eight transmitted words was in excess of 99 percent for a radius of about 1 meter at a range of 1.8 KM under very hazy conditions. However, the hit probabilities decrease rapidly as one proceeds radially outward from the beam center. If, however, we now transmit 128 words, then even at from $r = 3$ to 4 meters, we would find:

At $r = 3$ meters

$$\begin{aligned} P_{\text{near miss}} &= 1 - (1 - 0.035)^{128} \\ &= 1 - (0.965)^{128} = 1 - 0.01 \\ &= 99 \text{ percent} \end{aligned}$$

And, at $r = 3.5$ meters

$$\begin{aligned} P_{\text{near miss}} &= 1 - (1 - 0.02)^{128} \\ &= 1 - (0.98)^{128} = 1 - 0.07 = 93 \text{ percent} \end{aligned}$$

And, at $r = 4$ meters

$$\begin{aligned} P_{\text{near miss}} &= 1 - (1 - 0.01)^{128} \\ &= 1 - (0.99)^{128} = 1 - 0.276 \\ &= 72.4 \text{ percent} \end{aligned}$$

For the radial offsets less than $r = 3$ meters, the near miss probability would exceed 99 percent. However, since kill words:

- a. Are transmitted before near miss words
- b. Are decoded before near miss words
- c. Have priority over near miss words

Then we may construct the following graph, figure E-3, showing the probabilities of hit, near miss, and miss as a function of radial offset from the optimal aiming point, for a range of 1.8 KM under the conditions stated above. We note that from centerline to $r = 1$ meter, the hit probability is essentially unity. As one moves from $r = 1$ meter to $r = 3$ meters, the hit probability decreases but the near miss probability is so high that if a hit is not scored then a near miss almost certainly will be. Beyond 3 meters radial offset, the kill probability is quite low and is decreasing rapidly, although the near miss probability remains quite high out to about $r = 4$ meters where it begins to rapidly diminish. It is worth noting that the 99 percent probability points for hit and near miss occur at just about 1 meter and 3 meter radial offsets. These values are essentially the ideal of the original two laser near miss concept, yet they are the natural consequence of the physical effects of atmospheric scintillation and the selection of 8 code words for the kill beam and 128 code words for the near miss beam.

E.1.4 CONCLUSIONS AND XEOS ACTIONS

- a. For VES, the single tube transmitter concept appeared to have considerable merit and was selected as a design baseline approach.
- b. Data taken at 1.8 KM confirmed the reduction in detection probability with radial off-set from the aiming point.
- c. Analysis of an 8 word kill message followed by a 128 word near miss message indicated an effective kill beam diameter of about 1 meter and a concentric near miss zone having an effective diameter of about 3 meters, can be expected at a range of 1.8 KM.

56260

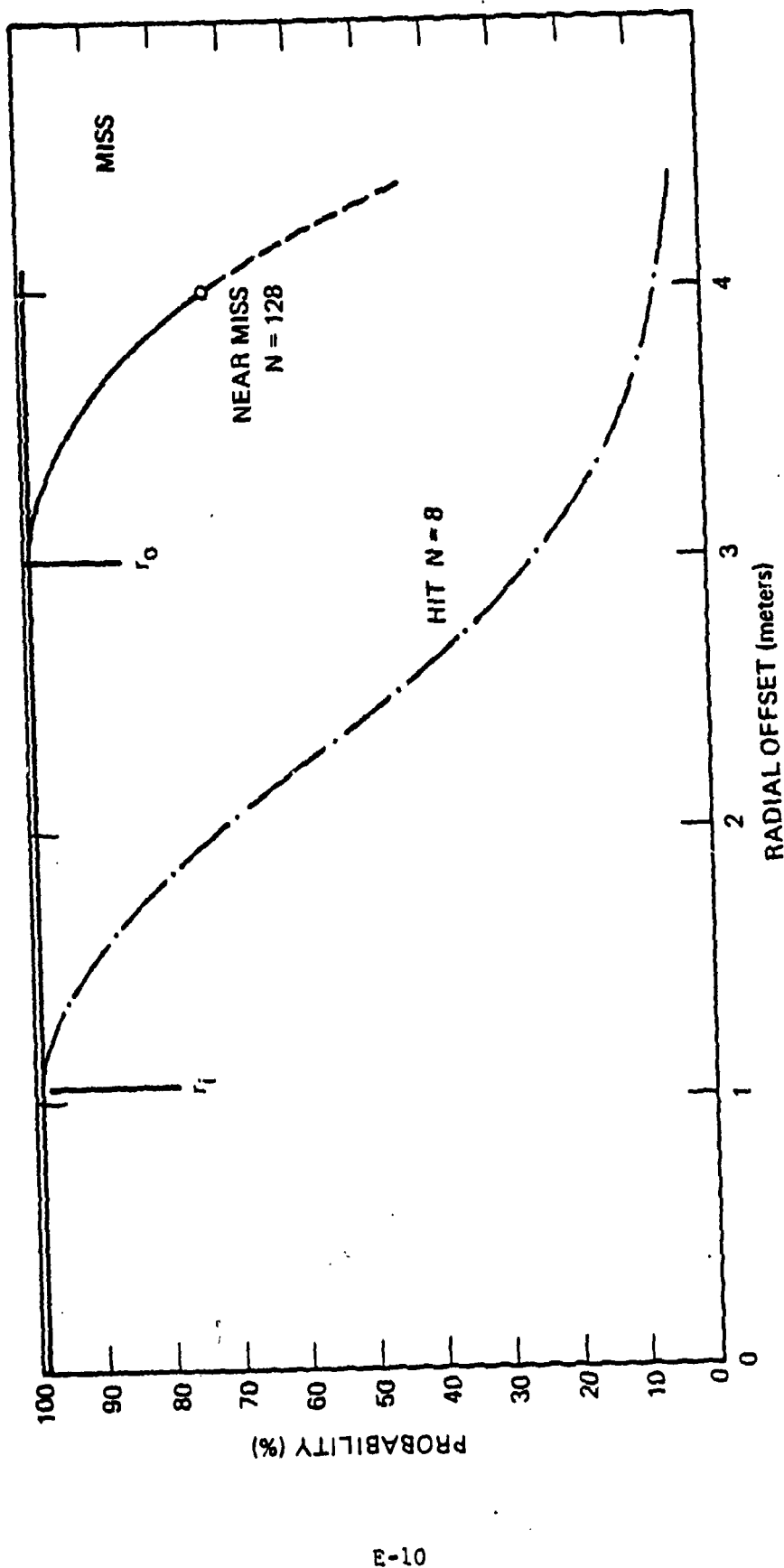


Figure E-3. Hit and Near Miss Detection Probabilities

- d. Additional testing of the single tube VES kill/near-miss concept, utilizing the ED MILES binary union code/decode concept, was required to establish full technical feasibility. The cost, size, weight, reliability, simplicity, and eye safety advantages of the single tube VES concept were so significant that this approach justified a parallel test program to verify the analysis.
- e. Based on the results of the previous analysis and preliminary tests, a MILES breadboard transmitter/encoder and receiver/decoder pair were fabricated. This encoder and decoder generated the proposed ED codes and utilized the "Boolean Union" decoding scheme discussed in this report.
- f. The breadboard equipment was used to develop experimental data on actual kill and near-miss zone sizes and kill and near-miss hit probabilities at ranges from 25 meters to 4 KM. The El Mirage tests were repeated with ED system hardware.

E.2 THE TES SINGLE TUBE APPROACH

For the VES system the effects of scintillation at long range have been shown to generate an effective near miss zone when numerous near miss words are transmitted. For the TES system the range values are considerably reduced and the effects of scintillation are considerably less important than for the VES case. However, in the VES case the laser transmitter is mounted on a very stable platform (e.g., a tank!) and there is negligible "aiming wander" during the transmission of a kill/near miss message even though that message may require over 400 milliseconds. In the TES case, the weapon is either an M16A1 rifle or a machine gun. Here we find that there are two weapon aiming perturbation effects:

- a. The motions induced as a result of firing blanks.
- b. The natural tremor motions associated with the human soldier.

E.2.1 EFFECTS OF HUMAN TREMOR

Relevant data regarding the effects of the motions resulting from blank fire and tremor upon aiming accuracy were gathered during blank fire enablement tests. In these tests an M16A1 rifle was fitted with an AD GaAs transmitter and was turned on in the continuous mode (i.e., firing continuous laser pulses at 3.2 KHz). Five detectors were spaced in a rectangular array, with one detector in the center. The mean inter-detector spacing was about 1 foot. Tests were performed at 100 meters (i.e., 328 ft.). Hence the mean angular spacing was about 1 part in 328 or about 3 milliradians. Six different persons were tested, firing at a stationary target in the standing, sitting, and prone positions. Under ideal conditions (i.e., no distractions, no target motion, no time limit and excellent target visibility) the typical tremor effects showed a 3 milliradian random motion of the laser beam. This was evident when the strip chart recording from all five detectors showed a wander from one detector to another. In many cases the tremor resulted in wander to a second or even a third detector. It can be concluded that tremor is responsible for a 3 to 10 milliradian random motion in the aiming point and is dependent upon individual proficiency. A portion of a strip chart showing the effects of tremor is seen in figure E-4.

Noting that time reads from right to left on the chart, it is seen that WITHOUT BLANK FIRE the individuals aiming point shifted from the lower right detector to a position encompassing both the lower right and center detectors, through the center detector and on to the upper left detector. Thus it is concluded that during the period of this strip chart recording the individual's aiming point was moving diagonally from the lower right towards the upper left as a result of tremor. Since the pulse repetition frequency (PRF) was 3.2 KHz then the time between pulses is 0.3125 milliseconds, and the time interval from essentially "lower right only" to "upper left only" was about 40 milliseconds.

56259

UPPER RIGHT

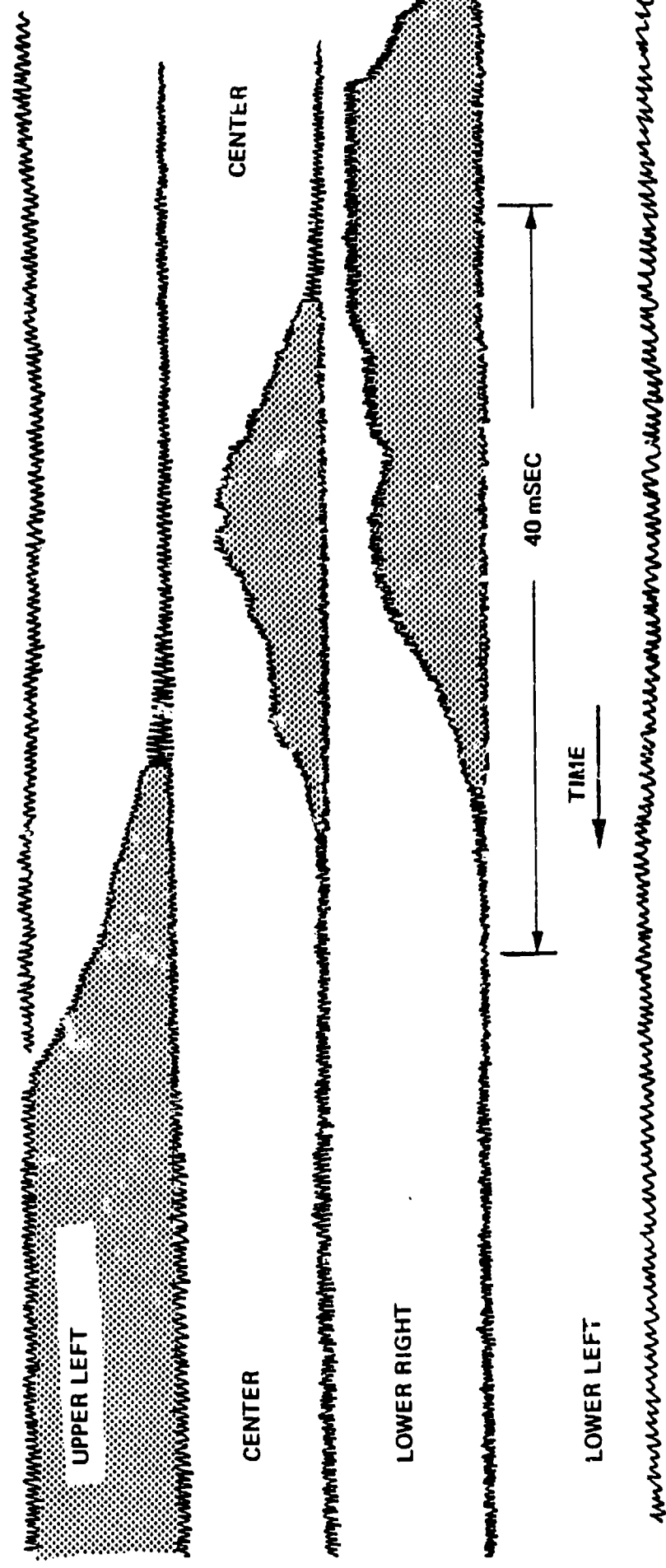


Figure E-4. Human Tremor, Strip Chart Recording

The TES system must be capable of firing 650 rounds per minute. This is equivalent to 10.83 rounds/second or 92.3 milliseconds/round. Since atmospheric scintillation will not have a major effect on TES performance, losing TES bits due to scintillation is unlikely. Thus, transmission of 4 kill words and receipt of 1 should be more than adequate. This will require a total time of 4 words/message x 11 bits/word x 0.333 msec/bit = 14.67 msec/message. This leaves about 78 msec for near miss information. If 24 near-miss words are transmitted and require receipt of 1 near-miss word to achieve a near miss, then each near-miss word will require 3.667 msec and the entire near-miss sequence will require the remaining 78 msec. Thus, all the available time between firings is utilized, which was not done on the AD system. Since it has been observed that angular perturbations as great as 4 to 10 milliradians can occur in 40 msec as the result of human tremor, then the 78 msec worth of near-miss information should be spread out over a zone of at least this order. Furthermore, since human tremor is expressed in milliradians, one would expect that the near-miss zone size would increase with range as a result of tremor. This is very realistic, since tremor is one of the major contributing factors to missing an actual target, and the effect with a real weapon does increase with range. At very short range the target subtends an angle much greater than the variations due to tremor, with the result that "one can hardly miss." At long range the target angular subtence is small compared to variations due to tremor.

Riflemen are taught to allow for tremor by breathing control. When the sight is aligned with the target, they squeeze off the round at that instant. Nonetheless, at long range, tremor remains a major cause of near miss. Thus, it is very appropriate that MILES should utilize the natural effects of human tremor as the basis of TES near miss. Essentially, what we are establishing is the following line of reasoning:

- a. If you are aimed exactly at the target, and hold steady for 14 msec, and the target is within 300 meters you will almost certainly score a kill.
- b. If you are aimed at the target for at least 3.67 msec but less than 14 msec, as the result of tremor, you probably will score a kill.
- c. If you are aimed at the target for less than 3.67 msec you will most likely not score a kill. However, if for any 3.67 msec period out of the next 78 msec natural tremor causes the aiming point to move back onto the target (remember, the soldier is trying to hit the target), then you will score a near miss.
- d. If you are initially aimed off the target, there are two additional possibilities:
 - (1) You will remain off the target for at least fourteen milliseconds thereby not scoring a kill, but will wander onto the target during the next 78 milliseconds which will score a near miss. The tremor data suggests that if your initial aiming point was within 3 milliradians of the target there is a high probability this will occur. If one is 10 milliradians off in the initial aiming point the probability will be lower. The above discussion is qualitatively correct.
 - (2) Tremor effects will cause the aiming point to move further off target and nothing will be registered. This is possible, but the fact that the soldier is trying to hit the target causes him to constantly attempt to restore the proper aiming point. The likelihood that he will never move the beam close enough to the target, for even a single near miss word out of the 24 transmitted, seems rather small. If this does occur, the system will, in effect, reward totally inaccurate aiming with a complete miss.

E.2.2 CONCLUSIONS AND XEOS ACTIONS

- a. The effects of human tremor causes angular displacement of the aiming point by amounts between 3 and 10 milliradians.
- b. The use of a significantly greater number of near-miss words, relative kill words, has the effect of increasing the effective near-miss zone size.

The effects of blank fire will cause a further increase in the dispersion of the aiming point.

- d. Preliminary tests utilizing a TES 0.67 watt output power GaAs laser transmitter were performed using a 30 word (AD words) encoder and a non-binary-union decoder. The decoder was required to successfully decode two (2) words rather than one since two AD words more closely simulate one ED word of weight 6. The transmitter was mounted on an M16A1 rifle and fired at a MWLD harness at a range of 300 meters. The rifle was hand-held in the standing position, and was fired with blanks 20 times. Nineteen successful near miss receipts were recorded. This test did not utilize the proposed kill and near miss codes, the 4 and 24 words per kill and near miss message respectively, or the Boolean Union decoder. Thus, these results did not firmly establish the proof of feasibility of the single tube TES concept. However, they did indicate a good chance for success. Further testing with the ED proof test model confirmed the analytical results.
- e. As with VES, we fabricated and assembled a TES laser encoder employing the proposed kill and near-miss codes and word count. TES decoder also had the Boolean Union decoder.
- f. The above equipment was used to perform experimental tests from 5 to 500 meters to obtain kill and near-miss zone size versus range. This study was conducted in parallel with the development of the existing TES 2-tube transmitter approach. However, cost, weight, size, reliability, ease of boresighting and eye safety advantages of the single tube TES concept were so significant that we performed this study as early as possible and the results of these tests were such that the single tube laser transmitter was selected for ED MILES design.
- g. A further means of miss beam enhancement is to drive the laser at a higher power during the miss beam code transmission. This was tested, proven, and also incorporated in the ED MILES design.

APPENDIX F
WEAPON SIMULATION
(HIT PROBABILITY VERSUS RANGE)

APPENDIX F
WEAPON SIMULATION
(HIT PROBABILITY VERSUS RANGE)

1.1 ~~INTRODUCTION~~

A computer program has been developed by XROS to provide a plot of hit probability versus range. This program is as a function of many weapon parameters which are listed in Table F-1.

The analytical development of this computer program was based upon the following building blocks:

1. The Beam Geometry Equation (DPG-001) which develops the error ellipse as a function of axial and radial position from the transmitter.
2. Radiation and Detection Report (Journal of Applied Optics, October 1970 or DPG-002) which tracks the probability of intercepting a single bit in the presence of saturated detection, as a function of the irradiance.
3. The Pulse Decoding Probability Analysis (DPD-130) which relates overall message detection probability to single bit detection probability for a generalized pulse-coded message.

1.2 ~~INPUT PARAMETERS AND COMPUTABLE VARIABLES~~

1.2.1 ~~INPUT PARAMETERS~~

There are a number of parameters which have been optimized for the propagation of noise waves through a communication atmosphere and are thus listed as fixed parameters in the computer program. Their symbols and values are listed below:

TABLE F-1
GLOSSARY OF PARAMETERS

<u>Variable Number</u>	<u>Symbol</u>	<u>Explanation</u>
	P_H	= Hit Probability = probability of successful receipt of a message. ($0 \leq P_K \leq 1$)
(1)	Range (R)	= Range from transmitter to detector, meters.
(2)	Radius (r)	= Radial offset from centerline of transmitted laser beam, meters (Note: Radius = 0 implies "on centerline.")
(3)	E_o	= Transmitter Output Energy = energy per pulse out of the transmitter (after allowance for temperature compensation and optical losses), ergs.
(4)	D_o	= Transmitter aperture diameter, meters.
(5)	Beta	= Equivalent circular beam divergence, radians.
(6)	Lambda (λ)	= Wavelength of radiation, microns.
(7)	M	= Number of words/message required for successful detection.
(8)	U	= Number of Boolean Unions. (Note: U = 2 = Binary Union)
(9)	W	= Weight of word = number of active bits/word.
(10)	N	= Number of words transmitted per message.
(11)	Sigma N	= RMS detector noise level, watts.
(12)	Eta	= Collection efficiency of detector (including cosine losses, dust losses, EMI shield transmission losses, and spectral filter transmission losses).
(13)	A	= Effective detector area, (meters) ² .
(14)	T	= Effective threshold, ergs/M ² .
(15)	Sigma S	= Square root of the log irradiance variance due to saturated scintillation.
(16)	α	= Atmospheric extinction coefficient (M ⁻¹).
(17)	c	= Cosine of the angle between laser beam and detector normal.

<u>Symbol</u>	<u>Value</u>	<u>Description</u>
U	2,	Number of Boolean Unions fixed at 2
W	6,	Weight of word = number of active bits per word out of 11 possible locations
λ	900 nm	Wavelength of the GaAs lasers used in the transmitters
η	57%	Detector collection efficiency including window losses, EMI shield losses, and RG830 filter losses
A	1 cm ²	Effective detector area per detector module
D _o	2 cm	Transmitter aperture diameter

F.2.2 VARIABLE PARAMETERS

There are a number of parameters which vary for weapons and targets. These are listed below with ranges of value.

<u>Symbol</u>	<u>Range</u>	<u>Description</u>
P _o	0.2W to 2W	Transmitter output power
T	0.60 - 200 ns	Optical pulselwidth (50% FWHM)
β_1	.4 - 4 mrad	50% pt gaussian primary beam spread perpendicular to laser junction
β_2	.63 - 4 mrad	50% pt gaussian primary beam spread in plane of junction
β_3	.63 - 5.6 mrad	10% pt beam spread
N	4 to 128	Number of words transmitted per message
T	$20-30 \times 10^{-6}$ ergs	Effective threshold of receiver in ergs

F.2.3 UNCONTROLLABLE PARAMETERS

These parameters vary with atmosphere, test conditions, and background illumination.

<u>Symbol</u>	<u>Range</u>	<u>Description</u>
R	0 to 4 KM	Range of target from transmitter
r	0 to 4M	Radial offset from the centerline of transmitted laser beam
σ_N	1.57 μ w to 3 μ w	RMS detector noise level*
σ_s	0.7 to 1.5	Square root of log irradiance variance due to saturated scintillation
α	4.6 to 0.12/kM	Atmospheric extinction coefficient (600M to 23 KM visibility)

In the preliminary release of this document (A001, Volume I) curves were shown based on an earlier computer program. These curves gave a good first order approximation of probability of hit versus range as a result of 16 variable parameters. The program gave results that had certain limitations.

- a. Results were good to only approximately ± 25 percent.
 - 1. The Boolean Union analysis (Appendix D) was only to a first order of approximation. It has since been revised and should now be very accurate.
 - b. The program only took centerline irradiance into consideration.
 - c. The program did not take into consideration multiple detectors, their locations, and their cosine effects.
 - d. The program was based on a simple gaussian laser profile model and not on the more complex actual laser beam profile.

The limitations of this earlier model have been overcome and the program gives results that agree much more closely with actual field measurements.

The following subsections present:

- F.3 Analysis of the laser beam profile as a tri-gaussian beam
- F.4 Presentation of a formula for the energy collected at the target as a function of multiple detectors at varying angles with respect to the laser beam

*High Range = Man system with 4 detectors in sun and signal.

Low Range = M113 APC side with all 6 detectors in signal, and 4 out of 6 equivalent detectors in sun.

- F.5 A discussion of the development of Bit Probability in the presence of scintillation
- F.6 A discussion of the development of word probability as a function of bit probability
- F.7 Presentation of the current computer program
- F.8 Examples of computer simulation showing the effects of visibility and target angle on the kill zone and the probability of hit versus range

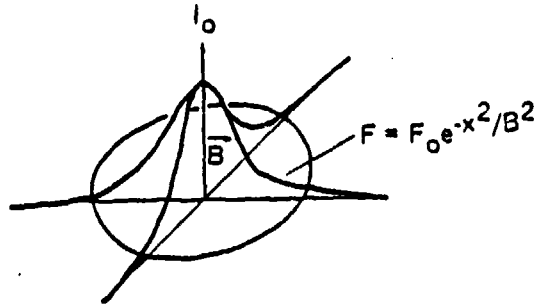
F.3 TRI-GAUSSIAN BEAM CONCEPT

In many cases the propagation of the narrow laser beam can be approximated by a Gaussian beam with an intensity distribution $I = I_0 e^{-x^2/\beta^2}$. This intensity distribution is shown in figure F-1A. In MILES simulation, the beam is not symmetrical, the far field beam is elliptical in shape. Thus, we must use a bi-Gaussian beam with two parameters β_1 and β_2 to simulate the far field parameters (see figure F-1B).

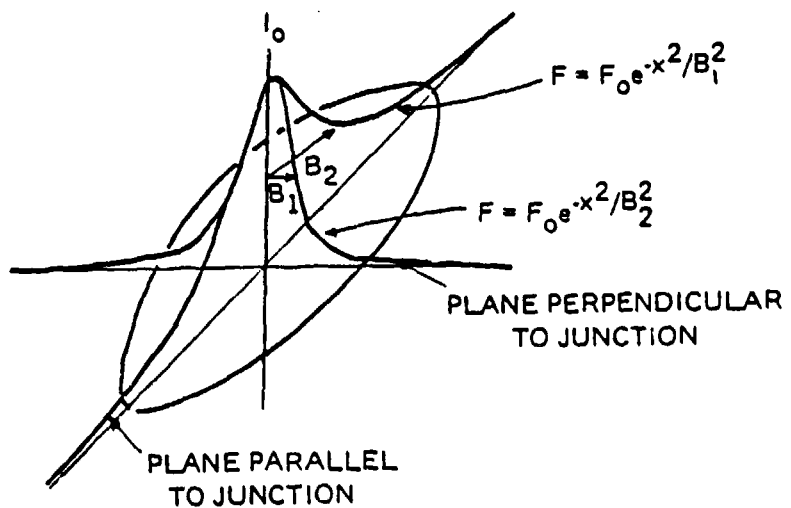
The near field intensity distribution is approximated by a third Gaussian. This Gaussian is assumed to be symmetrical in the vertical and horizontal planes. The form of the intensity distribution for MILES simulation takes the form of a tri-Gaussian equation shown below:

$$I = F_1 I_0 e^{-\left(\frac{x^2}{\beta_1^2} + \frac{y^2}{\beta_2^2}\right)} + F_2 I_0 e^{-\left(\frac{x^2 + y^2}{\beta_3^2}\right)}$$

In this equation, F_1 is the fraction of energy in the primary far field beam, and F_2 is the fraction of energy in the near field or "wings." The parameters F_1 , F_2 , β_1 , β_2 , and β_3 are determined empirically by examining various measured beam profiles using the MILES lens and 0.003 inch and 0.006 inch GaAs laser junctions at various focal positions.



A. SINGLE GAUSSIAN APPROXIMATION, SINGLE PARAMETER B
(CIRCULAR DISTRIBUTION)



B. BIGAUSSIAN APPROXIMATION, TWO PARAMETERS B_1, B_2
(ELLIPTICAL DISTRIBUTION)

Figure F-1. Laser Beam Profile Models

Analysis of the MILES transmitters assumes a beam profile characterized by three Gaussians. Two in the primary beam are characterized by Gaussian exponents B_1 , corresponding to the beam perpendicular to the laser junction and B_2 , corresponding to the beam in the plane of the junction. The beam "wings" which give the near field hit pattern are characterized by B_3 , assumed to be circularly symmetrical. A computer plot of beam profile for an M16 transmitter and the beam profile specification for a production M16A1 are shown in figures F-2 and F-3.

F.4 RECEIVER ENERGY CALCULATIONS

The position $X(N)$, $Y(N)$ and cosine of the angle $C(N)$ of each detector is used to determine the energy the target detector(s) collects for each transmitter aiming point.

The energy collected by the Nth detector is given below for a specific range R and aiming point X_0 , Y_0 with respect to the center of the target:

$$E(N) = \left[\frac{E_0 \cdot K \cdot F_1}{Y_1} \exp -A \left\{ \frac{J(N)^2}{(D_0 + R \cdot B_1)^2} + \frac{K^2(N)}{(D_0 + R \cdot B_2)^2} \right\} \right. \\ \left. + \frac{E_0 \cdot K \cdot F_2}{Y_2} \exp -A \left(\frac{J(N)^2 + K^2(2)}{Y_2^2} \right) \right] C(N) e^{-\alpha R} \quad (2)$$

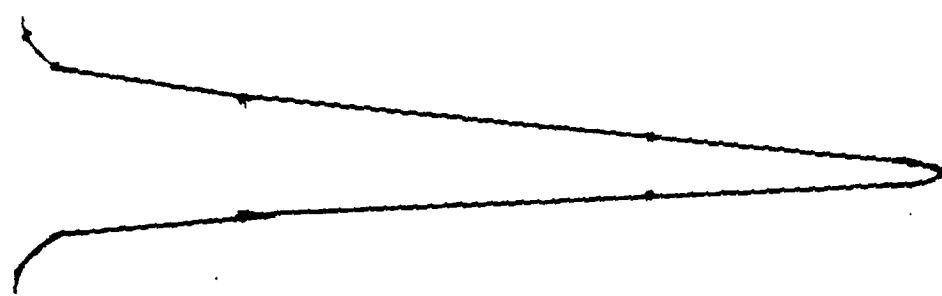
where:

$J(N)$ = horizontal distance between the aiming point and the Nth detector = abs $(X(N) - X_0)$

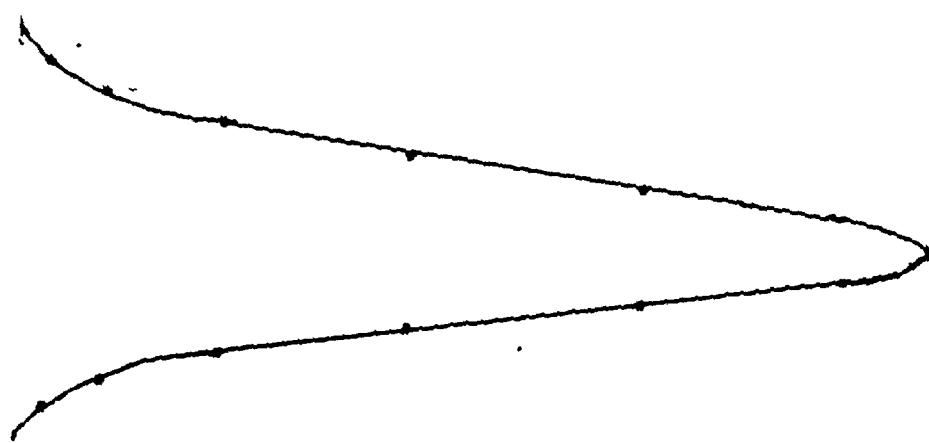
$K(N)$ = vertical distance between the aiming point and the Nth detector = absolute value $(Y(N) - Y_0)$

$$K = \frac{40 \log_e(10)}{(9 \cdot \pi)}$$

$$Y_1 = (D_0 + R \cdot B_1) * (D_0 + R \cdot B_2)$$



A. TRIGAUSSIAN BEAM PROFILE PERPENDICULAR TO JUNCTION



B. TRIGAUSSIAN BEAM PROFILE IN PLANE OF JUNCTION

Figure F-2. Computer Plot of Simulated Energy Output
For M16A1 Laser Transmitter

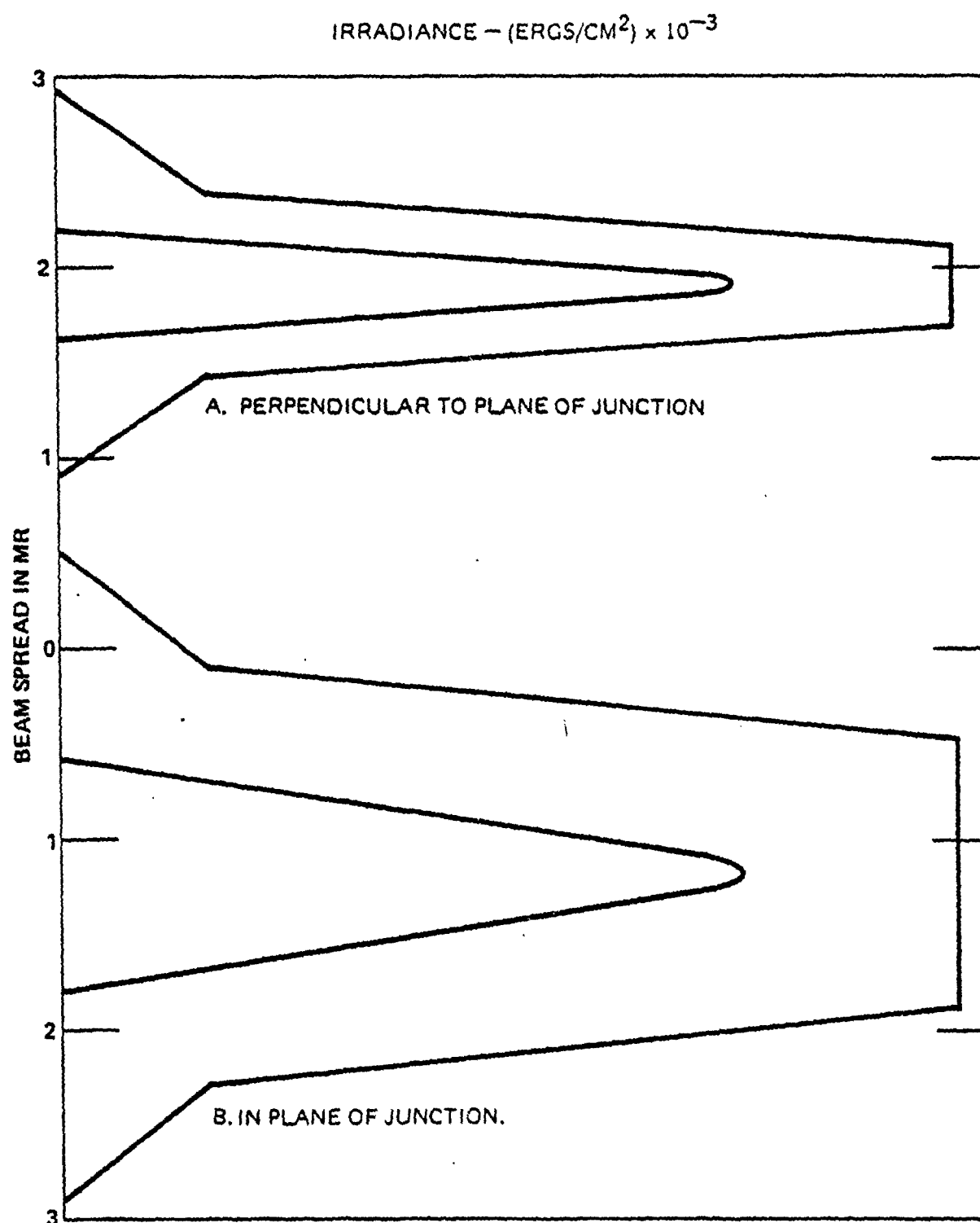


Figure F-3. Beam Profile Acceptance Criteria (min/max curves) For M16Al Laser Transmitter

61699

$$Y_2 = (D_o + R \cdot B_3)^2$$

$$A = 4 \log_e(10)$$

R = range

α = atmospheric absorption

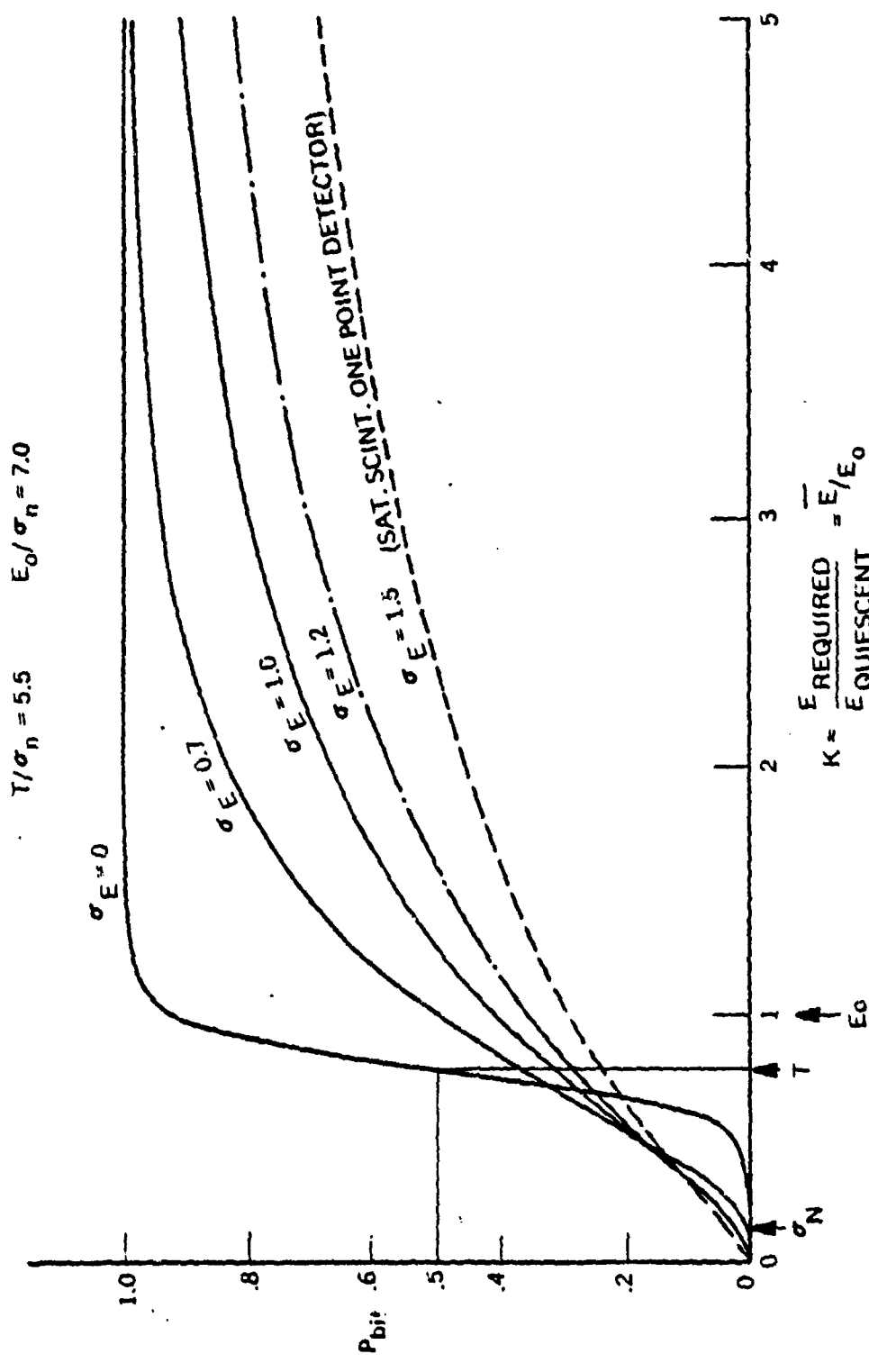
C(N) = cosine of the angle that the Nth detector makes with the laser beam

F.5 SCINTILLATION EFFECTS AND BIT DETECTION PROBABILITY

A laser pulse propagating through the atmosphere has the spatial and temporal properties of its irradiance distribution altered. Turbulence in the atmosphere cause the beam spread to increase slightly and produces intensity fluctuation about the average, called scintillation. The increase in beam spread due to atmospheric effects can be neglected for MILES analysis, however, the scintillation effects must be considered.

A paper by R. W. McMillan and N. P. Barnes, "Detection of Optical Pulses; the Effects of Atmospheric Scintillation"¹ allows the determination of the bit detection probability when the energy collected is known. Figure F-4 is a plot of the bit detection probability versus fraction of nominal required energy (K factor) for various values of c_E , the log amplitude standard deviation corrected for saturation and aperture averaging. With no scintillation present, $c_E=0.0$ we could have almost 100 percent probability of getting a hit when K=1 or the signal collected exceeds the threshold. With scintillation, however, the probability of getting a hit goes down with the same energy. A look-up table is used in the weapon simulation computer program to determine the probability of getting a bit through under a specific scintillation condition. Equation (2) gives the amount of energy collected at the target. The cosine of each angle is considered as is the atmospheric absorption. The ratio of this collected energy to the threshold energy, K factor, is determined. The hit detection probability is then determined from the look-up table.

61725



F-11

Figure F-4. Bit Detection Probability versus Fraction of Normal Required Energy

F.6 WORD AND HIT PROBABILITY DETERMINATION

In subsection F.4 we showed how to determine the probability that a bit transmitted is detected at the target. Once this bit probability is known, the word probability and hit probability can be calculated.

F.6.1 DEVELOPMENT OF THE EQUATIONS

Since Boolean Union decoding is employed in the MILES decoder, there are two chances that a bit can be received in a word slot. Let P be the calculated bit detection probability described in subsection F.4. The probability that at least one bit will be received is given by:

$$P_b = 1 - (1 - P)^2 \quad (3)$$

if we require 6 bits to be decoded in a word, then the probability that a word P_w is decoded is given by:

$$P_w = (1 - (1 - P))^6 \quad (4)$$

The numbers of words sent per round vary from weapon to weapon and this requires separate analysis of each weapon class.

For the case of a 105 mm main gun, there are 8 words sent and at least 2 words must be received to get a hit. There are C_2^8 or 28 ways that exactly two words can be received. Thus the probability that exactly 2 words are received is:

$$P_w(2) = C_2^8 P_w^2 (1 - P_w)^6$$

where P_w^2 is the probability that any two words are received and $(1 - P_w)^6$ is the probability that exactly 6 words were not received.

If exactly 3 words are received, we still get a hit. There are $C_3^8 = 56$ ways that exactly 3 words with 8 sent can be received:

$$P_W(3) = C_3^8 p_W^3 (1 - p_W)^5$$

The total probability that at least n words are received when m are sent can now be written by generalizing the two specific cases.

$$P_{hit} = \sum_{R=M}^N C_R^N p_W^R (1 - p_W)^{N-R} \quad \text{where } C_R^N = \frac{N!}{(N-R)! R!} \quad (5)$$

In conclusion, given a bit detection probability we can calculate the hit detection probability using equations 3, 4, and 5 as follows:

- a. Determine bit probability using Eq. 3
- b. Knowing bit probability, determine word probability using Eq. 4.
- c. Knowing word probability, determine hit probability using Eq. 5.

F.6.2 VALIDATION OF THE EQUATIONS

To validate the equations (Eqs. 3, 4, and 5) for obtaining the hit probability from word and bit probabilities, a computer simulation of the MILES decoding system was run for the various weapon classes. With bit probability as a variable, MILES type 6 weight words were generated. The computer performed Boolean Union decoding (i.e., or'd) on each consecutive pair of two words. For each selected set of criteria, 100 rounds were computer generated.

Figure F-5 shows the results of 3 of the 100 rounds fired for the 105 mm gun where a hit requires successful receipt of 2 words out of the 8 transmitted. For this set of 100 rounds, the bit probability was set at 50 percent. Bits were randomly generated by the computer. Several things should be noted from the figure.

INPUT WORDS REQUIRED, WORDS SENT

?2,8

INPUT BIT PROBABILITY

?50

NON UNION WORDS

	Word No.
0 1 1 1 1 1	1
0 0 1 0 0 1	2
1 1 0 0 1 0	3
0 1 0 1 0 0	4
0 1 0 1 1 1	5
0 0 1 1 1 0	6
0 0 0 1 0 1	7
1 0 1 0 0 0	8

BOOLEAN UNION WORDS

0 1 1 1 1 1	1
0 1 1 1 1 1	2
1 1 1 0 1 1	3
1 1 1 0 1 1	4
0 1 0 1 1 1	5
0 1 1 1 1 1	6
0 0 1 1 1 1	7
1 0 1 1 0 0	8

Words with Bits OR'D

0
1
2
3
4
5
6
7
8
0

Round No. 1

BIT PROB .479167 WORD PROB 0

NO HITS

INPUT BIT PROBABILITY

?50

NON UNION WORDS

	Word No.
1 0 0 1 1 1	1
0 1 0 0 1 1	2
1 1 0 0 1 1	3
1 1 0 1 1 0	4
1 0 1 1 1 1	5
1 1 1 0 1 1	6
1 0 0 0 1 0	7
1 1 1 1 0 1	8

BOOLEAN UNION WORDS

1 0 0 1 1 1	1
1 1 0 1 1 1	2
1 1 0 0 0 1	3
1 1 0 1 1 1	4
1 1 1 1 1 1	5
1 1 1 1 1 1	6
1 1 1 0 1 1	7
1 1 1 1 1 1	8

Words with Bits OR'D

0
1
2
3
4
5
6
7
8
0

Round No. 2

BIT PROB .666667 WORD PROB

.333333

WE HAVE A HIT

INPUT BIT PROBABILITY

?50

NON UNION WORDS

	Word No.
0 0 1 0 0 0	1
0 1 1 0 1 1	2
1 1 1 1 0 1	3
0 0 0 0 1 0	4
1 1 1 0 0 0	5
0 1 0 0 0 0	6
1 1 1 1 0 1	7
0 0 0 1 1 0	8

BOOLEAN UNION WORDS

0 0 1 0 0 0	1
0 1 1 0 1 1	2
1 1 1 1 1 1	3
1 1 1 1 1 1	4
1 1 1 0 1 0	5
1 1 1 1 0 0	6
1 1 1 1 0 1	7
1 1 1 1 1 1	8

Words with Bits OR'D

0
1
2
3
4
5
6
7
8
0

Round No. 3

BIT PROB .458333 WORD PROB

.333333

WE HAVE A HIT

INPUT BIT PROBABILITY

?

Figure F-5. Computer Simulation of Word Receipt Bit Detection Probability 60% for a 105 mm Gun.

- 1. First, the target response is the MBR decoder and Boolean logic decoding. The logic value is looked at twice by the decoder. This guarantees that the decoder receives a correct bit every time.
- 2. The word stage works. Most of the 4 words would have created 0 bits.
- 3. The bit stage works decoding. Rounds 1 and 2 each output 8 bits.

Figure 1 is a plot of the results of the computer simulation of the DMR decoding system. The curves for bit, word, and message probability values the computer was plotted manually from its simulated simulation data. The first point is a curve to the average of the message probability values of the generated test probability, namely 0.0001, 0.001, and 0.00000001 messages per iteration.

The second plot in figure 1 is the probability with results obtained using the 1.0, 0.1, and 0.0001 message set probabilities. Computer results were taken - except of course. Because 1.0 is the same assumed for decoding the computer does not program.

~~Computer Simulation Results~~

The computer program that was developed to determine self-corrected MBR probability is the first. The first is a program to determine the probability of the target for a fixed coding point on the target. The target is a sequence of integers for each one being tested. Each integer contains binary digits which are 0 or 1. These are probabilities.

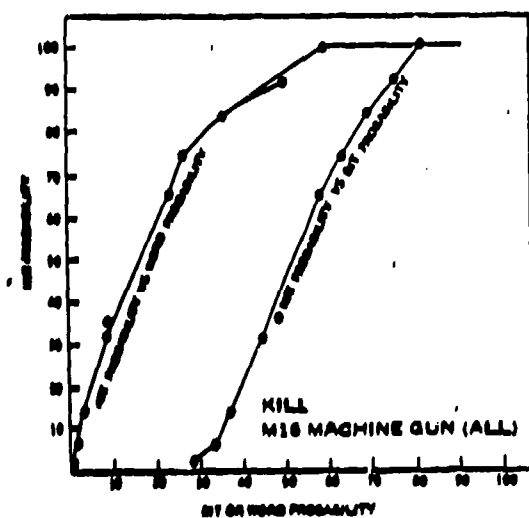
~~Computer Results for Coding Point = 20000 Bits~~

Figure 2 illustrates a second a fixed coding point is that target shown in table 1. The computer program runs the message from the computer to the computer to the test program to target system. Target

61797

WITH BOOLEAN UNION = 8 WORDS DECODES ARE POSSIBLE.
1 WORD REQUIRED OUT OF 4 SENT

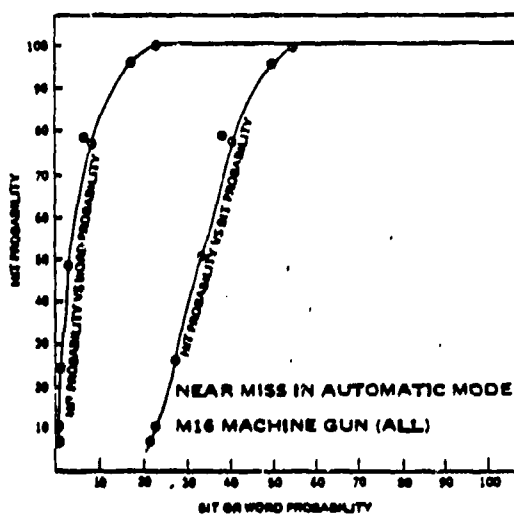
A.



61791

WITH BOOLEAN UNION 21 WORDS CAN BE DECODED
1 WORD REQUIRED OUT OF 20 SENT

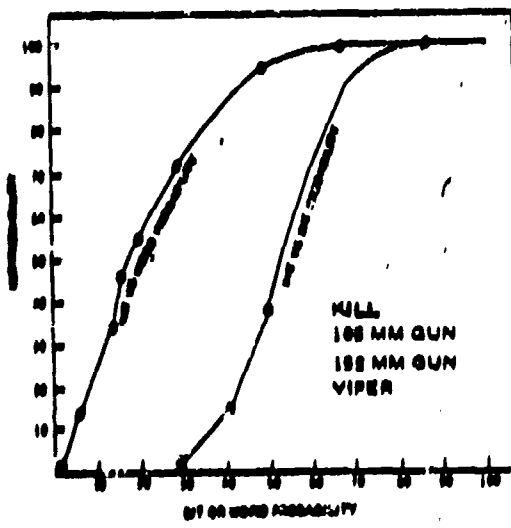
B.



61798

WITH BOOLEAN UNION = 9 WORDS ARE POSSIBLE.
1 WORD REQUIRED OUT OF 1 SENT KILL

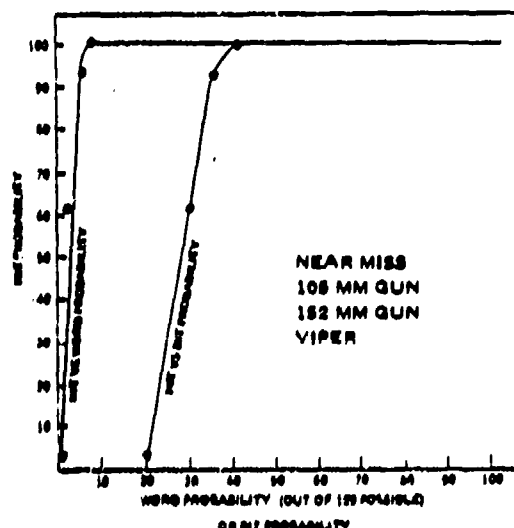
C.



61790

WITH BOOLEAN UNION = 119 WORDS ARE POSSIBLE.
2 WORDS REQUIRED OUT OF 128 WORD SENT

D.



61799

COMPUTER SIMULATION FOR HIT WORD, AND NOTWORD PROBABILITY
ADDED TO HIT PROBABILITY CALCULATION

H WORDS SENT. H WORDS REQUIRED PER MESSAGE FOR HIT
1 WORD SENT PER MESSAGE. 1 WORD REQUIRED PER MESSAGE

E.

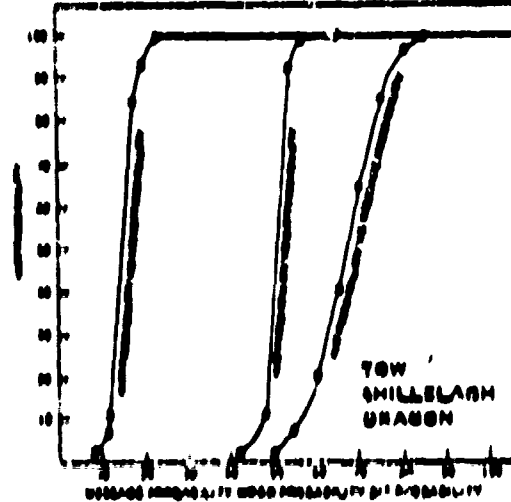


Figure F.5.
Computer Simulation — Hit Probability
As a Function of Bit, Word & Message
(Missile Only) Probabilities.

calculations are used in all MILES performance analyses because receivers are energy dependent and not peak power dependent as are most optical receivers.)

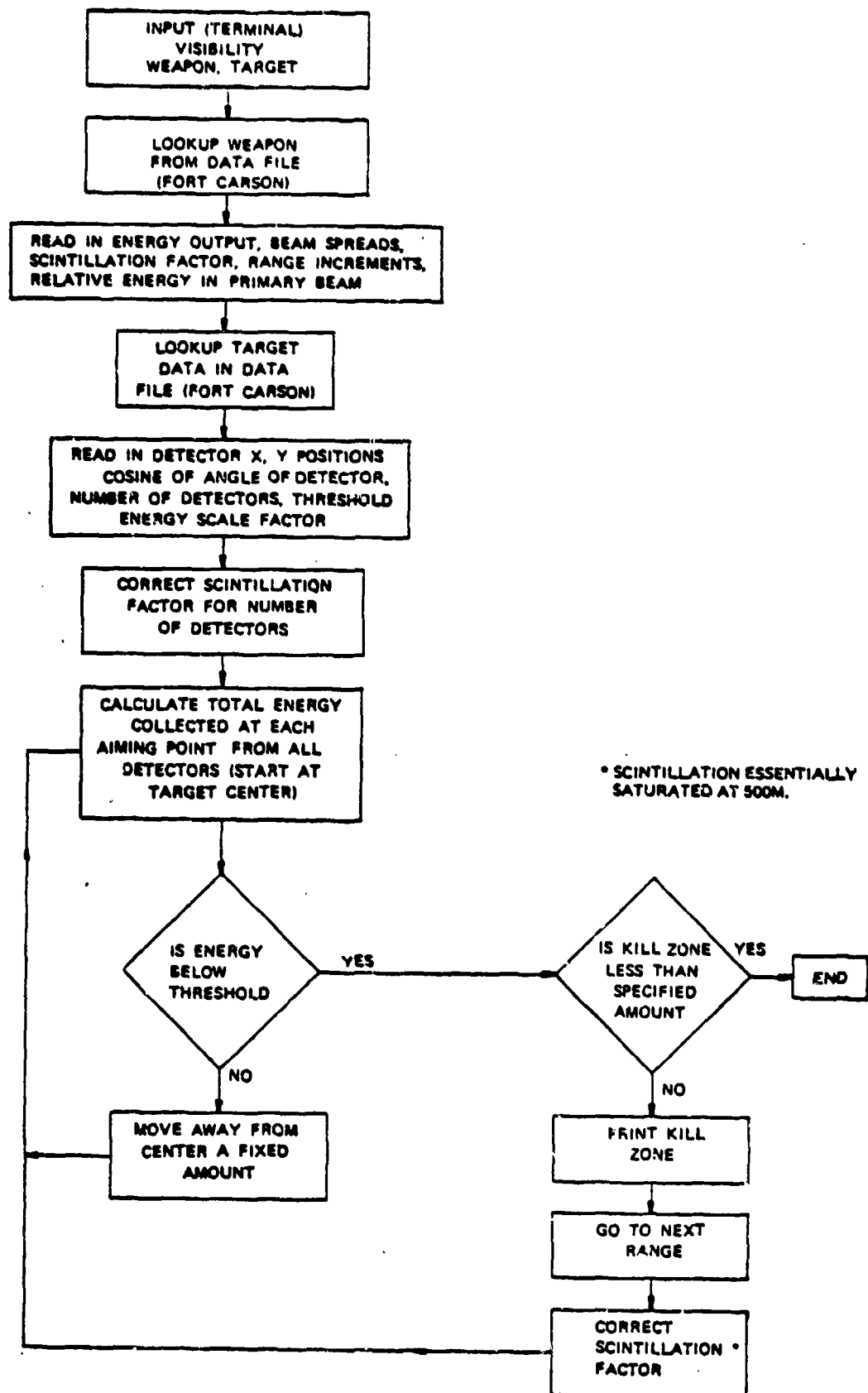
Figure F-7 is a simplified flow diagram of the computer program for determining centerline hit probability versus range. The actual program is included as table F-2.

The computer input requires the following data:

- N_7 = Number of detectors
- $r(x,y)$ = Detector position with respect to the target geometric center
- c = Cosine of the angle each detector makes with the transmitter optic axis
- E_0 = The energy output of the transmitter
- $\beta_1, \beta_2, \beta_3$ = The Gaussian exponents B_1, B_2, B_3 , of the transmitter
- σ_E = Scintillation factor
- F_1, F_2 = Fraction of energy in primary and secondary beams
- T = Receiver threshold energy, ergs
- K = K factor which depends on number of words sent, number of words required, σ_E (see figure 7)

In addition, data from the computer files are required:

- 1E A002 (table F-3)
Contains the visibility, weapon, target, number of words required for a hit or miss, the number of words sent, and the value of sigma e.
- *E FT CARSON (table F-3)
Contains weapon and target characteristics.
- F SCINTOUT (table F-4)
Contains hit probability versus K factor for various scintillation values.



61733

Figure F-7. Flow Diagram of Computer Program for Centerline P_H versus Range

TABLE F-2
COMPUTER PROGRAM FOR DETERMINING CENTERLINE HIT PROBABILITY

```

LIST
10 OPEN'A002' T0:2,1 INPUT
20 I INPUT:2,V,F$,TS,J,S,SS
100 DIM Q(45)
110 DIM L(45)
120 OPEN'SCINTOUT' T0:3,1 INPUT
150 I INPUT:3,B$
160 IF B$=S$ THEN 180
170 GOTO 150
180 I INPUT:3,B$
190 FOR N1=1 TO 45.1
200 I INPUT:3,L(N1)
210 NEXT N1
220 I INPUT:3,B$
230 FOR N1=1 TO 45.1
240 I INPUT:3,L(N1)
250 NEXT N1
260 *ALL DIMENSIONS ARE IN CM
290 OPEN 'FTCARSLN' T0:1,1 INPUT
300 I INPUT:1,W$
310 IF W$<>R$ GOTO 300
320 I INPUT:1,P,B1,B2,B3,K3,Z3,F1
330 I INPUT:1,PS
340 IF PS<>TS GOTO 330
350 I INPUT:1,N7
360 FOR B=1 TO N7+.1
370 I INPUT:1,X(B),Y(B),C(B)
380 NEXT B
390 I INPUT:1,T,S1,S2
420 DIM H(50)
430 DIM V(50)
440 *X(N),Y(N) IS POSITION OF NTH DETECTOR
450 *J(N) IS THE DISTANCE BETWEEN X AND X(N)
460 DIM N(8)
470 DIM I(8)
480 *K(N) IS THE DISTANCE BETWEEN Y AND Y(N)
490 *P= LASER XMITTER OUTPUT
500 *Z IS THE RANGE
510 D=2
520 *H IS THE ON AXIS IRRADIANCE AT Z
530 *F1 = FRACTION OF P IN GAUSSIAN B1
540 *F2 FRACTION OF POWER IN GAUSSIAN B
550 F2=1-F1
560 A=4* LOG(10)
570 *A1= ATMOSPHERIC AIR ABSORPTION PER CM
580 A1=2.84E-5/V
590 PRINT 'TRANSMITTER OUTPUT ENERGY 'P 'ERGS'

```

TABLE F-2

COMPUTER PROGRAM FOR DETERMINING CENTERLINE HIT PROBABILITY (Contd)

```

600 ;' VISIBILITY 'V' KM'
610 PRINT
620 PRINT
630 PRINT
640 ; TAB(2)'HIT PROBABILITY VS RANGE FOR 'RS' FIRING AT 'TS
650 PRINT
660 PRINT
670 *D=LENS DIAMETER IN CM
680 FOR Z=23 TO 5000E2 STEP Z3
690 B=(3*(1-.8*EXP(-Z/2.5E4))**T
700 B=0
710 K=40* LOG(10)/(9*3.1416)
720 Y1=(D+Z*B1)*(D+Z*B2)
730 Y2=(D+Z*B3)**2
740 Y=0
750 X=0
760 I=0
770 FOR N=1 TO N7+.1
780 J(N)=ABS(X-X(N))
790 K(N)=ABS(Y-Y(N))
800 H=P*K*F1/Y1*EXP(-A*(J(N)**2/(D+Z*B1)**2+K(N)**2/(D+Z*B2)**2))
810 H=(H+P*K*F2/Y2*EXP(-A*(J(N)**2+K(N)**2)/Y2))*EXP(-A*Z)
820 I=C(N)*H+I
830 NEXT N
840 IF I<10* T GOTO 870
850 G2=1
860 GOTO 940
870 T8=I/T
880 FOR N1=1 TO 45.1
890 IF L(N1)< T8 THEN 930
900 P8=Q(N1-1)+(Q(N1)-Q(N1-1))/(L(N1)-L(N1-1))*(T8-L(N1-1))
910 G=1-(1-P8)**2
911 G1=G**6
912 G2=1-(1-G1)**8
913 IF G=1 GOTO 915
914 G2=G2-S*G1*(1-G1)**(S-1)
915 IF G2<.001 GOTO 970
920 GOTO 940
930 NEXT N1
940 ; TAB(0)'"INT(Z/100)"TAB(6)"-'TAB(66*(G2+6))"-
950 NEXT Z
960 K(N)=ABS(Y-Y(N))
970 GOTO 20
980 END
990 ;
1000 ;
1010 ;
>

```

Table F-3
WEAPON AND TARGET CHARACTERISTICS

1E A002

EDIT HERE

*TY

1.000 23,105MM(NEAR-MISS), VEHICLE(STANDARD-TARGET), 2, 128, 1.00
 2.000 10,105MM(NEAR-MISS), VEHICLE(STANDARD-TARGET), 2, 128, 1.00
 3.000 3,105MM(NEAR-MISS), VEHICLE(STANDARD-TARGET), 2, 128, 1.00

--EOF HIT AFTER 3.

*F FICARS IN

*TY

1.000 DRAGON 1.3 .0025 .0041 .007	1.44 100E2 .44
2.000 M12 WICKILL) 1.4 .0036 .0013 .007 1.8 100E2 .44	
2.100 M12 W(NEAR-MISS) 3 .0036 .0013 .007 .83 100E2 .44	
3.000 105MM(ILL) 3.0 .0032 .0012 .015 1.8 100E2 .44	
3.100 105MM(NEAR-MISS) 4.0 .0032 .0012 .015 1.8 100E2 .44	
4.000 VIPER(ILL) .3 .005 .005 .007 1.3 25E2 .44	
4.100 VIPER(NEAR-MISS) 1 .005 .005 .007 1.3 25E2 .44	
5.000 MACHINE-GUNS(ILL) .32 .0006 .0016 .007 1.86 50E2 .44	
5.100 MACHINE-GUNS(NEAR-MISS) 1 .0006 .0016 .007 1.1 50E2 .44	
6.000 SHILLELAGH 3 .0032 .0012 .007 1.44 100E2 .44	
7.000 TOW 3 .0032 .0012 .007 1.44 100E2 .44	
8.000 M16(ILL) .25 .0006 .0016 .007 1.86 25E2 .44	
8.100 M16(NEAR-MISS) 1 .0006 .0016 .007 1.1 50E2 .44	
9.000 COAX(ILL-152MM) .36 .006 .006 .007 1.32 50E2 .44	
20.000 M60A1(SIDE) 7 - 15 1 40 .4 - 162 0 .2 - 115 0 .8 - 64 0 .9	
21.000 -10 0 1 48 0 1 107 0 1	
22.000 24E-6 400 200	
23.000 M60A1(FRONT) 5 44 40 .9 44 0 .94 90 0 .5 114 0 .3	
24.000 126 0 .05	
25.000 24E-6 400 200	
26.000 M60A1(REAR) 4 - 79 0 .93 - 20 0 .98 38 0 .98 98 0 .94	
27.000 24E-6 400 200	
28.000 M113(SIDE) 6 - 148 0 1 - 88 0 1 - 30 0 1 30 0 1 88 0 1 148 0 1	
29.000 24E-6 400 200	
30.000 M113(FRONT) 4 - 57 0 .7 - 18 0 .7 18 0 .7 57 0 .7	
31.000 24E-6 400 200	
32.000 M113(REAR) 4 - 63 0 .98 - 30 0 .98 0 0 .98 47 0 .98	
33.000 24E-6 400 200	
34.000 M551(SIDE) 7 - 82 30 .5 - 82 0 .17 - 82 0 .68	
35.000 -36 0 1 27 0 .98 60 0 .86 100 0 0	
36.000 24E-6 400 200	
37.000 M551(FRONT) 3 50 30 1 70 0 1 113 0 .5	
38.000 24E-6 400 200	
39.000 M551(REAR) 1 - 80 0 .7	
39.100 24E-6 400 200	
40.000 MAN(FRONT) 4 10 10 1 10 - 10 1 - 10 - 10 1 - 10 10 1	
41.000 24E-6 150 150	
42.000 VEHICLE(STANDARD-TARGET) 5 - 120 0 1 - 60 0 1 0 0 1 60 0 1 120 0	

1

43.000 24E-6 400 200

--EOF HIT AFTER 43.

TABLE F-4
HIT PROBABILITY VERSUS K FACTOR

FSCINRUT									
OTY	THRES/NOISE=			SIGNAL/NOISE=			SIGMA E=		
1.000	TP/	.100	.125	.150	.175	.200	.225	.250	.275
2.000	TP/	.100	.125	.150	.175	.200	.225	.250	.275
3.000	TP/	.350	.375	.400	.425	.450	.475	.500	.525
4.000	TP/	.600	.625	.650	.675	.700	.725	.750	.775
5.000	TP/	.850	.875	.900	.925	.950	.975	1.000	1.500
6.000	TP/	3.000	3.500	4.000	4.500	5.000			2.000
7.000	TP/	.000	.000	.000	.000	.000	.000	.000	.000
8.000	TP/	.001	.002	.003	.006	.009	.015	.023	.034
9.000	TP/	.097	.130	.171	.219	.274	.335	.401	.470
10.000	TP/	.676	.734	.788	.835	.875	.907	.933	1.000
11.000	TP/	1.000	1.000	1.000	1.000	1.000			1.000
12.000	TP/	.350	.375	.400	.425	.450	.475	.500	.525
13.000	TP/	.600	.625	.650	.675	.700	.725	.750	.775
14.000	TP/	.850	.875	.900	.925	.950	.975	1.000	1.500
15.000	TP/	3.000	3.500	4.000	4.500	5.000			2.000
16.000	TP/	.000	.000	.000	.000	.000	.000	.000	.000
17.000	TP/	.001	.002	.003	.009	.014	.021	.030	.039
18.000	TP/	.077	.091	.107	.123	.140	.157	.174	.192
19.000	TP/	.246	.261	.282	.300	.318	.335	.352	.369
20.000	TP/	.418	.434	.449	.464	.479	.493	.507	.518
21.000	TP/	.536	.560	.573	.592	.602			.600
22.000	TP/	.100	.125	.150	.175	.200	.225	.250	.275
23.000	TP/	.350	.375	.400	.425	.450	.475	.500	.525
24.000	TP/	.600	.625	.650	.675	.700	.725	.750	.775
25.000	TP/	.850	.875	.900	.925	.950	.975	1.000	1.500
26.000	TP/	3.000	3.500	4.000	4.500	5.000			2.000
27.000	TP/	.000	.000	.000	.000	.000	.000	.000	.000
28.000	TP/	.006	.011	.018	.026	.035	.044	.055	.066
29.000	TP/	.102	.115	.128	.141	.153	.166	.179	.192
30.000	TP/	.230	.242	.254	.266	.278	.290	.301	.313
31.000	TP/	.346	.356	.366	.377	.387	.396	.406	.564
32.000	TP/	.800	.840	.870	.893	.911			.746
33.000	TP/	.100	.125	.150	.175	.200	.225	.250	.275
34.000	TP/	.350	.375	.400	.425	.450	.475	.500	.525
35.000	TP/	.600	.625	.650	.675	.700	.725	.750	.775
36.000	TP/	.850	.875	.900	.925	.950	.975	1.000	1.500
37.000	TP/	3.000	3.500	4.000	4.500	5.000			2.000
38.000	TP/	.000	.000	.000	.000	.000	.000	.000	.000
39.000	TP/	.012	.018	.026	.033	.044	.054	.064	.075
40.000	TP/	.107	.116	.126	.139	.150	.160	.171	.181
41.000	TP/	.212	.222	.231	.241	.250	.260	.269	.278
42.000	TP/	.304	.312	.320	.326	.336	.344	.352	.481
43.000	TP/	.700	.743	.777	.805	.828			.575
44.000	TP/	.100	.125	.150	.175	.200	.225	.250	.275
45.000	TP/	.350	.375	.400	.425	.450	.475	.500	.525
46.000	TP/	.600	.625	.650	.675	.700	.725	.750	.775
47.000	TP/	.850	.875	.900	.925	.950	.975	1.000	1.500
48.000	TP/	3.000	3.500	4.000	4.500	5.000			2.000
49.000	TP/	.000	.000	.000	.000	.000	.000	.000	.000
50.000	TP/	.018	.026	.030	.034	.031	.039	.048	.055
51.000	TP/	.103	.111	.119	.127	.135	.143	.151	.159
52.000	TP/	.181	.188	.195	.202	.209	.216	.223	.229
53.000	TP/	.248	.254	.260	.266	.272	.278	.283	.380
54.000	TP/	.561	.561	.624	.652	.686			.513
55.000	TP/	.100	.125	.150	.175	.200	.225	.250	.275
56.000	TP/	.350	.375	.400	.425	.450	.475	.500	.525
57.000	TP/	.600	.625	.650	.675	.700	.725	.750	.775
58.000	TP/	.850	.875	.900	.925	.950	.975	1.000	1.500
59.000	TP/	3.000	3.500	4.000	4.500	5.000			2.000
60.000	TP/	.000	.000	.000	.000	.000	.000	.000	.000
61.000	TP/	.001	.002	.003	.003	.003	.008	.012	.019
62.000	TP/	.029							.012

F.7.2 PROGRAM FOR KILL/MISS ZONES VERSUS RANGE

This program is similar to the program described in F.7.1 except that the hit probability is fixed and the aiming point with respect to the detectors is a variable. Thus a plot of the kill or near miss zone versus range for a fixed hit probability is the computer printout. The collected energy is summed for each aiming point and when the energy falls below that required for a kill or miss, the computer plots a point.

The required energy differs for each weapon class and hit probability. To determine the required energy, the hit probability is calculated from the hit probability. The energy required is then looked up in table F-IV (or figure F-4).

The aiming points are then plotted for each range. The computer program scans both left and right and above and below the target center. Therefore, if the detectors are not symmetrically placed about the target center, or have differing cosine values, the kill zone is not symmetric about the target. The program is capable of plotting either hit or near miss zones for any given hit probability.

In the section that follows, computer printouts are included to show the use of the two computer programs.

F.8 WEAPON SIMULATION WITH THE COMPUTER

In the following subsections computer simulation is used to show the effects of visibility and target angle on hit probability versus range and the effect of visibility on the kill zone size.

F.8.1 HIT PROBABILITY VERSUS RANGE AS A FUNCTION OF VISIBILITY

The general shape of the rolloff of the centerline hit probability is constant as visibility changes. However, the range at which the hit probability starts rolling off decreases as the visibility is reduced. Figure F-8 shows the effects of visibility on a 105 mm main gun firing at the vehicle standard target (figure F-9).

F.8.2 HIT PROBABILITY VERSUS RANGE WITH TARGET ATTACK ANGLE AS A VARIABLE

The hit probability versus range for a 105 mm main gun firing at an M60A1 tank for various attack angles is given in figure F-8. When two belt segments are in the beam, the overall hit detection probability is:

$$P_T = 1 - (1-P_1)(1-P_2)$$

where $(1-P_1) \times (1-P_2)$ is the probability of not getting a signal on Belt 1 and Belt 2. Thus, if two belts each having a hit detection probability of (0.4) are "ored" together as in MILES, the detection probability is 0.64 which is significantly greater than that for each belt. Considering multiple belts greatly increases the difficulty in computer simulation but, as shown in the above case, is required.

F.8.3 90 PERCENT HIT AND NEAR MISS ZONES

The hit and near miss zones of each weapon firing at its standard target are presented. The kill and near miss energies of the MILES ED production units are used in the computer simulation. The following cases are analyzed. The near miss for TOW and Dragon are not included because there is no fixed near miss zone size.

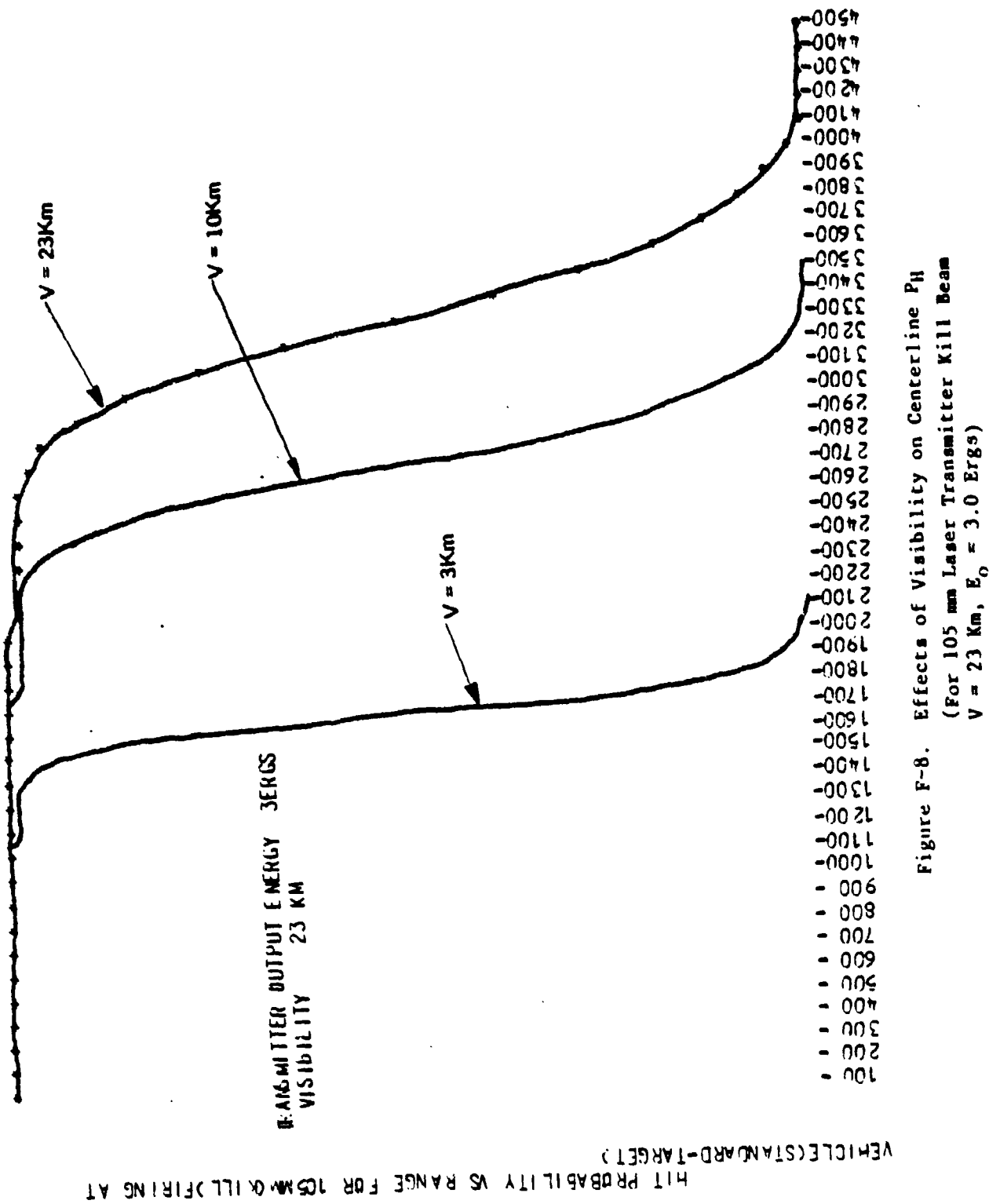


Figure F-8. Effects of Visibility on Centerline P_H
 (For 105 mm Laser Transmitter Kill Beam
 $V = 23 \text{ km}, E_0 = 3.0 \text{ Ergs})$

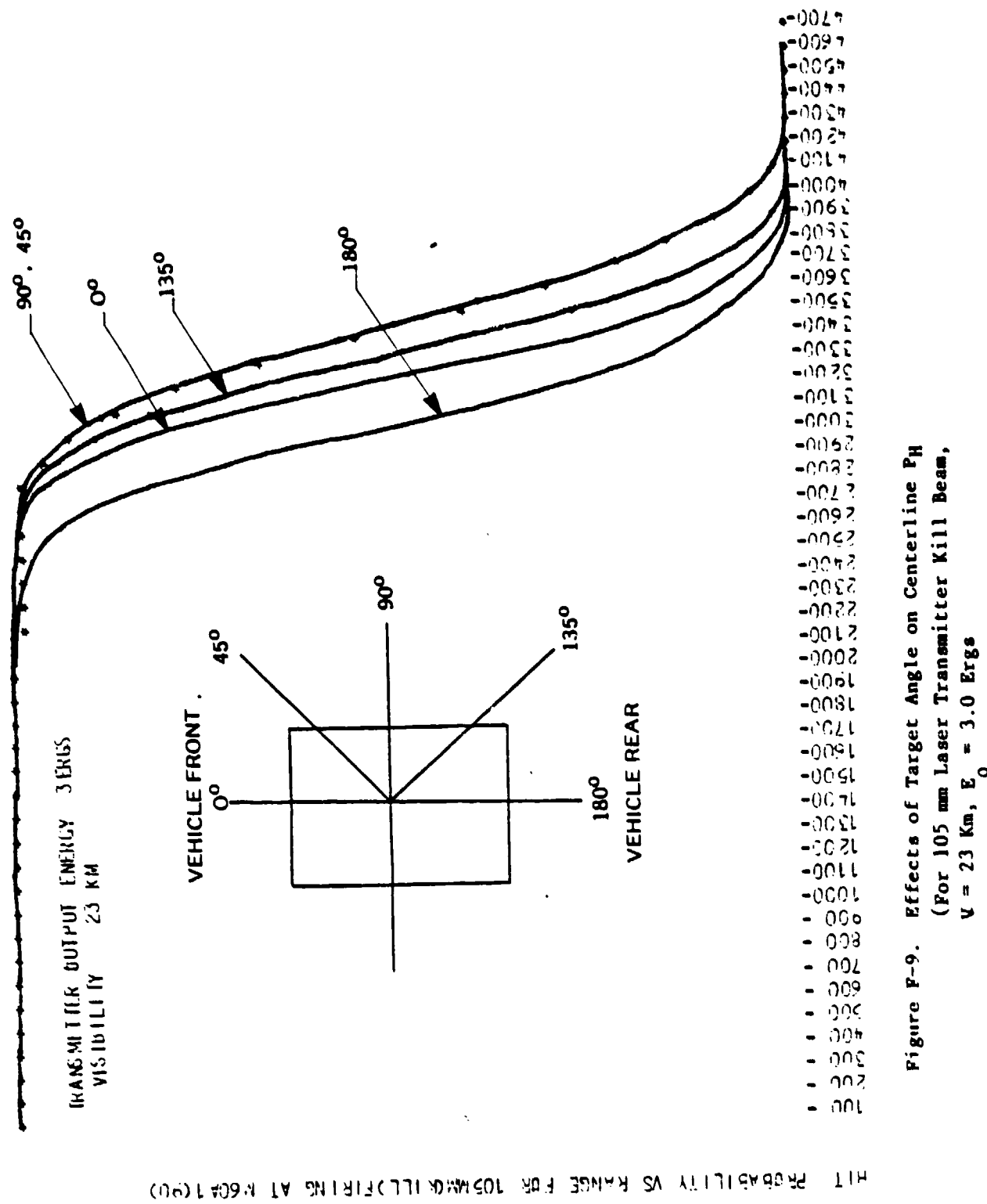


Figure P-9. Effects of Target Angle on Centerline PH
(For 105 mm Laser Transmitter Kill Beam,
 $V = 23 \text{ Km}$, $E_0 = 3.0 \text{ Ergs}$)

<u>Weapon</u>	<u>Standard Target</u>
M16	Man (figure F-10)
Machine Gun	Man
Shillelagh	Vehicle (figure F-11)
TOW	Vehicle
Dragon	Vehicle
105 mm	Vehicle
152 mm	Vehicle
Viper (figure F-15)	Vehicle

The hit and near miss curves are shown in figures F-12 through F-15.

F.8.4 KILL ZONE VERSUS RANGE WITH VISIBILITY AND PARAMETERS

The kill zone as a function of range is presented for various visibilities. The placement of the detectors is the overall determining factors for the kill zone size. This can be seen in figure F-16, which shows the kill zones for the 105 mm laser transmitter firing at the vehicle standard target. The man system hit probability and kill zone versus range is shown in figure F-17 for various visibilities.

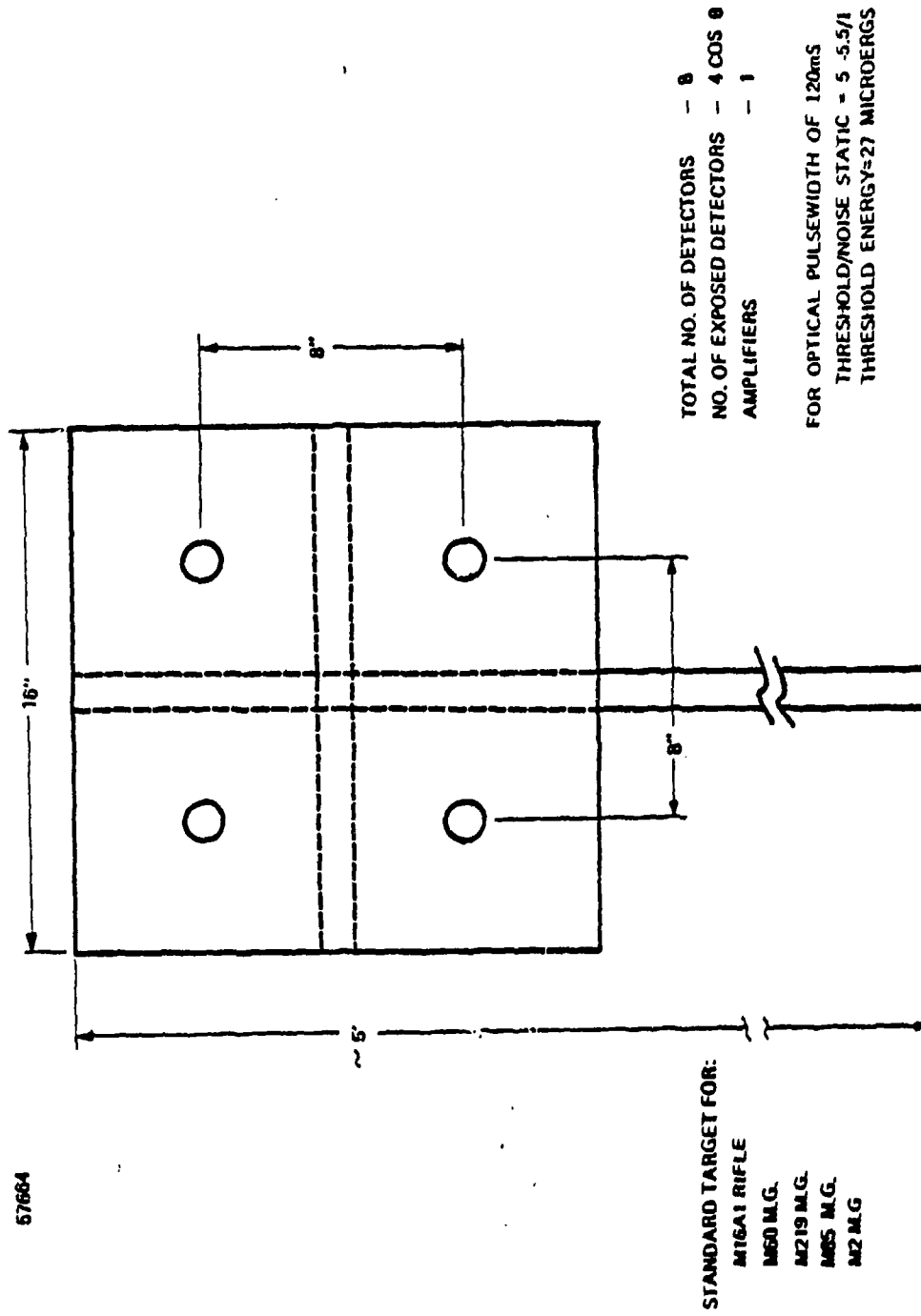
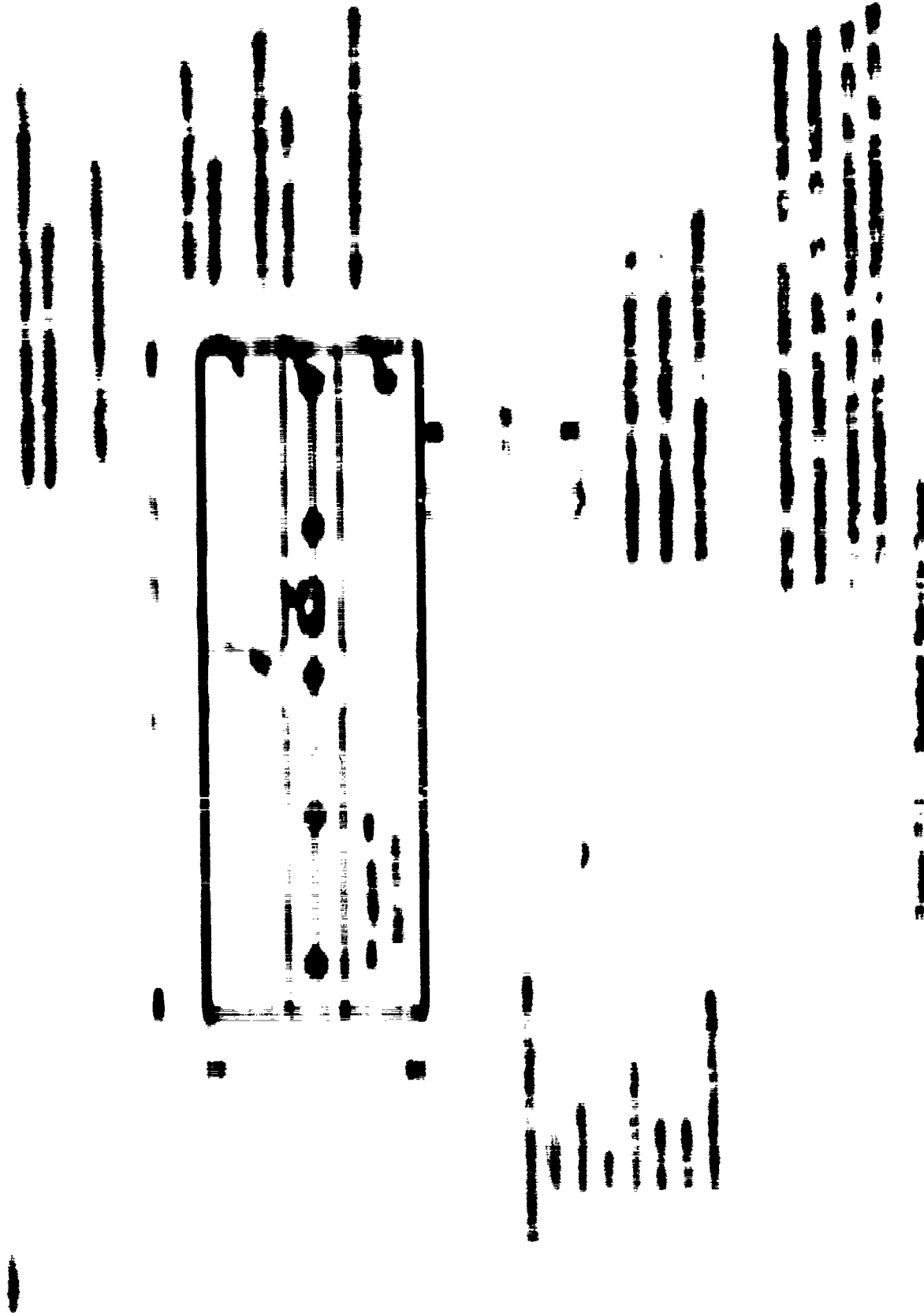


Figure F-10. Standard Man Target



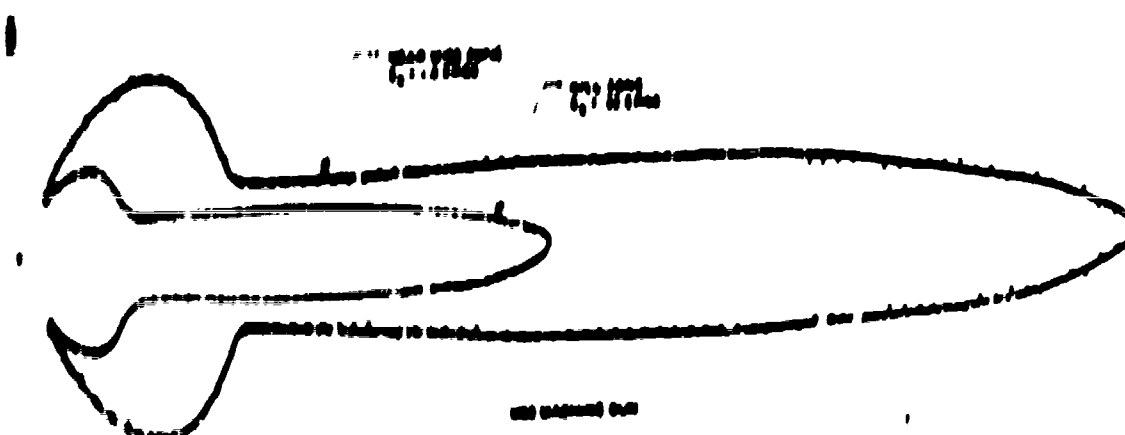
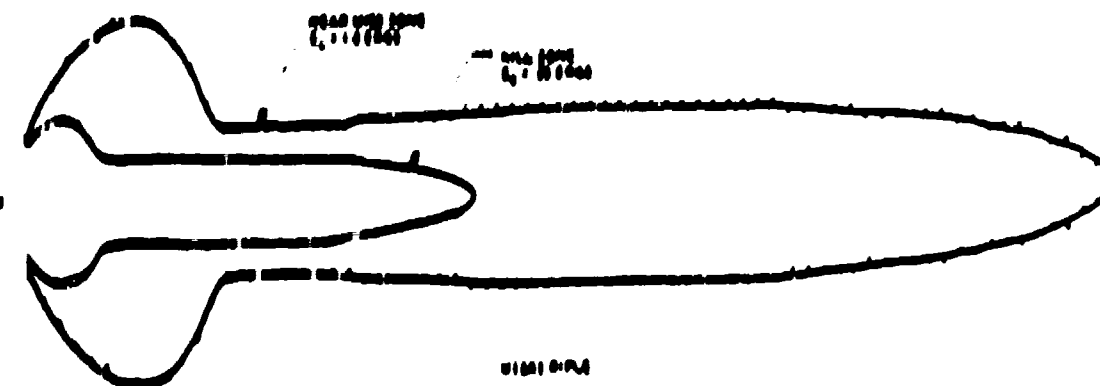


Figure 7-11 HIGH AND HIGH FREQUENCY SIMULATION
HIGH AND HIGH FREQUENCY BANDS
($V = 1$ V, $P_H = 0.01$)

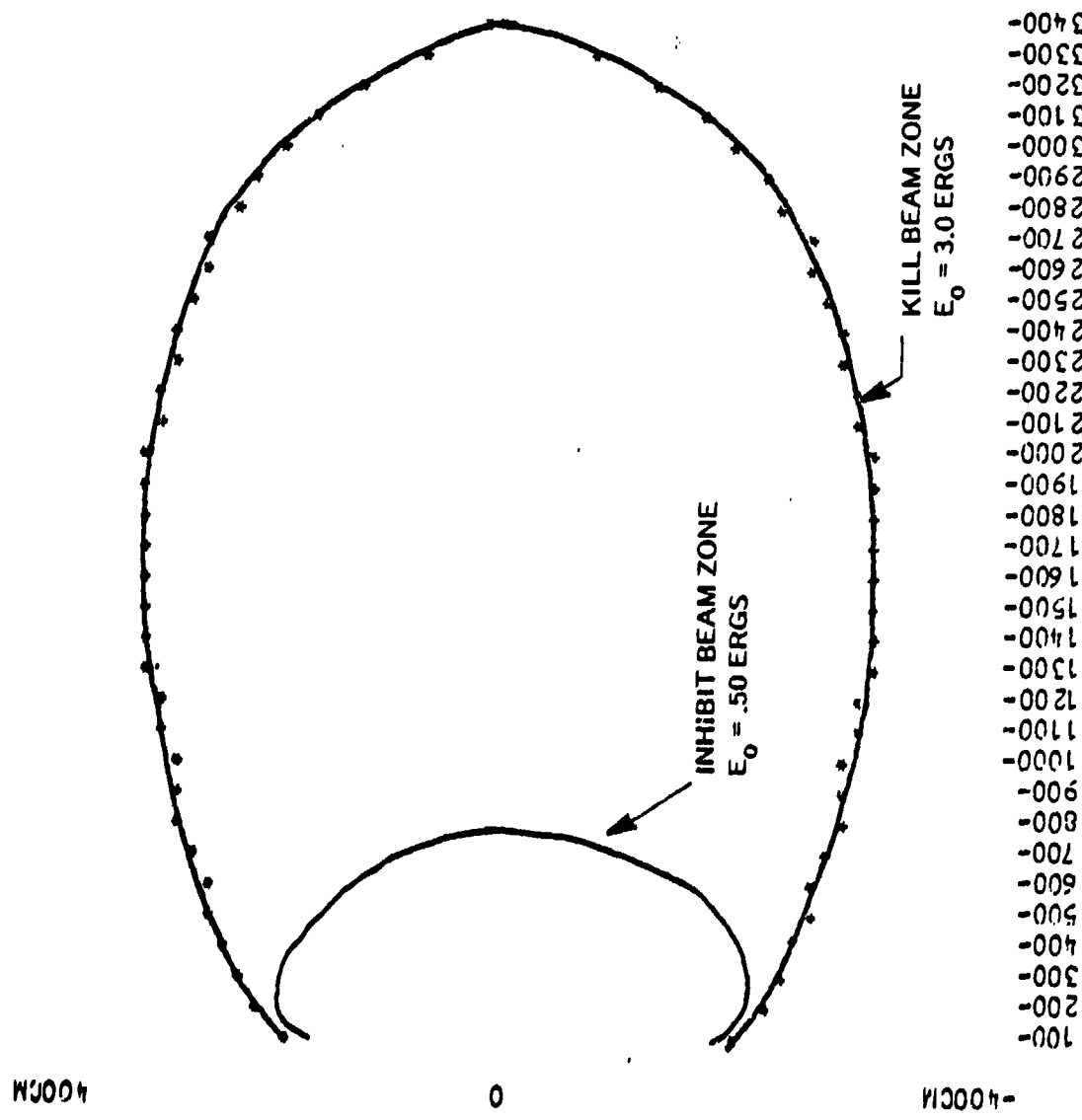


Figure F-13. Shillelagh Computer Simulation
 $V = 23$ Km, $P_H = 90\%$

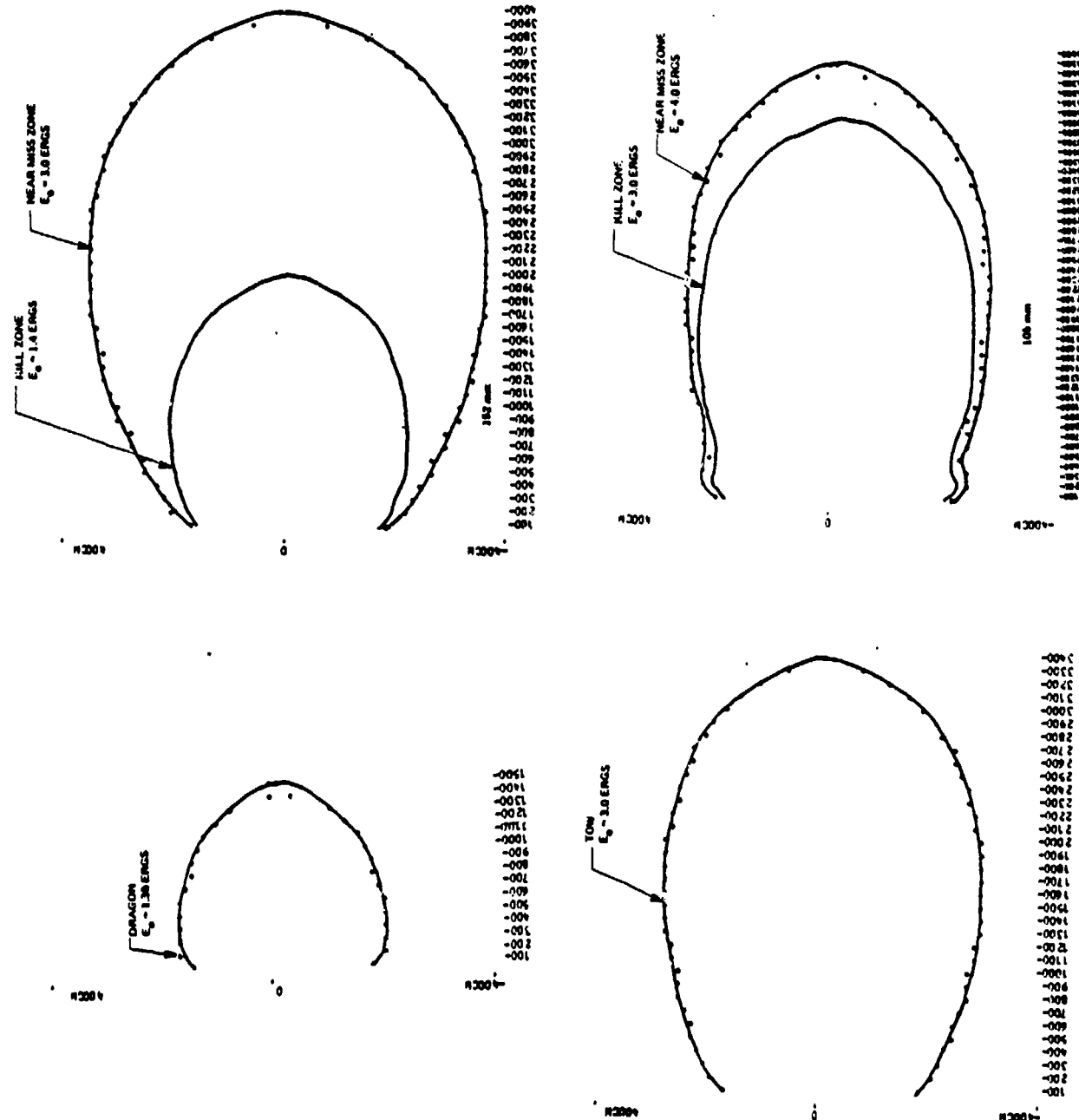


Figure F-14. Dragon, TOW, 105 mm, 152 mm Computer Simulation Kill and Near Miss Zones

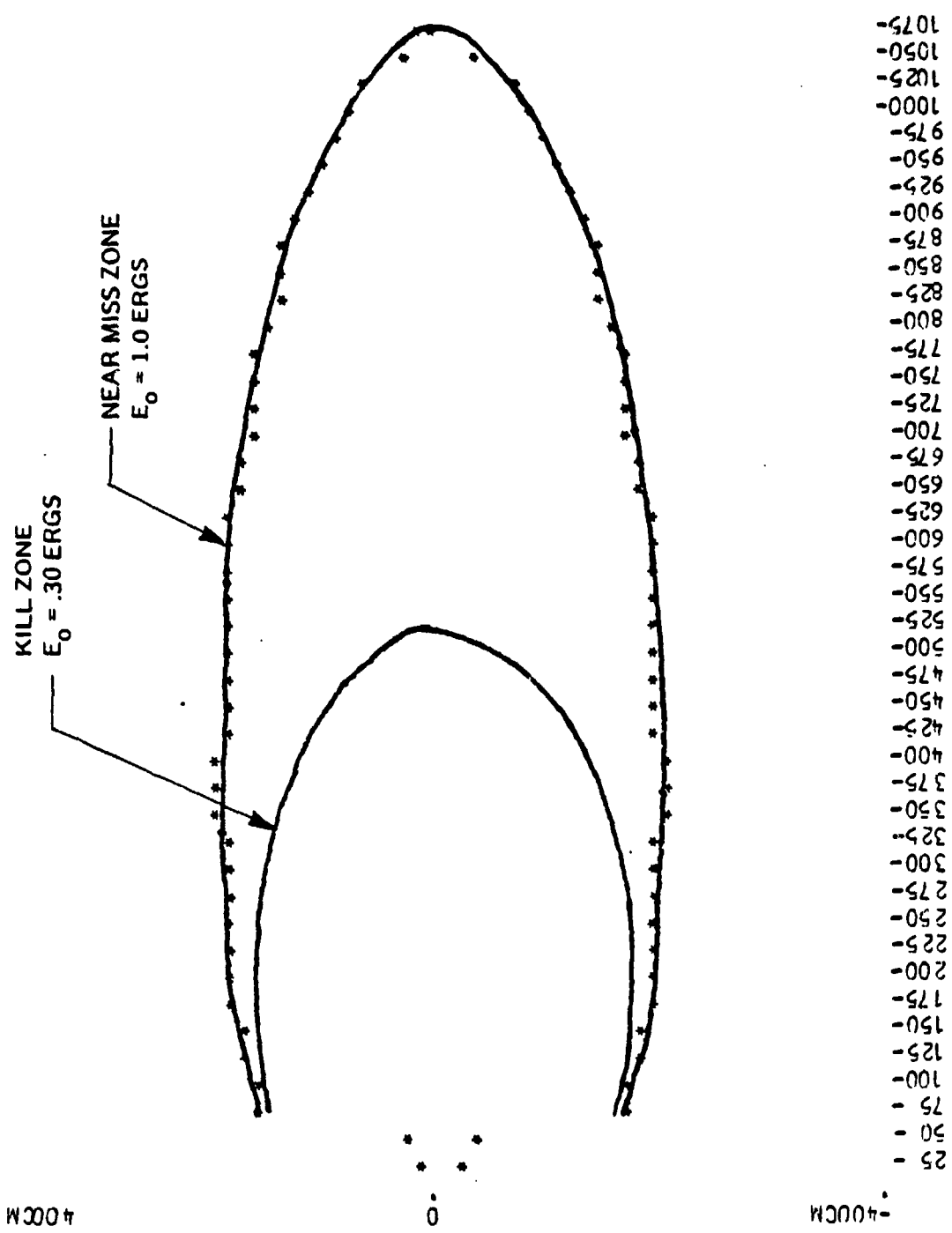


Figure F-15. Viper Computer Simulation Kill and Near Miss Zones
 $V = 23 \text{ Km}$, $P_H = 90\%$

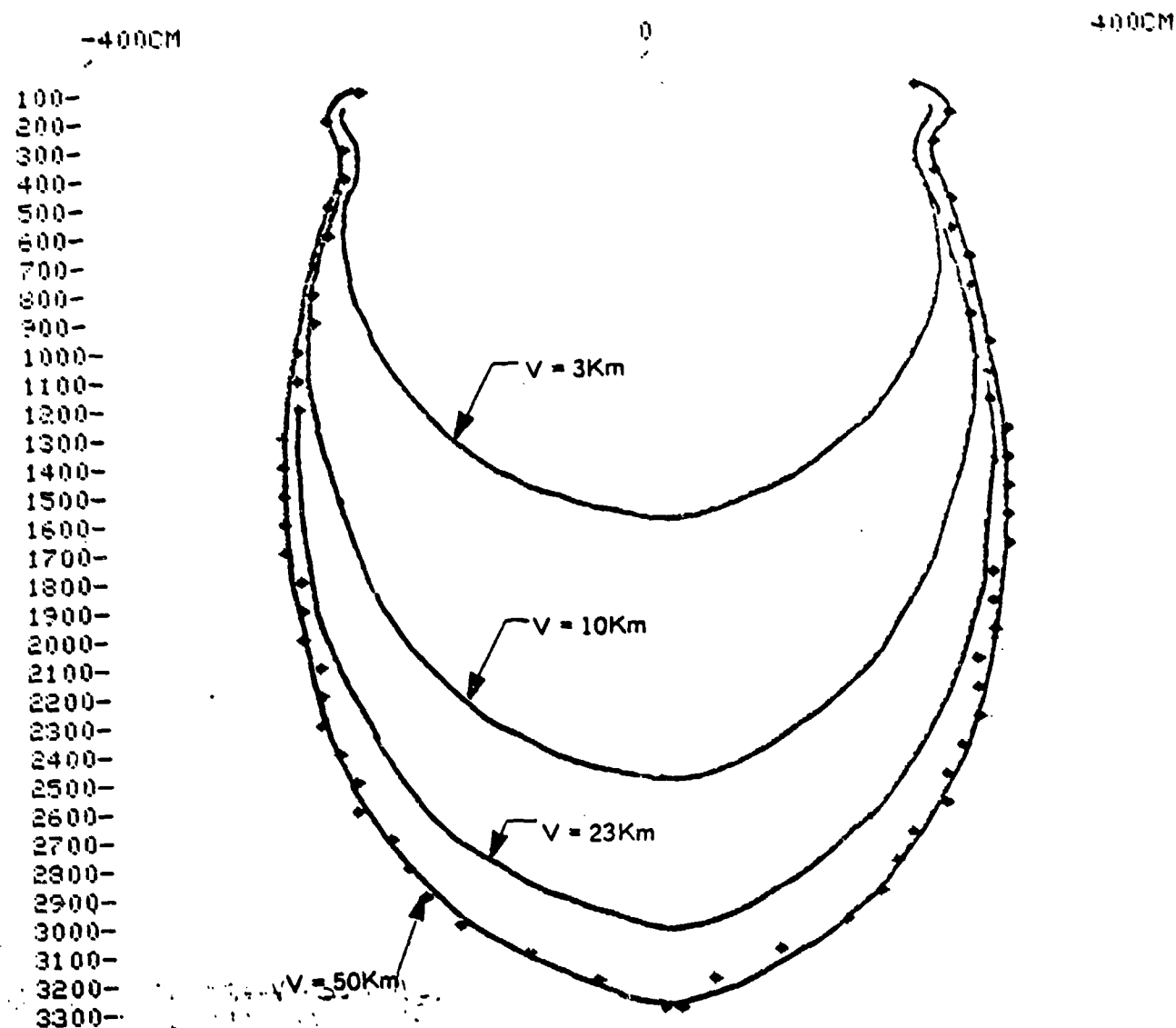


Figure F-16. Effect of Visibility on Kill Zone Size for
105 mm Laser Transmitter
Kill $E_0 = 3.0$ Ergs, $P_H = 90\%$

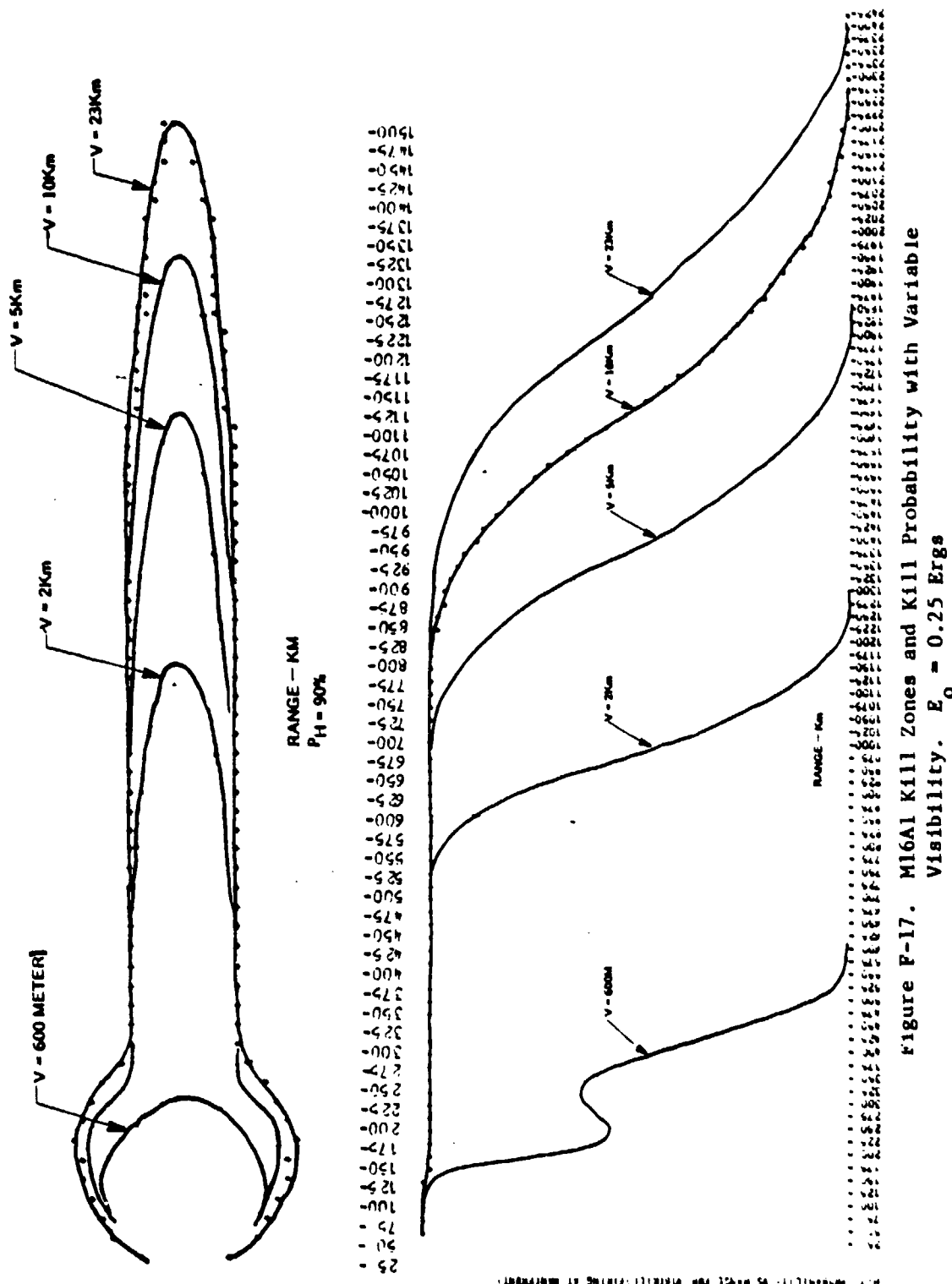


Figure F-17. MIGAL Kill Zones and Kill Probability with Variable Visibility. $E_0 = 0.25$ Ergs

APPENDIX G
GLOSSARY OF TERMS

\AA = Angstrom
AD = Advanced Development
APC = Armored Personnel Carrier
CATB = Combat Arms Training Board
CKD = Constant Kill Diameter
CVKI = Combat Vehicle Kill Indicator
CVLD = Combat Vehicle Laser Detector
DFS = Design File System
ED = Engineering Development
EMI = Electromagnetic Interference
FAR = Average False Alarm Rate
FWHM = Full Width Half Maximum
GaAs = Gallium Arsenide
Hz = Hertz
LAIR = Letterman Army Institute of Research
MILES = Multiple Integrated Laser Engagement System
MWLD = Man-Worn Laser Detector
NEP = Noise Equivalent Power
NTEC = Naval Training Equipment Center
PCM = Pulse-Code-Modulation
PRF = Pulse Repetition Frequency
S/N = Signal-to-Noise Ratio
TES = Target Engagement Simulator
TNR = Threshold-to-Noise Ratio
VES = Vehicle Engagement Simulator
 W/cm^2 = Watts per Square Centimeter

APPENDIX H

REFERENCES

1. Rice, RCA Electro-Optics Handbook
2. R. A. McClatchens and J. E. Selby, "Atmospheric Attenuation of Laser Radiation from 0.76 to 31.25 μ ," AFCRL-TR-74-0003, January 1974
3. V. I. Tatarski, Wave Propagation in a Turbulent Medium, McGraw-Hill, 1961
4. R. S. Lawrence and J. W. Strohbehn, "A Survey of Clear-Air Propagation Effects Relevant to Optical Communications," Proc. of the IEEE, Vol. 58, October 1970
5. D. L. Fried, "Propagation of Spherical Wave in a Turbulent Medium," J. Opt. Soc., Vol. 57, No. 2, February 1967
6. D. L. Fried and J. D. Cloud, "Propagation of an Infinite Plane Wave in a Randomly Inhomogeneous Medium," J. Opt. Soc. of Am., Vol. 56, No. 12, December 1966
7. R. E. Hufnagel and N. R. Stanely, J. Opt. Soc. Am., Vol. 54, 1964
8. R. Lutomirski, "Propagation Channel for the MILES System," Pacific-Sierra Research Report 610, July 1976
9. P. Jacobs, "Evaluation of the Effective Beam Geometry for a Laser Transmitter and a Threshold Detector," 8th NTEC Industry Conference, Orlando, Florida, November 1975
10. RCA Electro-Optics Handbook, EOH-11, p. 62, 1974
11. Satellite Environment Handbook, Ed. F. Johnson, Stanford University Press, pp. 78-83, 1961
12. Handbook of Geophysics and Space Environments, Ed. S. Valley, Chapter 16, pp. 16-1 - 16-9
13. "The Infrared Absorption Spectrum of Water," K. Ya Kondrat'yev, et al, NASA TTF-211, 1964
14. Infrared Physics and Engineering, J. Jamieson, et al, McGraw-Hill, New York, 1963, pp 46-47